GFZ

Helmholtz-Zentrum
POTSDAM

HELMHOLTZ-ZENTRUM POTSDAM
DEUTSCHES
GEOFORSCHUNGSZENTRUM

Sabine Wulf

Methods and applications of tephrochronology in sedimentary archives

Scientific Technical Report STR14/01

www.gfz-potsdam.de

HELMHOLTZ
GEMEINSCHAFT

Recommended citation:

Wulf, S. (2012), Methods and applications of tephrochronology in sedimentary archives.

Scientific Technical Report 14/01, GFZ German Research Centre for Geosciences.

Citation example for individual chapters:

Wulf, S. (2012) Tephra correlation and databases. In: Wulf, S. (2012), Methods and applications of tephrochronology in sedimentary archives (pp.23-24). *Scientific Technical Report 14/01, GFZ German Research Centre for Geosciences*.

Imprint

Helmholtz Centre Potsdam
GFZ German Research Centre for Geosciences

Telegrafenberg
D-14473 Potsdam

Published in Potsdam, Germany
Dezember 2012

ISSN 2190-7110

DOI: 10.2312/GFZ.b103-14010
URN: urn:nbn:de:kobv:b103-14010

This work is published in the GFZ series
Scientific Technical Report (STR)
and electronically available at GFZ website
www.gfz-potsdam.de

Sabine Wulf

Methods and applications of tephrochronology in sedimentary archives

Habilitation

zur Erlangung des akademischen Grades

„doctor rerum naturalium habilitatus"

(Dr. rer. nat. habil.)

in der Wissenschaftsdisziplin Geologie

eingereicht in Form einer kumulativen Arbeit an der

Mathematisch-Naturwissenschaftlichen Fakultät

der Universität Potsdam

Scientific Technical Report STR14/01

Universität Potsdam
Institut für Erd- und Umweltwissenschaften
und
Helmholtz-Zentrum Potsdam, Deutsches GeoForschungsZentrum GFZ
Sektion 5.2 – Klimadynamik und Landschaftsentwicklung

Methods and applications of tephrochronology in sedimentary archives

Habilitation

zur Erlangung des akademischen Grades
„doctor rerum naturalium habilitatus“
(Dr. rer. nat. habil.)

in der Wissenschaftsdisziplin Geologie

eingereicht in Form einer kumulativen Arbeit an der
Mathematisch-Naturwissenschaftlichen Fakultät
der Universität Potsdam

von

Dr. Sabine Wulf

Potsdam, Dezember 2012

Content

List of figures

List of tables

Scientific Technical Report STR14/01, Deutsches GeoForschungsZentrum GFZ. http://doi.org/10.2312/GFZ.b103-14010

Abstract

Tephra (volcanic ash) encompasses airborne material from explosive volcanic eruptions that can be dispersed by wind and deposited over large areas more or less synchronously. Despite its destructive nature, tephras are of great use in terms of independently dating and synchronizing different environments (land, ocean, ice). If deposited in sedimentary sites relatively close to the volcanic source, tephras can be easily detected as discrete visible layers. In further distal archives, however, only traces of tephras – often a lower number of fine grained (< 100 microns) volcanic glass shards – can be found due to sorting processes during the aerial tephra transport. The detection of these shards is quite difficult and may involve long and complicated processing of the tephra hosting material, depending on the type of sediments. Two types of methods are introduced for the tracing of non-visible tephras (cryptotephras) encompassing the destructive and non-destructive processing of sediments. The destructive methods comprise the time-consuming, successive removal of sediment components (i.e., organics, carbonates, biogenic silica, minerals) by chemical and/or physical separation, while the non-destructive methods include the scanning of sediments via optical inspection, magnetic susceptibility and µ-XRF elemental composition prior to tephra separation.

Once detected and extracted, the geochemical fingerprinting of volcanic glass shards allows an allocation of the tephra to its volcanic source and, if distinguishable, to an individual eruption. The date of the tephra eruption can be imported into the sediment age model allowing an additional dating of the sequence by an independent method (tephrochronology). The application of tephrochronology encompasses a variety of scientific questions in geology, palaeoclimatology, archaeology and neotectonics, which can be best demonstrated by examples from the Eastern Mediterranean. This region is ideal for tephrochronological studies due to the presence of high-explosive and frequently active volcanoes in Italy, Greece and Turkey that produced large amounts of geochemically diverse tephras during the Late Quaternary. Case studies involving the identification and application of widely dispersed ashes are presented in this thesis including the tephra records of Lago Grande di Monticchio in southern Italy, the Sea of Marmara (Greece/Turkey) and numerous other terrestrial and marine sites in southern Europe. Marker tephras like the Campanian Ignimbrite (39.3 ka BP) from Italy and the Y-2/Cape Riva tephra (22 ka BP) from Santorini emphasises the use as dating tools for the interpretation of e.g. abrupt climate changes and their relationship to human evolution, the development of past sea levels (e.g, Sea of

Scientific Technical Report STR14/01, Deutsches GeoForschungsZentrum GFZ. http://doi.org/10.2312/GFZ.b103-14010

Marmara, Black Sea) and the estimation of marine reservoir ages, the clarification of the chronostratigraphic position of palaeomagnetic excursions (e.g., the Laschamp and Mono Lake events) and the synchronization of palaeoenvironmental records in the Eastern Mediterranean in order to determine "leads and lags" of rapid climate changes. Annually laminated lake records in favourable wind positions to active volcanoes such as the 133 ka tephra record of Lago Grande di Monticchio are furthermore key sites for the over-regional linking of sedimentary records from central and southern Europe. From the socio-volcanological point of view, these records allow detailed insights into the frequency of explosive eruptions of nearby dangerous volcanoes (in the case of Monticchio the Campanian Province in southern Italy), and offer the potential to thoroughly investigate the relationship between rapid climate changes and the environmental impact of large tephra events. Last but not least, the study of the distribution of both visible and non-visible tephras contributes to the knowledge of past wind systems that can be applied to recent ash dispersal models of the 2010 Eyjafjallajökull and 2011 Grimsvötn eruptions in Iceland and vice versa.

Scientific Technical Report STR14/01, Deutsches GeoForschungsZentrum GFZ. http://doi.org/10.2312/GFZ.b103-14010

Zusammenfassung

Bei explosiven Vulkanausbrüchen entsteht Fallasche, die auch Tephra genannt wird und je nach Windbedingungen über weite Gebiete hinweg verteilt und +/- synchron abgelagert werden kann. Neben ihren zerstörerischen Charakter sind Tephren von großer wissenschaftlicher Bedeutung, da sie als unabhängige Zeit- und Synchronisationsmarker in verschiedenartigen Ablagerungsräumen (z.B. Land, Meer, Eis) eingesetzt werden können. In sedimentären Ablagerungsräumen nahe dem vulkanischen Ausbruchszentrum sind Tephren oft als diskrete Lagen sichtbar. In entfernteren (distale) Archiven sind aufgrund der Sortierungsprozesse während des äolischen Tephra-Transportes dagegen meist nur Spuren von Aschen – oft in Form von wenigen feinkörnigen (<100 µm) vulkanischen Gläsern – zu finden. Das Aufspüren dieser Gläser kann sehr schwierig sein und beinhaltet je nach Art des Tephra-führenden Sedimentes langwierige und komplexe Aufbereitungsprozesse. Hier werden zwei Arten von Methoden zur Suche von nicht sichtbaren Tephren (Kryptotephren) unterschieden: die destruktive Bearbeitung der Sedimente, die das sukzessive Entfernen von verschiedenen Sedimentkomponenten (z.B. Organik, Karbonate, biogenes Silizium, Minerale) durch chemische und/oder physikalische Separation beinhaltet, sowie vorgreifende materialschonende Methoden wie z.B. das Scannen der Sedimentsequenz mit Hilfe optischer-mikroskopischer Verfahren, der magnetischen Suszeptibilität und µ-XRF Element-zusammensetzung.

Nach dem Auffinden und der Extraktion von vulkanischen Gläsern erlaubt deren geochemischer „Fingerabdruck“ eine Zuordnung der Asche zu ihrem Ausbruchszentrum und, soweit möglich, zu einem bestimmten Ausbruchsereignis. Das Alter dieses Ereignisses kann dann in das Altersmodell der Sedimentsequenz integriert werden und bietet somit eine weitere unabhängige Datierungsmethode, die Tephrochronologie, an. Die Anwendung der Tephrochronologie umfasst eine Reihe wissenschaftlicher Fragestellungen in den Bereichen der Geologie, Paläoklimatologie, Archäologie und Neotektonik, die am besten anhand von Beispielen im östlichen Mittelmeerraum demonstriert werden können. Diese Region ist ideal für tephrochronologische Untersuchungen, da sie sich durch eine Vielzahl hochaktiver explosiver Vulkane in Italien, Griechenland und in der Türkei auszeichnet, die große Mengen an geochemisch diversen Aschen während des Spätquartärs produzierten. In dieser Arbeit werden Fallbeispiele zur Identifizierung und Anwendung von weitverbreiteten Tephren gezeigt, u.a. aus den Tephraprofilen des Lago Grande di Monticchio in Süditalien, des

Scientific Technical Report STR14/01, Deutsches GeoForschungsZentrum GFZ. http://doi.org/10.2312/GFZ.b103-14010

Marmara-Meeres (Griechenland/Türkei) und anderer terrestrischer und mariner Lokationen in Südeuropa. Insbesondere anhand des markanten Campanischen Ignimbrites (39.3 ka BP, Italien) und der Y-2/Cape Riva Asche (22 ka BP, Santorini) soll die Hilfe von Tephren als Datierungsmittel verdeutlicht werden, z.B. in der Interpretation von abrupten Klimaänderungen und ihre Auswirkung auf die menschliche Entwicklung, von Meeresspiegeländerungen (z.B. Marmara-Meer, Schwarzes Meer) und der Abschätzung von marinen Reservoir-Altern, der Klärung der chrono-stratigraphischen Stellung von paläomagnetischen Umpolungen (z.B. die Laschamp und Mono Lake Exkursionen) und der Synchronisierung von Paläoklimasequenzen im östlichen Mittelmeerraum zur Ermittlung von „leads“ und „lags“ rapider Klimaänderungen. Jahreszeitlich geschichtete Seesediment-Archive in günstiger Windposition zu aktiven Vulkanen, wie z.B. das 133 ka umfassende Tephra-Archiv des Lago Grande di Monticchio, sind dabei der Schlüssel für die überregionale Korrelation von Sedimentprofilen in Mittel- und Südeuropa. Vulkanologisch-soziologisch betrachtet sind diese Archive von großer Bedeutung, da sie detaillierte Informationen zur Häufigkeit von explosiven Ausbrüchen benachbarter, gefährlicher Vulkane (im Fall von Monticchio die Campanische Vulkanprovinz in Süditalien) liefern, und ferner die Möglichkeit bieten, Zusammenhänge zwischen rapiden Klimaänderungen und den Umweltauswirkungen von großen Vulkanausbrüchen zu studieren. Zu guter Letzt tragen Untersuchungen zur Verbreitung von sichtbaren Aschen und Kryptotephren zum Kenntnisstand vergangener Windsysteme bei, die wiederum auf moderne Aschenverbreitungsmodelle (siehe Ausbrüche des Eyjafjallajökull in 2010 und des Grimsvötn in 2011 auf Island) und umgekehrt angewandt werden können.

Scientific Technical Report STR14/01, Deutsches GeoForschungsZentrum GFZ. http://doi.org/10.2312/GFZ.b103-14010

Acknowledgements

My first and special thanks go to Prof. Dr. Achim Brauer and Prof. Dr. Jörg Negendank, who cordially supported me over the past years and who never stopped believing in the science of tephrochronology.

Likewise, I am very grateful to Prof. John Lowe and Prof. Siwan Davies for their kind willingness to participate in the habilitation committee.

My sincere gratitude goes to all my colleagues of Section 5.2 at the German Research Centre for Geosciences GFZ in Potsdam, in particular Christine Gerschke, Janina Baier, Markus Czymzik, Nadine Dräger, Peter Dulski, Ute Frank, Ulrike Kienel, Celia Martin-Puertas, Jens Mingram, Ina Neugebauer, Norbert Nowaczyk, Florian Ott, Sylvia Pinkerneil, Birgit Plessen, Georg Schettler, Michał Słoviński and Tina Swierczynski, for their overall support and stimulating discussions.

My special thanks go to Kristina Wutke, Miriam Gross, Elena Beckenbach, Jo Wesselhöfft and Justus Franke for their help in sample preparation and for sharing the "tephra enthusiasm".

Furthermore I would like to thank Oona Appelt for the support during EPMA measurements, Helga Kemnitz and Ilona Schaepan for SEM-EDS analyses and Brigitte Richert for µ-XRF scanning. From the thin section preparation laboratory, special thanks go to Gabi Arnold, Michael Köhler and Dieter Berger. I am furthermore grateful to Ursula Kegel and Petra Meier for all kind of help in the laboratory as well as Manuela Dziggel and Andreas Hendrich for graphical support.

During the past years of my research, I was very lucky to get to know to wonderful national and international colleagues of the tephrochronology community, with whom I shared fascinating and fruitful discussions. I am in particular grateful to Prof. Jörg Keller (University of Freiburg, Germany), Prof. Martine Paterne (CNRS Gif-sur-Yvette, France), Prof. Roberto Sulpizio (University of Bari, Italy), Prof. Gianni Zanchetta (University of Pisa, Italy), Dr. Biagio Giaccio (CNR Rome, Italy), Prof. Martin Menzies, Dr. Paul Albert, Dr. Chris Satow, Mark Hardiman (all Royal Hollow University of London, UK), Dr. Christine Lane, Dr. Victoria Smith (both University of Oxford, UK), Dr. Anna Bourne and Dr. Peter Abbott (both Swansea University, UK).

Last but not least I would like to express my heartily gratitude to all my friends and family for their love, support and inspiration.

Scientific Technical Report STR14/01, Deutsches GeoForschungsZentrum GFZ. http://doi.org/10.2312/GFZ.b103-14010

1 Introduction

1.1 Principles of tephrochronology

Explosive volcanic eruptions can produce large amounts of volcanic ash, so-called tephra that is dispersed synchronously over wide areas (e.g., Lowe, 2011). The crucial impact of airborne tephra on the human society and economy has been recently demonstrated by the 14 April-22 May 2010 eruptions of Eyjafjallajökull volcano in Iceland, resulting in an interruption in global air traffic for several days (e.g., Oxford-Economics, 2010; Oxford-Economics, 2011). This rather moderate size event (VEI=3) had an ash dispersal that was greater than previously reported for an event of this magnitude (Gudmundsson et al., 2012) and thus revealing a high complexity of the distribution and fallout pattern over northern and central Europe depending on prevailing and changing wind patterns (e.g., Langmann et al., 2012; Heinold et al., 2012; Weber et al., 2012; Gudmundsson et al., 2012). The eruptions of Eyjafjallajökull are therefore a unique example demonstrating the general lack in understanding these processes. Ash dispersal models developed for the Eyjafjallajökull eruptions in a first step contribute a better understanding of tephra distribution mechanisms of past eruptions that are, for instance, recorded as individual ash layers in terrestrial and marine environments. Vice versa, the study of proximal (near-vent) and distal (>15 km from the volcanic source) tephra deposits provides not only valuable information about past wind systems as revealed by their distribution (e.g., Pyle et al., 2006) but also about the explosive behaviour of the source volcanoes (e.g., de Vita et al., 1999; Cioni et al., 2003) and recurrence intervals of catastrophic eruptions (e.g., Palumbo, 1997). From a palaeoenvironmental perspective, in turn, the occurrence of individual tephra layers in sedimentary archives ("tephrostratigraphy"), especially those with a known age ("tephrochronology"), permits those archives to be synchronised (e.g., Thorarinsson, 1944). This methodology is now widely used to date and correlate glacial (e.g. polar ice caps), terrestrial (e.g., lake sediments, loess sequences, soils, lava flows), and marine sequences. Its application is mainly concentrated but not limited to questions in palaeoclimate/-environmental research (e.g., Newnham et al., 1995; Lowe, 2011 and references within), archaeology (e.g., Deino et al., 2010; Müller et al., 2011), and neo-tectonics (e.g., de Lange and Lowe, 1990; Funk et al., 2006).

In order to use a tephra layer from a sedimentary archive as a reliable isochrone, reliable dating and firm identification of each ash layer are crucial. Tephras can be dated by various techniques including ^{14}C, K/Ar, laser $^{39}Ar/^{40}Ar$, fission track, Thermo Luminescence (TL) and Electro-Spinning Resonance (ESR) dating methods (e.g., Pillans et al., 1996). The

Scientific Technical Report STR14/01, Deutsches GeoForschungsZentrum GFZ. http://doi.org/10.2312/GFZ.b103-14010

identification of tephra involves the determination of volcanic glass composition, referred to as chemical "fingerprinting" (e.g., Lowe, 2011 and references therein).

Aside from precise dating and chemical identification, the detection and processing of tephras for geochemical fingerprinting are crucial. Here, the search for non-visible tephras (cryptotephras) usually involves a time-consuming, systematic processing of sediment samples of long sequences (e.g., Turney, 1998; Blockley et al., 2005), which needs to be diminished and standardised by, for instance, prior scanning and evaluation of sedimentological data. The finding of cryptotephras is indicative of the future direction of tephra studies in many regards, last but not least for the establishment of complete tephrostratigraphies and detailed ash dispersal patterns of specific areas.

The Eastern Mediterranean is a unique area for tephrostratigraphical studies due to the partly wide dispersal of chemical different ashes from high-explosive, frequently active Late-Quaternary volcanoes in Italy, Greece and Anatolia/Turkey. In the past 60 years a large tephrostratigraphic data-base and correlation 'grid' has been established, mainly based on more than 30 major distal tephra layers detected in Eastern Mediterranean Sea cores and terrestrial records (e.g., Keller et al., 1978; Federman and Carey, 1980; Paterne et al., 1986; Narcisi and Vezzoli, 1999; Druitt et al., 1999; Wulf et al., 2004; Siani et al., 2004; Wulf et al., 2008; Calanchi and Dinelli, 2008; Giaccio et al., 2012). Recently, the study of cryptotephras has developed as a standard procedure for analysing marine and terrestrial records, and it has been shown that the number of cryptotephras preserved in those records can greatly outnumber visible ones (e.g., Bourne et al., 2010). This has enhanced the use of tephrostratigraphy as a tool for synchronising late Quaternary records in the Mediterranean.

1.2 Scientific goals

A major tephra program is provided by the UK RESET program (Response of Humans to Abrupt Environmental Transitions; http://c14.arch.ox.ac.uk/reset/embed.php?File=) that has been developed to systematically scan geological and archaeological records from Europe and North Africa to detect non-visible distal tephras, and to examine both their major and trace element glass compositions. Furthermore, a network of European scientists (Royal Holloway University of London (RHUL), Oxford University, Instituto Nazionale di Geofisica e Vulcanologia (INGV) Naples, Pisa and Catania, the Universities of Ankara, Edinburgh, Keele, Pisa, Roma Tre) has been established working currently on proximal tephra deposits, which will provide a reference major- and trace-element database against which to compare

Scientific Technical Report STR14/01, Deutsches GeoForschungsZentrum GFZ. http://doi.org/10.2312/GFZ.b103-14010

distal tephras. Until present, the RESET project has led to the discovery of multiple cryptotephra layers in different terrestrial and marine sites in Europe and North Africa in the time frame of the last 100,000 years leading to the conclusion that cryptotephras are more widespread and numerous than previously supposed (Lowe et al., 2012). In this respect, the medial-distal tephrochronological sequence of Lago Grande di Monticchio in southern Italy is a key reference record for matching proximal and distal tephras with Italian provenance.

The progressive results of the Monticchio tephra record are documented in the three enclosed manuscripts (Wulf et al., 2004; Wulf et al., 2008; Wulf et al., 2012). Moreover, the applied tephrochronological methods and the main uses of tephra markers are thoroughly discussed integrating results of tephra works from other sedimentary archives in Central and Southern Europe (Wulf et al., 2002; Ramrath et al., 1999; Brauer et al., 2007b, 2007c; Hamann et al., 2010; Kwiecien et al., 2008; Müller et al., 2011; Roeser et al., 2012; Neugebauer et al., 2012), the North Atlantic (Wulf et al., 2011) and the Americas (Haberzettl et al., 2007, 2008, 2009; Wulf et al., 2007; Kienel et al., 2009). Hence, a major scientific goal of this thesis is the evaluation of different methods and applications in the field of tephrochronology/ tephrostratigraphy, which is thought as a guide for the detection and extraction of visible and non-visible tephras in sedimentary records that are required to up-grade the tephrostratigraphical frameworks. This work is absolutely pivotal to making significant breakthroughs that will improve the dating and correlation of archaeological and geological sequences in southern Europe and adjacent seas. Accordingly, the wider scientific goals are:

- To contribute to important, long-standing questions about the timing, rate and natural effects of abrupt environmental transitions (AETs) during the past 135,000 years. Tephras in high-resolution terrestrial and marine archives are an outstanding dating and correlation tool for determining durations and ‘leads and lags’ of abrupt palaeoenvironmental changes (see the international COST-INTIMATE program (INTegration of Ice-core, Marine and TErrestrial record; http://cost-es0907.geoenvi.org/).
- To establish how these AETs may have affected human dispersal and development in prehistory. Widespread dispersed tephras in the Eastern Mediterranean can be used to date major phases of human immigration from Africa into Europe and their response to rapid climate changes. The RESET project, for instance, developed out of the fact that marked climatic changes have been proven to occur over as little as 20 years or less and that related human responses are of relevance today because of modern global warming.

Scientific Technical Report STR14/01, Deutsches GeoForschungsZentrum GFZ. http://doi.org/10.2312/GFZ.b103-14010

- To develop a more robust and complete record of past volcanic behaviour in order to estimate eruption recurrence intervals, magnitudes of volcanic activity and patterns and scales of ash dispersal. New tephra findings help to complement the record of explosive volcanism in areas of intense activity such as the Eastern Mediterranean. The volcanic record is used to determine the frequency and intensity of eruptions that is required for volcanic risk assessment in densely populated regions (i.e., central-southern Italy with the Mega-Cities of Rome and Naples). Dense pattern of tephra findings in addition with tephra thickness and grain size information will give clues about tephra dispersal patterns. In addition, the combination of high-resolution palaeo-records and tephra findings can provide important information such as prevailing wind and precipitation patterns during the time period of tephra eruption as derived from palaeo-proxy data of sediments.
- To provide more precise time-equivalent marker horizons (isochrones) for synchronising diverse records (marine, terrestrial, archaeological) throughout southern Europe and for potential bridging links to the Greenland ice cores.

Figure 1*: World map with zoom into Europe showing the sites of tephrochronological investigations mentioned in the manuscripts and text including main districts of Late Quaternary explosive volcanism. TP = Tenaghi Philippon.*

Scientific Technical Report STR14/01, Deutsches GeoForschungsZentrum GFZ. http://doi.org/10.2312/GFZ.b103-14010

1.3 Studied sites

The manuscripts of this thesis include tephra results from two sedimentary settings, each located in a terrestrial and marine environment in the Eastern Mediterranean.

The major focus of the studies is set on the tephra record of Lago Grande di Monticchio. Lago Grande di Monticchio is located about 120 km east of Naples in the Monte Vulture volcanic complex in the region of Basilicata, southern Italy (Fig. 1, Table 1). It is the larger of two small adjacent maar lakes that formed during the final phreatomagmatic eruptions of Monte Vulture stratovolcano at 132 ± 12 ka BP (Brocchini et al., 1994; Stoppa and Principe, 1998). Lago Grande di Monticchio is furthermore close (ca. 100-350 km) and in a downwind position to the active explosive volcanoes of the alkaline Roman Co-magmatic Province in central and southern Italy (Fig. 1). This favourable position resulted in the recording of a large number (n=345) of primary distal tephra deposits in the annually laminated lake sediments.

Lago Grande di Monticchio is furthermore a site of intense studies for palaeoclimate reconstruction since the early 1980's (e.g., Allen et al., 1999; Brauer et al., 2000; Brauer et al., 2007a). A first sediment core of 25.5 m was taken in a fen at the western margin of the lake (Watts, 1985), followed by three coring campaigns in the years 1990, 1994 and 2000 within the lake basin of Lago Grande di Monticchio, which recovered a total of eight partly overlapping sediment cores. The successive counting of varved sections and calculation of sedimentation rates in sections of poor varve preservation dated the base of the 103.1 m long, undisturbed composite sequence at 132,900 calendar years BP to the penultimate Glacial period (Zolitschka and Negendank, 1996; Brandt et al., 1999; Brauer et al., 2007a). This chronology was confirmed by independent dating methods such as radiocarbon dating (Zolitschka and Negendank, 1996; Hajdas et al., 1998) and tephrochronology (Newton and Dugmore, 1993; Narcisi, 1996; Wulf et al., 2004; Wulf et al., 2012).

Tephras in the Monticchio record are between 0.1 mm and >2 m thick and all originate from Plinian to sub-Plinian eruptions of southern and central Italian volcanoes (Wulf et al., 2004; Wulf et al., 2008; Wulf et al., 2012). Italian volcanism is subdivided into four provinces (Tuscan, Roman, Campanian, Sicilian-Aeolian) that have been active with temporal offsets since >7.3 Ma (Ferrara and Tonarini, 1985) and that produced particularly widespread tephra markers such as the Campanian Ignimbrite (Phlegrean Fields, 39.28 ± 0.11 ka BP; De Vivo et al., 2001).

Scientific Technical Report STR14/01, Deutsches GeoForschungsZentrum GFZ. http://doi.org/10.2312/GFZ.b103-14010

The second tephra study (Wulf et al., 2002) was carried out on marine sediments from the Sea of Marmara (between Turkey and Greece, Bosporus Strait and Strait of the Dardanelles) (Fig. 1, Table 1). Three, up to 10.61 m long piston cores (20 KLG, 21 KL, and 40 KL) were recovered during the R/V *Meteor* cruise M44/1 in January/February 1999 from a central plateau rising several hundred meters above a deep basin of the central Sea of Marmara between 566 m and 702 m water depth. Sediments are composed of silty clay of alternating brownish-grey, olive-greenish-grey to black colours reflecting changing redox conditions in the current bottom water. Based on radiocarbon dating the sediment sequences comprise the last ca. 26 ka BP. One discrete tephra marker layer of 1 cm to 7 cm thickness occurs in all three cores in-between or below a black horizon, which has been interpreted as the last seawater ingression >10.6 ka BP ago (Aksu et al., 1999; Çagatay et al., 2000). The Sea of Marmara is located in a more distal but favourable wind position to Italian volcanoes and close by high-magnitude explosive volcanoes of the Aegean Arc (Fig. 1). The latter in particular includes Thera volcano on the Island of Santorini, which erupted large amounts of tephra during the past 360 ka BP (i.e., Minoan Tuff = Z-2 Ash, 3.6 ka BP; Cape Riva Tuff = Y-2 Ash, 22 ka BP) (Druitt et al., 1999).

Other tephra archives discussed in this thesis comprise different lacustrine, peat or marine sedimentary sites in Central and Southern Europe, the North Atlantic and the Americas (Table 1, Figure 1). The results of respective tephra studies were published in a co-authorship in international peer-reviewed journals or conference proceedings (see Table 1).

Table 1: *Main characteristics of study sites mentioned in the text (see also Figure 1).*

Site	Coordinates of coring site	Setting	Time range of investigated tephras	Reference
Lago Grande di Monticchio (Italy)	40°56'N, 15°35'E	Maar lake	0 – 133 ka BP	Wulf et al. (2004, 2008, 2012)
Sea of Marmara	40°50'N, 27°46'E	Inland sea	0 – 26 ka BP	Wulf et al. (2002)
Piànico-Sèllere (northern Italy)	45°48'N, 10°02'E	Lake	Ca. 400 ka BP	Brauer et al. (2007b, 2007c)
Lago di Mezzano (Central Italy)	42°37'N, 11°56'E	Maar lake	0 – 34 ka BP	Ramrath et al. (1999) Wulf et al. (2008)
Tenaghi Philippon (Greece)	40°58'N, 24°13'E	Peat bog	7 – 73 ka BP	Müller et al. (2011)
Iznik (Turkey)	40°27'N, 29°32'E	Lake	0 – 36 ka BP	Roeser et al. (2012)
Black Sea	41°32'N, 30°53'E	Inland sea	0 – 25 ka BP	Kwiecien et al. (2008)
Levantine Sea	32°45′N, 34°39′E	Inland sea	0 – 27 ka BP	Hamann et al. (2010)
Rehwiese (Germany)	52°25'N, 13°12'E	Palaeo-lake	11.5 – 12.9 ka BP	Neugebauer et al. (2012)
HM03-133-10 (North Atlantic)	63°40'N, 06°05'W	Ocean	0 – 140 ka BP	Wulf et al. (2011)
Alberca (Mexico)	20°23'N, 101°12'W	Maar lake	0 – AD 1840	Kienel et al. (2009)
Rincón de Parangueo (Mexico)	20°25'N, 101°15'W	Maar lake	0 – AD 1840	Kienel et al. (2009)
Lake Nicaragua	11°53'N, 85°38'W	Lake	0 – 11.3 ka BP	Wulf et al. (2007)
Potrok Aike (Patagonia)	51°37'S, 69°10'W	Maar lake	0 – 55 ka BP	Haberzettl et al. (2007-2009)

Scientific Technical Report STR14/01, Deutsches GeoForschungsZentrum GFZ. http://doi.org/10.2312/GFZ.b103-14010

1.4 Structure of the Habilitation Thesis

This habilitation thesis is organized as a cumulative thesis. It is arranged into an introduction (chapter 1) followed by the syntheses of the results of multiple tephra studies (chapter 2 "Discussion"), which is sub-divided in a method part (chapter 2.1) and an application part (chapter 2.2). Chapter 3 encompasses a brief section about the challenges and perspectives in tephrochronology ("Conclusions and perspectives") followed by the list of references (chapter 4) and reprints of four first author manuscripts (chapter 5). Individual manuscripts were published in high-rank international peer-reviewed scientific journals and were the results of international and interdisciplinary collaboration projects. A brief outline of each manuscript and the own contribution in context with the individual co-authors to the scientific results are listed below.

Manuscript #1 – *"Tephrochronology of the 100 ka lacustrine sediment record of Lago Grande di Monticchio (southern Italy)"* by Wulf et al. (2004) is published in the journal "***Quaternary International***" and encompasses the description and dating of widespread tephra marker documented in the 100 ka tephra key site of Lago Grande di Monticchio in southern Italy. This study is the basis for the tephrochronological dating of lacustrine sediments. Co-Authors are A. Brauer and J.F.W. Negendank (project participants) as well as M. Kraml and J. Keller, who provided geochemical data from marine archives for detailed tephra correlation.

Manuscript #2 – *"Towards a detailed distal tephrostratigraphy in the Central Mediterranean: The last 20,000 yrs record of Lago Grande di Monticchio"* by Wulf et al. (2008), published in the "**Journal of Volcanology and Geothermal Research**", is the development of a detailed tephrostratigraphy of Late Glacial and Holocene tephra layers in the Central and Eastern Mediterranean using the lacustrine site of Monticchio as key site for the synchronisation of terrestrial and marine tephra archives. Co-Authors are M. Kraml and J. Keller (marine tephra archives), who kindly provided chrono-stratigraphical and geochemical data for two widespread marine ash layers from the Ionian Sea.

Manuscript #3 – *"The 100-133 ka record of Italian explosive volcanism and revised tephrochronology of Lago Grande di Monticchio"* by Wulf et al. (2012), published in "**Quaternary Science Reviews**" is an important follow-up of the results of tephrochronological studies of the 100 ka tephra sequence of Lago Grande di Monticchio

Scientific Technical Report STR14/01, Deutsches GeoForschungsZentrum GFZ. http://doi.org/10.2312/GFZ.b103-14010

published in Wulf et al. (2004) and Wulf et al. (2008). Manuscript #3 presents the tephra results of the extended 100-133 ka Monticchio profile and updates the tephrochronological framework for the entire 133 ka palaeoclimate record. My contribution as first author was the major-element glass analysis and correlation of Monticchio tephras as well as the interpretation of data. Four out of the twelve co-authors are members of the Monticchio project (J. Mingram, S. Lauterbach, S. Opitz, and A. Brauer) who helped to establish a detailed varve chronology and thus provided the timing of tephra deposition. Three co-authors from the Royal Holloway University of London (P. Albert, C. Satow, and E. Tomlinson) collaborated closely in the analysis of trace element data of individual glass shards of widespread tephra layers and therefore contributed to a firm geochemical correlation of crucial tephra markers. Further five co-authors provided valuable non-published geochemical and chronological data of distal marine (J. Keller and M. Paterne) and proximal-distal terrestrial (G. Sottili, B. Giaccio, and M. Viccaro) tephra correlatives that helped to establish a reliable Monticchio tephrochronology.

Manuscript #4 – "*Marine tephra from the Cape Riva eruption (22 ka) in the Sea of Marmara*" by Wulf et al. (2002), published in the journal "***Marine Geology***", gives a first time detailed description and precise land-sea correlation of a widespread Santorini ash (here labelled as Marmara Sea Tephra, MST) that has been detected as a valuable time marker in sediment cores of the Sea of Marmara (Eastern Mediterranean). As first author I contributed to the manuscript the description and interpretation of petrographical and geochemical data of the MST tephra and the background research of the proposed tephra correlative. Three co-authors from the Albert-Ludwigs-University Freiburg (M. Kraml, M. Schwarz, and J. Keller) provided valuable geochemical data of the Y-2 tephra correlative from proximal and distal marine sites for comparison. The interpretation of sedimentological data of the cores and the resulting palaeoceanography of the Sea of Marmara were obtained by four co-authors involved in the initial coring project (T. Kuhn, M. Inthorn, I. Kuscu, and P. Halbach).

Scientific Technical Report STR14/01, Deutsches GeoForschungsZentrum GFZ. http://doi.org/10.2312/GFZ.b103-14010

2 Discussion

This chapter presents a synthesis of tephra results as obtained from the sedimentary records of Lago Grande di Monticchio, Sea of Marmara and other terrestrial and marine archives from Europe and the Americas, and is subdivided into a methodical (2.1) and an application part (2.2).

2.1 Methods in tephrochronology

Tephra studies use a series of methods for the identification and extraction of volcanic ash material in different sedimentary archives. As illustrated by a series of experiences, these methods depend on the combination of both the composition of tephra and the type of the tephra hosting sediments. Since some of the tephra processing procedures – particular those for cryptotephras – are quite time consuming, it is necessary to perform an evaluation of sample material prior to extensive processing. In the following, a compilation is given for the tracing and processing of tephra layers in various sedimentary environments.

2.1.1 Identification of tephra

The detection of tephras encompasses various techniques ranging from simple optical identification of volcanic glass (the main tephra component beside phenocrysts and lithics), the use of changes in physical-chemical sediment parameters to sediment-destructive methods.

Optical methods

Tephras in distal lacustrine and marine sedimentary settings can be often distinguished from their host sediments by colour and /or grain sizes. Colours may range from white, pinkish, brown, grey to black, while grain sizes of tephra components are often coarser (fine silt to coarse sand) than the embedding sediments. In order to define a clastic layer as a tephra, the presence of volcanic glass is evidentiary. Attention has to be paid in terms of the interpretation of “primary” tephra fallout (deposition directly from the ash cloud) and “secondary” tephra material that has been re-deposited by intra-basin (i.e., subaqueous currents, turbidity currents) or catchment area processes (i.e., input by heavy rainfall, storms, or landslides). In the North Atlantic region, for example, secondary tephra deposition is enhanced by the rafting and subsequent melting of tephra-laden icebergs leading to a spatial

Scientific Technical Report STR14/01, Deutsches GeoForschungsZentrum GFZ. http://doi.org/10.2312/GFZ.b103-14010

offset and a time lag between eruption and deposition over timescales of centuries to millennia (e.g., Lackschewitz and Wallrabe-Adams, 1997; Brendryen et al., 2010). The microscopic inspection of potential tephra material is therefore essential to identify sedimentary matter such as reworked terrestrial plant remains in the lacustrine or ice-rafted debris in the marine setting that hint to a secondary deposition of tephra material. The study of large scale thin sections produced from undisturbed sediments can give extra valuable information about both tephra components and the depositional process (i.e., grading generated by the deposition of turbidity currents). Those thin section analyses can also be helpful for the detection of thin tephra layers that are not visible by naked eye. Here, the systematic scanning at high magnifications (200x to 500x) can be successful, but is difficult for diatom- and clastic-rich sediments.

Magnetic susceptibility

Depending on the composition of host sediments, a thin tephra layer (>0.1 mm) can be traced on the basis of its physical properties, i.e. by anomalous intensities in magnetic susceptibility (MS). In general, the intensity in MS depends on the concentration of magnetic minerals in a tephra. Those encompass Fe-Ti-Oxides and Fe-Sulphides that occur among the pheno-/xenocrystal assemblage and/or are present as microcrystal inclusions in juvenile (glass) components (e.g., Franz et al., 1997). The total concentration of magnetic minerals may also be an indicator for the chemical composition of a tephra, for instance the higher the concentration, the darker the glass, the more mafic is its composition.

Commonly, a tephra can be easily detected in sediments that are characterised by low concentrations of magnetic minerals such as organic-rich and evapoclastic deposits. For example, the relatively thick phonotrachytic Campanian Ignimbrite (CI) and the rhyolitic Y-2 ash layer from Santorini (22 ka BP) produced high MS signals in the peat sequence of Tenaghi Philippon (Greece) (Müller et al., 2011; U. Müller, personal communication 2008), but also thin ash layers (1 to 2.5 mm) such as the Central Mexican andesitic and rhyolitic tephras in the evapoclastic maar lake sequences of Hoya Alberca and Hoya Rincon de Parangueo (Kienel et al., 2009) can be traced this way.

Tephras deposited in sediments that are dominated by a regular input of Fe-Ti-Oxide rich clastic material (i.e., volcanic craters lakes, maar lakes) are more difficult to detect just on the basis of changes in the magnetic susceptibility. In the maar lake sediments of Lago Grande di Monticchio, for instance, magnetic susceptibility signals of K-alkaline tephras are often superimposed by increased MS values of the epiclastic material that has been re-

Scientific Technical Report STR14/01, Deutsches GeoForschungsZentrum GFZ. http://doi.org/10.2312/GFZ.b103-14010

deposited from the catchment area into the lake basin (Brandt, 1999). Another example from Lake Iznik (western Turkey) nicely demonstrates the correlation between the Fe-Ti-Oxide concentration in glass shards of tephras of different composition and their responding MS signals in clastic sediments that are dominated by metamorphic, sedimentary and volcanic rock fragments. Here, the Fe-Ti-oxide-rich glass shards of the rhyolitic Y-2 tephra are pointed out by a high peak in MS, while the juvenile components of the tephriphonolitic AP2 tephra from Vesuvius (ca. 3.5 ka BP; Rolandi et al., 1998) are characterized by low concentrations of magnetic microcrystals and thus produce decreased (negative) MS values compared to the host sediments (Roeser et al., 2012).

The detection of tephras on the basis of abrupt changes in magnetic susceptibility values not only depends on the type of host sediments but also on the thickness of a tephra layer. In general, cryptotephras are difficult to trace by this method, particular if the host sediments are rich in Fe-Ti-Oxide minerals. The finding of anomalous MS peaks, however, always requires a confirmation by microscopic inspection.

µ-XRF scanning

A new approach in tracing visible and non-visible tephras incorporates the evaluation of elemental composition data of host sediments that can be obtained by non-destructive µ-XRF core scanning (e.g., Francus et al., 2009; Kylander et al., 2011). High-resolution XRF scanning of sediment cores has its main application in the reconstruction of climate variability (Francus et al., 2009) and is today a routine measurement. The common core scanning uses 200 µm to 1 mm intervals, which are sufficient enough to detect thin tephra layers that are not visible by naked eye. The tracing of cryptotephras, in turn, requires a higher resolution µ-XRF scanning that can be obtained at 50-500 µm intervals on polished sediment blocks that have been prepared for the large-scale thin section preparation for microfacies analysis (Brauer et al., 2000). This method, however, is extremely time-consuming (*ca.* 0.5h to 5h per 1 cm section) and requires a thorough pre-evaluation of proxy data of the potential tephra-bearing sediment sections and a temporal localisation by the sediment chronology (i.e., varve counting).

The detection of a single tephra layer by XRF scanning is based on anomalous counts of specific chemical elements relative to its host sediment. The type of element depends on both the composition of the tephra and its hosting sediments. Table 2 provides an overview of tephras of different glass composition (mafic to felsic) and their relationship to different types of embedding sediments. Volcanic glass of basaltic to andesitic composition, for example, is

Scientific Technical Report STR14/01, Deutsches GeoForschungsZentrum GFZ. http://doi.org/10.2312/GFZ.b103-14010

characterized by high Fe, Ti and Ca concentrations, but not all of these elements may peak out in the XRF core scanning data. Marine calcareous sediments from the North Atlantic, for instance, occupy numerous dispersed and macroscopic visible basaltic tephras from Iceland that show increased counts of the elements Ti, Fe, Cl and Mn (Wulf et al., 2011). Those XRF signals, however, are absent for cryptotephras. Tephras of basaltic-andesitic composition documented in the organic-rich sediments of Lake Nicaragua show only high element counts in Fe and Ca (Wulf et al., 2007). In the varved evapoclastic sediments of central Mexican maar lakes, in turn, the andesitic tephra layers from Paricutín and Colima volcanoes are only traceable by the relative enrichment of the element Fe (Kienel et al., 2009). High counts in Ca synchronize with the Paricutín tephra, but this signal is clearly produced by the seasonal calcite layer in which the tephra is deposited (Kienel et al., 2009). Other examples are given from K-alkaline tephras detected in the sediments of Lago Grande di Monticchio. Primary fallout and reworked layers of the relative coarse grain phonolitic to trachytic ashes all feature high counts in K regardless of the composition of host sediments (organic, clastic to evapoclastic). Tephras deposited in calcareous sediments show in addition depletion in the elements Ca, Mn, Sr and Ti which make up the actual sediment composition (e.g., Wutke, 2012). One of these tephras, the tephriphonolitic AP2 tephra, has been successfully XRF traced as a non-visible tephra in sediments of the distal site of Lake Iznik, western Turkey (Roeser et al., 2012). In this clastic-rich archive, the AP2 tephra is indicated by increased counts of the elements K and Zr as well as decreased values of Rb, Sr, Zr, Cd and Cl. In the organic and diatom-rich lake sediments of Lago Grande di Monticchio, in turn, the very same but 3 cm thick AP2 tephra is characterized by increased counts in K, Si, Ca, Al, P, Mn, Sr, Fe and Ti, while S and Cl counts are decreased (Fig. 2).

Another example is given by the widespread phonolitic Laacher See Tephra (LST, 12,880 calendar years BP; Brauer et al., 1999a,b) from the Eifel Volcanic Field in western Germany (e.g., Schmincke et al., 1999; van den Bogaard and Schmincke, 1985). The LST was analysed in two lacustrine archives in northern (Rehwiese) and western Germany (Lake Meerfelder Maar, Eifel) (Neugebauer et al., 2012), both characterized by discriminative sediments varying from Fe-rich organic to calcareous and organo-clastic deposits, respectively. It is noticeable that the LST is generally pointed out by relatively high counts in Si, Ti, Al and K in both sites, although the glass composition of the LST is slightly variable. Other elements such as Mn additionally trace the LST in the organic to siderite/calcite-rich sediments of Rehwiese, while in Lake Meerfelder Maar also an enrichment of Ca, Ti, Rb and Sr as well as a decrease in Mn and Fe can be observed.

Scientific Technical Report STR14/01, Deutsches GeoForschungsZentrum GFZ. http://doi.org/10.2312/GFZ.b103-14010

Table 2: *List of tephras of different composition occurring in different types of sedimentary archives and their responding XRF signals. Mean tephra glass compositions (EPMA) are given on a water-free basis. B=basaltic, BA=basaltic-andesitic, P=phonolitic, TP=tephriphonolitic, Tr=trachytic, PTr=Phonotrachytic, A=andesitic, R=rhyolitic, RD=rhyodacitic, TrD=Trachydacitic. References: (1) Wulf et al. (2011); (2) Wulf et al. (2007); (3) Wulf et al., (2004); (4) Roeser et al. (2012); (5) Neugebauer et al. (2012); (6) Wulf et al. (2006); (7) Kienel et al. (2009); (8) Kwiecien et al. (2008); (9) Haberzettl et al. (2007); (10) Haberzettl et al. (2008).*

Tephra	Glass composition	SiO_2	TiO_2	Al_2O_3	FeO	MnO	MgO	CaO	Na_2O	K_2O	Cl	XRF signal increased	XRF signal decreased	Host sediments	Thickness of tephra (mm)
5e-low (North Atlantic) [1]	B	49.6	2.6	13.7	14.7	0.2	5.5	10.0	3.0	0.6	0.0	Ti, Fe, (Cl, Mn)	K	Calcareous	70
5e-Midt/DOS24s (North Atlantic) [1]	B	50.1	2.9	13.2	14.0	0.2	6.2	10.5	2.5	0.4	0.0	Ti, Fe	K	Calcareous	dispersed
5e-Midt/RHY (North Atlantic) [1]	B	50.7	2.4	13.9	12.5	0.2	6.3	11.0	2.7	0.4	0.0	None	None	Calcareous	crypto
SAT (Lake Nicaragua) [2]	BA	52.0	1.4	14.8	13.4	0.3	4.4	9.0	3.2	1.3	0.1	Fe, Ca	None	organic	1
AP2 (Monticchio) [3]	P-TP	57.3	0.4	21.0	3.2	0.1	0.4	3.4	6.1	7.5	0.7	K, Si, Ca, Al, P, Mn, Sr, (Fe, Ti)	S, Cl	organic	31
AP2 (Lake Iznik) [4]	P-TP	55.8	0.3	21.4	3.3	0.1	0.8	4.2	6.6	7.4	n.a.	K, Rb, Sr, Zr, Cd, Cl	None	clastic	lense
LST (Rehwiese) [5]	P	58.8	0.3	21.7	1.9	0.3	0.1	1.0	9.5	6.1	0.4	Si, Ti, Al, K, Mn	None	organic, Ca-Siderite rich	20
LST (Meerfelder Maar) [5]	P	60.6	0.6	20.6	2.3	0.2	0.4	1.9	5.7	7.5	n.a.	Si, Ti, Al, K, Ca, Rb, Sr,	Mn, Fe	organo-clastic	60
Schiava (Monticchio) [6]	Tr	64.9	0.4	17.8	2.3	0.1	0.3	2.6	3.5	7.9	0.5	K, Cl (Si, Ca)	Mn, Sr, Ti	calcareous	27
CI (Monticchio) [3]	PTr	61.9	0.4	19.2	2.9	0.2	0.4	1.7	5.7	6.9	0.8	K	None	calcareous	257
Paricutin (Central Mexico) [7]	A	58.6	1.6	15.2	8.3	0.2	3.7	6.0	4.3	1.7	0.4	Fe	None	evapoclastic	1
Colima 1913 AD (Central Mexico) [7]	A-R	55.6 77.0	2.3 0.1	16.6 12.9	8.4 0.9	0.2 0.0	2.2 0.0	5.0 0.4	4.9 3.9	4.0 4.5	0.8 0.0	Fe	None	evapoclastic	2.5
Z-2 (Black Sea) [8]	RD	73.5	0.3	13.7	2.1	0.1	0.3	1.5	5.0	3.2	0.3	None	None	clastic	1
Y-2 (Black Sea) [8]	RD	72.1	0.5	14.4	3.2	0.1	0.4	1.8	4.4	2.9	0.3	None	None	clastic	5
Y-2 (Lake Iznik) [4]	RD	72.0	0.4	14.3	3.3	0.1	0.4	1.7	5.1	2.6	n.a.	Zr, Cl	Al, K*, Ti, Fe	clastic	70
Hudson (H1) (12-12) (Potrok Aike) [9]	TrD	65.3	1.2	16.2	4.9	0.2	1.5	3	4.5	2.8	0.4	None	Fe, Ti, Mn	organo-clastic	1
Mt. Burney (12-15) (Potrok Aike) [9]	R	78.2	0.1	13.3	1.1	0.0	0.3	1.2	3.8	1.8	0.1	None	Fe, Ca, Ti	organo-clastic	10
Reclus (12-22) (Potrok Aike) [9]	RD	77.9 67.6	0.1 0.4	13.1 16.6	1.3 3.8	0.1 0.1	0.2 1.8	1.6 4.3	3.1 3.6	2.3 1.5	0.0 0.2	None	Ca, K, Sr	organo-clastic	20
Mt. Burney (6-8) (Potrok Aike) [10]	R	75.4	0.4	13.9	2.0	0.1	0.5	2.4	3.7	1.5	0.1	None	Ti, Fe, K	organo-clastic	10

As demonstrated by several studies, tephras of felsic composition are more difficult to detect by XRF core scanning (Table 2). Several dacitic to rhyolitic vitric ash layers identified in Laguna Potrok Aike, for instance, reveal none or only slight decreased signals in Fe, Ti, Ca, K, Mn and Sr within the organo-clastic lacustrine host sediments (Haberzettl et al., 2007, 2008). In the calcareous clastic sediments of the Black Sea, the elemental composition at the position of the two 1 and 5 mm thin rhyodacitic tephra layers Z-2 and Y-2 (Santorini) is not distinguishable from the host sediments (Kwiecien et al., 2008). However, thicker deposits (7 cm) of the very same Y-2 tephra show increased peaks in Zr and Cl but decreased signals in Al, Ti, Fe and K in the clastic sediments of Lake Iznik (Roeser et al., 2012).

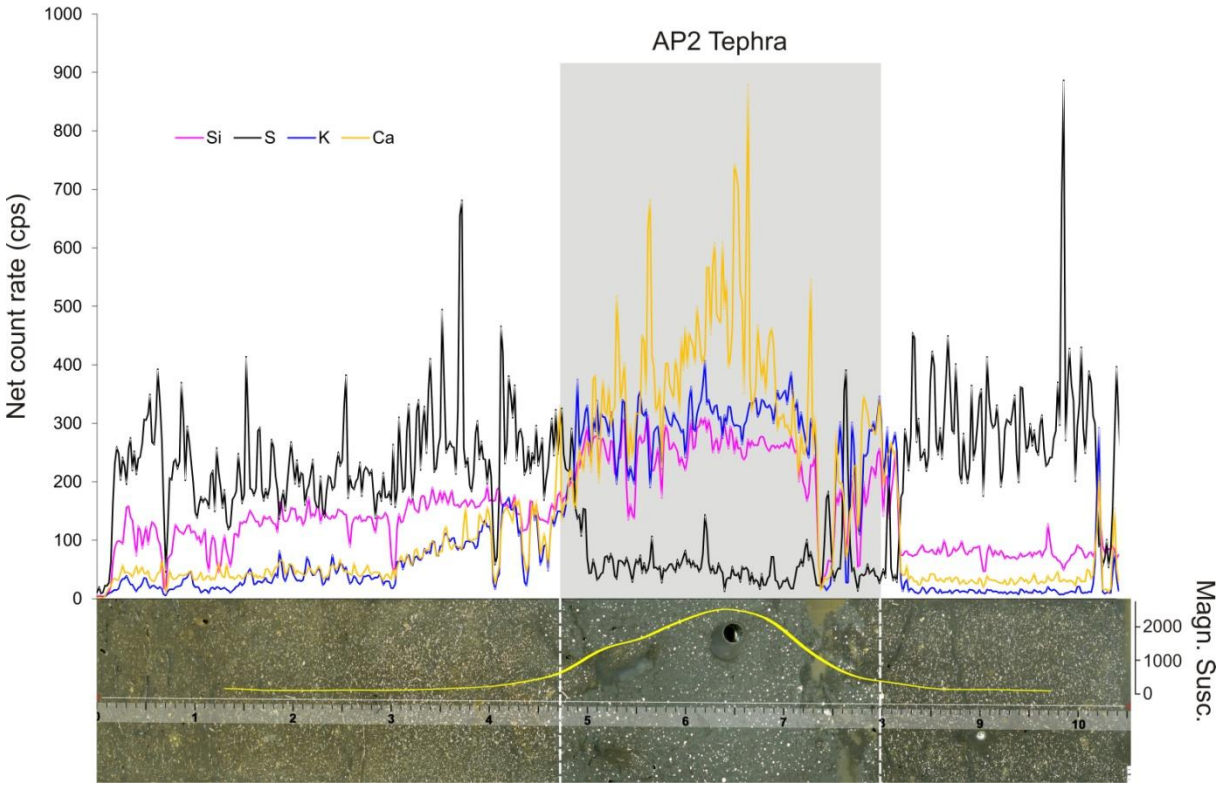

Figure 2: *Magnetic susceptibility and µ-XRF element profiles (Si, S, K, and Ca) of the AP2 tephra from Vesuvius (ca. 3.5 ka BP) in a polished sediment block from core LGM-L in Lago Grande di Monticchio.*

In summary, certain elements determined by µ-XRF core scanning are useful tools for tracing visible and non-visible tephras in sediments. The type of element is interpreted to depend on both the tephra glass chemistry and the composition of tephra hosting sediments. Increased counts of the elements Fe, Ti and/or Ca are, for example, expected for tephras of

Scientific Technical Report STR14/01, Deutsches GeoForschungsZentrum GFZ. http://doi.org/10.2312/GFZ.b103-14010

mafic composition (basalts to basaltic andesites). The element K, in turn, is a valuable indicator for K-alkaline tephras, while silicic glass shards (dacites to rhyolites) are rather difficult to trace. Regardless from their glass composition, some tephras show increased counts in chlorine (Cl), which may be falsely interpreted as an element that is enriched in volcanic glass. High Cl counts obtained on polished sediment blocks can rather be related to resin which is unfolded in core sections that are characterised by cracks and vesicles occurring along with grain sizes changes of sediments (i.e., coarse grained tephra material; P. Dulski, personal comment 2012). In marine and saline lacustrine sediment cores those spaces can be filled by secondary precipitated NaCl crystals resulting in higher counts of Cl during µ-XRF core scanning. The success of tephra tracing by µ-XRF core scanning also depends on the thickness of the ash layer and grain sizes of tephra components, for instance, the thinner (<1mm, cryptotephras) and finer grained the more difficult is the detection by µ-XRF-scanning.

As a conclusion, the results of µ-XRF measurements can be used only as a qualitative tool for the detection of tephras. Though a rough petrological classification of tephras seems to be possible by the XRF data, glass chemical compositions can be best obtained by high-precision microanalysis.

Sediment-destructive methods

Components of non-visible cryptotephras are usually dispersed in the sediments and may encompass only a few glass shards. Therefore, they are often hard to trace just on the basis of microscopic inspection, magnetic susceptibility or µ-XRF core scanning data. A different, but more time consuming method for tracing cryptotephras is the systematic sampling (i.e., 1 cm^3) and destructive processing of tephra hosting sediments. The extraction of volcanic glass basically encompasses the removal of sediment components other than volcanic glass shards. The type of procedure strongly depends on the composition of sediments and includes several steps that may be combined with each other (see the following chapter 2.1.2).

2.1.2 Tephra sample preparation

The extraction of glass shards of visible and non-visible tephras for determining the geochemical fingerprinting requires “clean” and concentrated samples. Thus, depending on the grade and type of contamination with embedding sediments a tephra sample can be pre-treated by several subsequent procedures (Fig. 3).

Scientific Technical Report STR14/01, Deutsches GeoForschungsZentrum GFZ. http://doi.org/10.2312/GFZ.b103-14010

Sieving

It is recommended to wet sieve pure tephra samples into a well sorted grain size fraction in order to remove the clay fraction and to facilitate the preparation of polished resin blocks or thin sections. The range of mesh sieve sizes can be chosen in terms of the mean grain sizes of the tephra samples, i.e. 63-125 µm or 125-250 µm. The search for cryptotephras applies the smallest mesh sieve sizes of 20-80 µm or 20-100 µm. In order to avoid contamination with former samples, the use of disposable polyester mesh sieves is recommended.

Chemical removal of organic matter and carbonates

Prior to sieving, samples rich in organic matter and/or carbonates are treated with "mild" chemicals such as diluted hydrogen peroxide and/or hydrochloric acid in order to dissolve the respective components. These processes also facilitate the dispersion of consolidated samples such as clumps of fine grain clays or dry-freezed sediments. Both chemicals can be applied successively with a rinsing process in between.

In detail, tephra samples contaminated with organic rich sediments are treated with a 5-10% hydrogen peroxide solution. Depending on the grade of contamination the sample is treated for 0.5 – >5 hours before thoroughly rinsing and sieving the residual tephra material. An alternative method is the combustion of abundant organic matter in, for example, peat sequences at 600°C for 4 hours in a muffle furnace (e.g., Pilcher and Hall, 1992). Tephra samples contaminated by calcareous matter (i.e., calcite precipitates, lime shell organism) are diluted in 10% hydrochloric acid for up to 24 hours.

Liquid density separation

The extraction of glass shards in mineral rich sediments requires the processing of liquid density separation. This method modified after Pilcher and Hall (1992), Turney (1998) and Blockley et al. (2005) uses the density liquid sodium-polytungstate (SPT) to separate heavier minerals such as pyroxenes, amphiboles and Fe-Ti-Oxides from lighter components such as diatoms, feldspars, quartz and volcanic glass. SPT uses DI water for density calibration and is applied to smaller samples (0.5g – 1g) that are common in tephra studies. The liquid density separation is applied after the chemical pre-treatment and sieving of the tephra sample and comprises two successive steps of standardised processing (for details see Blockley et al., 2005). In a first separation process a 1.95 g/cm^3 SPT solution is used to separate residual organics from the tephra material. The second process commonly applies a 2.55 g/cm^3 SPT solution that is supposed to separate the lighter volcanic glass from the heavier components.

Scientific Technical Report STR14/01, Deutsches GeoForschungsZentrum GFZ. http://doi.org/10.2312/GFZ.b103-14010

However, experiences have shown that non-vesicular, dark glass shards can be concentrated in the heavy sample fraction due to the higher density of these shards (e.g., Icelandic basaltic tephras, rhyolitic Vedde Ash, 12.1 ka BP). In these cases, both density fractions have been checked for glass shards.

Magnetic separation

Samples rich in light minerals such as feldspars and quartz are difficult to separate from volcanic glass due to their similar densities. In these cases, samples > 0.5g can be further processed by a magnetic separator accounting the fact that feldspars and quartz are characterised by non-magnetic properties in comparison to most Fe-Ti-oxide bearing glass shards. However, this procedure requires a careful treatment in order to avoid sample loss or contamination. In a test, magnetic separation has been successfully applied to the extraction of glass shards of the phonolitic Laacher See tephra in quartz rich sediments. Here, a Frantz Isodynamic Separator was used with an amperage setting between 0.4 and 0.8 A, a tilt of 11° and a slope of 13°. This method has also been turned out to be useful for the separation of Icelandic basaltic glass shards from mineral rich marine sediments (A. Griggs, personal comment 2012).

Removal of biogenic silica

Sediment components made up of biogenic silica (i.e., diatoms, chrysophyte cysts) can be abundant in lake sediments and are not removed during the sieving and liquid density separation processes due to glass-like properties. Diatoms, for example, show light densities between 2.0 and 2.25 g/cm^3 (e.g., Hurd and Theyer, 1977; Blockley et al., 2005), are optical anisotropic and reveal relatively small grain sizes (20-40 µm) that are in the range of cryptotephra shards. If abundant in a sample, the identification and extraction of volcanic glass is often difficult. However, biogenic silica can be dissolved in a 0.3M NaOH solution when heated in a water bath at 80°C for 3 hours (e.g., Rose et al., 1996). Alternatively, a treatment with a 2M $NaCO_3$ solution in a water bath at 70°C can be applied; this methods is less destructive and requires a longer (>5 hour) sample processing (G. Schettler, personal communication, 2011).

Scientific Technical Report STR14/01, Deutsches GeoForschungsZentrum GFZ. http://doi.org/10.2312/GFZ.b103-14010

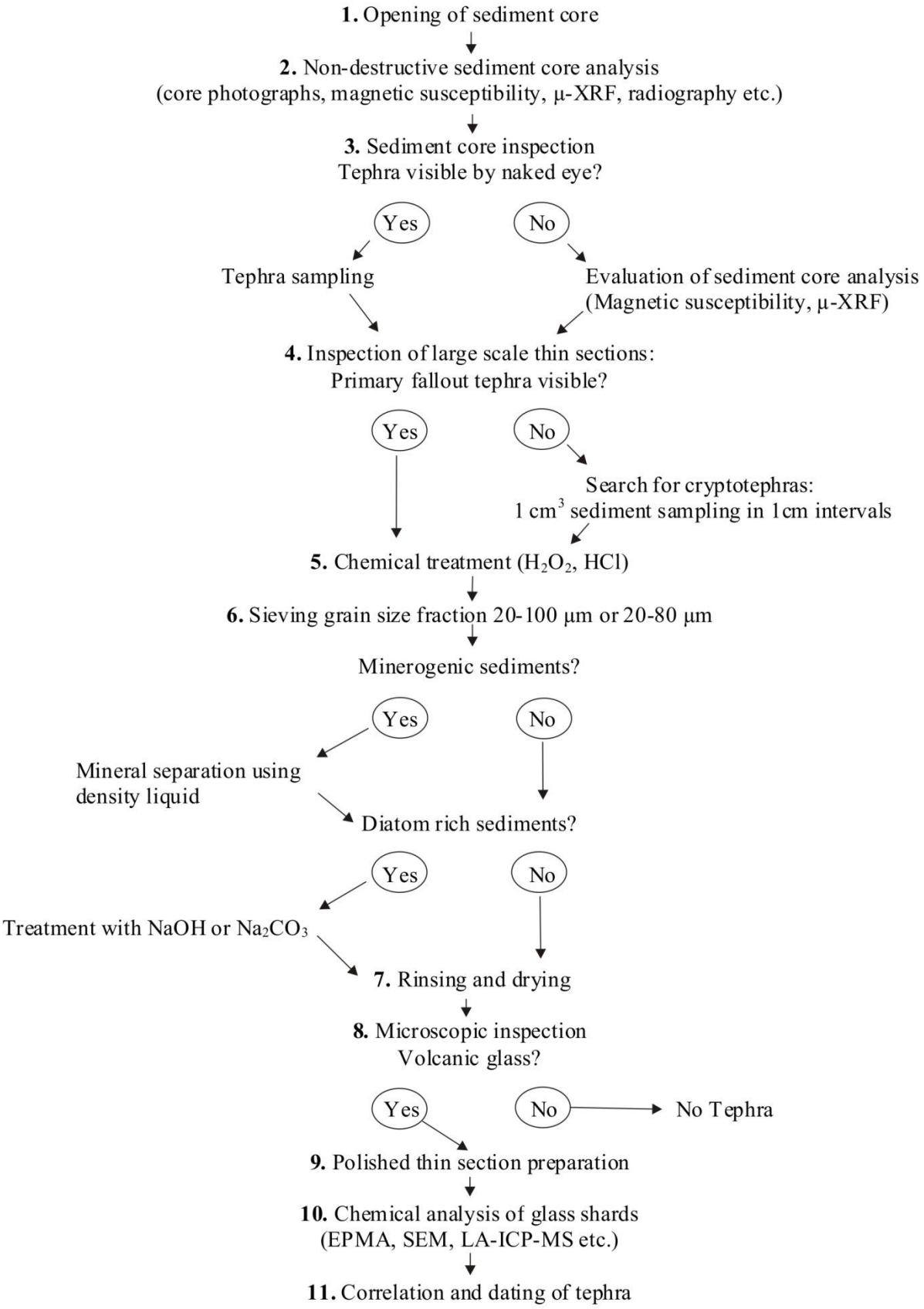

Figure 3: *Flow diagram showing the principles of tephra sample preparation and analysis in sedimentary cores.*

Scientific Technical Report STR14/01, Deutsches GeoForschungsZentrum GFZ. http://doi.org/10.2312/GFZ.b103-14010

Thin section preparation

The micro-analytical geochemical fingerprinting of tephra individual glass grains requires a smooth surface for measurements. Therefore, tephra grains need to be embedded in resin and mounted on a carrier, grinded to their surface which then will be fine polished. Depending on the amount of tephra material, different types of carriers can be used. Large amounts of volcanic glass samples commonly use the mounting on 2.8 x 4.8 cm frosted glass slides, on which the sample can be simply spread. Small quantity samples (less than 50 glass shards) are extracted under the microscope by handpicking using either a dry single-hair brush or a silica needle syringe (wet sample, C. Lane, personal comment 2010) and transferred to frosted glass slides or 1-Zoll epoxy stubs. Glass shards are concentrated in a marked area on the centre of the sample holder, carefully covered by resin and dried over several hours before the grinding and final polishing procedure (A. Bourne, personal comment 2012).

A different method has been applied to tephras that were detected on large scale thin section during microfacies analyses (Wulf et al., 2004). Here, the glass extraction procedure could be completely avoided by simply producing new 2.8 x 4.8 cm thin sections from the sediment blocks used for large-scale thin section preparation. This method has the advantage of systematically analysing different levels of the tephra deposit (i.e., top and basal parts) and it was successfully applied for the < 100 ka distal tephras of the Lago Grande di Monticchio record (e.g., Wulf et al., 2004; Wulf et al., 2008).

2.1.3 Tephra characterisation

Geochemical fingerprinting

The chemical composition of a tephra can be used to define its volcanic source and, if distinctive enough, its eruptive event. Methods applied mainly on proximal tephra deposits are X-ray fluorescence spectrometry (XRF), instrumental neutron activation analyses (INAA), and inductively coupled plasma mass spectrometry (ICP-MS) (e.g., Borchardt et al., 1971; Poli et al., 1987; Civetta et al., 1997; Landmann et al., 2011). Those methods have their limitations, because large tephra samples are required that are susceptible to contamination effects and that are often not present in distal volcanic archives. Therefore, methods such as electron probe microanalyses (EPMA) and laser ablation (LA) ICP-MS techniques are applied now to the analysis of individual volcanic glass shards for identification of distal tephras on the basis of their major- and respective trace-element composition (e.g., Smith and Westgate, 1969; Pearce et al., 1999). If sufficiently large chemical data-sets can be generated from

Scientific Technical Report STR14/01, Deutsches GeoForschungsZentrum GFZ. http://doi.org/10.2312/GFZ.b103-14010

various sites, then the chemical signatures obtained from several distal tephras can be assessed for matching chemical signatures. However, the frequent lack of individual micro-analytical glass data of proximal tephra deposits makes it often difficult to assign distal ash layers to specific volcanic events (e.g., Wulf et al., 2012).

The determination of the major and minor element composition of individual glass shards of a tephra preferable uses a high-precision electron probe micro-analyser with wavelength dispersive spectrometer (EPMA-WDS) or in some cases semi-quantitative SEM energy dispersive X-ray microanalysis (EDX) that may produce high-quality data if cross-checked with EMPA and adequate glass reference samples (e.g., Sulpizio et al., 2010b; Wutke, 2012). In general, data obtained by EPMA-WDS is comparable throughout different instruments and laboratories if using similar analytical set-up conditions (e.g., Hunt and Hill, 1993; Hunt and Hill, 1996). A common set-up in volcanic glass analysis is the use of a 15 kV voltage, a varying beam current between 5 to 20 nA and beam sizes between 5 and 20 µm depending on the size and vesicularity of glass shards. However, in order to reliable correlate tephras among different archives an interlaboratory comparison is necessary. An important step in undertaking such a comparison is the use of a geochemical homogenous secondary standard in order to check the quality of EPMA conditions prior to sample measurements (Froggatt, 1992). Glass standards applied for tephra studies are mainly rhyolitic in composition and include the KN-18 comendite obsidian from Kenia (Nielsen and Sigurdsson, 1981), the MPI-DING glasses (i.e., Atho-G and StHs6/80-G; Jochum et al., 2005), the Beloc meteoric glass standard (Jéhanno et al., 1992), the Vedde ash standard (Bard et al., 1994) and the Cannetto Lami obsidian from Lipari (Aeolian Islands, Italy) (Hunt and Hill, 1993). Detailed studies of the Lipari obsidian (Hunt and Hill, 1993; Hunt and Hill, 1996; Hunt and Hill, 2001; Brauer et al., 2007c) demonstrated the strong relationship between certain analytical setup conditions and the widely recognized loss of sodium and (to a lesser extent) potassium during EPMA measurements (e.g., Keller, 1981; Nielsen and Sigurdsson, 1981) (Fig. 4a, 4b). This loss in alkalis and the related increase in SiO_2 concentrations are strongly related to the intensity and diameter of the incident electron beam and exponentially related to the duration of exposure to the beam (e.g., Hunt and Hill, 2001; Brauer et al., 2007c). The largest effects, thus, are recognized with decreasing beam diameters; they are visible at beam sizes <15 µm and significant at beam diameters ≤ 10 µm (Fig. 4a).

The increase of beam intensities, in turn, seems to hardly influence the mobility of sodium when using beam diameters >10 µm (Fig. 4a), but may result in a strong decrease of fluorine concentration (Fig. 4b).

Scientific Technical Report STR14/01, Deutsches GeoForschungsZentrum GFZ. http://doi.org/10.2312/GFZ.b103-14010

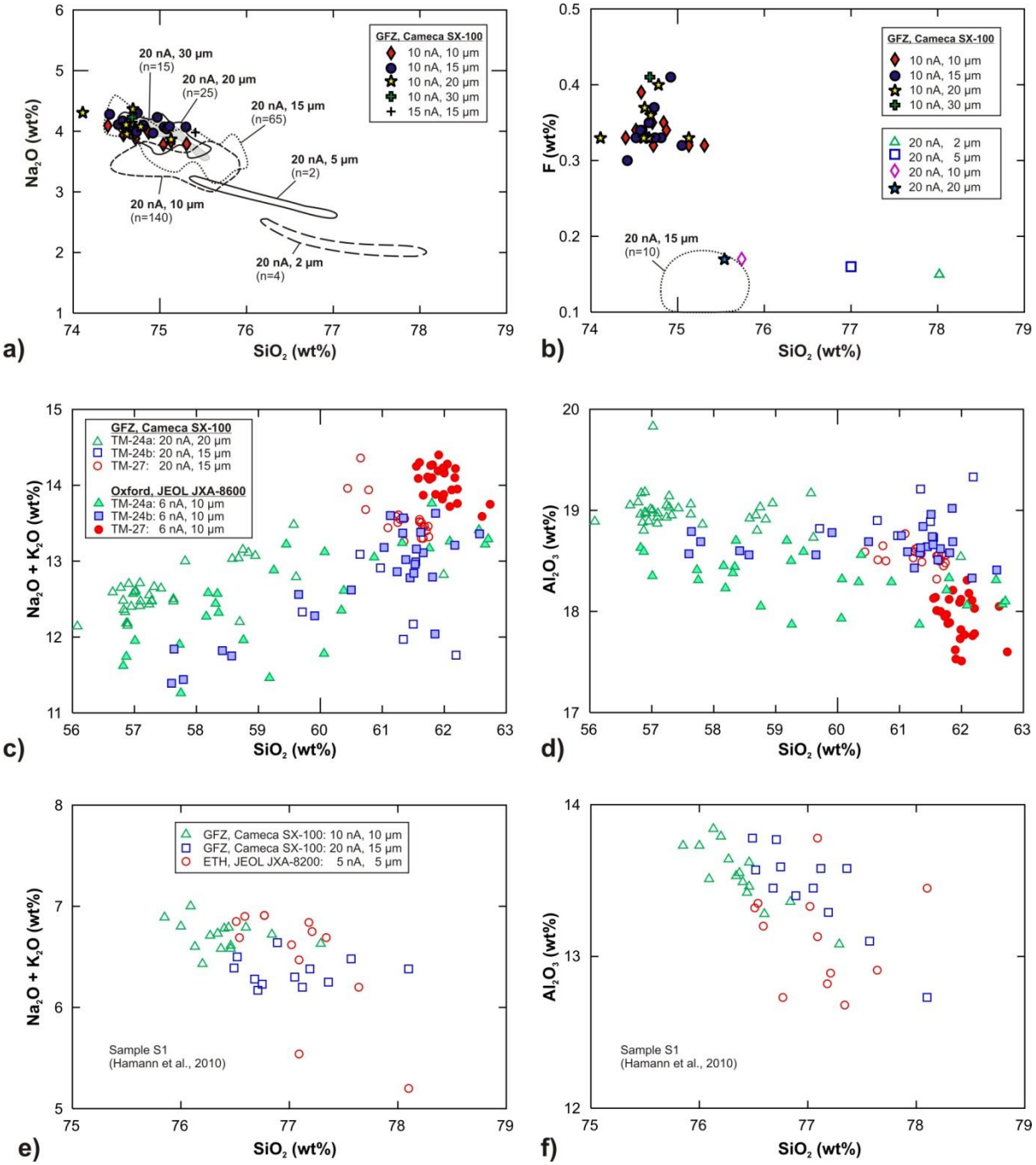

Figure 4: ***a) + b)*** *Results of the EPMA measurements of the Lipari obsidian reference standard using different analytical set-up conditions.* ***c) + d)*** *Comparison of major elemental glass data of three distal tephra layers - TM-24a, TM-24b and TM-27 - from the Lago Grande di Monticchio record analysed by EPMA at the GFZ Potsdam and the University of Oxford using a 15 kV voltage and varying beam currents and beam sizes (data from Wulf et al., 2012).* ***e) + f)*** *Comparison of major elemental glass data of the S1 tephra (8.8 ka BP) obtained by EPMA at the GFZ Potsdam (unpublished data) and ETH Zürich (Hamann et al., 2010) at a 15 kV voltage and different beam currents and beam sizes.*

The application of different analytical setups for a single tephra can provide different results as demonstrated by an interlaboratory comparison of distal tephras from the Monticchio

Scientific Technical Report STR14/01, Deutsches GeoForschungsZentrum GFZ. http://doi.org/10.2312/GFZ.b103-14010

record (Wulf et al., 2012) using a CAMECA SX-100 instrument at the GFZ German Research Centre for Geosciences in Potsdam and a JEOL JXA-8600 instrument at the University of Oxford, UK (Fig. 4c and 4d). Here, not only deviations in Na_2O and SiO_2 concentrations are visible, but also a systematic offset in Al_2O_3 concentrations occurs. Similar effects are observed for an EMPA comparison between the GFZ and ETH Zürich (Switzerland) laboratories (Fig. 4e and 4f). The examples presented express the strong need for the verification either by using comparable analytical setup conditions across different laboratories or by data cross-checking with identical international glass standards, which is only given for some labs, so far.

The determination of the major and minor element glass composition is in most cases sufficient for the correlation of tephras with their volcanic sources. However, the attribution to specific volcanic events sometimes requires further geochemical discrimination that can be obtained by LA-ICP-MS trace elemental data of single glass shards (e.g., Pearce et al., 1999; Pearce et al., 2007; Pearce et al., 2011). The results of tephra studies of the Lago Grande di Monticchio record, for example, have shown that most tephras originate from Campanian volcanoes (n>250) and that the chemical signatures of those tephras, mainly phonolitic to trachytic in composition, are difficult to discriminate from each other only on the basis of their major-element glass composition. Due to the relatively close position of Monticchio lake to the source volcanoes, some of the Campanian tephras have been identified using additional discriminatory tools such as the presence of certain diagnostic phenocrysts and lithic clasts, the observation of the structure, grain size distribution and precise stratigraphic position of each tephra layer. In hyper-distal archives, however, that additional information is limited, and tephra correlation mostly relies on comparison of glass chemistry. Accordingly, pilot projects in close cooperation with members of the RESET consortium have been conducted to test the potential for precisely linking Monticchio tephras with proximal and distal tephras from other sites in southern Europe. Using trace-element glass data obtained by LA-ICP-MS techniques, Tomlinson et al. (2012) and Wulf et al. (2012) have confirmed and/or re-allocated the provenance of several of the major visible Campanian tephras at Monticchio originally determined by Wulf et al. (2004), whilst experiments conducted by Smith et al. (2011) indicate the necessity to revise the provenance attributions of some of the Holocene Campanian tephras within the Monticchio sequence. These proof-of-concept results have demonstrated the viability of this new technique at least for the analysis of Monticchio tephras as well as the urgent need to use this approach to test the provenance allocations based on EMPA major-element composition in general.

Scientific Technical Report STR14/01, Deutsches GeoForschungsZentrum GFZ. http://doi.org/10.2312/GFZ.b103-14010

Glass shard morphology

In addition to the geochemical fingerprinting the analysis of the morphological features of volcanic ash components can be of great value for the correlation of tephras (for more details see Lowe, 2011). The classical particle shape analysis involves simple measurements of the circularity, compactness, elongation and rectangularity that allow a good discrimination between juvenile clasts related to different eruption processes, such as magmatic and phreatomagmatic eruption styles (e.g., Dellino and La Volpe, 1996; Eiriksson et al., 1996). A new approach, the fractal geometry analysis, is another popular technique with the potential to quantify fragmentation and transport mechanisms of pyroclastic particles (e.g., Maria and Carey, 2007), which has been successfully applied for the supportive correlation of the Holocene marine S1 tephra with a specific Anatolian volcanic event (Hamann et al., 2010).

2.1.4 Tephra correlation and databases

The allocation of tephras to a provenance and a certain volcanic event requires the availability of an adequate geochemical-petrological data set (preferable EPMA glass data) of tephra equivalents from proximal and distal sites. For European tephras, those data sets are mostly accessible for single widespread and well-studied marker layers such as the Late Glacial Laacher See tephra (van den Bogaard and Schmincke, 1985; Schmincke et al., 1999; Riede et al., 2011; http://www.tephrabase.org/), the 3.6 ka Minoan ash from Santorini (e.g., Druitt et al., 1999), the 12.1 ka Vedde Ash from Iceland (e.g., Lane et al., 2012a) or the Campanian Ignimbrite (Phlegrean Fields, Italy, 39.3 ka BP; Civetta et al., 1997; De Vivo et al., 2001; Giaccio et al., 2008). For the North Atlantic volcanic region (e.g., Iceland, Jan Mayen) a comprehensive geochemical EPMA data set of tephras is available for the last ca. 300 ka BP (e.g., Haflidason et al., 2000; Wastegard and Rasmussen, 2001; Wallrabe-Adams and Lackschewitz, 2003; Wastegard et al., 2006; Brendryen et al., 2010; Larsen et al., 1999; Zillén et al., 2002; Kristjánsdóttir et al., 2007; Wastegard and Davies, 2009; see also http://www.tephrabase.org/). In the eastern Mediterranean, numerous visible and non-visible tephras in distal terrestrial and marine sediment records have been EPMA fingerprinted for the time interval of the last 200 ka BP so far (e.g., Federman and Carey, 1980; Narcisi and Vezzoli, 1999; Wulf et al., 2004; Wulf et al., 2008; Bourne et al., 2010; Wulf et al., 2012), but respective EPMA glass data of proximal deposits for detailed comparison are only provided for the last ca. 40 ka BP (e.g., Turney et al., 2008; Smith et al., 2011; Zanchetta et al., 2011). This in particular applies for tephras from the Italian peninsula and is well demonstrated by

Scientific Technical Report STR14/01, Deutsches GeoForschungsZentrum GFZ. http://doi.org/10.2312/GFZ.b103-14010

the results of tephra studies of the Lago Grande di Monticchio sediment sequence (Wulf et al., 2012). Here, so far only 28 out of 345 tephra layers (18 layers < 40 ka BP) could be reliable correlated with known and well dated eruptive events due to the lack of comparable single grain data of proximal deposits (Wulf et al., 2012). In this regard, a major contribution will be made by the upcoming EPMA database of the "RHOXTOR research network" (RESET program, http://c14.arch.ox.ac.uk/rhoxtor/embed.php?File=).

The correlation of tephras based on glass chemical composition uses simple bi-plots of major, minor or trace elements (see Fig. 4) that can be generated by the programs like Excel or IGPET (Carr, 2012). Statistical techniques to aid correlation may involve similarity coefficients (Borchardt et al., 1971) that have been successfully applied for the comparison of mainly distal Campanian and Etnean tephras (e.g., Wulf et al., 2008), or coefficients of variation that are useful for the identification and quantification of the abundances of dispersed ash of multiple volcanic sources in marine sediments (see details in Lowe, 2011). Again, those statistical methods are only meaningful, if the glass composition of distal and proximal tephra deposits were obtained by comparable analytical conditions of EPMA instruments.

2.1.5 Dating of tephra

Beside the geochemically-based correlation, the stratigraphical position and the dating of an assigned tephra event need to be carefully evaluated. The age of a tephra can be established by radiocarbon dating of associated organic material or for older deposits by K/Ar, laser $^{40}Ar/^{39}Ar$, fission track, TL or ESR dating of primary mineral constituents. Those dates, however, can exhibit large statistical errors due to contamination effects, such as the presence of volcanic CO_2 distorting radiocarbon results (e.g., Deeming et al., 2010), or the limiting size of minerals and/or the inclusion of secondary xenocrystals in K/Ar and $^{40}Ar/^{39}Ar$ dating (e.g., Villa, 1991). A better resolved age estimates is achievable if the tephras are associated with annually-laminated archives, as for example in polar ice cores, lake sediments or deep marine deposits (e.g., Grönvold et al., 1995; Brauer et al., 1999a; Wulf et al., 2004; Bahk et al., 2000).

Potential problems associated with the tephra radiocarbon dating are well demonstrated by the Avellino Tephra of Vesuvius (ca. 4 ka BP). Here, numerous ^{14}C dates of proximal and distal deposits, obtained during the past four decades by different analytical techniques (conventional and AMS radiocarbon dating), provide a wide age range of 1300

Scientific Technical Report STR14/01, Deutsches GeoForschungsZentrum GFZ. http://doi.org/10.2312/GFZ.b103-14010

years of tephra deposition. Some of those dates require a re-evaluation due to the improvement of ^{14}C age precision by the recent development of the analytical precision, and a reliable ^{14}C tephra date can only be approved if dated independently by other dating methods. The precise dating of the Laacher See tephra, as an another example, took more than five decades and used three different dating techniques (^{14}C, $^{39}Ar/^{40}Ar$ and varve counting) that provided a concordant timing of the eruptive event of 12.88 ka BP (van den Bogaard, 1995; Brauer et al., 1999a; Baales et al., 2002).

Eastern Mediterranean K-rich tephras that are older than the ^{14}C dating range (>40 ka BP; Lowe and Walker, 1997) are commonly directly dated by $^{39}Ar/^{40}Ar$ and K/Ar (whole rock, K-feldspar, K-rich volcanic glass), whereby the $^{39}Ar/^{40}Ar$ dates on individual sanidine phenocrysts have been proven to provide the most reliable dates (e.g., De Vivo et al., 2001; Giaccio et al., 2012). However, since the dating of finer grains (< 200 µm) is quite complex (e.g., Kraml, 1997), most timings of distal tephras are derived from age interpolation of sapropel and/or oxygen isotope chronologies (e.g., Keller et al., 1978; Paterne et al., 1986, 1988, 2008). This dating method in particular applies to the timing of older Icelandic tephras that lack in K-rich components (e.g., Wastegard and Rasmussen, 2001; Brendryen et al., 2010).

If well established, high-resolution varve chronologies from sites close to active explosive volcanoes such as the Eifel maar lakes in Western Germany (e.g., Zolitschka et al., 1995; Brauer et al., 1999a) or Lago Grande di Monticchio in southern Italy are another extremely valuable tool for independently dating younger and older tephras (e.g., Narcisi, 1996; Wulf et al., 2004; Wulf et al., 2012).

Scientific Technical Report STR14/01, Deutsches GeoForschungsZentrum GFZ. http://doi.org/10.2312/GFZ.b103-14010

2.2 Application of tephra studies

Tephra layers from different sediment archives that have been successfully correlated with reliable dated volcanic events can be used as valuable dating and synchronisation tools in order to answer a series of scientific questions in geology, volcanology, geomorphology, pedology, glaciology, palaeoecology, palaeoclimatology, palaeolimnology and archaeology. The application of tephrochronology in regional palaeoenvironmental studies includes, for example, the dating of the hydrological variability of lakes (e.g., Haberzettl et al., 2007, 2008) or the reconstruction of storm frequencies and magnitudes (e.g., Page et al., 2010 in Lowe, 2011). In southern Europe, tephra studies encompass a wider field of application in the dating and synchronisation of both terrestrial and marine sequences. The majority of palaeoenvironmental records in the Eastern Mediterranean are composed of homogeneous (non-varved) sediments recovered from holomictic lakes or marine environments that are often difficult to date. Many longer chronologies are established by orbital tuning based on biostratigraphies and oxygen isotope curves (e.g., Paterne et al., 2008; Belmecheri et al., 2010; Müller et al., 2011), while radiocarbon dating of shorter sequences (<40 ka BP) can reveal inherent sources of errors such as the contamination of samples with "old" (hard water effect; e.g., Oldfield et al., 1997) or "dead" carbon (mixing with older volcanic CO_2; e.g., Hajdas et al., 1998). This latter problem can be avoided by ^{14}C dating exclusively terrestrial macrofossils, which are, however, rare in the oceans and in the central and deepest parts of lakes. In this respect, the finding of tephra layers is extremely helpful to ***support and /or establish independent chronologies*** for both the dating of sediments and the evaluation of radiocarbon-based age models. Examples for this nature of tephra application are in particular given from the marine and terrestrial environment in the eastern part of the Mediterranean Sea. The finding of the so called Y-2 tephra (Santorini, *ca.* 22 ka BP) in marine sediment cores from the Sea of Marmara – a sea enclosed between the normal marine Aegean Sea in the south and the brackish Black Sea in the northeast (Fig. 5) – was used, for instance, to establish a reliable time and correlation marker in the north-eastern part of the Mediterranean Sea by importing the weighted mean of radiocarbon age obtained on the firmly correlated terrestrial counterpart into the rather "weak" age model of the sediment sequences (Wulf et al., 2002). Furthermore, this tephra study enabled the detailed correlation of single cores from the Sea of Marmara, which in turn was applied for the ***reconstruction of the Late Glacial-Holocene sea level*** in this region. The very same Y-2 tephra in addition to the younger Z-2 Ash from Santorini (*ca.* 3.6 ka BP) was used to ***estimate sea surface radiocarbon reservoir ages*** in

Scientific Technical Report STR14/01, Deutsches GeoForschungsZentrum GFZ. http://doi.org/10.2312/GFZ.b103-14010

sediments of the nearby Black Sea (Kwiecien et al., 2008) (Fig. 5). Here, the radiocarbon ages of terrestrial tephra equivalents were compared with ^{14}C ages of marine ostracod and gastropod shells indicating an offset of *ca.* 1450 ^{14}C years during the Last Glacial, a gradual reduction of the reservoir age to *ca.* 1000 ^{14}C years in the Bølling-Allerød warm period and to *ca.* 400 ^{14}C years in recent times. The knowledge of radiocarbon reservoir ages are crucial not only for the interpretation of radiocarbon chronologies of marine sediment sequences but also for the understanding of biological-chemical-physical processes on land and in the Ocean basin that can lead to a more detailed ***interpretation of abrupt climate changes in the past*** (Kwiecien et al., 2008).

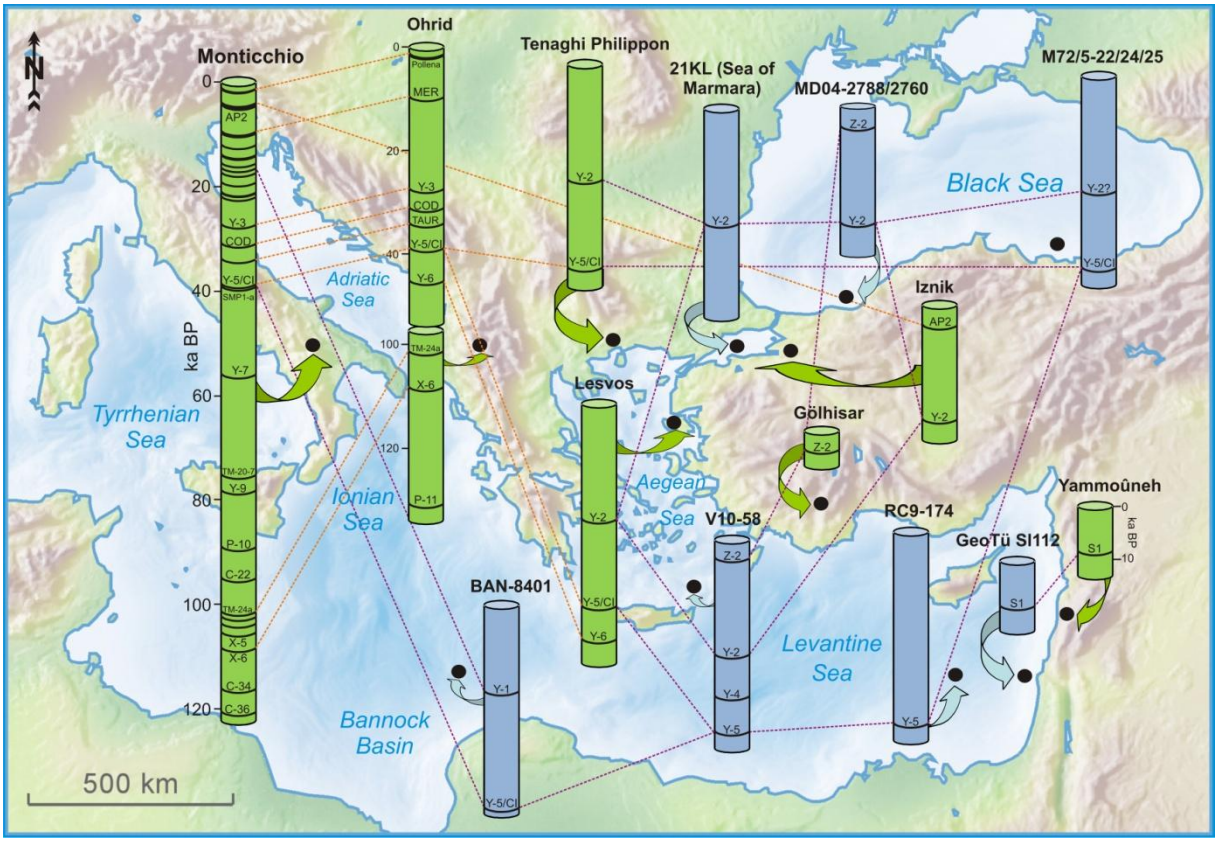

Figure 5: *Tephrostratigraphical linking of the Lago Grande di Monticchio record with selected terrestrial and marine palaeoclimate sequences in the Eastern Mediterranean.* <u>*References:*</u> *Lago Grande di Monticchio, Italy (Wulf et al., 2004; Wulf et al., 2008; Wulf et al., 2012); Lake Ohrid, Macedonia/Albania (Sulpizio et al., 2010b); Tenaghi Philippon, Greece (Müller et al., 2011); Megali Limni, Lesvos Island, Greece (Margari et al., 2007); 21KL, Sea of Marmara (Wulf et al., 2002); MD04-2788/2760, SW' Black Sea (Kwiecien et al., 2008); M72/5-22/24/25, SE' Black Sea (Kind, 2008; Nowaczyk et al., 2012); Lake Iznik, Turkey (Roeser et al., 2012); Lake Gölhisar, Turkey (Eastwood et al., 1999); Lake Yammoûneh (Develle et al., 2009); GeoTü SL112, Levantine Sea (Hamann et al., 2010); RC9-174, Levantine Sea (Keller et al., 1978); V10-58, Aegean Sea (Keller et al., 1978); BAN-8401, Bannock Basin (Vezzoli, 1991).*

Scientific Technical Report STR14/01, Deutsches GeoForschungsZentrum GFZ. http://doi.org/10.2312/GFZ.b103-14010

Vice versa, a finding of a thitherto unknown distal Early Holocene tephra layer (S1-tephra) in a south-eastern Levantine Sea core (Fig. 5) could be precisely dated by radiocarbon dating of planktonic foraminifera (Hamann et al., 2010) by using a reservoir age of *ca.* 400 ^{14}C years which, in turn, resulted from tephrochronological constraints of Adriatic Sea cores (Central Mediterranean; Siani et al., 2001; Siani et al., 2004). The detailed source allocation in Anatolia and the dating of the S1-tephra is in strong agreement with a distal tephra finding on land (Develle et al., 2009) (Fig. 5) and therefore provides both a ***new time constrain for the proximal tephrostratigraphical record*** and a reliable Holocene synchronisation marker for the very eastern part of the Mediterranean Sea ***linking the marine record with terrestrial profiles*** from the Near East (Develle et al., 2009).

Another example from the Black Sea sediments demonstrates the use of the enormous widespread Campanian Ignimbrite (CI), in combination with 16 independent radiocarbon ages and tuning to the NGRIP time scale to precisely ***date the spatial dynamics of the geomagnetic field*** during the Laschamp excursion (*ca.* 41 ka BP). This chronology, on the one hand, places the virtual geomagnetic pole data (VGPs) obtained from several individual lava flows from the Massif Central (France) into a chronological order which has not been achieved unambiguously before by radiometric dating (see Nowaczyk et al., 2012, and references therein). On the other hand, the finding of the CI together with the Laschamp excursion and Dansgaard-Oeschger climatic oscillation validates the ^{39}Ar/^{40}Ar age of CI proximal deposits (39.28 ± 0.11 ka BP ^{39}Ar/^{40}Ar, De Vivo et al., 2001, *versus* 39.4 ka BP in Black Sea sediments) and for the first time places the CI in a clear and direct stratigraphic context with those events. Accordingly, the CI eruption occurred between Greenland Interstadial 9 and 8 in the middle of the cooler Heinrich event H4, approximately 1600 years after the Laschamp event (Fig. 6). This information will facilitate the finding of the CI as a cryptotephra in high-latitude, northern-hemispheric climate archives (i.e., North Atlantic sediment cores, Greenland ice core records), which is essential for the over-regional linking of palaeoclimate signals. A similar chronostratigraphic validation of the CI is provided by the Tenaghi Philippon peat sequence in Greece (Müller et al., 2011) (Fig. 6). Here, the CI and Y-2 tephras in combination with a high-resolution AMS radiocarbon chronology dated the high-resolution pollen record, which, in turn, was used to study the ***effects of abrupt climate changes and major volcanic eruptions on human evolution*** during the last Glacial period. The site of Tenaghi Philippon in the Eastern Mediterranean is of particular interest because this area served as a gateway in the process of immigration of Anatomically Modern Humans

Scientific Technical Report STR14/01, Deutsches GeoForschungsZentrum GFZ. http://doi.org/10.2312/GFZ.b103-14010

(AMHs) from Africa into Europe ca. 60 to 48 ka ago. The results of the Tenaghi Philippon pollen record strongly contradict the hypothesis that the combined effects of natural hazards – like the CI volcanic eruption (Golovanova et al., 2010) or the Laschamp-Mono Lake geomagnetic events (Valet and Valladas, 2010) – and the severe climatic cooling during Heinrich Event H4 (*ca.* 40 ka BP) triggered the extinction of the Neanderthals in Europe. Müller et al. (2011) and Lowe et al. (2012) rather suggest that the earlier successive spread of AMHs during a period of extreme and rapid climate changes (i.e., Heinrich Event H5 climatic deterioration to warmer Greenland Interstadial 12, 48-47 ka BP) led to a competitive exclusion of the Neanderthals.

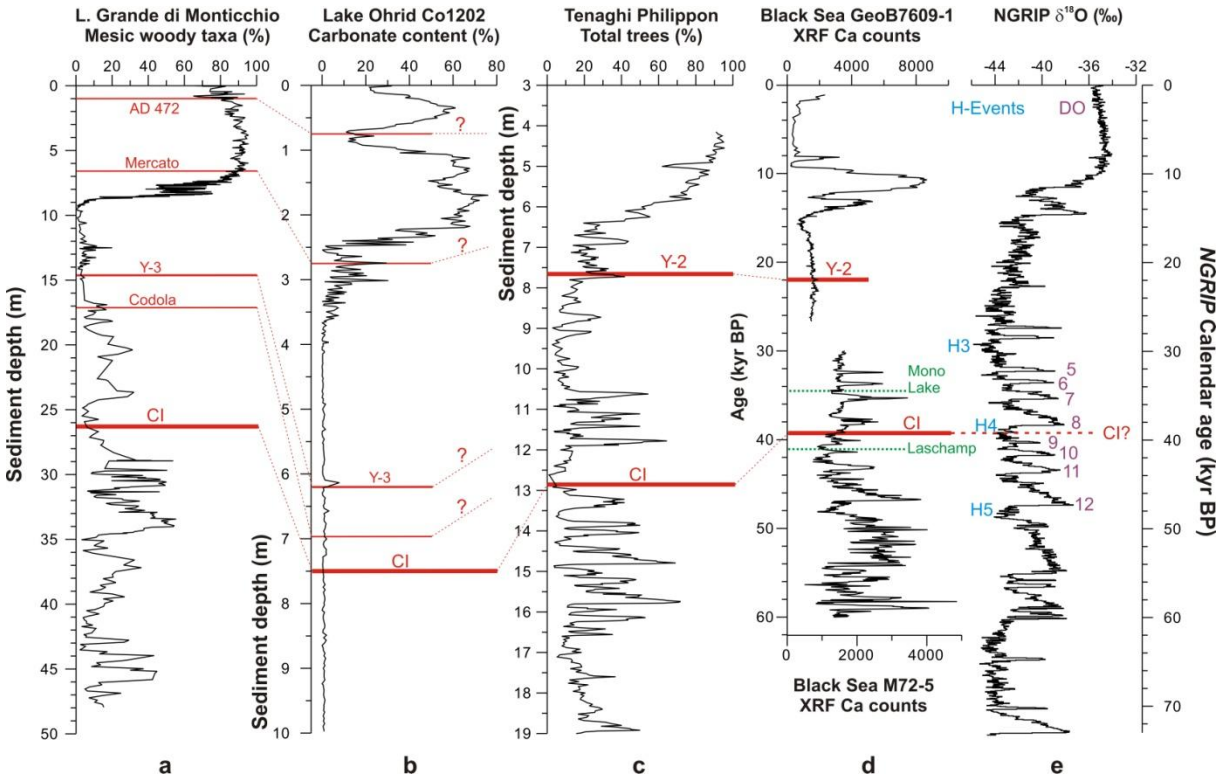

Figure 6: *Chronostratigraphical position of major tephras (red bars) and tephrostratigraphic linking of selected terrestrial (a-c) and marine (d) palaeoclimate records in the Eastern Mediterranean as well as proposed position of the Campanian Ignimbrite (CI) in NGRIP Greenland ice core (e). Data from a) Brauer et al. (2007a), Wulf et al. (2004); b) Vogel et al. (2010), Sulpizio et al. (2010b); c) Müller et al. (2011); d) Kwiecien et al. (2009), Nowaczyk et al. (2012); e) North Greenland Ice Core Project Members (2004).*

Moreover, the presentation of a clear chronostratigraphic position of the CI within and not as proposed by Fedele et al. (2008) at the onset of the Heinrich event H4 in the terrestrial pollen records of Tenaghi Philippon (Müller et al., 2011) and Lago Grande di Monticchio (Brauer et al., 2007a) and as well as in the high-resolution Black Sea sediments (Nowaczyk et al., 2012)

Scientific Technical Report STR14/01, Deutsches GeoForschungsZentrum GFZ. http://doi.org/10.2312/GFZ.b103-14010

(Fig. 6) rules out an interaction of the CI eruption (volcanic winter) with the atmospheric systems that may have triggered or accelerated the hemispheric climatic deterioration. Nevertheless, the CI eruption must have had a strong but short-termed impact on life and the environment near the volcanic source.

Italian marker tephras like the CI/Y-5 (39.3 ka) in Tenaghi Philippon (Müller et al., 2011), the AP2 tephra (Vesuvius, ca. 3.5 ka BP) in Lake Iznik in north-western Turkey (Roeser et al., 2012) and the Y-6 tephra (Pantelleria, ca. 45 ka BP) in Megali Limni/Lesvos Island, Greece (Margari et al., 2007), enable not only the correlation of marine and terrestrial records in the very eastern part of the Mediterranean but also the ***supra-regional linking*** with palaeoenvironmental records from the Balkans, the Italian peninsular and Central Mediterranean Sea cores (Fig. 5, Fig. 7). Here, the high-resolution tephrostratigraphic record of Lago Grande di Monticchio in southern Italy is in a particular key position for the synchronisation of widespread Italian tephra markers (e.g., Zolitschka et al., 2000; Wulf et al., 2008). So far, a total number of 32 out of 345 distal tephra layers in the Monticchio record can be used for linking Eastern Mediterranean records for the last *ca.* 110 ka BP (Fig. 5, Fig. 7).
The Monticchio tephra record not only synchronizes short and longer marine and terrestrial sequences that are located in a favourable wind position east of Monticchio and adjacent volcanic sources (i.e., southern Adriatic Sea cores, Lake Shokra, Lake Ohrid, Lake Prespa, Tenaghi Philippon, Lake Iznik), but also closely ties up circum-Central Mediterranean archives (Fig. 5, Fig. 7). Relatively thick, widespread tephra markers are the Y-1 tephra/Biancavilla Ignimbrite from Mount Etna (*ca.* 17.4 ka BP), the Campanian Y-3 and Y-5/CI tephras (*ca.* 30.7 and 39.3 ka BP), the Y-7/Monte Epomeo Green Tuff from Ischia (*ca.* 56 ka BP) and the Campanian X-5 and X-6 doublet tephra layers (*ca.* 105.6 and 108.3 ka BP, respectively). Those tephras, originally defined by Keller et al. (1978) in Ionian Sea cores, provide the fundamental basis for the Central Mediterranean tephrostratigraphical framework. The recent finding of numerous Italian cryptotephras in the marine and terrestrial environment now enables a more detailed correlation of the Monticchio sequence with long (>100 ka BP) palaeoclimate records from the Central Adriatic Sea (Bourne et al., 2010), the Tyrrhenian Sea (e.g., Paterne et al., 1986, 1988, 2008) and the Balkans (e.g., Wagner et al., 2008; Sulpizio et al., 2010b) (Fig. 7). Further findings are expected in the more distal sites of Tenaghi Philippon (M. Hardiman, personal comment 2012), the Aegean Sea (C. Satow, personal comment 2012) and the Sea of Marmara (Wulf and Catagay, in progress).

Scientific Technical Report STR14/01, Deutsches GeoForschungsZentrum GFZ. http://doi.org/10.2312/GFZ.b103-14010

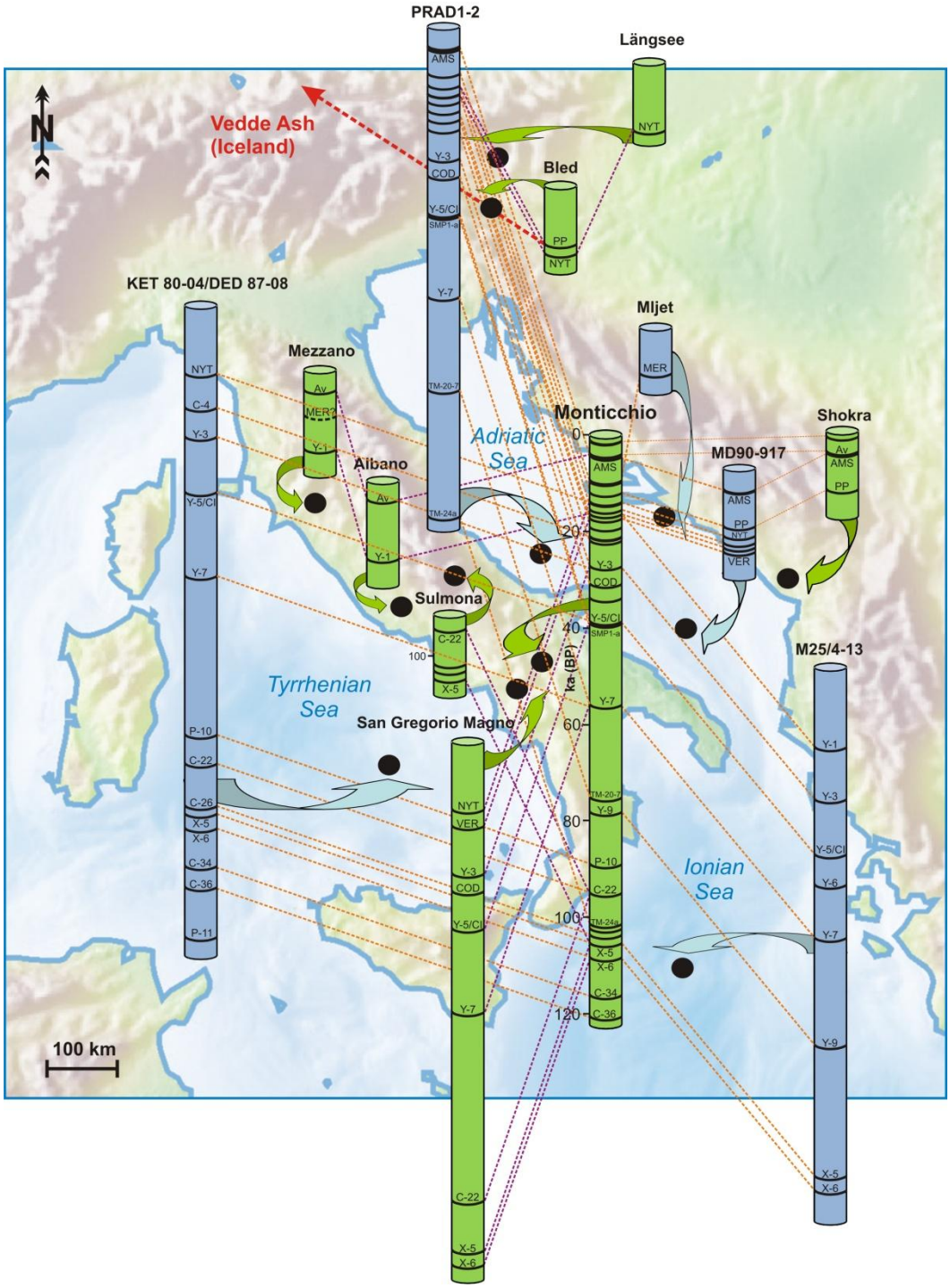

Figure 7: *Tephrostratigraphical synchronisation of terrestrial and marine sediment records in the Central Mediterranean. References: Lago Grande di Monticchio, southern Italy (Wulf et al., 2004; Wulf et al., 2008; Wulf et al., 2012); PRAD1-2, central Adriatic Sea (Bourne et al., 2010); MD90-917, southern Adriatic Sea (Siani et al., 2004); Lago di Mezzano, central Italy (Ramrath et al., 1999); Lago di Albano, central Italy (Calanchi et al., 1996); Sulmona Basin, Central Italy (Giaccio et al., 2012); San Gregorio Magno basin, southern Italy (Munno and Petrosini, 2007); KET 8004/DED 87-08, Tyrrhenian Sea (Paterne et al., 1986, 1988, 2008); M25/4-13, Ionian Sea (Keller et al., 1996; Kraml, 1997); Mljet, Croatia (Jahns and van den Bogaard, 1998); Längsee, Austria (Schmidt et al., 2002); Lake Bled, Slovenia (Lane et al., 2011a); Lake Shokra, Albania/Montenegro (Sulpizio et al., 2010a).*

Scientific Technical Report STR14/01, Deutsches GeoForschungsZentrum GFZ. http://doi.org/10.2312/GFZ.b103-14010

A large breakthrough in terms of a ***transalpine tephra synchronisation*** was made by the findings of Late Glacial Italian marker tephras, the Pomici Principali tephra (PP, 12.1 ka BP) and the Neapolitan Yellow Tuff (NYT, 13.6 ka BP) in combination with the Icelandic Vedde Ash in Lake Bled, Slovenia (Lane et al., 2011a) (Fig. 7). The Younger Dryas "Vedde Ash" (VA, 12,121 ± 114 years BP GICC05, Rasmussen et al., 2006) has so far been used as an important stratigraphic marker for the dating and linking of the terrestrial records in Central and Northern Europe (e.g., Mangerud et al., 1984; Birks et al., 1996; Wastegard et al., 1998; Wastegard et al., 2000a; Wastegard et al., 2000b; Davies et al., 2001; Blockley et al., 2007; Koren et al., 2008; Lane et al., 2012a, 2012b) with marine sequences from the Norwegian and North Atlantic Seas (e.g., Ingólfsson et al., 1997; Knudsen and Eiríksson, 2002; Austin et al., 2011) and Greenland ice cores (e.g., Grönvold et al., 1995; Mortensen et al., 2005; Lane et al., 2011b). In several terrestrial archives in Central Europe, the Vedde Ash co-exists with the Late Allerød "Laacher See tephra" (LST, 12,880 calendar years BP), allowing ***"differential dating"*** of the temporal section of the Late Glacial to Interglacial transition (e.g., Blockley et al., 2007; Lane et al., 2012b). Each tephra has been exceptionally well dated and therefore forms an essential anchoring point in annually laminated sediments for the ***determination of ages and durations of stadials and interstadials*** such as the transition of the warmer Allerød period to the cooler/drier Younger Dryas (e.g., Rasmussen et al., 2006; Brauer et al., 1999b; Lane et al., 2011b; Neugebauer et al., 2012). In order to estimate the environmental impact of current global warming, this information is essential to understand the process of climate change, for example the order and duration of responses of changes in atmospheric carbon dioxide concentration, air and deep-water temperatures, ice volumes (Shackleton, 2000), aquatic biological systems and vegetation on land. For the Late Glacial period, the existence of such "***leads and lags***" is indicated by the significant difference of the dating of the Younger Dryas onset in varved sediments in Lake Meerfelder Maar (12,679 calendar years BP; Brauer et al., 1999b; Brauer et al., 2008) and Rehwiese palaeolake (12,675 calendar years BP; Neugebauer et al., 2012) in W' and NE' Germany, respectively, and in the NGRIP Greenland ice core (12,846 ± 138 calendar years BP; GICC05; Rasmussen et al., 2006). This time lag of ca. 170 years in the terrestrial records might not be explained by dating errors of the independent chronologies alone, but may rather suggests a longer response of lake systems in respect to atmospheric changes in the North Atlantic region. However, in order to test this hypothesis of hemispheric climatic non-synchronicity further independently dated, high-temporal (preferable varved) and tephra bearing sequences for this time interval are required from Europe (i.e. NE' Germany and Poland).

Scientific Technical Report STR14/01, Deutsches GeoForschungsZentrum GFZ. http://doi.org/10.2312/GFZ.b103-14010

Further challenges of palaeoclimate research are the study and interpretation of past climate transitions that approximate today's climate conditions, i.e. the transition from the last Interglacial (Eemian, MIS 5.5) into the cooler Early Glacial period (Early Weichselian, MIS 5.4). In the Eastern Mediterranean, this transitional period is marked by the eruption of two widespread Italian tephras, the X-5 and X-6 tephras (Keller et al., 1978), both precisely dated by $^{39}Ar/^{40}Ar$ and/or varve counting at 105.6 ka BP (X-5) and 108.3 ka BP (X-6) (Kraml, 1997; Giaccio et al., 2012; Wulf et al., 2012) (Fig. 8).

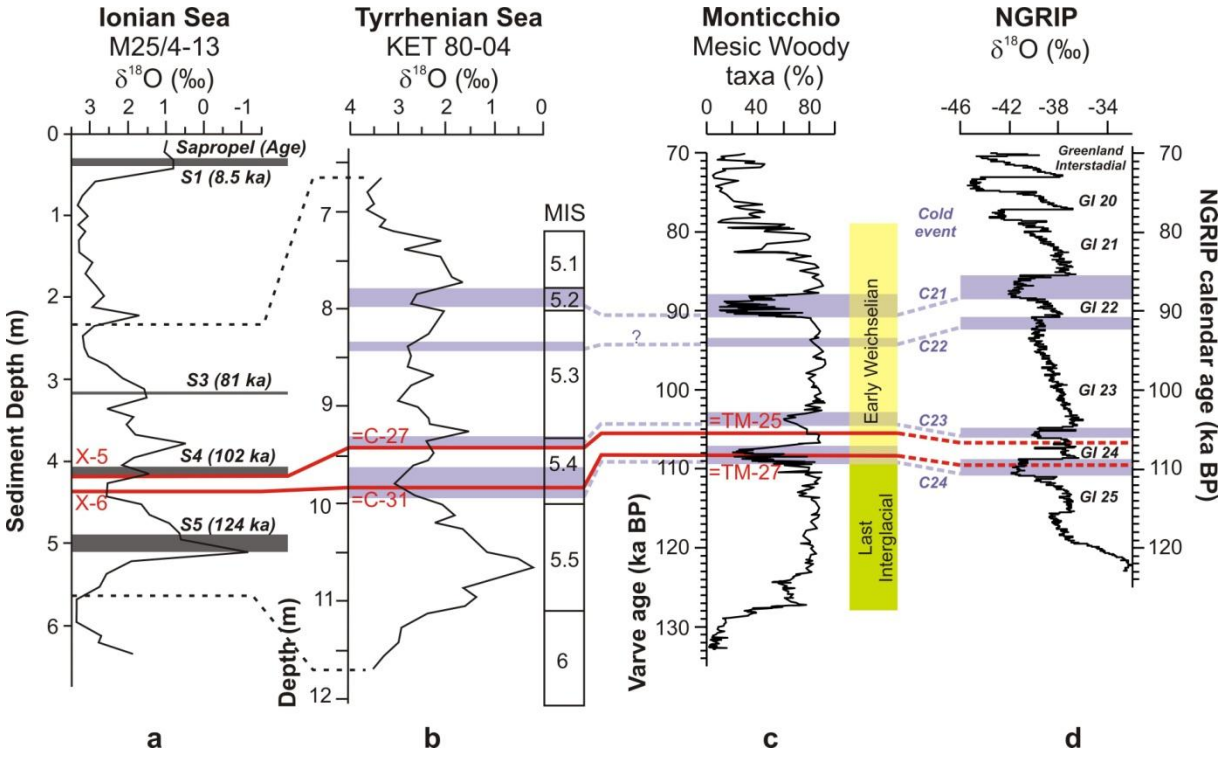

Figure 8: *Chronostratigraphic position of the X-5 (=C-27=TM-25) and X-6 (=C-31=TM-27) tephra layers in sediments of the (**a**) Ionian Sea (Kraml, 1997), (**b**) the Tyrrhenian Sea (Paterne et al., 2008),(**c**) Lago Grande di Monticchio (Brauer et al., 2007a; Wulf et al., 2012), correlated with (**d**) the $\delta^{18}O$ record of the NGRIP Greenland ice core record (North Greenland Ice Core Project Members, 2004), modified after Giaccio et al. (2012). Note that the Monticchio and Greenland records are plotted against their own independent time scales, while the Central Mediterranean marine records are plotted against core depths.*

Similar to the Late Glacial tephra pairs "LST/Vedde" in Central-Northern Europe, the X-5/X-6 couplet has the potential as a dating and synchronisation tool for determining "leads and lags" of rapid climate and environmental changes in the Eastern Mediterranean at this important climatic boundary (e.g., Brauer et al., 2007a; Giaccio et al., 2012). The Monticchio

Scientific Technical Report STR14/01, Deutsches GeoForschungsZentrum GFZ. http://doi.org/10.2312/GFZ.b103-14010

record is so far the only terrestrial sequence in the Mediterranean that provides both a high-resolution palaeoclimate record of the Last Interglacial/Early Glacial transition and a clear stratigraphic position (Fig. 8) and independent varve dating of the X-5 and X-6 tephras (Wulf et al., 2012). The Monticchio ages and stratigraphic positions of the X-5 and X-6 tephras are consistent with the chronostratigraphic position of tephras within MIS 5.4 in adjacent Ionian and Tyrrhenian Sea sediments (Fig. 8). Furthermore, wiggle-matching of $\delta^{18}O$ curves of the same (lower resolution) marine records with the NGRIP Greenland ice core places the tephras within the C-24 cold event (X-6) and Greenland Interstadial GI24 (X-5). A comparison of proposed tephra ages estimated from the Greenland Ice Core Chronology (North Greenland Ice Core Project Members, 2004) with varve ages inferred from the Monticchio chronology exhibits a deviation of *ca.* 1000 years (<1%) for each tephra, whereupon the ice core ages appear older (Fig. 8). These age differences can be either related to dating errors (up to 5% for both chronologies) and/or to lagged climatic responses in the Eastern Mediterranean.

In order to test any of these hypotheses further long and high-resolution palaeoclimate sequences from this region are required. From the terrestrial environment, Lake Ohrid in the Balkans (Fig. 5) has already proven a longer but incomplete record documenting at least the X-6 tephra (Sulpizio et al., 2010b). The Tenaghi Philippon peat bog in Greece (Fig. 5, Fig. 6) has the potential for both high-resolution palynological dating of the sequence and the finding of the X-5 and X-6 cryptotephras (U. Müller, personal comment 2012). A long lacustrine record in the Western Mediterranean, the Villarquemado palaeolake in NE Spain, also covers the Last Interglacial-Glacial transition dated independently by OSL (Moreno et al., 2012) but difficult to confirm by tephrochronology due to the lack of Italian and Greek tephras in the western part of the Mediterranean. The high-resolution marine record PRAD1-2 from the Adriatic Sea, located near the Monticchio site, covers the last 370 ka BP (Piva et al., 2008a, b) and has already proven its tephrochronological potential for the last 105 ka BP (Bourne et al., 2010). The extension of the PRAD1-2 tephra record (A. Bourne, personal comment 2012) will contribute to a better understanding of the temporal shifts of palaeoclimate signals during the Last Interglacial/Early Glacial period as inferred from the Monticchio record.

Apart from its role as a regional and supra-regional synchronisation tool, the Monticchio tephra record provides a number of further applications. Those encompass, for instance, the

- verification of the varve supported sedimentation rate chronology of sediments by establishing an independent tephrochronology (Wulf et al., 2004; Wulf et al., 2012),

Scientific Technical Report STR14/01, Deutsches GeoForschungsZentrum GFZ. http://doi.org/10.2312/GFZ.b103-14010

- the development of a detailed tephrostratigraphy of Campanian explosive eruptions for the last 133 ka including the discovery and varve dating of so far unknown tephra events (Wulf et al., 2006; Wulf et al., 2008),
- the establishment of a time series of tephra events to determine frequencies of e.g. Campanian volcanic activities and to check on the theory whether climate/sea level changes have impacted the explosivity of Mediterranean volcanoes as postulated by McGuire et al. (1997) (see Vos et al., 1999, Wulf et al., 1999),
- the provision of a large set of EPMA glass data serves as a data base for comparison with other terrestrial and marine records (see upcoming RESET data base) and
- the study of environmental impacts of major tephra events in the distal Monticchio location (Wutke, 2012).

Thus, the Monticchio tephra record has been proven an exceptional key record for the understanding of both palaeoclimatic and volcanological processes in the Mediterranean.

Scientific Technical Report STR14/01, Deutsches GeoForschungsZentrum GFZ. http://doi.org/10.2312/GFZ.b103-14010

3 Conclusions and perspectives

The use of tephras as reliable dating and correlation tools in sedimentary archives has turned out to be less problematic for the time frame of the last 200 ka BP, though in particular older tephra deposits often lack in single grain geochemical (glass) data and/or chronostratigraphical information. Some issues can also arise for tephra deposits that show initial stages of glass chemical alteration and thus prohibit a reliable correlation with proximal and distal equivalents. Those are mainly tephras deposited in a saline to hypersaline milieu (i.e., evapoclastic sediments of Mexican maar lakes; Kienel et al., 2009), or in terrestrial environments that are prone to weathering (alteration by humic acids) such as open-access soils, loess and palaeo-lake deposits (e.g., Pouclet et al., 1999; Brauer et al., 2007b). The combination of both, the lack in chemical-chronostratigraphical data and glass chemical alteration can lead to a serious misinterpretation of the timing of tephra deposition, as demonstrated by the case study of the Interstadial record of the Piànico-Sèllere palaeo-lake (Northern Italy) (e.g., Pinti et al., 2001; Brauer et al., 2007b; Brauer et al., 2007c; Pinti et al., 2007; Roulleau et al., 2009). However, these problems can be only overcome by the development of detailed tephrostratigraphies of older deposits that include high-precision dating and single grain major (and trace) elemental glass data.

Large effort was made during the last decade to improve the European tephrostratigraphic framework. The finding of new visible and non-visible tephras in high-resolution sedimentary records in the Eastern Mediterranean region in the frame of the RESET and INTIMATE projects contributed to an increased awareness of the importance of tephra studies by the palaeoclimate and volcanology communities. However, the trend of finding cryptotephras of even smaller grain sizes now raises a number of issues that are related to the processing and analysis of tephra glass shards. In terms of an analytical restriction, large effort was recently made to develop new techniques to overcome the limiting 10 µm beam size during EPMA and LA-ICP-MS measurements (e.g., Hayward, 2011; Pearce et al., 2011). Therefore, the main future challenge of tephra research will be the development of the existing and/or new techniques for tracing and extracting cryptotephras of grain sizes smaller than 20 µm. This is also an important factor for the reconstruction of tephra dispersal; this general lack in knowledge can be overcome, for instance, by the study of recent eruptions, e.g. the Icelandic eruptions of the Eyjafjalljökull in April/May 2010 and Grimsvötn in May 2011 (Kerminen et al., 2011). Volcanic ash dispersal maps generated by satellites and aircraft

Scientific Technical Report STR14/01, Deutsches GeoForschungsZentrum GFZ. http://doi.org/10.2312/GFZ.b103-14010

monitoring suggest a wide tephra dispersal of these rather medium sized eruptions. It is one of the challenges now to confirm those maps by tephra findings in artificial traps (pollen traps, etc.) and in high resolution lake and ocean deposits (see current ICLEA projects). These studies in combination with an improvement of geochemical data sets and radiometric dating of proximal and distal tephra deposits will help to establish a dense, over-regional tephrostratigraphical network and more detailed ash dispersal maps in both Northern and Southern Europe. The improvement of the accuracy and precision of age determination of sediment sequences (i.e., ^{14}C, $^{39}Ar/^{40}Ar$), U-Th, OSL) together with a dense tephrostratigraphic framework over large areas such as the Greenland – Near East transect enable the direct correlation of palaeoclimate records from remote regions on a common time scale, without using the palaeoenvironmental record itself as a correlation tool (i.e., wiggle matching of $\delta^{18}O$ signals). This is the only way to determine and quantify leads and lags in climate change, which are essential for the understanding of future environmental impacts in response to current global warming. In order to meet the increasing demand from society to improve predictions of future climates, the quantification of time lags of subsequent climate and/or environmental changes is crucial for the detection of future precursor changes at an early stage that can help society to adapt to new climatic conditions.

Scientific Technical Report STR14/01, Deutsches GeoForschungsZentrum GFZ. http://doi.org/10.2312/GFZ.b103-14010

4. References

Aksu, A.E., Hiscott, R.N., Yasar, D., 1999. Oscillating Quaternary water levels of the Marmara Sea and vigerous outflow into the Aegean Sea from the Marmara Sea - Black Sea drainage corridor. Marine Geology 153, 275-302.

Allen, J.R.M., Brandt, U., Brauer, A., Hubberten, H.-W., Huntley, B., Keller, J., Kraml, M., Mackensen, A., Mingram, J., Negendank, J.F.W., Nowaczyk, N.R., Oberhänsli, H., Watts, W.A., Wulf, S., Zolitschka, B., 1999. Rapid environmental changes in southern Europe during the last glacial period. Nature 400, 740-743.

Austin, W.E.N., Telford, R.J., Ninnemann, U.S., Brown, L., Wilson, L.J., Small, D.P., Bryant, C.L., 2011. North Atlantic reservoir ages linked to high Younger Dryas atmospheric radiocarbon concentrations. Global and Planetary Change 79, 226-233.

Baales, M., Jöris, O., Street, M., Bittmann, F., Weninger, B., Wiethold, J., 2002. Impact of the late glacial eruption of the Laacher See volcano, Central Rhineland, Germany. Quaternary Research 58, 273-288.

Bahk, J.J., Chough, S.K., Han, S.J., 2000. Origins and paleoceanographic significance of laminated muds from the Ulleung Basin, East Sea (Sea of Japan). Marine Geology 162, 459-477.

Bard, E., Arnold, M., Mangerud, J., Paterne, M., Labeyrie, L., Dupart, J., Melieres, M., Sonstegaard, E., Duplessy, J., 1994. The North-Atlantic atmosphere-sea surface ^{14}C gradient during the Younger Dryas climatic event. Earth and Planetary Science Letters 126, 275-287.

Belmecheri, S., von Grafenstein, U., Andersen, N., Eymard-Bordon, A., Régnier, D., Grenier, C., Lézine, A.-M., 2010. Ostracod-based isotope record from Lake Ohrid (Balkan Peninsula) over the last 140 ka. Quaternary Science Reviews 29, 3894-3904.

Birks, H.H., Gulliksen, S., Haflidason, H., Mangerud, J., 1996. New radiocarbon dates for the Vedde Ash and the Saksunarvatn Ash from Western Norway. Quaternary Research 45, 119-127.

Blockley, S., Pyne-O'Donnell, S.D.F., Lowe, J.J., Matthews, I.P., Stone, A., Pollard, M., Turney, C.S.M., Molyneux, E.G., 2005. A new and less destructive laboratory procedure for the physical seperation of distal glass tephra shards from sediments. Quaternary Science Reviews 24, 1952-1960.

Blockley, S.P.E., Lane, C.S., Lotter, A.F., Pollard, A.M., 2007. Evidence for the presence of the Vedde Ash in Central Europe. Quaternary Science Reviews 26, 3030-3036.

Borchardt, G.A., Harward, M.E., Schmitt, R.A., 1971. Correlation of volcanic ash deposits by activation analysis of glass separates. Quaternary Research 1, 247-260.

Bourne, A.J., Lowe, J.J., Trincardi, F., Asioli, A., Blockley, S., Wulf, S., Matthews, I.P., Piva, A., Vigliotti, L., 2010. Distal tephra record for the last ca 105,000 years from core PRAD 1-2 in the central Adriatic Sea: implications fro marine tephrostratigraphy. Quaternary Science Reviews 29, 3079-3094.

Brandt, U., 1999. Rekonstruktion von Säkularvariationen des Erdmagnetfeldes der letzten 100.000 Jahre - Untersuchungen an Sedimenten aus dem Lago di Mezzano und dem Lago Grande di Monticchio, Italien. University of Potsdam, p. 119.

Brandt, U., Nowaczyk, N.R., Ramrath, A., Brauer, A., Mingram, J., Wulf, S., Negendank, J.F.W., 1999. Palaeomagnetism of Holocene and Late Pleistocene sediments from Lago di Mezzano and Lago Grande di Monticchio (Italy): initial results. Quaternary Science Reviews 18, 961-976.

Brauer, A., Endres, C., Negendank, J.F.W., 1999a. Lateglacial calendar year chronology based on annually laminated sediments from Lake Meefelder Maar, Germany. Quaternary International 61, 17-25.

Brauer, A., Endres, C., Günther, C., Litt, T., Stebich, M., Negendank, J.F.W., 1999b. High resolution sediment and vegetation responses to Younger Dryas climate change in varved lake sediments from Meerfelder Maar, Germany. Quaternary Science Reviews 18, 321-329.

Brauer, A., Mingram, J., Frank, U., Günter, C., Schettler, G., Wulf, S., Zolitschka, B., Negendank, J.F.W., 2000. Abrupt environmental oscillations during the Early Weichselian recorded at Lago Grande di Monticchio, southern Italy. Quarternary International 73/74, 79-90.

Brauer, A., Allen, J.R.M., Mingram, J., Dulski, P., Wulf, S., Huntley, B., 2007a. Evidence for last interglacial chronology and environmental change from Southern Europe. PNAS 104, 450-455.

Brauer, A., Wulf, S., Mangili, C., Moscariello, A., 2007b. Tephrochronological dating of varved interglacial lake deposits from Piànico-Sèllere (Southern Alps, Italy) to around 400 ka. Journal of Quaternary Science 22, 85-96.

Brauer, A., Wulf, S., Mangili, C., Appelt, O., Moscariello, A., 2007c. Reply: Tephrochronological dating of varved interglacial lake deposits from Piànico-Sèllere (Southern Alps, Italy) to around 400 ka. Journal of Quaternary Science 22, 415-418.

Scientific Technical Report STR14/01, Deutsches GeoForschungsZentrum GFZ. http://doi.org/10.2312/GFZ.b103-14010

Brauer, A., Haug, G.H., Dulski, P., Sigman, D.M., Negendank, J.F.W., 2008. An abrupt wind shift in western Europe at the onset of the Younger Dryas cold period. Nature Geoscience 1, 520-523.

Brendryen, J., Haflidason, H., Sejrup, H.P., 2010. Norwegian Sea tephrostratigraphy of marine isotope stages 4 and 5: Prospect and problems for tephrochronology in the North Atlantic region. Quaternary Science Reviews 29, 847-864.

Brocchini, D., La Volpe, L., Laurenzi, M.A., Principe, C., 1994. Storia evolutiva del Monte Vulture. Plinius 12, 22-25.

Çagatay, M.N., Görür, N., Algan, O., Eastoe, C., Tchapalyga, A., Ongan, D., Kuhn, T., Kuscu, I., 2000. Late Glacial-Holocene palaeoceanography of the Sea of Marmara: timing of connections with the Mediterranean and the Black Sea. Marine Geology 167, 191-206.

Calanchi, N., Dinelli, E., 2008. Tephrostratigraphy of the last 170 ka in sedimentary successions from the Adriatic Sea. Journal of Volcanology and Geothermal Research 177, 81-95.

Calanchi, N., Dinelli, E., Lucchini, F., Mordenti, A., 1996. Chemostratigraphy of late Quaternary sediments from Lake Albano and central Adriatic Sea cores (PALICLAS Project), In: Guilizzoni, P., Oldfield, F. (Eds.), Palaeoenvironmental Analysis of Italian Crater Lake and Adriatic Sediments, pp. 247-263.

Carr, M.J., 2012. Igpet for Windows. Terra Softa Inc., http://home.comcast.net/~carrvolcano/site/?/page/Igpet/.

Cioni, R., Sulpizio, R., Garruccio, N., 2003. Variability of the eruption dynamics during a Subplinian event: the Greenish Pumice eruption of Somma-Vesuvius (Italy). Journal of Volcanology and Geothermal Research 124, 89-114.

Civetta, L., Orsi, G., Pappalardo, L., Fisher, R.V., Heiken, G., Ort, M., 1997. Geochemical zoning, mingling, eruptive dynamics and depositional processes; the Campanian Ignimbrite, Campi Flegrei caldera, Italy. Journal of Volcanology and Geothermal Research 75, 183 - 219.

Davies, S.M., Turney, C.S.M., Lowe, J.J., 2001. Identification and significance if a visible, basalt-rich Vedde Ash layer in a Late-glacial sequence on the Isle of Skye, Inner Hebrides, Scotland. Journal of Quaternary Science 16, 99-104.

de Lange, P.J., Lowe, D.J., 1990. History of vertical displacement of Kerepehi fault at Kopouatai bog, Hauraki Lowlands, New Zealand, since c. 10 700 years ago. New Zealand Journal of Geology and Geophysics 33, 277-283.

de Vita, S., Orsi, G., Civetta, L., Carandente, A., D' Antonio, M., Deino, A., di Cesare, T., Di Vito, M.A., Fisher, R.V., Isaia, R., Marotta, E., Necco, A., Ort, M., Pappalardo, L., Piochi, M., Southon, J., 1999. The Agnano-Monte Spina eruption (4100 years BP) in the restless Campi Flegrei caldera (Italy). Journal of Volcanology and Geothermal Research 91, 269-301.

De Vivo, B., Rolandi, G., Gans, P.B., Calvert, A., Bohrson, W.A., Spera, F.J., Belkin, H.E., 2001. New constraints on the pyroclastic eruptive history of the Campanian volcanic plain (Italy). Mineral. Petrol. 73, 47-65.

Deeming, K.R., McGuire, B., Harrop, P., 2010. Climate forcing of volcano lateral collapse: evidence from Mount Etna, Sicily. Phil. Trans. R. Soc. A 368, 2559-2577.

Deino, A.L., Scott, G.R., Saylor, B., Alene, B., Angelini, J.D., Haile-Selassie, Y., 2010. 40Ar/39Ar dating, paleomagnetism, and tephrochemistry of Pliocene strata of the hominid-bearing Woranso-Mille area, west-central Afar Rift, Ethiopia. Journal of Human Evolution 58, 111-126.

Dellino, P., La Volpe, L., 1996. Fragmentation versus transportation mechanism in the pyroclastic sequence of Monte Pilato-Rocche Rosse (Lipari, Italy). Journal of Volcanology and Geothermal Research 64, 211-231.

Develle, A.-L., Williamson, D., Gasse, F., Walter-Simonnet, A.-V., 2009. Early Holocene volcanic ash fallout in the Yammoûneh lacustrine basin (Lebanon): Tephrochronological implications for the Near East. Journal of Volcanology and Geothermal Research 186, 416-425.

Druitt, T.H., Edwards, L., Mellors, R.M., Pyle, D.M., Sparks, R.S.J., Lanphere, M., Davies, M., Barriero, B., 1999. Santorini Volcano. Geological Society, London.

Eastwood, W.J., Pearce, N.J.G., Westgate, J.A., Perkins, W.T., Lamb, H.F., Roberts, N., 1999. Geochemistry of Santorini tephra in lake sediments from Southwest Turkey. Global and Planetary Change 21, 17-29.

Eiriksson, J., Sigurgeirsson, M.A., Hoelstad, T., 1996. Image analysis and morphometry of hydromagmatic tephra particles from the Reykjanes volcanic system, Iceland. Jökull 44, 41-56.

Fedele, F.G., Giaccio, B., Hajdas, I., 2008. Timescales and cultural process at 40,000 BP in the light of the Campanian Ignimbrite eruption, Western Eurasia. Journal of Human Evolution 55, 834-857.

Federman, A.N., Carey, S.N., 1980. Electron microprobe correlation of tephra layers from Eastern Mediterranean abyssal sediments and the island of Santorini. Quaternary Research 13, 160 - 171.

Scientific Technical Report STR14/01, Deutsches GeoForschungsZentrum GFZ. http://doi.org/10.2312/GFZ.b103-14010

Ferrara, G., Tonarini, S., 1985. Radiometric geochronology in Tuscany: results and problems. Rendiconti della Società Italiana di Mineralogia e Petrologia 40, 11-124.

Francus, P., Lamb, H., Nakagawa, T., Marshall, M., Brown, E., members, S.P., 2009. The potential of high-resolution X-ray fluorescence core scanning: Applications in paleolimnology. PAGES news 17, 93-96.

Franz, G., Breitkreuz, C., Coyle, D.A., El Hur, B., Heinrich, W., Paulick, H., Pudlo, D., Smith, R., Steiner, G., 1997. The alkaline Meidob volcanic field (Late Cenozoic, northwest Sudan). Journal of African Earth Sciences 25, 263 - 291.

Froggatt, P.C., 1992. Standardization of the chemical analysis of tephra deposits. Report of the ICCT working group. Quaternary International 13/14, 93-96.

Funk, J., Mann, P., McIntosh, K.D., Wulf, S., Dull, R., Perez, P., Strauch, W., 2006. Results from NICLAKES survey of active faulting beneath lake Nicaragua, Central American volcanic arc, AGU 2006 Fall Meeting, San Francisco, California.

Giaccio, B., Isaia, R., Fedele, F.G., Di Canzio, E., Hoffecker, J., Ronchitelli, A., Sinitsyn, A.A., Anikovich, M., Lisitsyn, S.N., Popov, V.v., 2008. The Campanian Ignimbrite and Codola tephra layers: Two temporal/stratigraphic markers for the Early Upper Palaeolithic in southern italy and eastern Europe. Journal of Volcanology and Geothermal Research 177, 208-226.

Giaccio, B., Nomade, S., Wulf, S., Isaia, R., Sottili, G., Cavuoto, G., Galli, P., Messina, P., Sposato, A., Sulpizio, R., Zanchetta, G., 2012. The late MIS 5 Mediterranean tephra markers: a reappraisal from peninsular Italy terrestrial records. Quaternary Science Reviews 56, 31-45.

Golovanova, L.V., Doronichev, V.B., Cleghorn, N.E., Koulkova, M.A., Sapelko, T.V., Shackley, M.S., 2010. Significance of ecological factors in the Middle to Upper Paleolithic Transition. Current Anthropology 51 (5), 655.

Grönvold, K., Óskarsson, N., Johnsen, S.J., Clausen, H.B., Hammer, C.U., Bond, G., Bard, E., 1995. Ash layers from Iceland in the Greenland GRIP ice core correlated with oceanic and land sediments. Earth and Planetary Science Letters 135, 149-155.

Gudmundsson, M.T., Thordarson, T., Höskuldsson, Á., Larsen, G., Björnsson, H., Prata, F.J., Magnússon, E., Högnadóttir, T., Petersen, G.N., Hayward, C.L., Stevenson, J.A., Jónsdóttir, I., 2012. Ash generation and distribution from the April-May 2010 eruption of Eyjafjallajökull, Iceland. Scientific Reports 2, 1-12.

Haberzettl, T., Corbella, H., Fey, M., Janssen, S., Lücke, A., Mayr, C., Ohlendorf, C., Schäbitz, F., Schleser, G.H., Wille, M., Wulf, S., Zolitschka, B., 2007. Lateglacial and Holocene wet-dry cycles in southern Patagonia: chronology, sedimentology and geochemistry of a lacustrine record from Laguna Potrok Aike, Argentina. The Holocene 17, 297-310.

Haberzettl, T., Kück, B., Wulf, S., Anselmetti, F., Ariztegui, D., Corbella, H., Fey, M., Janssen, S., Lücke, A., Mayr, C., Ohlendorf, C., Schäbitz, F., Schleser, G.H., Wille, M., Zolitschka, B., 2008. Hydrological variability in southeastern Patagonia and explosive volcanic activity in the southern Andean Cordillera during Oxygen Isotope Stage 3 and the Holocene inferred from lake sediments of Laguna Potrok Aike, Argentina. Palaeogeography, Palaeoclimatology, Palaeoecology 259, 213-229.

Haberzettl, T., Anselmetti, F.S., Wulf Bowen, S., Fey, M., Mayr, C., Zolitschka, B., Ariztegui, D., Mauz, B., Ohlendorf, C., Kastner, S., Lücke, A., Schäbitz, F., Wille, M., 2009. Late Pleistocene dust deposition in the Patagonian steppe - extending and refining the paleoenvironmental and tephrochronological record from Laguna Potrok Aike back to 55 ka. Quaternary Science Reviews 28, 2927-2939.

Haflidason, H., Eiriksson, J., van Kreveld, S., 2000. The tephrochronology of Iceland and the North Atlantic region during the Middle and Late Quaternary: a review. Journal of Quaternary Science 15, 3-22.

Hajdas, I., Bonani, G., Zolitschka, B., Brauer, A., Negendank, J.F.W., 1998. ^{14}C ages of terrestrial macrofossils from Lago Grande di Monticchio (Italy). Radiocarbon 40, 803 - 807.

Hamann, Y., Wulf, S., Ersoy, O., Ehrmann, W., Aydar, E., Schmiedl, G., 2010. First evidence of a distal early Holocene ash layer in Eastern Mediterranean deep-sea sediments derived from the Anatolian volcanic province. Quaternary Research 73, 497-506.

Hayward, C., 2011. High spatial resolution electron probe microanalysis of tephras and melt inclusions without beam-induced chemical modification. The Holocene 22, 119-125.

Heinold, B., Tegen, I., Wolke, R., Ansmann, A., Mattis, I., Minikin, A., Schumann, U., Weinzierl, B., 2012. Simulations of the 2010 Eyjafjallajökull volcanic ash dispersal over Europe using COSMO-MUSCAT. Atmospheric Environment 48, 195-204.

Hunt, J.B., Hill, P.G., 1993. Tephra geochemistry: a discussion of some persistent analytical problems. The Holocene 3, 271-278.

Scientific Technical Report STR14/01, Deutsches GeoForschungsZentrum GFZ. http://doi.org/10.2312/GFZ.b103-14010

Hunt, J.B., Hill, P.G., 1996. An inter-laboratory comparison of the electron probe microanalysis of glass geochemistry. Quaternary International 34-36, 229-241.

Hunt, J.B., Hill, P.G., 2001. Tephrological implications of bean size - sample-size effects in electron microprobe analysis of glass shards. Journal of Quaternary Science 16, 105-117.

Hurd, D.C., Theyer, F., 1977. Changes in the physical and chemical properties of biogenic silica from the central equatorial Pacific: Part II. Refractive index, density, and water content of acid-cleaned samples. American Journal of Science 277, 1168-1202.

Ingólfsson, Ó., Björck, S., Haflidason, H., Rundgren, M., 1997. Glacial and climatic events in Iceland reflecting regional North Atlantic climate shifts during the Pleistocene-Holocene transition. Quaternary Science Reviews 16, 1135-1144.

Jahns, S., van den Bogaard, C., 1998. New palynological and tephrostratigraphical investigations of two salt lagoons on the island of Mljet, south Dalmatia, Croatia. Vegetation History and Archaeobotany 7, 219 - 234.

Jéhanno, C., Boclet, D., Froget, L., Lambert, B., Robin, E.R., Rocchia, R., Turpin, L., 1992. The cretaceous-Tertiary boundary at Beloc, Haiti: No evidence for an impact in the Caribbean Area. Earth and Planetary Science Letters 109, 229-241.

Jochum, K.P., Pfänder, J., Woodhead, J.D., Willbold, M., Stoll, B., Herwig, K., Amini, M., Abouchami, W., Hofmann, A.W., 2005. MPI-DING glasses: New geological reference materials for in situ Pb isotope analysis. Geochemistry, Geophysics, Geosystems 6.

Keller, J., Ryan, W.B.F., Ninkovich, D., Altherr, R., 1978. Explosive volcanic activity in the Mediterranean over the past 200,000 yr as recorded in deep-sea sediments. Geological Society of America Bulletin 89, 591 - 604.

Keller, J., 1981. Quaternary tephrochronology in the Mediterranean region, In: Self, S., Sparks, R.S.J. (Eds.), Tephra Studies. Reidel, Dordrecht, pp. 227-244.

Keller, J., Kraml, M., Scheld, A., 1996. Late Quaternary tephrochronological correlation between deep-sea sediments and the land record in the Central Mediterranean, 30th International Geological Congress, Beijing, p. 204.

Kerminen, V.-M., Niemi, J.V., Timonen, H., Aurela, M., Frey, A., Carbone, S., Saarikoski, S., Teinilä, K., Hakkarainen, J., Tamminen, J., Vira, J., Prank, M., Sofiev, M., Hillamo, R., 2011. Characterization of a volcanic ash episode in southern Finland caused by the Grimsvötn eruption in Iceland in May 2011. Atmospheric Chemistry and Physics 11, 12227-12239.

Kienel, U., Wulf Bowen, S., Byrne, R., Park, J., Böhnel, H., Dulski, P., Luhr, J.F., Siebert, L., Haug, G.H., Negendank, J.F.W., 2009. First lacustrine varve chronologies from Mexico: impact of droughts, ENSO and human activity since AD 1840 as recorded in maar sediments from Valle de Santiago. Journal of Paleolimnology 42, 587-609.

Kind, J., 2008. Paleoenvironmental changes during the last glacial period as reconstructed from sediment cores in the SE Black Sea. Diploma Thesis, Technical University Bergakademie Freiberg, p. 84.

Knudsen, K.L., Eiríksson, J., 2002. Application of tephrochronology to the timimg and correlation of palaeoceanographic events recorded in Holocene and Late Glacial shelf sediments off North Iceland. Marine Geology 191, 165-188.

Koren, J.H., Svendsen, J.I., Mangerud, J., Furnes, H., 2008. The Dimna-Ash - 12.8 14C ka-old volcanic ash in Western Norway. Quaternary Science Reviews 27, 85-94.

Kraml, M., 1997. Laser-$^{40}Ar/^{39}Ar$-Datierungen an distalen marinen Tephren des jung-quartären mediterranen Vulkanismus (Ionisches Meer, METEOR-Fahrt 25/4), Geowissenschaftliche Fakultät. Albert-Ludwigs-University Freiburg i.Br., p. 216.

Kristjánsdóttir, G.B., Stoner, J.S., Jennings, A.E., Andrews, J.T., Grönvold, K., 2007. Geochemistry of Holocene cryptotephras from the North Iceland Shelf (MD99-2269): intercalibration with radiocarbon and palaeomagnetic chronostratigraphies. The Holocene 17, 155-176.

Kwiecien, O., Arz, H.W., Lamy, F., Wulf, S., Bahr, A., Röhl, U., Haug, G.H., 2008. Estimated reservoir ages of the Black Sea since the Last Glacial. Radiocarbon 50, 1-20.

Kylander, M.E., Lind, E.M., Wastegard, S., Löwemark, L., 2011. Recommendations for using XRF core scanning as a tool in tephrochronology. The Holocene 22, 371-375.

Lackschewitz, K.S., Wallrabe-Adams, H.J., 1997. Composition and origin of volcanic ash zones in Late Quaternary seidments from the Reykjanes Ridge: evidence for ash fallout and ice-rafting. Marine Geology 136, 209-224.

Scientific Technical Report STR14/01, Deutsches GeoForschungsZentrum GFZ. http://doi.org/10.2312/GFZ.b103-14010

Landmann, G., Steinhauser, G., Sterba, J.H., Kempe, S., Bichler, M., 2011. Geochemical fingerprints by activation analysis of tephra layers in lake Van sediments, Turkey. Applied Radiation and Isotopes 69, 929-935.

Lane, C.S., Andri, M., Cullen, V.L., Blockley, S.P.E., 2011a. The occurrence of distal Icelandic and Italian tephra in the Lateglacial of Lake Bled, Slovenia. Quaternary Science Reviews 30, 1013-1018.

Lane, C.S., Blockley, S.P.E., Bronk Ramsey, C., Lotter, A.F., 2011b. Tephrochronology and absolute centennial scale synchronisation of European and Greenland records for the last glacial to interglacial transition: A case study of Soppensee and NGRIP. Quaternary International 246, 145-156.

Lane, C.S., Blockley, S.P.E., Mangerud, J., Smith, V.C., Lohne, O.S., Tomlinson, E.L., Matthews, I.P., Lotter, A.F., 2012a. Was the 12.1 ka Icelandic Vedde Ash one of a kind? Quaternary Science Reviews 33, 87-99.

Lane, C.S., Blockley, S.P.E., Lotter, A.F., Finsinger, W., Filippi, M.L., Matthews, I.P., 2012b. A regional tephrostratigraphic framework for central and southern European climate archives during the Last Glacial to Interglacial transition: comparisons north and south of the Alps. Quaternary Science Reviews 36, 50-58.

Langmann, B., Folch, A., Hensch, M., Matthias, V., 2012. Volcanic ash over Europe during the eruption of Eyjafjallajökull on Iceland, April-May 2010. Atmospheric Environment 48, 1-8.

Larsen, G., Dugmore, A., Newton, A.J., 1999. Geochemistry of historical-age silicic tephras in Iceland. The Holocene 9, 463-471.

Lowe, D.J., 2011. Tephrochronology and its application: A review. Quaternary Geochronology 6, 107-153.

Lowe, J.J., Walker, M.J.C., 1997. Reconstructing Quaternary Environments. Addison Wesley Longman Limited, Essex.

Lowe, J.J., Barton, N., Blockley, S., Bronk Ramsey, C., Cullen, V.L., Davies, W., Gamble, C., Grant, K., Hardiman, M., Housley, R., Lane, C.S., Lee, S., Lewis, M., MacLeod, A., Menzies, M.A., Müller, W., Pollard, M., Price, C., Roberts, A.P., Rohling, E.J., Satow, C., Smith, V.C., Stringer, C.B., Tomlinson, E.L., White, D., Albert, P., Arienzo, I., Barker, G., Boric, D., Carandente, A., Civetta, L., Ferrier, C., Guadelli, J.-L., Karkanas, P., Koumouzelis, M., Müller, U.C., Orsi, G., Pross, J., Rosi, M., Shalamanov-Korobar, L., Sirakov, N., Tzedakis, P.C., 2012. Volcanic ash layers illuminate the resilience of Neanderthals and earl modern humans to natural hazards. PNAS.

Mangerud, J., Lie, S.E., Furnes, H., Kristiansen, I.L., Lomo, L., 1984. A Younger dryas ash bed in western Norway and its possible correlations with tephra in cores from the Norwegian Sea and the North Atlantic. Quaternary Research 21, 85-104.

Margari, V., Pyle, D.M., Bryant, C., Gibbard, P.L., 2007. Mediterranean tephra stratigraphy revisited: Results from a long terrestrial sequence on Lesvos Island, Greece. Journal of Volcanology and Geothermal Research 163.

Maria, A., Carey, S., 2007. Quantitative discrimination of magma fragmentation and pyroclastic transport processes using the fractal spectrum technique. Journal of Volcanology and Geothermal Research 161, 234-246.

McGuire, W.J., Howarth, R.J., Firth, C.R., Solow, A.R., Pullen, A.D., Saunders, S.J., Stewart, I.S., Vita-Finzi, C., 1997. Correlation between rate of sea-level change and frequency of explosive volcanism in the Mediterranean. Nature 389, 473 - 476.

Moreno, A., González-Sampériz, P., Morellón, M., Valero-Garcés, B.L., Fletcher, W.J., 2012. Northern Iberian abrupt climate change dynamics during the last glacial cycle: A view from lacustrine sediments. Quaternary Science Reviews 36, 139-153.

Mortensen, A.K., Bigler, M., Grönvold, K., Steffensen, J.P., Johnsen, S.J., 2005. Volcanic ash layers from the Last Glacial Termination in the NGRIP ice core. Journal of Quaternary Science 20, 209-219.

Müller, U.C., Pross, J., Tzedakis, P.C., Gamble, C., Kotthoff, U., Schmiedl, G., Wulf, S., Christanis, K., 2011. The role of climate in the spread of modern humans into Europe. Quaternary Science Reviews 30, 273-279.

Munno, R., Petrosini, P., 2007. The late Quaternary tephrostratigraphical record of the San Gregorio Magno basin (southern Italy). Journal of Quaternary Science 22, 247-266.

Narcisi, B., 1996. Tephrochronology of a late quaternary lacustrine record from the Monticchio Maar (Vulture Volcano, southern Italy). Quaternary Science Reviews 15, 155 - 165.

Narcisi, B., Vezzoli, L., 1999. Quaternary stratigraphy of distal tephra layers in the Mediterranean - an overview. Global and Planetary Change 21, 31-50.

Neugebauer, I., Brauer, A., Dräger, N., Dulski, P., Wulf, S., Plessen, B., Mingram, J., Herzschuh, U., Brande, A., 2012. A Younger Dryas varve chronology from the Rehwiese palaeolake record in NE-Germany. Quaternary Science Reviews 36, 91-102.

Scientific Technical Report STR14/01, Deutsches GeoForschungsZentrum GFZ. http://doi.org/10.2312/GFZ.b103-14010

Newnham, R.M., de Lange, P.J., Lowe, D.J., 1995. Holocene vegetation, climate, and history of a raised bog complex, northern New Zealand, based on palynology, plant macrofossils and tephrochronology. The Holocene 5, 267-282.

Newton, A.J., Dugmore, A.J., 1993. Tephrochronology of Core C from Lago Grande di Monticchio, In: Negendank, J.F.W., Zolitschka, B. (Eds.), Paleolimnology of European Maar Lakes. Springer-Verlag, Berlin, Heidelberg, pp. 333 - 348.

Nielsen, C.H., Sigurdsson, H., 1981. Quantitative methods for electron microprobe analysis of sodium in natural and synthetic glasses. American Mineralogist 66, 547-552.

North Greenland Ice Core Project members, 2004. High-resolution record of Northern Hemisphere climate extending into the last interglacial period. Nature 431(7005), 147-151.

Nowaczyk, N.R., Arz, H.W., Frank, U., Kind, J., Plessen, B., 2012. Dynamics of the Laschamp geomagnetic excursion from Black Sea sediments. Earth and Planetary Science Letters 351-352, 54-69.

Oldfield, F., Crooks, P., Harknedd, D., Petterson, G., 1997. AMS radiocarbon dating of organic fractions from varved lake sediments: an empirical test of reliability. Journal of Paleolimnology 18, 87-91.

Oxford-Economics, 2010. The Economic impacts of air travel restrictions due to volcanic ash report for airbus.

Oxford-Economics, 2011. UK Economic losses due to volcanic ash air travel restrictions.

Page, M.J., Trustrum, N.A., Orpin, A.R., Carter, L., Homez, B., Cochran, U.A., Mildenhall, D.C., Rogers, K.M., Brackley, H.L., Palmer, A.S., Northcote, L., 2010. Storm frequency and magnitude in response to Holocene climate variability, Lake Tutira, north-eastern New Zealand. Marine Geology 270, 30-44.

Palumbo, A., 1997. Chaos hides and generates order: an application to forecasting the next eruption of Vesuvius. Journal of Volcanology and Geothermal Research 79, 139 - 148.

Paterne, M., Guichard, F., Labeyrie, J., Gillot, P.Y., Duplessy, J.C., 1986. Tyrrhenian Sea tephrochronology of the oxygen isotope record for the past 60,000 years. Marine Geology 72, 259 - 285.

Paterne, M., Guichard, F., Labeyrie, J., 1988. Explosive activity of the South Italian volcanoes during the past 80,000 years as determined by marine tephrochronology. Journal of Volcanology and Geothermal Research 34, 153-172.

Paterne, M., Guichard, F., Duplessy, J.C., Siani, G., Sulpizio, R., Labeyrie, J., 2008. A 90,000-200,000 yrs marine tephra record of Italian volcanic activity in the Central Mediterranean Sea. Journal of Volcanology and Geothermal Research 177, 187-196.

Pearce, N.J.G., Westgate, J.A., Perkins, W.T., Eastwood, W.J., Shane, P., 1999. The application of laser ablation ICP-MS to the analysis of volcanic glass shards from tephra deposits: bulk glass and single shard analysis. Global and Planetary Change 21, 151-171.

Pearce, N.J.G., Denton, J.S., Perkins, W.T., Westgate, J.A., Alloway, B.V., 2007. Correlation and characterisation of individual glass shards from tephra deposits using trace element laser ablation ICP-MS analyses: current status and future potential. Journal of Quaternary Science 22, 721-736.

Pearce, N.J.G., Perkins, W.T., Westgate, J.A., Wade, S.C., 2011. Trace element microanalysis by laser ablation ICP-MS: the quest for comprehensive chemical characterisation of single sub-10µm volcanic glass shards. Quaternary International 246, 57-81.

Pilcher, J.R., Hall, V.A., 1992. Towards a tephrochronology for the Holocene of the north of Ireland. The Holocene 2, 255-259.

Pillans, B., Kohn, B.P., Berger, G., Froggatt, P., Duller, G., Alloway, B., Hesse, P., 1996. Multi-method dating comparison for mid-Pleistocene Rangitawa tephra, New Zealand. Quaternary Science Reviews 15, 641-653.

Pinti, D.L., Quidelleur, X., Chiesa, S., Ravazzi, C., Gillot, P.-Y., 2001. K-Ar dating of an early Middle Pleistocene distal tephra in the interglacial varved succession of Piànico-Sèllere (Southern Alps, Italy). Earth and Planetary Science Letters 188, 1-7.

Pinti, D.L., Quidelleur, X., Rouchon, V., Gillot, P.Y., Chiesa, S., Ravazzi, C., 2007. Comment: "Tephrochronological dating of varved interglacial lake deposits from Piànico-Sèllere (Southern Alps, Italy) to around 400 ka" by Achim Brauer, Sabine Wulf, Clara Mangili, Andrea Moscariello. Journal of Quaternary Science 22, 411-414.

Piva, A., Asioli, A., Schneider, R.R., Trincardi, F., Andersen, N., Colmenero-Hidalgo, E., Dennielou, B., Flores, J.-A., Vigliotti, L., 2008a. Climatic cycles as expressed in sediments of the PROMESS1 borehole PRAD1-2, central Adriatic, for the last 370 ka: 1. Integrated stratigraphy. Geochemistry, Geophysics, Geosystems 9 (3), 1-21.

Piva, A., Asioli, A., Andersen, N., Grimalt, J.O., Schneider, R.R., Trincardi, F., 2008b. Climatic cycles as expressed in sediments of the PROMESS1 borehole PRAD1-2, central Adriatic, for the last 370 ka: 2. Paleoenvironmental evolution. Geochemistry, Geophysics, Geosystems 9 (3), 1-21.

Scientific Technical Report STR14/01, Deutsches GeoForschungsZentrum GFZ. http://doi.org/10.2312/GFZ.b103-14010

Poli, S., Chiesa, S., Gillot, P.-Y., Gregnanin, A., Guichard, F., 1987. Chemistry versus time in the volcanic complex of Ischia (Gulf of Naples, Italy): evidence of successive magmatic cycles. Contributions to Mineralogy and Petrology 95, 322 - 335.

Pouclet, A., Horvath, E., Gabris, G., Juvigné, E., 1999. The Bag Tephra, a widespread tephrochronological marker in Middle Europe: chemical and mineralogical investigations. Bulletin of Volcanology 60, 265-272.

Pyle, D.M., Ricketts, G.D., Margari, V., van Andel, T.H., Sinitsyn, A.A., Praslov, N.D., Lisitsyn, S., 2006. Wide dispersal and deposition of distal tephra during the Pleistocene 'Campanian Ignimbrite/Y5' eruption, Italy. Quaternary Science Reviews 25, 2713-2728.

Ramrath, A., Zolitschka, B., Wulf, S., Negendank, J.F.W., 1999. Late Pleistocene climatic variations as recorded in two Italian maar lakes (Lago di Mezzano, Lago Grande di Monticchio). Quaternary Science Reviews 18, 977-992.

Rasmussen, S.O., Andersen, K.K., Svensson, A.M., Steffensen, J.P., Vinther, B.M., Clausen, H.B., Siggaard-Andersen, M.L., Johnsen, S.J., Larsen, L.B., Dahl-Jensen., D., Bigler, M., Röthlisberger, R., Fischer, H., Goto-Azuma, K., Hanssom, M.E., Ruth, U., 2006. A new Greenland ice core chronology for the last glacial termination. Journal of Geophysical Research D: Atmospheres, 111.

Riede, F., Bazely, O., Newton, A.J., Lane, C.S., 2011. A Laacher See-eruption supplement to Tephrabase: Investigating distal tephra fallout dynamics. Quaternary International 246, 134-144.

Roeser, P.A., Franz, S.O., Litt, t., Ülgen, U.B., Hilgers, A., Wulf, S., Wennrich, V., Ön, S.A., Viehberg, F., Cagatay, N., Melles, M., 2012. Lithostratigraphic and geochronological framework for the paleoenvironmental reconstruction of the last ~36 ka cal BP from a sediment record from Lake Iznik (NW Turkey). Quaternary International 274, 73-87.

Rolandi, G., Petrosino, P., McGeehin, J., 1998. The interplinian activity at Somma-Vesuvius in the last 3500 years. Journal of Volcanology and Geothermal Research 82, 19 - 52.

Rose, N.L., Golding, P.N.E., Battarbee, R.W., 1996. Selective concentration and enumeration of tephra shards from lake sediment cores. The Holocene 6, 243-246.

Roulleau, E., Pinti, D.L., Rouchon, V., Quidelleur, X., Gillot, P.Y., 2009. Tephrochronostratigraphy of the lacustrine interglacial record of Piànico, Italian southern Alps: identifying the volcanic sources using radiogenic isotopes and trace elements. Quaternary International 204, 31-43.

Schmidt, R., van den Bogaard, C., Merkt, J., Müller, J., 2002. A new Lateglacial chronostratigraphic tephra marker for the south-eastern Alps: The Neapolitan Yellow Tuff (NYT) in Längsee (Austria) in the context of a regional biostratigraphy and palaeoclimate. Quaternary International 88, 45-56.

Schmincke, H.-U., Park, C., Harms, E., 1999. Evolution and environmental impacts of the eruption of Laacher See Volcano (Germany 12,900 BP. Quaternary International 61, 61-72.

Shackleton, N.J., 2000. The 100,000-year Ice Age cycle identified and found to lag temperature, carbon dioxide and orbital eccentricity. Science 289, 1897-1902.

Siani, G., Paterne, M., Michel, E., Sulpizio, R., Sbrana, A., Arnold, M., Haddad, G., 2001. Mediterranean Sea surface radiocarbon reservoir age changes since the last glacial maximum. Science 294, 1917-1920.

Siani, G., Sulpizio, R., Paterne, M., Sbrana, A., 2004. Tephrostratigraphy study for the last 18,000 ^{14}C years in a deep-sea sediment sequence for the South Adriatic. Quaternary Science Reviews 23, 2485-2500.

Smith, D.G.W., Westgate, J.A., 1969. Electron probe technique for characterising pyroclastic deposits. Earth and Planetary Science Letters 5, 313-319.

Smith, V.C., Isaia, R., Pearce, N.J.G., 2011. Tephrostratigraphy and glass compositions of post-15 kyr Campi Flegrei eruptions: implications for eruption history and chronostratigraphic markers. Quaternary Science Reviews 30, 3638-3660.

Stoppa, F., Principe, C., 1998. Eruption style and petrology of a new carbonatitic suite from the Mt. Vulture (Southern Italy): The Monticchio Lakes Formation. Journal of Volcanology and Geothermal Research 80, 137-153.

Sulpizio, R., Van Welden, A., Caron, B., Zanchetta, G., 2010a. The Holocene tephrostratigraphic record of Lake Shkodra (Albania and Montenegro). Journal of Quaternary Science 25, 633-650.

Sulpizio, R., Zanchetta, G., D'Orazio, M.D., Vogel, H., Wagner, B., 2010b. Tephrostratigraphy and tephrochronology of lakes Ohrid and Prespa, Balkans. Biogeosciences Discussions 7, 3931-3967.

Thorarinsson, S., 1944. Tefrokronologiska studier pa Island. Geogr. Analer, 1-215.

Tomlinson, E.L., Arienzo, I., Civetta, L., Wulf, S., Smith, V.C., Hardiman, M., Lane, C.S., Carandente, A., Orsi, G., Rosi, M., Müller, W., Menzies, M.A., 2012. Geochemistry of the Phlegrean Fields (Italy) proximal sources for major Mediterranean tephras: Implications for the dispersal of Plinian and co-ignimbritic components of explosive eruptions. Geochimica et Cosmochimica Acta 93, 102-128.

Scientific Technical Report STR14/01, Deutsches GeoForschungsZentrum GFZ. http://doi.org/10.2312/GFZ.b103-14010

Turney, C.S.M., 1998. Extraction of rhyolitic component of Vedde microtephra from minerogenic lake sediments. Journal of Paleolimnology 19, 199-206.

Turney, C.S.M., Blockley, S.P.E., Lowe, J.J., Wulf, S., Branch, N.P., Mastrolorenzo, G., Swindle, G., Nathan, R., Pollard, M.A., 2008. Geochemical characterization of Quaternary tephras from the Campanian Province, Italy. Quaternary International 178, 288-305.

Valet, J.-P., Valladas, H., 2010. The Laschamp-Mono Lake geomagnetic events and the extinction of Neanderthal: a causal link or a coincidence? Quaternary Science Reviews 29, 27-28, 3887-3893.

van den Bogaard, P., Schmincke, H.-U., 1985. Laacher See Tephra: A widespread isochronous late Quaternary tephra layer in central and northern Europe. Geological Society of America Bulletin 96, 1554-1571.

van den Bogaard, P., 1995. $^{40}Ar/^{39}Ar$ ages of sanidine phenocrysts from Laacher See Tephra (12,900 yr BP): Chronostratigraphic and petrological significance. Earth Planet. Sci. Lett. 133, 163-174.

Vezzoli, L., 1991. Tephra layers in Bannock Basin (Eastern Mediterranean). Marine Geology 100, 21 - 34.

Villa, I., 1991. Excess Ar geochemistry in potassic volcanites. Schweizer Mineralogische und Petrographische Mitteilungen 71, 205-219.

Vogel, H., Wagner, B., Zanchetta, G., Sulpizio, R., Rosén, P., 2010. A paleoclimate record with tephrochronological age control for the last glacial-interglacial cycle from Lake Ohrid, Albania and Macedonia. Journal of Paleolimnology 44, 295-310. http://doi.pangaea.de/10.1594/PANGAEA.770103

Vos, H., Wulf, S., Negendank, J.F.W., 1999. Lago Grande di Monticchio - time series analysis of tephra deposition. Terra Nostra 99/10, 107-112.

Wagner, B., Sulpizio, R., Zanchetta, G., Wulf, S., Wessel, M., Daut, G., Nowaczyk, N., 2008. The last 40 ka tephrostratigraphic record of lake Ohrid, Albania and Macedonia: a very distal archive for ash dispersal from Italian volcanoes. Journal of Volcanology and Geothermal Research 177, 71-80.

Wallrabe-Adams, H.J., Lackschewitz, K.S., 2003. Chemical composition, distribution, and origin of silicic volcanic ash layers in the Greenland-Iceland-Norwegian Sea: explosive volcanism from 10 to 300 ka as recorded in deep-sea sediments. Marine Geology 193, 273-293.

Wastegard, S., Björck, S., Possnert, G., Wohlfahrt, B., 1998. Evidence for the occorrence of Vedde Ash in Sweden; radiocarbon and calendar age estimates. Journal of Quaternary Science 13, 271-274.

Wastegard, S., Turney, C.S.M., Lowe, J.J., Roberts, S.J., 2000a. New discoveries of the Vedde Ash in southern Sweden and Scotland. Boreas 29, 72-78.

Wastegard, S., Wohlfarth, B., Subetto, D.A., Sapelko, T.V., 2000b. Extending the known distribution of the Younger Dryas Vedde Ash into northwestern Russia. Journal of Quaternary Science 15, 581-586.

Wastegard, S., Rasmussen, T.L., 2001. New tephra horizons from Oxygen Isotope Stage 5 in the North Atlantic: correlation potential for terrestrial, marine and ice-core archives. Quaternary Science Reviews 20, 1587-1593.

Wastegard, S., Rasmussen, T.L., Kuijpers, A., Nielsen, T., van Weering, T.C.E., 2006. Composition and origin of ash zones from marine Isotope stages 3 and 2 in the North Atlantic. Quaternary Science Reviews 25, 2409-2419.

Wastegard, S., Davies, S.M., 2009. An overview of distal tephrochronology in northern Europe during the last 1000 years. Journal of Quaternary Science 24, 500-512.

Watts, W.A., 1985. A long pollen record from Laghi di Monticchio, southern Italy: a preliminary account. Journal of the Geological Society of London 142, 491 - 499.

Weber, K., Eliasson, J., Vogel, A., Fischer, C., Pohl, T., van Haren, G., Meier, M., Grobéty, B., Dahmann, D., 2012. Airborne in-situ investigations of the Eyjafjallajökull volcanic ash plume on Iceland and over north-western Germany with light aircrafts and optical particle counters. Atmospheric Environment 48, 9-21.

Wulf, S., Negendank, J.F.W., Mingram, J., Zolitschka, B., Vos, H., 1999. Explosivity of South-Italian volcanoes and climate change during the last 110,000 years, IUGG 99, Birmingham, England, p. 174.

Wulf, S., Kraml, M., Kuhn, T., Schwarz, M., Inthorn, M., Keller, J., Kuscu, I., Halbach, P., 2002. Marine tephra from the Cape Riva eruption (22 ka) of Santorini in the Sea of Marmara. Marine Geology 183, 131-141.

Wulf, S., Brauer, A., Kraml, M., Keller, J., Negendank, J.F.W., 2004. Tephrochronology of the 100 ka lacustrine sediment record of Lago Grande di Monticchio (southern Italy). Quaternary International 122, 7-30.

Wulf, S., Brauer, A., Mingram, J., Zolitschka, B., Negendank, J.F.W., 2006. Distal tephras in the sediments of Monticchio maar lakes, In: Principe, C. (Ed.), La geologia del monte Vulture. Consiglio Nazionale delle Ricerche, pp. 105-122.

Scientific Technical Report STR14/01, Deutsches GeoForschungsZentrum GFZ. http://doi.org/10.2312/GFZ.b103-14010

Wulf, S., Dull, R.A., Mann, P., McIntosh, K.D., Gardner, J.E., 2007. Late Pleistocene/Holocene paleoclimate reconstruction and eruptive history of Central American volcanoes from bottom sediments of Lake Nicaragua, AGU Fall Meeting, San Francisco, USA.

Wulf, S., Kraml, M., Keller, J., 2008. Towards a detailed distal tephrostratigraphy in the Central Mediterranean: The last 20,000 yrs record of Lago Grande di Monticchio. Journal of Volcanology and Geothermal Research 2008, 118-132.

Wulf, S., Baier, J., Haug, G.H., Dokken, T., Jansen, E., Dulski, P., Nowaczyk, N., Brauer, A., 2011. A 140 ka medial-distal marine record of Icelandic tephra events: examples from core HM03-133-10 (Norwegian Sea), Marine Tephrochronology Meeting, Burlington House, London, UK.

Wulf, S., Keller, J., Paterne, M., Mingram, J., Lauterbach, S., Opitz, S., Sottili, G., Giaccio, B., Albert, P.G., Satow, C., Tomlinson, E.L., Viccaro, M., Brauer, A., 2012. The 100-133 ka record of Italian explosive volcanism and revised tephrochronology of Lago Grande di Monticchio. Quaternary Science Reviews 58, 104-123.

Wutke, K., 2012. Large Pleistocene eruptions of Campanian volcanoes and their environmental impacts - a case study from Lago Grande di Monticchio, Southern Italy, Department of Geography. Justus-Liebig-University Giessen, p. 114.

Zanchetta, G., Sulpizio, R., Roberts, N., Cioni, R., Eastwood, W.J., Siani, G., Caron, B., Paterne, M., Santacroce, R., 2011. Tephrostratigraphy, chronology and climatic events of the Mediterranean basin during the Holocene: An overview. The Holocene 21, 33-52.

Zillén, L.M., Wastegard, S., Snowball, I.F., 2002. Calendar year ages of three mid-Holocene tephra layers identified in varved lake sediments in west central Sweden. Quaternary Science Reviews 21, 1583-1591.

Zolitschka, B., Negendank, J.F.W., Lottermoser, B.G., 1995. Sedimentological proof and dating of the early Holocene volcanic eruption of Ulmener Maar (Vulkaneifel, Germany). Geologische Rundschau 84, 213-219.

Zolitschka, B., Negendank, J.F.W., 1996. Sedimentology, dating and palaeoclimatic interpretation of a 76.3 ka record from Lago Grande di Monticchio, southern Italy. Quaternary Science Reviews 15, 101 - 112.

Zolitschka, B., Wulf, S., Negendank, J.F.W., 2000. Circum-Mediterranean lake records as archives of climatic and human history. Quaternary International 73/74, 1-5.

Scientific Technical Report STR14/01, Deutsches GeoForschungsZentrum GFZ. http://doi.org/10.2312/GFZ.b103-14010

5. Manuscripts

5.1 Manuscript #1

"Tephrochronology of the 100 ka lacustrine sediment record of Lago Grande di Monticchio (southern Italy)" *(S. Wulf, M. Kraml, A. Brauer, J. Keller & J.F.W. Negendank, 2004: Quaternary International)*

Scientific Technical Report STR14/01, Deutsches GeoForschungsZentrum GFZ. http://doi.org/10.2312/GFZ.b103-14010

Available online at www.sciencedirect.com
SCIENCE DIRECT®
Quaternary International 122 (2004) 7–30

Tephrochronology of the 100 ka lacustrine sediment record of Lago Grande di Monticchio (southern Italy)

Sabine Wulf[a,*], Michael Kraml[b], Achim Brauer[a], Jörg Keller[c], Jörg F.W. Negendank[a]

[a] GeoForschungsZentrum Potsdam, Section 3.3, Climate Dynamics and Sediments, Telegrafenberg, D-14473 Potsdam, Germany
[b] Bundesanstalt für Geowissenschaften und Rohstoffe, Stilleweg 2, D-30655 Hannover, Germany
[c] Institut für Mineralogie, Petrologie und Geochemie, Albert-Ludwigs-Universität Freiburg, Albertstrasse 23b, D-79104 Freiburg i.Br., Germany

Abstract

The results of a tephrochronological study on 340 distal tephra layers intercalated within 72.5 m of sediments in Lago Grande di Monticchio (southern Italy) are outlined. This maar lake provides a continuous, high temporal resolution record of climate and environmental change for the last 100 kyr. From a total of 340 intercalated tephra layers, 42 prominent tephras have been selected for detailed microscopic, chemical and chronological investigations in order to obtain a second chronological fundament complementary to the varve-supported sedimentation rate chronology providing in combination a high precision timescale of this important palaeoclimatic record. All these tephra layers have been correlated with highly explosive eruptions of Central and South Italian volcanoes. The historically dates, radiometric, radioisotopic and interpolated ages of 26 correlated tephra events and direct laser $^{40}Ar/^{39}Ar$ dates for Monticchio tephra layers are consistent with ages of tephra deposition provided by the independent sedimentation rate chronology of Monticchio sediments with a mean deviation of ~5%. Aside from its tephrochronological purpose, the study of tephra layers in the Monticchio sediments also contributes to a better knowledge of the explosive history of Italian volcanoes and the dispersal of erupted tephra material.

1. Introduction

Several scientific projects have been established during the past years in order to reconstruct the palaeoclimatic and palaeoenvironmental development of terrestrial sites, not only on national but also on a European level (e.g. the European Lake Drilling Project (ELDP), Euromaar). Maar lake sediments in the circum-Mediterranean region are of special interest. Such deposits provide (a) potentially continuous records covering a time span from the present day back through several glacial/interglacial cycles (e.g. Lac du Bouchet), (b) a high temporal resolution due to high sedimentation rates and the preservation of annual laminations and (c) considerable potential for tephrochronological investigations due to the vicinity to explosive volcanoes. The ~100 ka sediment record from the maar lake Lago Grande di Monticchio in southern Italy has the potential for studying both the environmental change during the last Glacial/Interglacial cycle (e.g. Zolitschka and Negendank, 1996; Allen et al., 1999; Brauer et al., 2000) and the explosive history of nearby volcanoes. A total number of 340 distal tephra layers are preserved in the sediments of Lago Grande di Monticchio, most of them primary air fall deposits that previously have been dated by an independent varve-supported sedimentation rate chronology. Initial results of physical and chemical investigations on 14 major ash deposits occurring in the upper part of the sediment record have suggested that most tephras originate from South Italian explosive volcanoes (Newton and Dugmore, 1993; Narcisi, 1996). This paper reports on the tephrochronology of the complete 100 ka record compiled on the base of new geochemical and chronological data of 42 prominent tephra layers.

2. The study site

Lago Grande di Monticchio (40°56′N, 15°35′E, 656 m a.s.l.) is located 120 km east of Naples in the Monte

*Corresponding author. Fax: +49-331-2881302.
E-mail address: wulf@gfz-potsdam.de (S. Wulf).

1040-6182/$ - see front matter © 2004 Elsevier Ltd and INQUA. All rights reserved.
doi:10.1016/j.quaint.2004.01.028

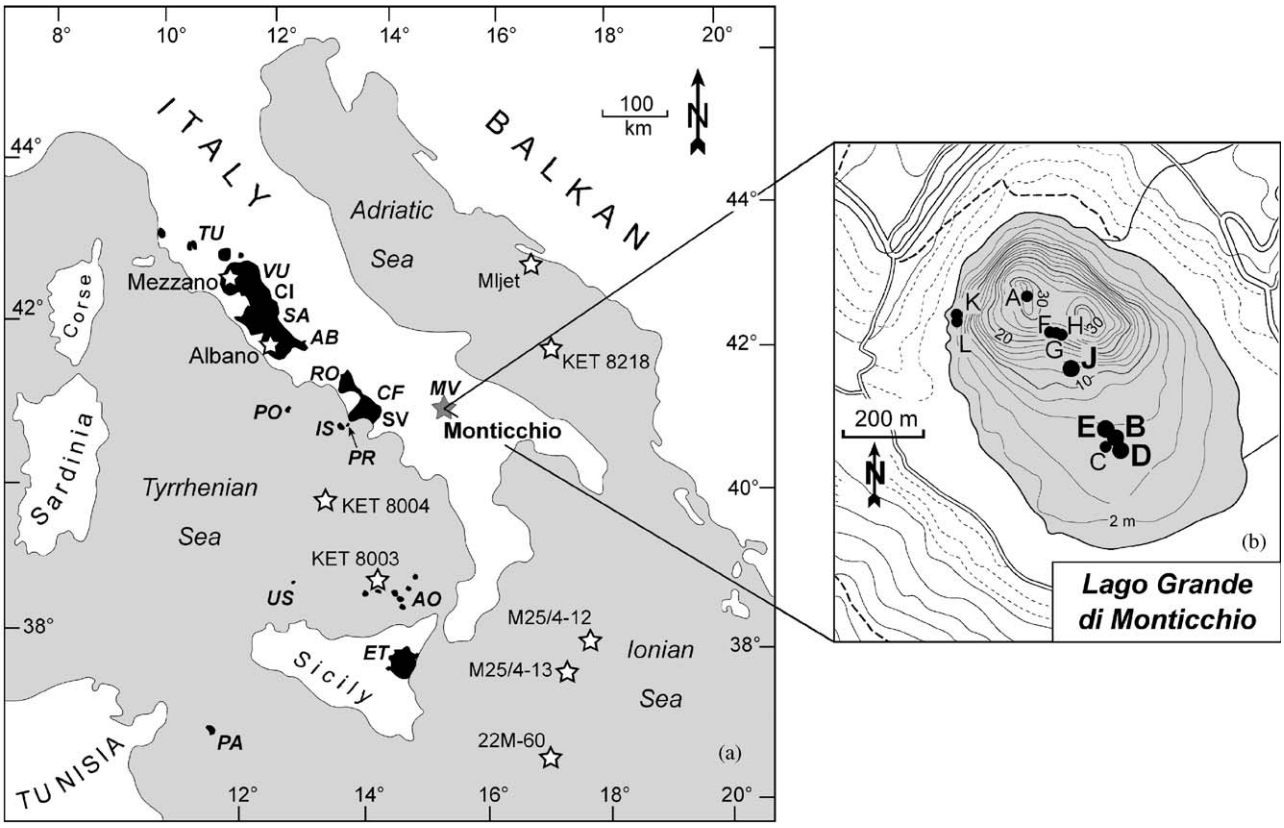

Fig. 1. (a) Schematic map of the distribution of Quaternary Italian volcanoes, location of Lago Grande di Monticchio (grey star) and other lacustrine and marine sites mentioned in the text (white stars). Abbreviations of volcanic districts: TU = Tuscany. Roman Province: VU = Vulsini Hills, CI = Cimini District (including Vico volcano), SA = Sabatini Volcanic District, AB = Alban Hills. Campanian Province: PO = Ponza Islands, RO = Roccamonfina, CF = Phlegrean Fields (Phlegrean Fields), SV = Vesuvius, IS = Ischia Island, PR = Procida-Vivara, MV = Monte Vulture. Aeolian and Sicilian District: US = Ustica Island, AO = Aeolian Islands, ET = Etna, PA = Pantelleria. (b) Bathymetric map and position of coring sites at Lago Grande di Monticchio. Studied cores are labelled in bold.

Vulture volcanic complex in the region of Basilicata, southern Italy (Fig. 1a). It represents the larger of two adjacent maar lakes that were formed 132 ± 12 ka ago during the last phreatomagmatic eruptions in a caldera on the western slopes of Monte Vulture (Brocchini et al., 1994; Stoppa and Principe, 1998). Volcanic activity of Monte Vulture started approximately 740 ka ago with a main phase between 660 and 480 ka (Brocchini et al., 1994). Because of the alkaline composition of erupted products, Monte Vulture has been assigned to the Roman Comagmatic Province (Washington, 1906). Volcanoes of this district are located 100–350 km west to northwest of Lago Grande di Monticchio (Fig. 1a) and are characterized by intense explosive activity during the late Quaternary.

Lago Grande di Monticchio (LGM) has a lake surface area of 0.4 km^2 and a maximum water depth of 36 m (Fig. 1b). Its present trophic state is eutrophic to polytrophic. The catchment area of LGM mainly comprises phonotephritic pyroclastic and epiclastic deposits of the younger volcanic period of Monte Vulture.

3. Materials and chronology

During coring campaigns in 1990 and 1994, a total number of 11 sediment cores with a maximum length of 65 m were recovered within the basin of Lago Grande di Monticchio (Fig. 1b) using a modified Livingston piston corer. Based on macroscopic and microscopic correlations, four overlapping sediment cores were chosen to construct a continuous composite profile of 72.5 m length (Zolitschka and Negendank, 1996; Brauer et al., 2000; Fig. 2). In general, sediments are organic-rich to minerogenic-calcareous in composition and laminated for the most part of the record. Annual laminations (organic varves), in turn, are restricted to ~10% of the total sequence. The chronology of the sediment record has been established by counting the varved sections and calculating sedimentation rates in sections of poor varve preservation and non-laminated parts (Zolitschka and Negendank, 1996; Brauer et al., 2000). This 'varve-supported sedimentation rate chronology' provides an age of 101,670 yr BP for the base of the record (Fig. 10) with a roughly estimated dating error of 5–10% (Brandt

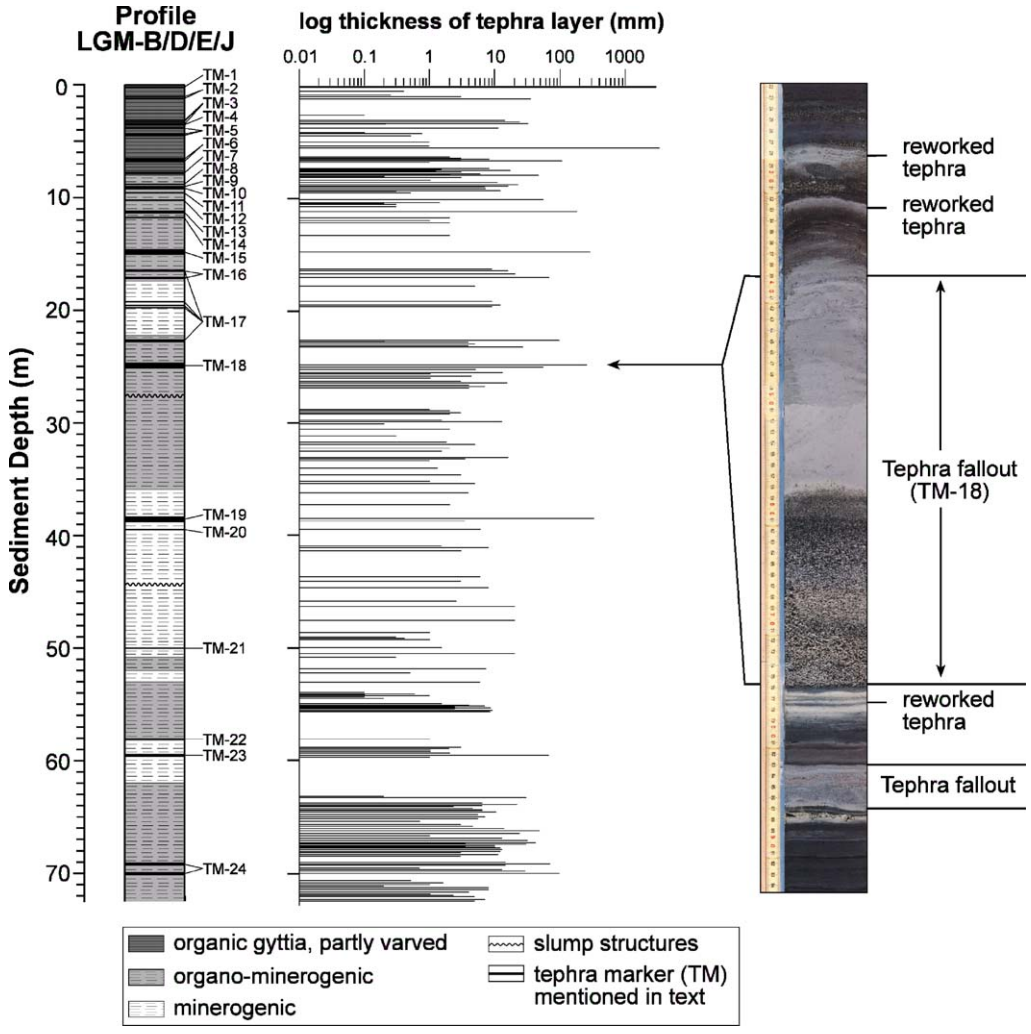

Fig. 2. Sedimentology and tephrostratigraphy of composite profile LGM-B/D/E/J from Lago Grande di Monticchio (left). Example of fallout and reworked tephra deposition in the Monticchio sediments (right).

et al., 1999; Brauer et al., 2000). The younger part of the chronology has been confirmed by several radiocarbon datings on macrofossils occurring in the sediments and laser $^{40}Ar/^{39}Ar$ dates on distal tephra layers (Watts, 1985; Robinson et al., 1993; Watts et al., 1996a; Hajdas et al., 1998).

4. Tephrochronological methods

In addition to numerous (epi-) clastic layers, a total number of 340 distal tephra layers occur within the Monticchio record, ranging in thickness from 0.1 mm to 33.2 cm (Fig. 2). Most of the tephra layers visible by naked eye are supposed to be primary air fall deposits. Only a few ash layers ($n < 20$) may be re-deposited due to subsequent erosional and depositional processes around the catchment and in the lake as described by (e.g.) Boygle (1999). Epiclastic layers have been distinguished from distal tephra layers on the base of the absence of fresh volcanic glasses and their typical assemblage of lithics (volcanic and sedimentary rock fragments), pheno- and xenocrysts (green clinopyroxene, hornblende, k-feldspar, plagioclase, nepheline, biotite, hauyn, leucite, sodalite).

Single tephra layers were described in respect of their macroscopic and microscopic features. The mineral/lithic assemblage and chemical composition of tephra layers were determined on polished thin sections, which were prepared using the freeze-fry technique and subsequent impregnation of sediment with epoxy resin (Brauer et al., 2000). Microscopic inspection of these thin sections additionally provided information about the original structure of tephra layers and grain size distribution of tephra components. For chemical classification, major-element analyses on single glass shards of tephra layers were carried out using a Cameca SX-100 electron microprobe (WDS) with an accelerating voltage of 15 kV and a beam current of 20 nA. Large beam sizes of diameter 15 and 20-μm were chosen because of the

loss of sodium during electron microprobe analysis of volcanic glass (Nielsen and Sigurdsson, 1981; Hunt and Hill, 1993). Peak counting times were 20 s for each element, except for Na analysed 10 s. Instrumental calibration used interlaboratory natural mineral and glass reference materials (Lipari obsidian; Hunt and Hill, 1996). At least ten glass shards per tephra were measured according to the homogeneity of samples. Individual analyses of glass shards with total oxide sums lower than 95 wt% have been excluded. The data of accepted analyses of individual tephra layers were recalculated to 100 wt% and given as a mean with 1σ standard deviation of n glass shards. Chemical classification is based on the Total-Alkali-Silica diagram after Le Bas et al. (1986).

5. Chemical and mineralogical features of tephras

For distinguishing and correlating tephras, the major-element glass chemistry of individual tephra layers is the most powerful method. In general, chemical analyses on micro-pumices, scoria and glass shards do not reflect any hydration processes and, therefore, suggest that major elements in volcanic glass remain stable in the lake environment during the 100 kyr time period (see also Wulf, 2000). The characterization of the mineral and lithic assemblage, in turn, was a supplementary useful correlative tool, although it is known that preferential settling of tephra with distance from the volcanic source can lead to significant variations in mineralogical-lithological composition (e.g. Fisher and Schmincke, 1984).

The major-element glass chemistry of the 340 distal tephra layers in the Monticchio record shows a broad spectrum of predominantly alkaline basic, intermediate and acid volcanics (Fig. 3, Table 2). According to their silica and total alkali contents, tephras can be divided in five petrogenetic groups: (A) alkali-trachytes, (B) high-K-alkaline trachytes to phonolites and latites, (C) K-alkaline phonolites, tephriphonolites, phonotephrites and foidites (slightly to highly under saturated rocks), (D) Na-alkaline trachydacites to rhyolites and (E) calc-alkaline volcanics, trachyandesites to trachydacites. These groups are characterized by following common mineral associations: (A) sanidine–biotite–aegerine–augite; (B) sanidine–plagioclase–augite–biotite ± olivine ± leucite; (C) augite–diopside–leucite–sanidine–plagioclase–biotite ± nepheline; (D) plagioclase–alkali-feldspar–augite–amphibole; and (E) plagioclase–augite–hypersthene. In addition to the primary mineral associations, some tephras contain extraordinary types of minerals, like e.g. acmite (TM-20) or scapolite (TM-4; Table 1). Different portions of apatite and Fe–Ti-oxides microcrysts occur in juvenile clasts of most tephra layers.

6. Origin of tephra layers

For correlation of tephra layers, a careful inspection of possible volcanic sources was required taking into

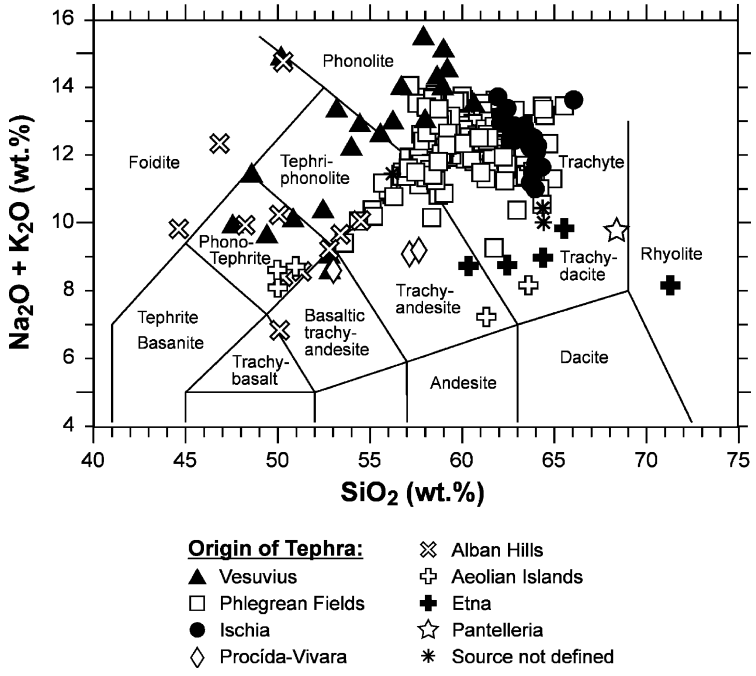

Fig. 3. Total-Alkali-Silica diagram after Le Bas et al. (1986) showing the mean values of electron microprobe analyses (water-free) of glass shards of 340 distal tephra layers occurring in the Monticchio record.

Table 1
Depths, ages, composition and origin of correlated distal tephra layers occurring in the sediment record of Lago Grande di Monticchio

Tephra	Depth (cm)	Varve age (yr BP)	Thickness (mm)	Colour of tephra	Phenocrysts	Lithics	Chemistry	Origin	Volcanic event
TM-1	6.1	90	9.0	Grey	cpx, amp, kf, plg, bt, lc, ap	T, V, C	P/TP	Vesuvius	AD 1631
TM-2a	110.4	1420	3.0	Dark grey	lc, cpx, bt, ol, kf, plg	T, V, C	TP/PT	Vesuvius	AD 512
TM-2b	115.3	1440	35.0	Dark grey	cpx, ol, amp, lc, kf, plg, bt	T, V, C	F/P–BtrA	Vesuvius	Pollena, AD 472
TM-3a (L1)[a]	309.9	3990	22.0	Grey	lc, bt, cpx, plg, kf	T, V, C	TP/P	Vesuvius	AP4
TM-3b (L2)[a]	313.9	4020	24.0	Light grey	cpx, lc, bt, plg, kf, ap	V, T	P	Vesuvius	AP3
TM-3c (L3)[a]	328.3	4150	31.0	White–grey	cpx, bt, lc, kf, plg, (amp)	V, C, T	P	Vesuvius	AP2
TM-4	345.6	4310	6.0	White–grey	kf, cpx, so, plg, bt, ne, sc	V, C	P	Vesuvius	Avellino
TM-5a	370.2	4620	11.0	White	kf, cpx, bt, plg, ap	V	P/Tr	Phlegrean Fields	Agnano Monte Spina, D1?
TM-5b	373.7	4660	3.0	White	kf, cpx, bt, plg, ap	V	Tr	Phlegrean Fields	Agnano Monte Spina
TM-5c	421.3	5390	0.8	Grey	kf, cpx, bt, plg, ap	—	P	Phlegrean Fields	Agnano Monte Spina, B1?
TM-5d	441.3	5680	0.5	Grey	kf, cpx, bt, plg, ap	—	P/Tr	Phlegrean Fields	Agnano Monte Spina
TM-6a	655.0	9620	8.0	Grey	cpx, kf, plg, bt, amp	V, C, T	P/Tr	Vesuvius	Mercato (Pomici e proietti)
TM 6b (L4)[a]	668.5	9680	106.0	White–grey-green	kf, plg, cpx, bt, me, ne	V, T, C	P–P/TP–Tr	Vesuvius	Mercato (Pomici Gemelle)
TM-7a	777.5	12,170	6.0	Brown	kf, plg, cpx, bt, lc, ol	T, V	L/TP	Phlegrean Fields	Pomici Principali (top)
TM-7b (L5)[a]	789.0	12,180	47.0	Grey-brownish	kf, plg, cpx, bt, ol, lc	T, V	P	Phlegrean Fields	Pomici Principali (base)
TM-8 (L6)[a]	864.5	14,120	22.0	Light brown	kf, plg, cpx, ol, bt, ap	V	Tr–L/TP	Phlegrean Fields	Neapolitan Yellow Tuff
TM-9 (L7)[a]	883.4	14,560	18.0	White	kf, plg, cpx, bt	V	Tr	Phlegrean Fields	Tufi Biancastri (VM1)
TM-10a	901.6	15,030	4.0	Pink-brownish	kf, plg, bt, cpx	V	Tr	Phlegrean Fields	Lagno Amendolare (top)
TM-10b	907.7	15,220	7.0	Pink–grey	kf, bt, cpx	V	Tr/P	Phlegrean Fields	Lagno Amendolare
TM-10c	913.0	15,300	1.0	Grey-brownish	plg, kf, bt, cpx	V	Tr	Phlegrean Fields	Lagno Amendolare
TM-10d	920.9	15,550	4.0	Light grey	kf, plg, bt, cpx	V	Tr	Phlegrean Fields	Lagno Amendolare (base)
TM-11	957.0	16,440	0.5	Dark brown	plg, kf, cpx, amp, ap	V, T	TrD–TrA	Mt. Etna	Biancavilla Ignimbrite, Y-1
TM-12 (L8)[a]	1015.5	17,560	55.0	Grey	kf, plg, cpx, bt, amp, ne, lc	V, C, T	P	Vesuvius	Greenish (Verdoline)
TM-13 (L9)[a]	1117.1	19,280	170.0	White–black	kf, plg, cpx, bt, amp	T, V, C	Tr–L/TP–BtrA	Vesuvius	Pomici di Base
TM-14	1176.6	20,150	2.0	Dark brown	kf, plg, cpx, bt, ol	T, V, S	BtrA	Procida	Solchiaro
TM-15 (L10)[a]	1471.9	23,930	286.0	Beige	kf, plg, bt, cpx	V, T	Tr	Phlegrean Fields	Y-3
TM-16a	1650.5	26,130	16.0	Dark brown	lc, cpx, kf, plg, bt	T, C, V	TP - Tr	Vesuvius	Codola (top)
TM-16b (L11)[a]	1710.4	26,790	68.0	White–dark brown	cpx, kf, plg, bt, ti	T, C, V	Tr/P	Vesuvius	Codola (base)
TM-17a	1633.7	25,930	9.0	Brown	lc, cpx, bt, kf, plg, ne, ap	C, V, T	PT	Alban Hills	Peperino Albano Ignimbrite
TM-17b	1638.0	25,990	7.0	Brown–black	lc, cpx, bt, kf, plg, ne, ap	C, V, T	PT	Alban Hills	Peperino Albano Ignimbrite
TM-17c	1917.6	29,690	9.0	Grey-brown	cpx, kf, plg, bt, ap	C, V, T	TP	Alban Hills	
TM-17d	1948.5	29,870	12.0	Dark brown	cpx, kf, plg, bt, ap	C, V, T	PT–TP	Alban Hills	Peperino Albano
TM-17e	1963.0	29,900	9.0	Grey–brown	cpx, kf, plg, bt, ap	C, V, T	PT–TP/L	Alban Hills	(units I—IV)
TM-17f	2270.4	30,530	97.0	Grey–brown	cpx, bt, kf, lc	V, C, S, T	—	Alban Hills	
TM-18 (L12)[a]	2495.2	32,970	257.0	Beige–grey	kf, plg, bt, cpx	V, S, T	Tr–P	Phlegrean Fields	Campanian Ignimbrite, Y-5
TM-19 (L14)[a]	3863.8	56,250	332.0	Beige–greenish	kf, bt, cpx, plg	V	Tr	Ischia	Tufo Verde Epomeo *ss.*
TM-20	3953.7	57,570	6.0	Beige	kf, bt, plg, cpx, ac, ti	V	Tr	Ischia	UMSA, Y-7
TM-21	5004.0	74,540	1.5	Pale brown–pink	plg, cpx, opx, bt, kf, ap	V, T	TrA–TrD	Stromboli	Petrazza Tuffs, Y-9
TM-22	5824.3	85,320	1.0	Pale brown	kf, plg, cpx, ap	-	TrD/R	Pantelleria	Ante Green Ignimbrite, P-10
TM-23	5964.9	85,670	66.0	Light brown	cpx, kf, bt, plg, lc, ne, ap	V, C, S, T	—	Sabatini	Tufo di Baccano
TM-24a	6929.7	97,770	70.0	Pink–brownish	plg, cpx, bt, kf, (lc)	T, V, S	Tr	Campanian	X-5 (Pumice fallout)
TM-24b	7019.8	98,750	97.0	Pale brown	plg, kf, cpx, bt	(V)	Tr	Province	X-5 (Co-ignimbrite)

Abbreviations: kf = sanidine, plg = plagioclase, cpx = clinopyroxene, opx = orthopyroxene, bt = biotite, amp = amphibole, ol = olivine, lc = leucite, so = sodalite, ne = nepheline, sc = scapolite, ap = apatite, me = melanite, ac = acmite, ti = titanite; T = tachylites; V = volcanics; C = carbonatic rocks, skarns; S = sedimentary rocks (sand-, siltstones); Tr = Trachyt, P = Phonolite, TP = Tephriphonolite, PT = Phonotephrite, F = Foidite, BtrA = Basaltic Trachyandesite, TrA = Trachyandesite, L = Latite, TrD = Trachydacite, R = Rhyolite.

[a] L1–L14, nomenclature of tephra layers after Narcisi (1996).

account (a) the vicinity of explosive volcanoes and prevailing wind directions, (b) the timing of high-explosive eruptions (<102 ka) and (c) the petrology of erupted products. During the Late Quaternary, numerous explosive volcanoes were active in central and southern Europe. In central Europe, volcanism of the Auvergne (Massif Central, France) lasted until 6000 yr BP. However, the eruption of larger volumes of pyroclastics occurred from (e.g.) the Mont Dore Massif before the considered time span (3.8 Ma–250 ka; Boivin et al., 1991). The Eifel volcanic district in western Germany produced the phonolitic Laacher See Tephra at 12,900 ± 560 yr, which is widespread only in central and northern Europe (van den Bogaard, 1995; Schmincke et al., 1999). In the Mediterranean, explosive activity is known from volcanoes of the Italian Peninsula, the Hellenic Arc (e.g. Santorini) and Central Anatolia (Turkey). Although the tephra fallout of Hellenic and Anatolian volcanic eruptions is mainly calc-alkaline in composition and dispersed only in the very eastern part of the Mediterranean (Keller et al., 1978; Druitt et al., 1995), the Italian potassic volcanoes provide a more likely source for tephras, also due to their relative proximity and the favourable downwind location of the Monticchio maar lake. During the last 102 kyr, most of the Italian volcanoes were active, particularly those of the nearby Campanian Province, 100–150 km west of Lago Grande di Monticchio (Fig. 1a). High-explosive eruptions of Vesuvius, the Phlegrean Fields, the Islands of Ischia and Procida-Vivara have produced numerous tephra layers, also occurring in deep-sea sediments of the eastern Mediterranean Sea (e.g. Keller et al., 1978; Paterne et al., 1986, 1988; Narcisi and Vezzoli, 1999; Keller et al., in prep.). Volcanic activity of the Roman Province in central Italy, 260–350 km northwest of Monticchio (Fig. 1a), was restricted to final phreatomagmatic eruptions of the Alban Hills and the Sabatini Volcanic District during this period. Late Quaternary highly explosive eruptions also occurred at the Aeolian Islands, Etna and the Island of Pantelleria, 280–540 km south to southwest of the Monticchio maar lake (Fig. 1a). In the following section, the primary chronological and petrological features of the Italian high-explosive volcanoes are discussed.

7. Campanian province

7.1. Vesuvius

Vesuvius stratovolcano, located 20 km east of Naples, started its activity approximately 25 ka ago (Santacroce, 1987). During this period, four caldera-forming events have been recognized, each occurring during major Plinian eruptions (Cioni et al., 1999). In the last 3600 years, volcanic activity was characterized by several sub-Plinian eruptions and minor strombolian-vulcanian events (Rolandi et al., 1998; Andronico and Cioni, 2002). The last historical eruption occurred in AD 1944. From the petrological viewpoint, the Vesuvius pyroclastics display a wide variability from nearly saturated (trachytes–phonolites) changing with time to highly under saturated high-potassic rocks (leucititic phonolites to tephrites) (e.g. Santacroce, 1987).

7.2. Phlegrean fields

Volcanism at the Phlegrean Fields (CF), bordered on the western district of Naples, commenced more than 60 kyr ago and was mainly explosive (Rosi and Sbrana, 1987; Orsi et al., 1996; Pappalardo et al., 1999). The recent caldera structure resulted from two main collapses related to the high-explosive eruptions of the 'Campanian Ignimbrite' (CI, 37 ka) and the 'Neapolitan Yellow Tuff' (NYT, 14 ka BP). Volcanism between the CI and NYT eruptions was restricted to minor hydromagmatic eruptions. After the NYT-event, about 72 eruptions occurred in three epochs of volcanic activity (Di Vito et al., 1999). The most recent eruption formed the Monte Nuovo tuff cone in AD 1538. Phlegrean Fields pyroclastic products are typical high-K-trachytic to phonolitic in composition with K_2O contents $\gg Na_2O$ (e.g. Rosi and Sbrana, 1987).

7.3. Island of Ischia

Volcanism at the Island of Ischia was mainly characterized by large pyroclastic and numerous small monogenetic eruptions. Five phases of Ischia volcanic activity have been distinguished (Poli et al., 1987; Vezzoli, 1988): The initial period of pre-Monte Epomeo activities comprises an older phase of high pyroclastic activity at >150 ka and a younger period of lava dome emplacements between 150 and 75 ka. The following phase included the eruption of huge ignimbrites of the Tufo Verde Epomeo at ca 56 ka and the thick pyroclastic deposits of the Citara Formation between 48 and 33 ka (Poli et al., 1987). The eruption phase between 28 and 18 ka as well as the youngest historical phase (10 ka BP–AD 1302) were dominated by the emplacement of lava flows and minor deposition of pyroclastic fallout originating from monogenetic cones. Ischia volcanics show a typical uniform peralkalic trachytic composition with K_2O contents $\leqslant Na_2O$ (e.g. Poli et al., 1987).

7.4. Island of Procida-Vivara

Volcanic activity of the double-Island of Procida-Vivara in the Gulf of Naples was restricted between 40 and 14 ka BP and characterized mainly by low-energetic

explosive eruptions (Scandone et al., 1991). Only two high-explosive events occurred, the eruption of the 'Fiumicello' and the more widespread 'Solchiaro' pyroclastics at 31 and 19 ka BP, respectively. Deposits of these formations are trachybasaltic in composition (Rosi et al., 1988; Scandone et al., 1991).

8. Roman province

8.1. Alban Hills

The Alban Hills, situated 15 km southeast of Rome, are formed from a huge volcanic complex (Federico et al., 1994). Volcanic activity at the Alban Hills started 630 ka ago with the alternating eruption of lavas and large pyroclastic units, ultrapotassic in composition (Trigila, 1995). During the younger phreatomagmatic phase starting at 106 ka, several maar craters were formed accompanied by the eruption of small-volume basic ignimbrites (e.g. Lago di Albano, Lago di Nemi; Trigila, 1995). One of the most recent products are the tephritic-foiditic 'Peperino Albano' phreatomagmatic ignimbrites erupting at ca 30 ka BP (De Vries in Fornaseri et al., 1963; Giordano et al., 2002).

8.2. Sabatini Volcanic District

The Sabatini Volcanic District, located approximately 30 km northwest of Rome, was the site of intense volcanic activity, which started at 600 ka and continued until 40 ka (De Rita and Zanetti, 1986; De Rita et al., 1993). Huge volumes of leucite-rich phonotrachytic pyroclastic flows and surges were emplaced during the older period, while highly explosive activity was concentrated between 288 ka and the final hydromagmatic eruptions of "Baccano", "Martignano" and "Stracciacappa" (De Rita et al., 1993).

9. Sicilian-aeolian province

9.1. Mount Etna

Mount Etna, located on the eastern coast of Sicily, is the largest active volcano in Europe. Its persistent activity is mainly effusive with products of mugearitic, hawaiitic and basaltic composition, although tephra-producing events occurred. For the time interval 100 ka to the Present, five periods of explosive activity, mainly eruptions of strombolian to sub-Plinian and Plinian benmoreitic types, have been identified (Coltelli et al., 2000). The highest energy eruptions of Plinian magnitude produced two pyroclastic fallout deposits at 100–80 ka (Unit B) and 17 ka cal. BP (Unit D), respectively.

9.2. Aeolian islands

The Aeolian arc comprises seven mainly calc-alkaline volcanic islands that were active during the Late Pleistocene. Major explosive eruptions are known from Salina, Lipari, Vulcano and Stromboli, but most of them showing a restricted dispersal of fallout products on a local to regional scale (Keller, 1982). One of the largest volcanic events was the eruption of the trachyandesitic 'Petrazza Tuffs' of Stromboli dated at 79 ka (Hornig-Kjarsgaard et al., 1993).

9.3. Island of Pantelleria

Volcanism on the Island of Pantelleria started at least 300 kyr ago and was characterized by the emplacement of felsic and minor mafic peralkaline volcanic rocks (Cornette et al., 1983; Civetta et al., 1984; Mahood and Hildreth, 1986). Huge volumes of welded ignimbrites were erupted between 133 and 79 ka ('Ante-Green Ignimbrites') and at $\sim$50 ka ('Green Tuff'). Tephra fallout from these eruptions are widely dispersed to the North and Northeast, and deposited within deep-sea sediments of the Tyrrhenian and Ionian Seas (Keller et al., 1978; Paterne et al., 1988, 1990).

10. Results of tephra correlation

According to the chemical, mineralogical and lithological data, all distal tephra layers in the Monticchio record have been correlated with Italian explosive volcanoes located in the Roman, Campanian and Sicilian-Aeolian provinces. More than 300 tephras originate from the nearby Campanian volcanoes including Vesuvius, the Phlegrean Fields and the Islands of Ischia and Procida-Vivara. A minor number of tephra layers derive from high-explosive eruptions of the Alban and Sabatini Hills, the Aeolian Island volcanoes, Mount Etna, and Pantelleria Island. These tephras are easy to distinguish due to their conspicuous chemical composition (Fig. 3). For the Campanian volcanoes, there are more difficulties in distinction between eruptions from the same volcano, particular those of Ischia and the Phlegrean Fields, due to the homogeneity of erupted magmas. From all 340 tephras, it was possible to reliably correlate 42 explosive events, some well-dated, that form 24 tephra units representing certain eruptive cycles from different Italian volcanoes through a combination of geochemical, mineralogical and stratigraphical data of individual tephra layers. Single tephra layers are marked with letters in alphabetic order from the top to the base of the tephra unit (e.g. TM-2a, TM-2b etc.) and dated by the varve-supported sedimentation rate chronology (rounded varve yr BP, 1950). In the following, the essential features of composition, age,

Table 2
Selected electron microprobe major-element data (water-free) of glass shards from correlated distal tephra layers occurring in the sediment record of Lago Grande di Monticchio

Tephra	TM-1		TM-2a		TM-2b		TM-2b		TM-3a		TM-3b		TM-3c		TM-4		TM-5a		TM-5b		TM-5c		TM-5d	
Varve age	90	SD	1420	SD	1440a	SD	1440b	SD	3990	SD	4020	SD	4150	SD	4310	SD	4620	SD	4660	SD	5390	SD	5680	SD
SiO_2	53.14	0.51	48.44	0.69	50.26	0.99	52.82	1.28	54.45	0.43	56.25	0.15	57.13	0.74	55.91	0.95	59.83	0.84	60.74	0.38	58.16	0.21	60.80	0.68
Ti_2O	0.50	0.08	0.83	0.09	0.50	0.07	1.67	0.07	0.56	0.04	0.45	0.01	0.36	0.05	0.13	0.02	0.48	0.05	0.46	0.02	0.45	0.03	0.47	0.05
Al_2O_3	21.08	0.55	19.19	0.48	21.65	0.20	16.77	0.66	20.13	0.15	20.24	0.06	20.93	0.52	23.44	0.31	18.85	0.09	18.76	0.16	19.87	0.18	18.74	0.22
FeO	4.43	1.00	7.23	0.56	4.80	0.24	8.39	1.37	4.94	0.25	4.27	0.18	3.33	0.51	1.43	0.24	3.65	0.38	3.31	0.21	3.62	0.16	3.23	0.50
MnO	0.17	0.05	0.26	0.31	0.20	0.04	0.19	0.04	0.15	0.03	0.14	0.01	0.13	0.03	0.11	0.02	0.14	0.02	0.13	0.02	0.13	0.03	0.15	0.04
MgO	0.65	0.24	2.85	0.69	0.64	0.20	3.11	0.13	0.99	0.15	0.75	0.05	0.43	0.14	0.06	0.02	0.73	0.19	0.60	0.04	0.65	0.05	0.58	0.08
CaO	5.09	0.53	8.89	0.68	5.89	0.62	7.29	1.23	5.24	0.38	4.34	0.08	3.33	0.37	1.64	0.24	2.74	0.38	2.48	0.07	3.19	0.08	2.24	0.15
Na_2O	7.35	0.68	4.33	0.68	7.92	0.36	3.46	0.24	4.75	0.25	4.74	0.24	6.25	0.74	8.83	0.43	4.34	0.23	4.33	0.20	5.33	0.10	5.09	0.41
K_2O	6.58	1.33	6.86	1.04	6.94	0.73	5.07	0.98	8.11	0.35	8.21	0.05	7.47	0.97	7.82	0.48	8.59	0.13	8.56	0.33	7.96	0.16	8.16	0.34
P_2O_5	0.23	0.29	0.59	0.13	0.29	0.17	1.11	0.06	0.19	0.06	0.15	0.01	0.08	0.04	0.03	0.03	0.13	0.06	0.10	0.04	0.12	0.04	0.09	0.05
Cl	1.01	0.15	0.69	0.11	1.07	0.19	0.15	0.10	0.65	0.04	0.61	0.01	0.70	0.07	0.40	0.23	0.65	0.06	0.69	0.06	0.62	0.04	0.59	0.14
F	0.00	0.00	0.00	0.00	0.14	0.11	0.00	0.00	0.00	0.00	0.00	0.00	0.02	0.03	0.49	0.16	0.00	0.00	0.00	0.00	0.05	0.00	0.00	0.00
Total	100.00	$n=5$	100.00	$n=10$	100.00	$n=6$	100.00	$n=3$	100.00	$n=15$	100.00	$n=5$	100.00	$n=17$	100.00	$n=10$	100.00	$n=8$	100.00	$n=17$	100.00	$n=23$	100.00	$n=8$

Tephra	TM-6a		TM-6b		TM-6b		TM-6b		TM-7a		TM-7b		TM-8		TM-8		TM-9		TM-10b		TM-10d		TM-11	
Varve age	9620	SD	9680a	SD	9680b	SD	9680c	SD	12,170	SD	12,180	SD	14,120a	SD	14,120b	SD	14,560	SD	15,220	SD	15,550	SD	16,440a	SD
SiO_2	60.06	0.95	58.73	0.31	55.57	0.00	62.83	0.00	55.69	0.25	58.38	0.89	61.66	0.11	56.77	0.24	63.39	0.50	61.94	0.16	60.46	0.89	60.67	1.20
Ti_2O	0.30	0.10	0.14	0.03	0.44	0.00	0.10	0.00	0.77	0.05	0.49	0.05	0.43	0.03	0.60	0.03	0.37	0.09	0.42	0.02	0.46	0.03	1.47	0.11
Al_2O_3	20.63	0.53	21.43	0.20	18.49	0.00	20.77	0.00	18.34	0.18	18.78	0.44	18.35	0.08	18.51	0.08	18.32	0.44	18.50	0.09	18.49	0.08	17.01	0.50
FeO	2.24	0.47	1.80	0.13	5.13	0.00	0.72	0.00	5.92	0.32	4.17	0.46	2.87	0.07	5.32	0.09	2.03	0.62	2.29	0.11	3.82	0.64	5.49	0.63
MnO	0.13	0.04	0.18	0.03	0.36	0.00	0.05	0.00	0.14	0.01	0.13	0.04	0.15	0.04	0.14	0.02	0.30	0.43	0.12	0.02	0.15	0.06	0.18	0.03
MgO	0.16	0.07	0.07	0.01	1.02	0.00	0.02	0.00	2.13	0.14	1.00	0.53	0.44	0.03	1.63	0.07	0.38	0.26	0.43	0.02	0.82	0.21	1.88	0.43
CaO	2.42	0.41	1.77	0.25	5.98	0.00	1.75	0.00	5.04	0.39	3.50	0.85	2.18	0.03	4.83	0.15	1.94	0.12	2.27	0.07	2.98	0.38	3.85	0.54
Na_2O	5.59	1.07	8.58	0.18	7.22	0.00	4.71	0.00	3.50	0.10	3.89	0.21	4.91	0.13	3.50	0.07	4.71	0.54	4.85	0.25	3.97	0.40	5.23	0.64
K_2O	8.03	0.85	6.76	0.54	5.35	0.00	8.96	0.00	7.67	0.18	9.02	0.49	8.49	0.08	8.00	0.07	8.16	0.71	8.73	0.27	8.30	0.12	3.29	0.25
P_2O_5	0.05	0.03	0.02	0.02	0.03	0.00	0.00	0.00	0.39	0.12	0.16	0.06	0.05	0.03	0.36	0.06	0.04	0.02	0.06	0.04	0.14	0.05	0.61	0.21
Cl	0.51	0.15	0.58	0.04	0.52	0.00	0.12	0.00	0.53	0.04	0.62	0.06	0.62	0.01	0.44	0.02	0.45	0.22	0.50	0.03	0.53	0.04	0.42	0.04
F	0.01	0.03	0.10	0.09	0.01	0.00	0.00	0.00	0.00	0.00	0.00	0.00	0.00	0.00	0.00	0.00	0.00	0.00	0.00	0.00	0.00	0.00	0.00	0.00
Total	100.00	$n=13$	100.00	$n=10$	100.00	$n=1$	100.00	$n=1$	100.00	$n=10$	100.00	$n=19$	100.00	$n=4$	100.00	$n=5$	100.00	$n=12$	100.00	$n=14$	100.00	$n=3$	100.00	$n=9$

Tephra	TM-11		TM-12		TM-13		TM-13		TM-13		TM-13		TM-14		TM-15		TM-16a		TM-16a		TM-16b		TM-17a	
Varve age	16,440b	SD	17,560	SD	19,280a	SD	19,280b	SD	19,280c	SD	19,280d	SD	20,150	SD	23,930	SD	26,130a	SD	26,130b	SD	26,790	SD	25,930	SD
SiO_2	65.53	0.23	59.56	0.59	52.91	0.99	54.25	0.74	60.25	0.53	62.54	0.44	53.02	0.38	62.29	0.79	52.46	1.69	62.31	0.14	58.65	0.65	50.07	0.68
Ti_2O	0.82	0.04	0.35	0.03	1.35	0.09	0.74	0.16	0.42	0.02	0.31	0.03	1.63	0.06	0.38	0.03	0.79	0.09	0.36	0.01	0.50	0.06	0.93	0.07
Al_2O_3	17.05	0.11	19.00	0.22	16.50	0.18	18.99	0.62	18.67	0.21	18.47	0.33	17.30	0.02	18.39	0.20	19.07	0.86	18.47	0.07	19.72	0.41	19.76	0.60
FeO	3.32	0.07	3.45	0.14	8.46	0.18	6.16	0.31	3.69	0.29	2.68	0.12	8.54	0.22	3.27	0.29	7.07	0.61	3.22	0.02	3.67	0.33	7.56	0.82
MnO	0.20	0.02	0.15	0.03	0.16	0.01	0.14	0.03	0.16	0.03	0.18	0.03	0.15	0.01	0.13	0.04	0.16	0.03	0.07	0.01	0.12	0.03	0.19	0.04
MgO	0.88	0.07	0.31	0.07	3.39	0.22	2.19	0.15	0.59	0.14	0.29	0.12	3.08	0.14	0.61	0.15	1.85	0.31	0.60	0.00	0.55	0.14	1.98	0.30
CaO	1.88	0.13	3.37	0.19	7.12	0.55	6.76	1.88	3.78	0.50	2.65	0.26	6.96	0.25	2.19	0.22	7.13	1.24	2.08	0.04	4.30	0.95	8.30	0.67
Na_2O	6.12	0.37	4.41	0.20	2.95	0.24	3.64	1.04	3.82	0.11	4.51	0.29	4.15	0.09	3.85	0.44	3.66	0.43	3.95	0.02	3.40	0.49	4.31	0.53
K_2O	3.71	0.05	8.75	0.34	5.90	0.15	6.38	0.36	8.09	0.31	7.80	0.25	4.44	0.16	8.37	0.55	6.67	0.62	8.57	0.13	8.59	0.40	5.93	0.67
P_2O_5	0.14	0.02	0.07	0.03	1.09	0.10	0.48	0.06	0.10	0.03	0.04	0.03	0.59	0.03	0.12	0.06	0.71	1.05	0.08	0.04	0.10	0.04	0.41	0.10
Cl	0.47	0.03	0.75	0.05	0.22	0.03	0.34	0.05	0.55	0.06	0.66	0.05	0.18	0.01	0.52	0.11	0.56	0.11	0.39	0.02	0.50	0.08	0.73	0.12
F	0.00	0.00	0.00	0.00	0.00	0.00	0.00	0.00	0.00	0.00	0.00	0.00	0.00	0.00	0.00	0.00	0.00	0.00	0.00	0.00	0.00	0.00	0.00	0.00
Total	100.00	$n=4$	100.00	$n=16$	100.00	$n=5$	100.00	$n=2$	100.00	$n=5$	100.00	$n=9$	100.00	$n=2$	100.00	$n=20$	100.00	$n=11$	100.00	$n=2$	100.00	$n=6$	100.00	$n=12$

Tephra	TM-17b		TM-17c		TM-17d		TM-17e		TM-18		TM-19		TM-20		TM-21		TM-21		TM-22		TM-24a		TM-24b	
Varve age	25,990	SD	29,690	SD	29,870	SD	29,900	SD	32,970	SD	56,250	SD	57,570	SD	74,540a	SD	74,540b	SD	85,320	SD	97,770	SD	98,750	SD
SiO_2	48.30	0.76	53.41	0.66	50.10	1.05	51.31	0.10	61.85	0.49	62.80	0.42	62.40	0.85	61.31	1.25	63.59	0.77	68.37	1.58	57.58	0.89	61.11	0.83
Ti_2O	0.91	0.07	0.76	0.14	0.92	0.05	0.86	0.04	0.42	0.02	0.57	0.04	0.57	0.04	0.71	0.10	0.99	0.06	0.63	0.08	0.50	0.05	0.40	0.03
Al_2O_3	19.40	0.36	18.71	0.93	18.43	0.45	18.86	0.22	19.16	0.22	18.98	0.19	19.00	0.23	18.90	0.90	16.01	0.09	14.45	1.00	19.02	0.18	19.00	0.23
FeO	7.28	0.56	6.93	0.86	7.52	0.43	6.96	0.07	2.94	0.09	2.66	0.10	2.76	0.36	4.32	0.51	5.40	0.31	4.97	0.12	4.30	0.41	3.35	0.31
MnO	0.15	0.04	0.17	0.03	0.17	0.03	0.15	0.03	0.24	0.02	0.28	0.07	0.24	0.03	0.11	0.02	0.15	0.03	0.24	0.02	0.14	0.02	0.13	0.05
MgO	2.45	0.16	1.79	0.39	3.90	0.51	3.43	0.08	0.35	0.02	0.35	0.06	0.38	0.11	1.27	0.40	1.48	0.26	0.35	0.07	1.14	0.19	0.63	0.19
CaO	10.18	0.72	7.55	0.64	9.47	0.79	8.76	0.12	1.74	0.07	1.16	0.10	1.21	0.28	5.68	0.82	3.60	0.30	0.82	0.20	4.05	0.48	2.57	0.29
Na_2O	3.61	0.34	2.96	0.17	2.59	0.13	2.63	0.05	5.67	0.71	6.77	0.45	6.64	0.44	4.19	0.25	4.03	0.06	5.37	0.45	4.25	0.14	4.04	0.47
K_2O	6.48	0.81	6.70	0.65	5.82	0.14	5.94	0.11	6.85	0.29	5.90	0.29	6.24	0.47	3.03	0.39	4.13	0.19	4.40	0.20	8.38	0.32	8.35	0.29
P_2O_5	0.73	0.43	0.53	0.50	0.73	0.05	0.73	0.04	0.05	0.03	0.05	0.03	0.06	0.04	0.31	0.05	0.40	0.04	0.09	0.03	0.25	0.06	0.11	0.02
Cl	0.65	0.05	0.62	0.07	0.48	0.03	0.48	0.02	0.78	0.05	0.62	0.13	0.64	0.07	0.21	0.03	0.30	0.01	0.39	0.12	0.52	0.04	0.40	0.19
F	0.01	0.02	0.00	0.00	0.00	0.00	0.00	0.00	0.19	0.17	0.00	0.00	0.00	0.01	0.00	0.00	0.00	0.00	0.00	0.00	0.00	0.00	0.00	0.00
Total	100.00	$n=9$	100.00	$n=12$	100.00	$n=9$	100.00	$n=12$	100.00	$n=43$	100.00	$n=24$	100.00	$n=17$	100.00	$n=5$	100.00	$n=4$	100.00	$n=10$	100.00	$n=34$	100.00	$n=6$

SD = 1σ standard deviation, n = number of analysed glass shards.

correlation and dispersal of the 24 tephra units and associated individual tephra layers are established, each ordered by number from the youngest to the oldest deposit (see also Tables 1–3).

10.1. TM-1

The youngest tephra in 6 cm depth in the Monticchio record, TM-1 (90 varve yr BP), is a 9 mm thick layer mainly made up of essential loose crystals and white-greyish, moderate to high vesicular and microcrysts-bearing juvenile pumice clasts (Fig. 9a). Lithic fragments are abundant in TM-1 comprising sand-sized tachylites, altered intermediate lavas and sparse carbonate rocks. From the chemical point of view, glass of tephra TM-1 shows a tephriphonolitic to phonolitic composition with remarkably high values of Al_2O_3. Both the chemical and mineralogical composition of TM-1 suggest a correlation with the Plinian fallout deposits of the AD 1631 eruption of Vesuvius (Fig. 4). Fallout products of this eruption are widely dispersed reaching as far east as Turkey (Rolandi et al., 1993a; Rosi et al., 1993). In the Monticchio record, the historical AD 1631 tephra forms an important marker for the precise dating of sediments.

10.2. TM-2

Two single, adjacent ash layers of 3 and 35 mm thickness characterize tephra unit TM-2, deposited ca 1 m below TM-1. The older tephra TM-2b (1440 varve yr BP) forms a reversely graded ash layer consisting of strongly porphyritic white pumices and less vesicular brown-greenish juvenile clasts with leucite, biotite and clinopyroxene phenocrysts. Lithic fragments of tachylites, mafic to intermediate lavas, sedimentary and metamorphosed carbonate rocks, and essential crystals are abundant and increase towards the top of the ash layer. Because of the heterogeneity of glass composition ranging from foiditic-phonolitic and basaltic trachyandesitic, TM-2b has been correlated with the pumice-fallout of the Plinian AD 472 'Pollena' eruption of Vesuvius (Fig. 4). The overlying thinner tephra TM-2a (1420 varve yr BP) is characterized by a similar assemblage of phenocrysts and lithics. Glass shards are nearly non-vesicular, greenish to light brownish in colour and bear abundant crystals of leucite. According to its homogenous tephriphonolitic-foiditic composition, tephra TM-2a has been assigned to the historical AD 512 eruption associated with the late phase of the Pollena eruptive cycle. Both the AD 472 and 512 eruptions are poorly known owing to the existence of only rare historic reports (Rolandi et al., 1998). The occurrence of the related tephras at the distal site of Monticchio suggests more or less widespread fallout to the East for both eruptions.

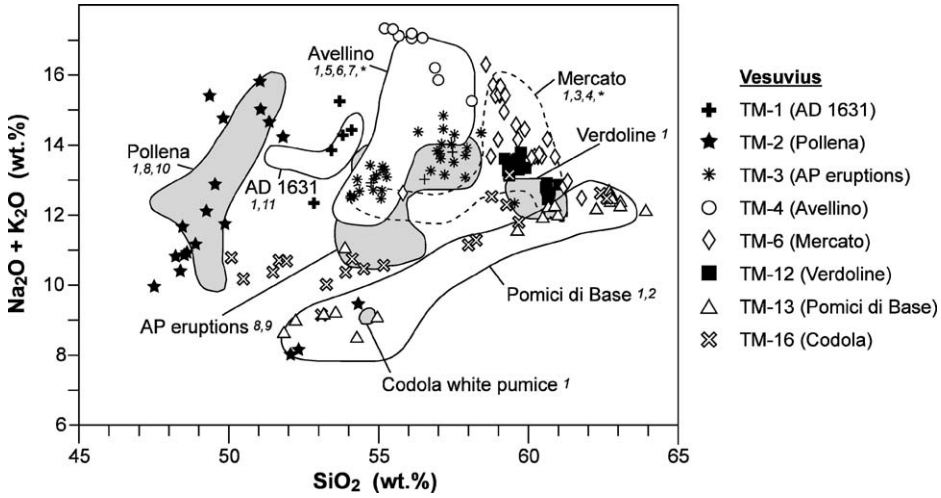

Fig. 4. Chemical discrimination diagram SiO_2 (wt%) vs. Na_2O+K_2O (wt%) showing the correlations of distal tephra markers in the Monticchio record (symbols) with distinct volcanic eruptions (fields) of Vesuvius. Chemical data of near-vent and distal tephra equivalents are used for comparison: [1] XRF, Santacroce (1987), Cioni et al. (2003); [2] XRF, Landi et al. (1999); [3] EMP, Jahns and van den Bogaard (1998); [4] SEM-EDS, Rolandi et al. (1993b); [5] EMP, Signorelli et al. (1999b); [6] SEM-EDS, Cioni et al. (2000); [7] SEM-EDS, Calanchi et al. (1996b); [8] SEM-EDS, Rolandi et al. (1998); [9] XRF, Andronico and Cioni (2002); [10] XRF, Ayuso et al. (1998); [11] SEM-EDS, Rolandi et al. (1993a); * EMP data of near-vent deposits, this study.

10.3. TM-3

Three prominent pyroclastic layers of unit TM-3 occur between 3.1 and 3.3 m depth showing the typical phonolitic to tephriphonolitic composition of younger Vesuvius pyroclastic products. As already suggested by Narcisi (1996), these tephra layers can be related to the inter-Plinian activities between the Avellino and AD 79 Pompeii eruptions of Vesuvius. During this time period at least six major eruptions occurred showing a favourable dispersal axis direction of tephra products to the East and Northeast (Rolandi et al., 1998; Andronico and Cioni, 2002). Based on the comparison with new geochemical and petrological data of near-vent deposits (Andronico and Cioni, 2002), a more specific correlation of tephra unit TM-3 with these eruptive events was possible (Fig. 4).

Tephra TM-3a (3990 varve yr BP) is represented by a 22 cm thick, thinly laminated and fine-grained ash layer with large amounts of lithic fragments, biotite phenocrysts and sparse brown low-vesicular juvenile clasts. Abundant leucite crystals, mostly coated by fine-grained reddish ash, form pisolite-rich horizons, particularly in the upper part of the deposit. Accordingly, we have correlated tephra TM-3a with the sub-Plinian eruption AP4 of Vesuvius, which has not been dated so far except by the 'varve-supported sedimentation rate chronology' of Monticchio sediments.

Tephra TM-3b (4020 varve yr BP) is characterized by a similar thick pisolite bearing, ash deposit. Two coarse ash laminations are visible made up of abundant phenocrysts, lithic fragments (mafic to intermediate lavas) and light brownish, moderately vesicular juvenile clasts with sparse leucite and abundant apatite microcrysts. The petrographical and chemical composition of TM-3b corresponds to that of the fallout products of Unit A of the AP3 sub-Plinian eruption dated at 2710 ± 60 ^{14}C a BP by Rolandi et al. (1998). Tephra from the AP3 eruption is also preserved in the eastern sector of Vesuvius (Andronico and Cioni, 2002), corroborating in combination with the occurrence in the Monticchio maar a widespread dispersal to the East.

Tephra TM-3c (4150 varve yr BP) is subdivided into two successive layers that sum up a total thickness of 31 mm. The basal sub-layer is a reverse-graded white pumice fallout with a broad variety of volcanic and sedimentary rock fragments. The upper part of the deposit comprises a green-brownish, thinly stratified internal ash layer made up of grey to brown juvenile fragments with varying grades of vesicularity. TM-3c has been assigned to the pyroclastics of the AP2 eruption dated by ^{14}C at a mean age of 3170 ± 110 a BP (Santacroce, 1987; Rolandi et al., 1998). With the deposition in the Monticchio maar lake, the AP2 tephra is more widely dispersed to the East than previously supposed.

10.4. TM-4

Tephra TM-4 (4310 varve yr BP) in ca 3.5 m depth comprises two sub-layers, a basal 5 mm thick white pumice fallout and a directly overlying grey ash layer of 1 mm thickness. White highly vesicular pumices and large euhedral phenocrysts of sanidine, zoned Ti-rich

clinopyroxene, sodalite, scapolite and nepheline dominate the basal layer. Abundant limestone fragments, sparse green-brownish vitrics and large highly vesicular grey pumice fragments rich in clinopyroxene and apatite microcrysts, characterize the fine-grained grey ash layer. The chemical composition of glass shards of both sublayers is Na-phonolitic to Na-tephriphonolitic (Table 2; Fig. 4). Because of its unique composition, TM-4 has been correlated with the 'Avellino' Plinian eruption of Vesuvius dated at a mean age of 3675 ± 57 ^{14}C a BP (Alessio et al., 1973; Delibrias et al., 1979; Vogel et al., 1990; Andronico et al., 1995; Di Vito et al., 1998; Rolandi et al., 1998). An AMS radiocarbon dating on *Abies* seed overlying the TM-4 tephra in the Monticchio record gave an older age of 3920 ± 50 a BP (4514–4159 a cal. BP, 2σ error range; Watts et al., 1996b). The Avellino tephra forms a widespread Holocene ash marker in Italian terrestrial sites. The occurrences of pumice fallouts in the Monticchio maar lake (white and grey pumices) as well as in the crater lakes of Mezzano and Albano in central Italy (grey pumices) are in accordance with the shifting wind directions from ENE to NNE during the Avellino eruption as postulated by Santacroce (1987) and Cioni et al. (2000).

10.5. TM-5

Tephra unit TM-5 comprises four single tephra layers TM-5a to TM-5d between 3.7 and 4.4 m depth, which all are characterized by a homogenous phonotrachytic composition of glass shards. The lower thin ash layers TM-5d and TM-5c (5680 and 5390 varve yr BP) are composed of large K-feldspar and clinopyroxene phenocrysts, juvenile clasts with quenched minerals, and both brownish and white pumice fragments with low to moderate vesicularity. The overlying white tephra layers TM-5b and TM-5a (4660 and 4620 varve yr BP) are made up of colourless highly vesicular pumice fragments, and additionally contain large biotite crystals and sparse xenolithic fragments (lavas, greenish tuff). All tephra layers of unit TM-5 have been assigned to the long-duration 'Agnano Monte Spina' (AMS) eruption phase of the Phlegrean Fields (Fig. 5). The thickest tephra TM-5a (11 mm) most likely corresponds to the upper fallout unit D1 of the AMS eruption dated at 4130 ± 50 ^{14}C a BP (de Vita et al., 1999). An equivalent tephra has been found in marine sediment cores from the western Adriatic Sea (Calanchi et al., 1998) confirming in combination with the AMS tephra in the Monticchio maar a wide dispersal to the ENE.

10.6. TM-6

Tephra unit TM-6 is made up of two distinct layers intercalated in 6.5 and 6.7 m sediment depth. The basal 10.6 cm thick tephra deposit TM-6b (9680 varve yr BP) consists of two reversely graded white pumice layers, which are separated by a 1 cm thick grey-greenish ash horizon enriched in phenocrysts and lithic fragments. The highly vesicular glass components of the white tephra layers comprise two geochemically heterogeneous populations (Fig. 4): a predominately phonolitic (pumices) and a minor tephriphonolitic group (scoria). The thin overlying tephra layer TM-6a (9620 varve yr BP), in turn, is rich in lithics and trachyphonolitic juvenile clasts, which are embedded in a fine-grained calcareous groundmass. Tephra TM-6b has been correlated with the 'Mercato' Plinian eruption of Vesuvius dated at 8098 ± 71 ^{14}C a BP (mean age derived from Delibrias et al., 1979; Andronico et al., 1995; Zanchetta et al., 2000). Tephra TM-6a is similar in chemical and mineralogical composition to a lithic-rich pumice-fall level at the top of the near-vent Mercato deposits, the so-called 'Pomici e Proietti' (Delibrias et al., 1979; Santacroce, 1987). The heterogeneous glass chemistry of tephra layers TM-6a and TM-6b also corresponds to the tri-modal glass composition obtained on the Veliko Jezero tephra that has been detected in Holocene sediments at the Island of Mljet, Croatia (Jahns and van den Bogaard, 1998) and to the V-1 tephra found in marine sediments of the southern Adriatic Sea (core KET 8218; Paterne et al., 1988; Fig. 1a). Both occurrences in the Monticchio record and in the Adriatic Sea confirm the proposed easterly distribution of air fall products of both the Mercato and succeeding 'Pomici e Proietti' eruption (Santacroce, 1987; Rolandi et al., 1993b).

10.7. TM-7

Tephra unit TM-7 in 7.8–7.9 m depth consists of two adjacent tephra layers with distinct chemical composition. The basal tephra deposit TM-7b (12,180 varve yr BP) is a 47 mm thick pumice fallout characterized by white, highly vesicular phonolitic pumices changing upwards to darker scoria (Fig. 9b). Lithic fragments comprise altered tuffs at the base and fresh volcanic rocks in the upper part of the deposit. The overlying thin tephra layer TM-7a (12,170 varve yr BP) is made up of light brownish, leucite bearing glass shards showing a latitic to tephriphonolitic composition. Both tephra layers have been correlated with the 'Agnano Pomici Principali' (APP) eruption of the Phlegrean Fields (Fig. 5), whereby TM-7b represents the base and TM-7a the top of APP near-vent deposits. The APP tephra in proximal sites has been dated at an age of $10{,}320 \pm 50$ ^{14}C a BP (Di Vito et al., 1999), which is in good agreement with an AMS radiocarbon age of $10{,}550 \pm 150$ a BP obtained on terrestrial macrofossils sampled 7 cm below the TM-7b tephra in the Monticchio record (Hajdas et al., 1998). The occurrence in

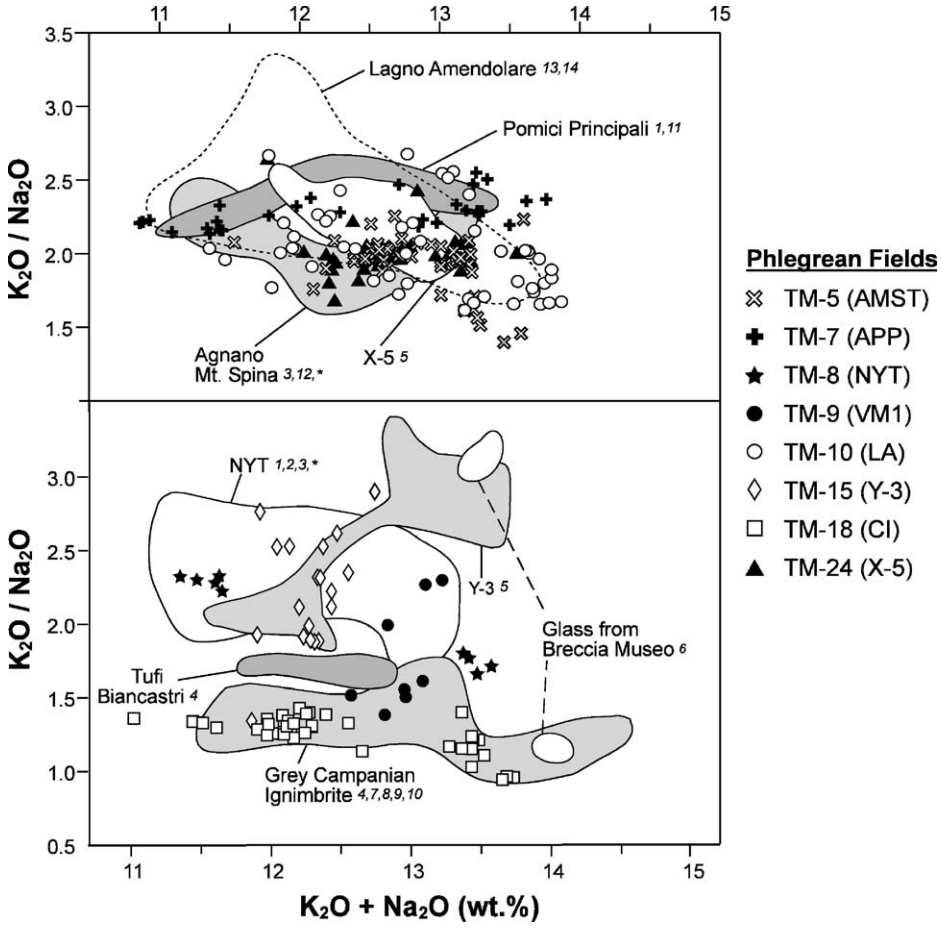

Fig. 5. Chemical discrimination diagram K_2O+Na_2O (wt%) vs. K_2O/Na_2O showing the correlations of distal tephra markers in the Monticchio record (symbols) with distinct volcanic eruptions (fields) of the Phlegrean Fields. Chemical data of near-vent and distal tephra equivalents are used for comparison: [1] SEM-EDS, Paterne et al. (1986); [2] XRF, Scarpati et al. (1993); [3] EMP, Calanchi et al. (1998); [4] ICP-AES, Pappalardo et al. (1999); [5] EMP, Keller et al. (in prep.); [6] EMP, Melluso et al. (1995); [7] XRF, Signorelli et al. (1999a); [8] XRF, Rosi and Sbrana (1987); [9], SEM-EDS, Vezzoli (1991); [10] ICP-AES, Civetta et al. (1997); [11] ICP-AES, D'Antonio et al. (1999); [12] XRF, de Vita et al. (1999); [13] XRF, Andronico (1997); [14] XRF, Santacroce (1987); ∗ EMP data of near-vent deposits, this study.

Monticchio as well as in an Adriatic Sea core (Paterne et al., 1988) indicates an ENE dispersal axis of the APP products.

10.8. TM-8

Tephra TM-8 (14,120 varve yr BP) in 8.6 m depth forms a 2.2 cm thick succession of three normal graded fallout beds. These are characterized by light brownish, moderately vesicular blocky pumices embedded in a fine grained glassy groundmass, and differ in the amounts of phenocrysts and lithic fragments (lavas, altered tuffs). Because of the heterogeneous trachytic to latitic-tephriphonolitic composition of glass shards (Fig. 5), TM-8 is related to the phreatomagmatic eruption of the 'Neapolitan Yellow Tuffs' (NYT) of the Phlegrean Fields dated at a mean age of $12{,}300 \pm 300$ ^{14}C a BP (Alessio et al., 1971, 1973). The distal facies of the NYT also occurs in marine sediment cores from the Tyrrhenian and Adriatic Seas (Paterne et al., 1988; Calanchi et al., 1998) and in the lacustrine record of Längsee (Austria; Schmidt et al., 2002), where it forms an important chronological marker for the early Late Glacial. Those occurrences together with the relative large thickness of the NYT tephra in the Monticchio sediments suggest that its proposed NNE dispersal (Scarpati et al., 1993) was temporary preceded or replaced by a more easterly dispersal direction.

10.9. TM-9

The single tephra layer TM-9 (14,560 varve yr BP) in 8.8 m depth is yet another thick ash deposit mainly made up of white highly vesicular pumice fragments, sparse phenocrysts and lithic fragments (altered tuffs, lavas). Because of its trachytic glass chemistry and stratigraphic position, TM-9 has been correlated with the 'Tufi Biancastri' erupted from the Phlegrean Fields (Fig. 5). In the near-vent area the Tufi Biancastri form a thick succession of numerous white pyroclastic fall and flow

deposits, which have been dated by laser $^{40}Ar/^{39}Ar$ technique at ages between 14.6±0.6 and 17.9±0.5 ka (Pappalardo et al., 1999). So far, only one single tephra deposit of the Tufi Biancastri, the so-called VM1 tephra, has been detected in distal sites east of the eruptive centre (Andronico, 1997). The identical chemical composition and stratigraphic position between the NYT (12.3 uncal. ka BP) and the older Lagno Amendolare pyroclastics (13 uncal. ka BP) at these sites and in the more distal Monticchio maar suggest a correlation of both the VM1 and the TM-9 tephra with the younger 14.6 ka Tufi Biancastri event. Both tephra occurrences confirm the easterly dispersal of Tufi Biancastri products.

10.10. TM-10

Tephra unit TM-10 comprises four successive ash layers between 9 and 9.2 m depth. The basal layer TM-10d (15,550 varve yr BP) is made up of white highly vesicular pumices, abundant juvenile clasts with quenched minerals, altered pumices and minor amounts of phenocrysts. The composition of the overlying tephras TM-10c, TM-10b and TM-10a, dated at 15,300, 15,220 and 15,030 varve yr BP, respectively, is similar to TM-10d except for the additional presence of brownish glass. Because of the trachytic to trachyphonolitic glass chemistry (Fig. 5), tephra unit TM-10 has been related to the white and brownish pumice fall deposits of the 'Lagno Amendolare' (LA) eruption dated at 13,070±90 ^{14}C a BP (Andronico, 1997). Its age is in good agreement with both an AMS dating of macrofossils directly overlying tephra TM-10a at 12,540±130 a BP (Watts et al., 1996a) and the time span of LA base and top deposits obtained by the Monticchio sedimentation rate chronology. The Lagno Amendolare eruption has only recently been related to Phlegrean Fields activity. From the exposure at the northern flank of Vesuvius volcano and the detection of the distal facies in the Adriatic Sea (Siani et al., 2001), an easterly dispersal axis direction has been reconstructed for the LA tephra (Andronico, 1997).

10.11. TM-11

Tephra layer TM-11 (16,440 varve yr BP) in 9.6 m depth is a thin brown ash layer made up of brown to black low-vesicular juvenile clasts (Fig. 9c), abundant plagioclase phenocrysts and lithic fragments of basaltic composition. Because of the unique Na-alkaline trachydacitic to trachyandesitic composition of volcanic glass, TM-11 has been correlated with a younger Plinian eruption of Etna (Fig. 7). Here, the final eruptions of the Ellittico volcanic centre formed two couple of pumice layers in the near-vent deposits, the so-called unit D, which were widely dispersed towards the E and SE (Coltelli et al., 2000). The same eruptive events are considered to have produced the 'Biancavilla-Montalto Ignimbrites', which are dated at 14,180±260 ^{14}C a BP (Delibrias et al., 1986). The distal facies of unit D has been interpreted to be identical with the 'Y-1' tephra occurring in numerous deep-sea cores of the eastern Mediterranean Sea and in terrestrial sediment records from central Italy (Keller et al., 1978; Paterne et al., 1986, 1988; Vezzoli, 1991; Calanchi et al., 1996a; Narcisi, 1993; Ramrath et al., 1999). The northern distribution of Y-1 is still under discussion. Referring to the results of pyroclastic studies in the medial-distal part of the Etna volcano, Coltelli et al. (2000) excluded northward Plinian fallout of unit D and newly considered a dispersion and sedimentation of finer Y-1 pyroclasts from a high-atmospheric circulation. The detection of the Biancavilla Ignimbrite in the Monticchio record, however, confirms at least partial transport to the North.

10.12. TM-12

The 5.5 cm thick tephra layer TM-12 (17,560 varve yr BP) in 10.2 m depth is defined by five alternating grey and brownish-black horizons, generally showing a normal grading of components. Juvenile clasts are greyish in colour, moderate to low vesicular and often rich in microcrysts (Fig. 9d); lithic fragments of volcanic and carbonatic origin are abundant and increase towards the top. The homogenous trachytic glass composition and the mineral assemblage of TM-12 suggest a correlation with the 'Greenish Pumice' sub-Plinian eruption of Vesuvius (Fig. 4), which took place at 15,970±70 ^{14}C a BP (Siani et al., 2001). Its related pyroclastics are widely dispersed to the ENE, and also occur in Adriatic Sea cores in 170 km distance from the source (Cioni et al., 2003).

10.13. TM13

One of the most prominent tephra in the Monticchio record is the 17 cm thick tephra TM-13 (19,280 varve yr BP) in 11.1 m depth. From the bottom to the top, this deposit comprises (A) a basal 4.1 cm thick greyish pumice layer changing upwards to a dark scoria bed with abundant phenocrysts and volcanic lithics, (B) a white to light brownish reversely graded pumice layer (1.4 cm) containing high-vesicular juvenile clasts, abundant phenocrysts and lithic fragments at the top, (C) a transitional horizon (4.5 cm), in which light coloured pumice gradually change upwards to dark grey scoria and (D) a grey–black scoria layer (7 cm) rich in crystals and volcanic and carbonatic lithics. The chemical composition of glass shards of TM-13 is heterogeneous and range from trachytic to latitic. Both, the chemistry and the composition of sub-layers correlate with the

basal pumice fall deposits of the Plinian 'Pomici di Base' eruption of Vesuvius (Fig. 4). The 'Pomici di Base' pyroclastics, formerly named as 'Sarno' pyroclastics, are dated at 18,300±180 ^{14}C a BP and dispersed to an easterly direction (Andronico et al., 1995; Bertagnini et al., 1998; Landi et al., 1999). Up to now, the Monticchio maar lake is known as the most distal site, where the Pomici di Base tephra has been detected.

10.14. TM-14

The 2 mm thin tephra layer TM-14 (20,150 varve yr BP) in 11.8 m depth is dark brown in colour and made up of greenish-brown to minor white juvenile clasts, abundant phenocrysts and lithics fragments. Glass shards show a basaltic-trachyandesitic chemical composition (Fig. 6). According to the petrological features and the stratigraphical position tephra TM-14 has been correlated with the 'Solchiaro' eruption of Procida-Vivara dated at 19,620±270 ^{14}C a BP (Alessio et al., 1976). So far, the distal facies of the Solchiaro tephra is known as marine 'C-4' tephra that solely occurs in sediment core KET 8004 of the Tyrrhenian Sea (Fig. 1a; Paterne et al., 1986). Its new occurrence in the Monticchio maar lake approximately 140 km east of the volcanic centre suggests that the Solchiaro eruption was of greater magnitude than previously supposed.

10.15. TM-15

A further thick pyroclastic deposit is represented by tephra TM-15 (23,930 varve yr BP) in 14.7 m depth. It consists of brownish co-ignimbritic ashes interbedded with coarse-grained horizons of highly vesicular pumices (Fig. 9e), sparse large phenocrysts and lithic fragments. The homogenous K-trachytic chemistry of glass shards corresponds most likely to the glass chemistry of the marine 'Y-3' tephra occurring in deep-sea cores from the Ionian Sea (Keller et al., 1978; Kraml, 1997; Fig. 5). In core M25/4-13, tephra Y-3 has been dated at 25.3±3.0 ka by an interpolation using the Mediterranean sapropel chronology (Kraml, 1997). Based on the geochemical and stratigraphical comparison with proximal CF pyroclastics, we suggest a correlation of tephra TM-15 and Y-3 with an eruption that produced a lithic-rich pyroclastic flow overlying the Grey Campanian Ignimbrite (37 ka) in proximal sites of the Phlegrean Fields (Rolandi, 1988; Scandone et al., 1991). This flow deposit, named as 'Breccia Museo', has been dated by ^{14}C at a mean age of 21,299±170 a BP (Lirer et al., 1991; Melluso et al., 1995). However, both its occurrence in marine sites located southeast of the eruptive centre and its large thickness in the Monticchio record implies a widespread tephra dispersal from a Plinian column to the ESE.

10.16. TM-16

Two single tephra layers form tephra unit TM-16 in 16.5 and 17.1 m depth, respectively. The basal tephra TM-16b (26,790 varve yr BP) is made up of a thin white trachytic pumice level that grade into a massive ashy horizon with large brownish-black, low vesicular pumices (tachylites), phenocrysts and limestone fragments. The younger tephra TM-16a (26,130 varve yr BP) comprises a massive black horizon at the base and a brownish calcareous scoria layer with low vesicular, leucite-rich juvenile clasts covered by pisolite-rich ashes. The tephriphonolitic composition of glass shards of TM-16a matches well with a single chemical determination obtained on pumice of near-vent deposits of the Plinian 'Codola' eruption dated at 25,100±400 ^{14}C a BP (Alessio et al., 1974; Fig. 4). This eruption is poorly

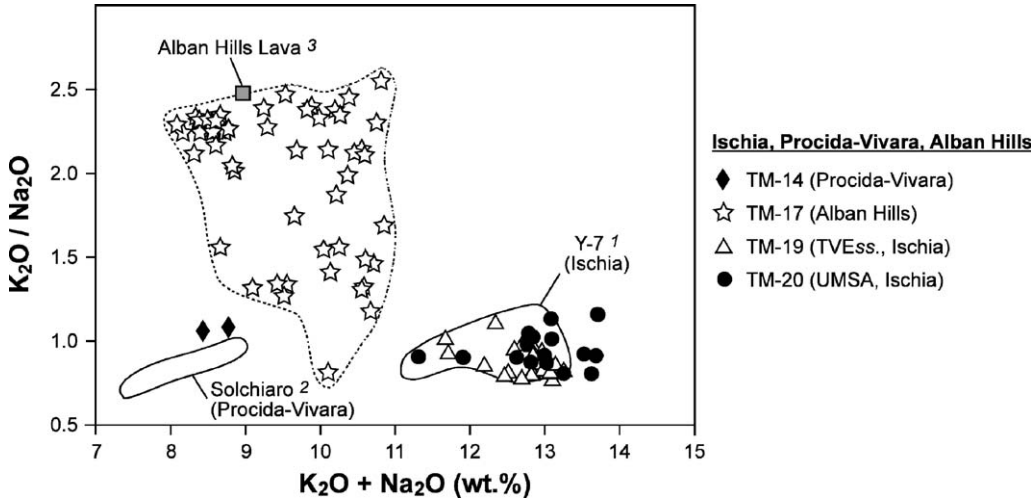

Fig. 6. Chemical discrimination diagram K_2O+Na_2O (wt%) vs. K_2O/Na_2O showing the correlations of distal tephra markers in the Monticchio record (symbols) with distinct volcanic eruptions (fields) of Ischia, Procida-Vivara and Alban Hills. Chemical data of near-vent and distal tephra equivalents are used for comparison: [1] EMP, Keller et al. (in prep.); [2] SEM-EDS, Paterne et al. (1986); [3] XRF, Trigila (1995).

known and considered to originate from Vesuvius (Santacroce, 1987).

10.17. TM-17

Six single tephra layers between 16.3 and 22.7 m depth with similar composition make up tephra unit TM-17. The basal tephra layer TM-17f (30,530 varve yr BP) forms the thickest pyroclastic deposit. It is mainly composed of coarse-grained, altered pumices (max. 2 mm), abundant xenoliths and large phenocrysts. Juvenile clasts are sparse and occur only in the lower part of the deposit. TM-17f is overlain by the fine-grained, tephriphonolitic to phonotephritic ash layers TM-17e, TM-17d and TM-17c dated at 29,900, 29,870 and 29,690 varve yr BP, respectively. These tephras are characterized by low vesicular, light-brownish glass shards bearing apatite microcrysts, abundant sedimentary and volcanic rock fragments, and a similar mineral assemblage like tephra TM-17f. The upper part of tephra unit TM-17 comprises the more fine-grained, dark brownish to blackish tephra layers TM-17b and TM-17a (25,990 and 25,930 varve yr BP). These ashes are mainly made up of green-brownish, leucite-rich glass shards (Fig. 9f), phonotephritic in composition, and less abundant phenocrysts and lithic fragments (carbonates, tuffs). A reliable correlation of tephra unit TM-17 has been established by the comparison with unpublished whole rock chemical data of 'Peperino Albano' pyroclastics of Lago di Albano (Alban Hills; G. Cavarretta pers. comment, 1999). In detail, tephra layer TM-17f has been related to the initial eruption phase of the Peperino Albano, that has produced a pyroclastic flow unit of similar composition dated at 29,700 ± 400 ^{14}C a BP (De Vries in Fornaseri et al., 1963). Tephra layers TM-17b and TM-17a most likely correspond to the final phreatomagmatic basic ignimbrite eruption of the Peperino Albano. Having these data on hand, the products of the Peperino Albano have been precisely re-dated by the Monticchio varve-supported sedimentation rate chronology between 30.5 and 25.9 ka. Moreover, their occurrence in the Monticchio maar implies a widespread distribution of more than 260 km ESE from its source, which, in turn, implies a higher energy of the related eruption than previously supposed.

10.18. TM-18

Tephra TM-18 (32,970 varve yr BP) in 25 m depth comprises a basal pumice fallout and a direct overlying vitric ash deposit of 17 and 8.7 cm thickness, respectively (see photo, Fig. 2). The pumice fallout is composed of several sub-layers of alternating light grey, coarse grained (<7 mm), highly vesicular pumices, brownish glass shards (Fig. 9g), lithic fragments and phenocrysts. The fine-grained vitric ash layer (<100 μm), in turn, is interpreted to represent a distal co-ignimbritic fallout deposit. The homogenous peralkalic trachytic glass composition of both the pumice fallout and vitric ash layer of TM-18 is identical with proximal fallout deposits of the 'Campanian Ignimbrite' (CI) and ensuing 'Gray Campanian Ignimbrite' (GCI) eruptions of the Phlegrean Fields, respectively (Fig. 5). These events dated at 37.1 ± 0.4 ka (Deino et al., 1994; Rosi et al., 1999) are among the largest eruptions occurring in the Mediterranean during the Late Quaternary. Their distal facies are known as the marine Y-5 tephra that occurs in numerous deep-sea cores from the Eastern Mediterranean Sea as far as 1660 km ESE from its volcanic source (e.g. Keller et al., 1978; Thunell et al., 1979; Vinci, 1985; Paterne et al., 1988; Vezzoli, 1991).

10.19. TM-19

Tephra TM-19 (56,250 varve yr BP) in 38.6 m depth forms the thickest pyroclastic deposit in the sediments of the Monticchio record. It is beige-greenish in colour and mainly composed of Y-shaped glass shards (Fig. 9h), minor contents of phenocrysts and volcanic lithics. TM-19 has been directly dated by Laser ^{40}Ar/^{39}Ar on individual sanidines at an age of 55 ± 2 ka (Watts et al., 1996a). Because of its peralkaline trachytic composition and chronological conformity, TM-19 has been interpreted to be the distal co-ignimbritic fallout facies of the 'Tufo verde Epomeo sensu strictu' eruption of Ischia (TVEss; ca 55 ka; Rosi et al., 1988; Fig. 6). So far, the distal facies of TVEss products has only been found in deep-sea sediment from the Tyrrhenian Sea, here named as C-18 tephra (Paterne et al., 1988). The large thickness in the Monticchio site, however, implies a huge-volume eruption and a rather easterly dispersal direction of the TVEss tephra.

10.20. TM-20

Tephra TM-20 (57,570 varve yr BP) in 39.5 m depth is a thin layer with comparable peralkaline trachytic composition as the overlying tephra TM-19. It is made up of highly vesicular white pumices with abundant phenocrysts and volcanic lithics. Because of the presence of titanite and a conspicuous yellow Na-pyroxene (acmite), TM-20 has been correlated with the marine 'Y-7' tephra occurring in deep-sea sediment from the Ionian Sea (Fig. 6). Y-7 has been dated by laser ^{40}Ar/^{39}Ar on sanidine at 56 ± 4 ka (Kraml, 1997; Allen et al., 1999). Its correlation with a terrestrial counterpart is still under discussion. Keller et al. (in prep.) suggest a correlation with the acmite-bearing 'Unità di Monte San Angelo' (UMSA) of Ischia, which was produced during an initial phase of the Tufo Verde Epomeo eruption (Rosi et al., 1988). However, the minor thickness in the

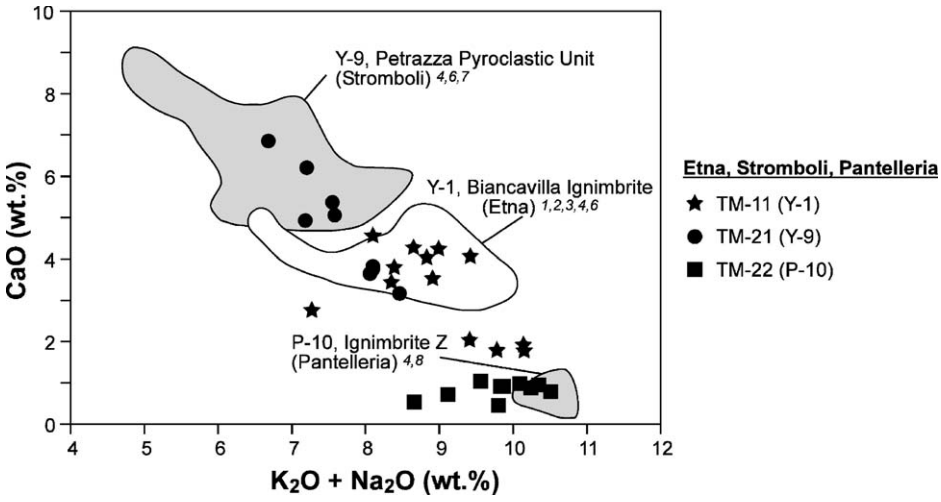

Fig. 7. Chemical discrimination diagram $K_2O + Na_2O$ (wt%) vs. CaO (wt%) showing the correlations of distal tephra markers in the Monticchio record (symbols) with distinct volcanic eruptions (fields) of Etna, Stromboli and Pantelleria. Chemical data of near-vent and distal tephra equivalents are used for comparison: [1] SEM-EDS, Vezzoli (1991); [2] SEM-EDS, Calanchi et al. (1996a); [3] SEM-EDS, Narcisi (1993); [4] SEM-EDS, Paterne et al. (1988); [5] XRF, Coltelli et al. (2000); [6] EMP, Keller et al. (in prep.); [7] XRF, Hornig-Kjarsgaard et al. (1993); [8] XRF, Civetta et al. (1984).

Monticchio record implies a preferable dispersal of the Y-7 tephra to the SE.

10.21. TM-21

The 1.5 mm thick tephra layer TM-21 (74,540 varve yr BP) in 50 m depth is composed of sparse grey to brownish pyroxene-bearing pumices, abundant phenocrysts and minor volcanic rock fragments. The mineral assemblage and the heterogeneous trachyandesitic to trachydacitic glass geochemistry coincide most likely with the marine 'X-1' tephra occurring in deep-sea sediments from the Ionian and Tyrrhenian Seas (Keller et al., 1978; Paterne et al., 1988). The X-1 tephra, calc-alkaline in composition, is attributed to the Aeolian Arc volcanism (McCoy, 1981; Paterne et al., 1988) and has to be distinguished from the andesitic tephra layer 'X-1' of Santorini, which has been found in a similar stratigraphical position in deep-sea cores from of the Aegean and Levantine Seas (Keller et al., 1978, 1998; Kraml et al., 1998). In order to avoid future confusion of names, we suggest a renaming of the Aeolian 'X-1' tephra into 'Y-9' tephra. While the terrestrial counterpart of 'Y-9' is still under discussion, we supply evidence for a correlation of both the 'Y-9' and TM-21 tephra with the 'Petrazza Pyroclastics' of Stromboli volcano on the base of the petrological, chemical and chronological matching (Fig. 7). The Petrazza near-vent deposits comprise conspicuous orange and grey pumice and scoria layers of andesitic composition, which are stratigraphical interbedded between lava flows dated at 85.3 ± 2.0 and 64.3 ± 4.9 ka, respectively (Hornig-Kjarsgaard et al., 1993; Gillot and Keller, 1993). Based on the interpolation of astronomically calibrated time scales, more restricted age estimates are given for the 'Y-9'

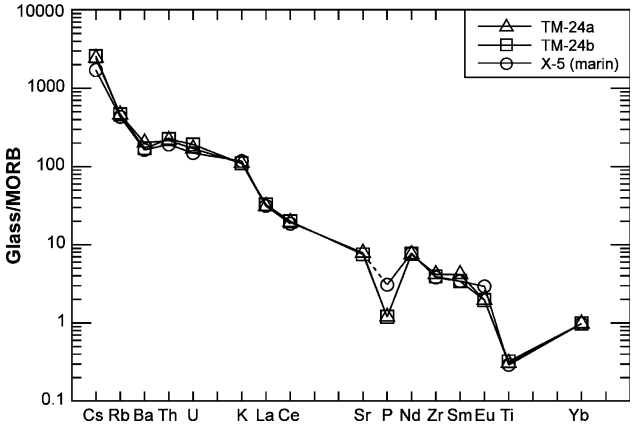

Fig. 8. Spider diagram for discriminating tephra layers TM-24a, TM-24b and the marine X-5 tephra occurring in deep-sea cores 22M-60, M25/4-12 and M25/4-13 from the Ionian Sea (see also Fig. 1a). Trace element data on glass shards are obtained by INAA technique (Keller et al., in prep). Compositions are normalized to the MORB composition from Sun and McDonough (1989).

tephra in the Ionian Sea at 75.3 ka (core M25/4–12; Kraml, 1997) and for tephra '860-03' in the Tyrrhenian Sea at 77.1 ka (core KET 8003; Paterne et al., 1988; Fig. 1), respectively. The occurrences of the distal facies of 'Petrazza Pyroclastics' in the Monticchio sediments and in deep-sea cores from the Tyrrhenian and Ionian Seas confirm the wide dispersion to the NE as already suggested by Morche (1988).

10.22. TM-22

Tephra TM-22 (85,320 varve yr BP) in 58.2 m depth is defined as a thin, fine-grained vitric ash layer that is mainly composed of tubular and Y-shaped glass shards,

and very sparse feldspar and clinopyroxene phenocrysts. Its Na-trachydacitic to rhyolitic glass chemistry and stratigraphical position coincide most likely with that of the distal P-10 tephra from the Tyrrhenian deep-sea core KET 8004 (Fig. 7), which is dated by an oxygen isotope stratigraphy at 84.0 ka BP (Paterne et al., 1990). In terrestrial sites, Morche (1988) has identified a tephra layer with a similar chemical composition and stratigraphical position at the base of the Petrazza pyroclastics on Stromboli volcano (Gillot and Keller, 1993; Hornig-Kjarsgaard et al., 1993). Both, the marine and the terrestrial distal tephra layers can be related to the 'Ignimbrite Z Unit' of Pantelleria, which erupted at 79.3 ± 4.2 ka (Mahood and Hildreth, 1986). The occurrence of distal fallout products of 'Ignimbrite Z' on Stromboli volcano and within the sediments of the Tyrrhenian Sea and the Monticchio maar lake suggest a widespread dispersal of these products to the NNE.

10.23. TM-23

Tephra TM-23 (85,670 varve yr BP) in 59.7 m depth forms a conspicuous, 6.6 cm thick and coarse grained (max. 5 mm) ash layer with lithic fragments, altered pumices and abundant phenocrysts of clinopyroxene (Ti-augite), feldspar, biotite and leucite. Most of the few volcanic glasses are altered or entirely devitrificated and, therefore, it was not possible to attain electron

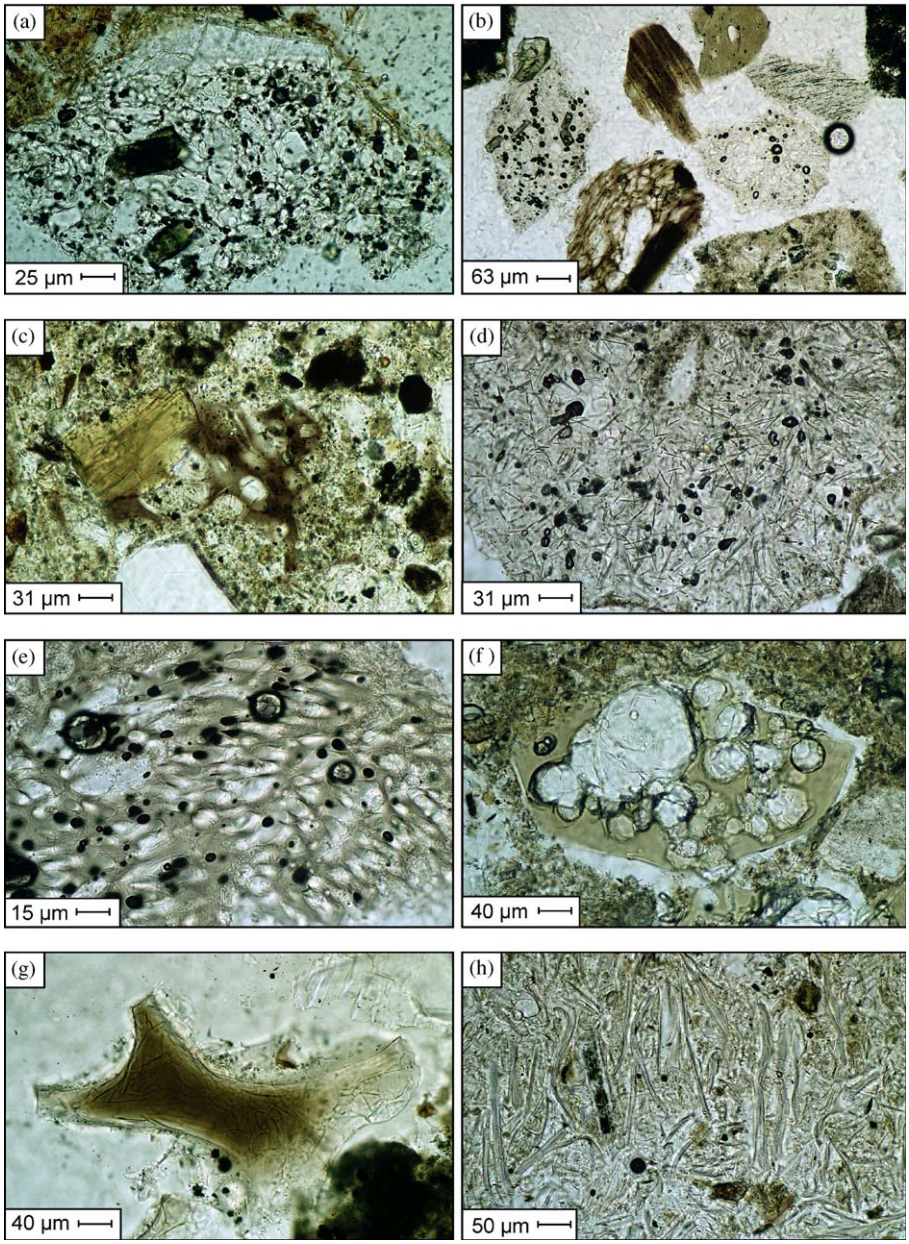

Fig. 9. Microscopic images of volcanic glass from selected distal tephra layers occurring in the Monticchio sediments. (a) TM-1, (b) TM-7b, (c) TM-11, (d) TM-12, (e) TM-15, (f) TM-17a, (g) TM-18, (h) TM-19.

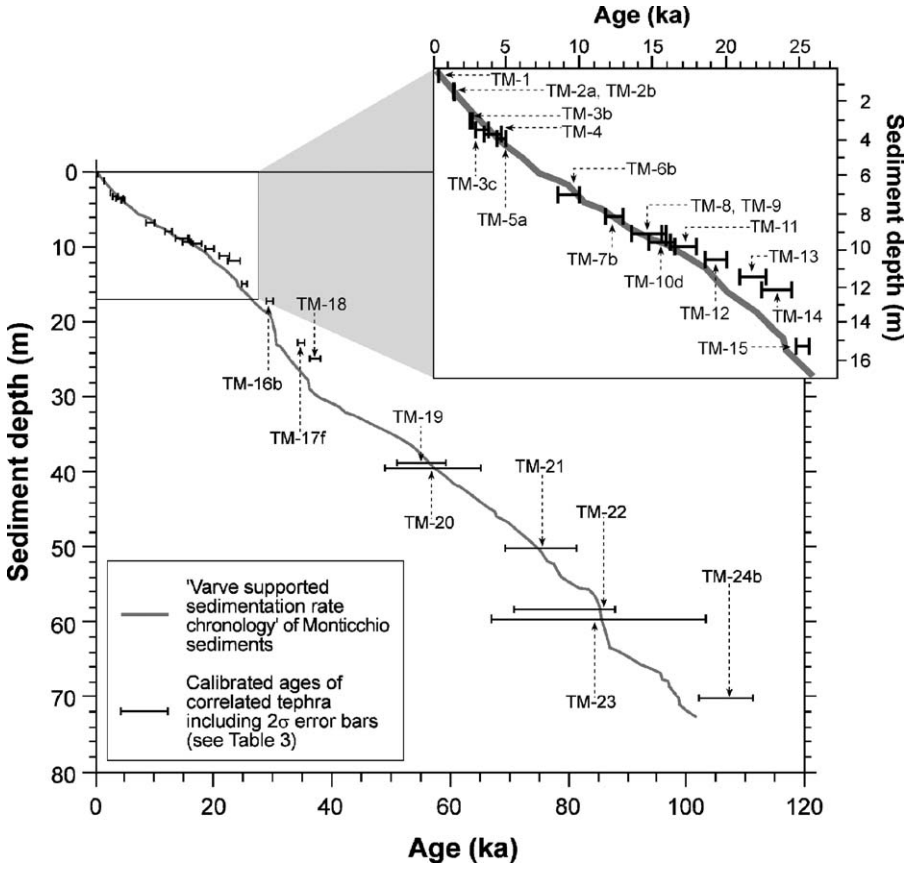

Fig. 10. Comparison of the 'varve-supported sedimentation rate chronology' of Monticchio sediments with the tephrochronology obtained on 26 distal tephra layers.

microprobe data. However, a trachytic-phonolitic composition can be roughly estimated by the refractive index of glass ($n<1.54$) and the assemblage of phenocrysts of tephra TM-23. According to its unique composition and stratigraphical position in the Monticchio record, tephra TM-23 has been correlated with the initial phase of hydromagmatic explosions of the 'Baccano' centre dated by K/Ar at 85 ± 9 ka (Villa, 1984 in Fornaseri, 1985). The related proximal pyroclastic deposits are characterized by layers of accretionary lapilli rich in sedimentary, volcanic and holocrystalline lithics bearing leucite, biotite and pyroxene (De Rita et al., 1993). Hitherto, pyroclastics of the Baccano hydromagmatic eruptions were found only in the near-vent area or in the southern distal part of the volcanic edifice. The occurrence of Baccano products in the Monticchio sediments, approximately 310 km ESE of the volcanic centre, implies widespread fallout from a Plinian column.

10.24. TM-24

Two thick tephra deposits in 69.3 m and 70.2 m depth, respectively, form tephra unit TM-24. The older tephra TM-24b (98,750 varve yr BP) has been defined as a fine-grained, nearly pure vitric ash deposit that originate from a co-ignimbritic eruption column. The younger tephra TM-24a (97,770 varve yr BP), in turn, is characterized by a coarse grained white and brown pumice fallout with abundant large phenocrysts and lithic fragments. Both, TM-24b and TM-24a are K-trachytic in composition and show an identical trace element chemistry, which corresponds to that of the marine 'X-5' tephra occurring in deep-sea sediments of the Ionian Sea (Figs. 5 and 8). The X-5 tephra has been precisely dated at 105 ± 2 ka by laser $^{40}Ar/^{39}Ar$ technique (Kraml, 1997; Allen et al., 1999). Although its origin is still unknown, the chemical and mineralogical composition of tephra X-5 suggests a volcanic source within the Campanian Province. However, the occurrence of two distinct tephra layers in the high-resolution lacustrine record indicate that the single X-5 tephra layer in deep-sea cores from the Ionian Sea represents a mixture of distal fallout products deriving from both a Plinian and a co-ignimbritic eruption column (Figs. 9 and 10).

11. Discussion of chronology

With the objective of constructing a high-resolution tephrochronological framework for the 100 ka Monticchio sediment record, a total of 26 datings of correlated proximal (near-vent) and distal tephra layers have been

Table 3
Comparison of tephra ages obtained from the varve-supported sedimentation rate chronology of Monticchio sediments (rounded varve ages in yr BP 1950) with historical recorded, radiometric, radioisotopic and interpolated ages of correlated volcanic events referred from literature

Tephra	Varve age (yr BP 1950)	Raw date of tephra event (yr)[a]	Calibrated 2σ age range	Dating method	Dated material
TM-1	90 (AD 1860)	AD 1631	369	Historical record	—
TM-2a	1420 (AD 530)	AD 512	1488	Historical record	—
TM-2b	1440 (AD 510)	AD 472	1528	Historical record	—
TM-3b	4020	2710±60 BP	2948–2745 BP	^{14}C	Charcoal (proximal tephra)
TM-3c	4150	3170±110 BP[b]	3727–2797 BP	^{14}C	Charcoal (proximal tephra)
TM-4	4310	3675±57 BP[b]	4569–3523 BP	^{14}C	Charcoal, underlying paleosols (proximal tephra)
TM-5a	4620	4130±50 BP	4830–4448 BP	^{14}C	Charcoal (proximal tephra)
TM 6b	9680	8098±71 BP[b]	9649–8484 BP	^{14}C	Underlying and intercalated paleosols (proximal tephra)
TM-7b	12,180	10,320±50 BP	12,761–11,769 BP	^{14}C	Underlying charcoal (proximal tephra)
TM-8	14,120	12,300±300 BP[b]	15,636–13,550 BP	^{14}C	Underlying paleosols (proximal tephra)
TM-9	14,560	14,600±600	15,80013,400	^{40}Ar/^{39}Ar	Sanidine (proximal tephra)
TM-10d	15,550	13,070±90 BP	16,209–14,638 BP	AMS^{14}C	Underlying paleosols (distal tephra)
TM-11	16,440	14,180±260 BP	17,788–16,252 BP	^{14}C	Underlying charcoal (proximal tephra)
TM-12	17,560	15,970±70 BP	18,989–18,654 BP	^{14}C	Charcoal (proximal tephra)
TM-13	19,280	18,300±180 BP	22,557–20,972BP	^{14}C	Underlying paleosols (proximal tephra)
TM-14	20,150	19.620±270 BP	24,239–22,327BP	^{14}C	Underlying paleosols (proximal tephra)
TM-15	23,930	21,299±170 BP[b]	25,490–24,700 BP	^{14}C	Underlying paleosols (proximal tephra)
		25,300±3000	*31,300–19,300*	*Interpolation*	S*apropel* (*marine tephra*)
		31.000±8000[c]	*47,000–15,000*	*^{40}Ar/^{39}Ar*	*Sanidine* (*TM-15*)
TM-16b	26,790	25,100±400 BP	29,921–28,896 BP	^{14}C	Underlying paleosols (proximal ? tephra)
TM-17f	30,530	29,700±400 BP	35,083–34,194 BP	^{14}C	Charcoal (proximal tephra)
TM-18	32,970	37,100±400	38,200–36,600	^{40}Ar/^{39}Ar	Sanidine (proximal tephra)
		37,000±3000[c]	*38,000–34,000*	*^{40}Ar/^{39}Ar*	S*anidine* (*TM-18*)
		35,000±1000[c]	*37,000–33,000*	*^{40}Ar/^{39}Ar*	*Sanidine* (*TM-18*)
TM-19	56,250	55,000±2000[c]	59,000–51,000	^{40}Ar/^{39}Ar	Sanidine (TM-19)
		58,000±5000[c]	*68,000–48,000*	*^{40}Ar/^{39}Ar*	*Sanidine* (*TM-19*)
TM-20	57,570	56,000±4000	65,000–49,000	^{40}Ar/^{39}Ar	Sanidine (marine tephra)
TM-21	74,540	75,300±3000	81,300–69,300	Interpolation	Sapropel (marine tephra)
TM-22	85,320	79,300±4200	87,700–70,900	K/Ar	Sanidine (proximal tephra)
TM-23	85,670	85,000±9000	103,000–67,000	K/Ar	Sanidine (proximal tephra)
TM-24b	98,750	105,000±2000	111,000–102,000	^{40}Ar/^{39}Ar	Sanidine (marine tephra)

Radiocarbon ages <10 ka BP are calibrated by the tree-ring calibration curve after Stuiver et al. (1998). Radiocarbon ages >10 ka BP are calibrated by U/Th disequilibria data on corals using the second-order polynomial equation after Bard et al. (1998). For an accurate comparison, laser ^{40}Ar/^{39}Ar ages were recalculated against international standard GA 1550 at 98.8 Ma following the recent inter-calibration after Renne et al. (1998). Sapropel ages are interpolated from the astronomically calibrated Mediterranean sapropel chronology after Lourens et al. (1996). For this dating, an analytical uncertainty of 3000 years has been assumed (e.g. Lourens et al., 1996). Dates in italics are not used for constructing the tephrochronological model.

[a] References see text.

[b] Weighted average of radiocarbon datings.

[c] Direct datings of distal Monticchio tephra layers (Watts et al., 1996a; R. Walter, pers. comment 1998).

Scientific Technical Report STR14/01, Deutsches GeoForschungsZentrum GFZ. http://doi.org/10.2312/GFZ.b103-14010

compiled from the literature (Table 3, Fig. 10). These chronological data primary comprise radiometric and radioisotopic datings (laser Ar/Ar, K/Ar). In addition, ages are included deriving from historical records of recent volcanic eruptions (<2000 yr BP) and from interpolation of the Mediterranean sapropel chronology.

In summary, the tephrochronological framework from 0 to 31 ka has been established by (1) three historically recorded eruption ages, (2) 15 AMS- and conventional ^{14}C dates from charcoals intercalated within tephra deposits or from underlying paleosols, and (3) one laser $^{40}Ar/^{39}Ar$ date of sanidines of a correlated proximal tephra. The tephrochronology for the older part of the Monticchio record (>31 ka) is mainly derived from laser Ar/Ar ages obtained on sanidines of (A) one correlated proximal tephra deposit (TM-18), (B) a single Monticchio tephra layer (TM-19) and (C) two marine tephra equivalents (TM-20, TM-24b). For the lower part, one single interpolated sapropel age (TM-21) and two K/Ar ages of correlated near-vent tephra deposits (TM-22, TM-23) are included.

Comparing the sedimentation rate and tephra chronologies (Table 3, Fig. 10) revealed a mean deviation of less than 5%, but for some specific sections of the record significant discrepancies appear:

(1) The youngest tephra TM-1, which has been correlated with the historical AD 1631 eruption of Vesuvius is dated by the sedimentation rate chronology at AD 1860. The discrepancy in the Monticchio sediment dating might be explained by the missing uppermost part of the sediment or poor preservation of annual lamination.
(2) From 17–20 ka, calibrated ^{14}C ages of tephra layers TM-12 to TM-14 gradually become older than the corresponding sedimentation rate time scale (Fig. 10, Table 3). This might be due to an increasing underestimation of sedimentation rates or to problems with the radiocarbon calibration, which for this part is based on U/Th dating on corals. Since the age discrepancy for TM-14 is rather large (>2000 years) a combination of both factors might be as well possible. In addition, problems with single ^{14}C dates on paleosol have to be taken into account.Astonishingly, for TM-15 the sedimentation rate age again is in agreement within error ranges to tephra ages derived from a ^{14}C-dating of an underlying paleosol, a sapropel interpolation of a marine tephra equivalent (Y-3) and a laser Ar/Ar dating of TM-15 itself, which however, reveals a large error of ±8000 years.
(3) The section with the largest age discrepancies between the sedimentation rate chronology and tephrochronology is the one between ca 30 and 40 ka. The varve age for TM-18—the Campanian Ignimbrite—of ca 32,970 (±1650) yr BP is about 4000 years younger than the laser Ar/Ar age of 37,100 ± 3000 yr directly obtained on TM-18 and the generally accepted mean age of 37,100 ±400 yr derived from a number of laser Ar/Ar datings of sanidines from related proximal pyroclastic deposits (Deino et al., 1994). This confirms suggested problems with the sedimentation rate chronology either due to a general underestimation of sedimentation rates or due to one or more hiatuses. Detailed micro-stratigraphic analyses are ongoing to clarify this problem. Recent dating of a tephra layer in a marine core which is assumed to correspond to the Campanian Ignimbrite even suggest an age of 41 ka for this volcanic event (Ton-That et al., 2001). This would enlarge the age discrepancy to ca 8000 years. However, in contrast to the Monticchio record, where the single well-known successive phases of this event are individually recorded thus giving clear evidence of a correct correlation, there might be a mixture of distinct tephra layers in the marine record probably due to bioturbation or redeposition. Therefore, it is very likely that the chronological problem of the Monticchio sedimentation rate time scale for this event is not more than about 4000 missing years. Astonishingly, the next older marker layer (TM-19) again shows very good agreement between both time scales. Accepting the problems with the sedimentation rate time scale as the cause for the age discrepancy for the TM-18 tephra would, consequently, mean that in between TM-18 and TM-19 sedimentation rates must be over-estimated by about the same amount (i.e. ca 4000 years). Therefore, the sedimentation rate chronology for this time period will be re-investigated.
(4) Chronologies of the lower part of the Monticchio record (>56 ka) are in agreement within the 2σ error ranges. Nevertheless, one single laser Ar/Ar tephra age at the base of the record (TM-24b) indicates a slight underestimation of varve ages, probably due to the lack of overlapping sediment cores in the lower section between 76 and 102 ka. For this time interval, varve counting and estimation of sedimentation rates will be re-investigated including material from newly recovered overlapping sediment cores.

12. Conclusions

Laminated sediments recovered from Lago Grande di Monticchio provide detailed information about the explosive activity of nearby Italian volcanoes during at least the past 100 kyr. The 340 distal tephra layers occurring in the Monticchio record have been characterized chemically and mineralogically. Most of the

tephras ($n = 313$) derive from volcanic eruptions of the Campanian province, which still represents an area of high volcanic risk for the Naples Metropolitan area. Other tephra layers ($n = 17$) are related to high-explosive events of Roman and Sicilian-Aeolian volcanoes or are not possible to correlate with a distinct volcanic source ($n = 10$). These findings provide new information about the explosive history of Italian volcanoes and the distribution of emitted tephra. Thus the detection of several tephras like, for example, the Interplinian AP tephras from Vesuvius (TM-3) or the Solchiaro tephra from Procida-Vivara (TM-14) proved a wider distribution of eruption clouds than previously thought. Moreover, numerous ($n > 300$) tephra events like e.g. the eruption of the Peperino Tuffs from Albano (TM-17) could be re-dated or, like the Interplinian AP4 eruption of Vesuvius (TM-3a) dated for the first time by the Monticchio sedimentation rate chronology. For some of the larger events the rapid succession of eruptions within a short time is clearly recorded in the Monticchio record due to the high sedimentation rate and absence of sediment mixing due to bioturbation or subaqueous currents.

A total number of 42 Monticchio tephra layers could be precisely correlated with known and partly well dated explosive events. Radiometric and radioisotopic dating of 26 of these tephra events is in agreement with tephra ages obtained by the varve supported sedimentation rate chronology with an estimated mean deviation of about 5%. Significant discrepancies appear for the period from ca 30–40 and 85–100 ka, which confirm previously assumed problems with the sedimentation rate chronology. Thus detailed tephrochronological studies can be a valuable tool for identification of problematic sections in the chronology of long palaeoclimatic records.

Acknowledgements

The authors wish to thank theirs colleagues and the GFZ coring team for their technical and scientific expertise. M. Köhler, G. Arnold, D. Berger and K. Reinhold (GFZ Potsdam) are acknowledged for laboratory help particularly with regards to the production of thin sections, and O. Appelt, Dr. D. Rhede and Dr. W. Seifert for the technical assistance during electron microprobe measurements. We are grateful to Prof. R. Cioni, Prof. G. Cavarretta, Prof. G. Orsi, Dr. L. Pappalardo, Dr. R. Sulpizio and A. Di Muro for their hospitality and fruitful discussions on the Italian volcanism. Moreover, we thank Dr. C. Principe and an anonymous reviewer for revising the manuscript and for constructive comments.

Financial support for coring campaigns and tephrochronological studies has been provided by the GeoForschungsZentrum Potsdam and the German Research Foundation (DFG), respectively, with grant NE 154/33. It is a contribution to the European Lake Drilling Program (ELDP).

References

Alessio, M., Bella, F., Improta, S., Belluomini, G., Cortesi, C., Turi, B., 1971. University of Rome Carbon-14 dates IX. Radiocarbon 13, 395–411.

Alessio, M., Bella, F., Improta, S., Belluomini, G., Calderoni, G., Cortesi, C., Turi, B., 1973. University of Rome Carbon-14 dates X. Radiocarbon 15, 165–178.

Alessio, M., Bella, F., Improta, S., Belluomini, G., Calderoni, G., Cortesi, C., Turi, B., 1974. University of Rome Carbon-14 dates XII. Radiocarbon 16, 358–367.

Alessio, M., Bella, F., Improta, S., Belluomini, G., Calderoni, G., Cortesi, C., Turi, B., 1976. University of Rome Carbon-14 dates XIV. Radiocarbon 18, 321–349.

Allen, J.R.M., Brandt, U., Brauer, A., Hubberten, H.-W., Huntley, B., Keller, J., Kraml, M., Mackensen, A., Mingram, J., Negendank, J.F.W., Nowaczyk, N.R., Oberhänsli, H., Watts, W.A., Wulf, S., Zolitschka, B., 1999. Rapid environmental changes in southern Europe during the last glacial period. Nature 400, 740–743.

Andronico, D., 1997. La Stratigrafia dei prodotti dell'eruzione di Lagno Amendolare (Phlegrean Fields, Napoli). Atti della Societ Toscana di Scienze Naturali Memoirs, Serie A 104, 165–178.

Andronico, D., Cioni, R., 2002. Contrasting styles of Mount Vesuvius activity in the period between the Avellino and Pompeii Plinian eruptions, and some implications for assessment of future hazards. Bulletin of Volcanology 64, 372–391.

Andronico, D., Calderoni, G., Cioni, R., Sbrana, A., Sulpizio, R., Santacroce, R., 1995. Geological map of Somma-Vesuvius Volcano. Periodico di Mineralogia 64, 77–78.

Ayuso, R.A., De Vivo, B., Rolandi, G., Seal II, R.R., Paone, A., 1998. Geochemical and isotopic (Nd–Pb–Sr–O) variations bearing on the genesis of volcanic rocks from Vesuvius, Italy. Journal of Volcanology and Geothermal Research 82, 53–78.

Bard, E., Arnold, M., Hamelin, B., Tisnerat-Laborde, N., Cabioch, G., 1998. Radiocarbon calibration by means of mass spectrometric $^{230}Th/^{234}U$ and ^{14}C ages of corals. An updated data base including samples from Barbados, Mururoa and Tahiti. Radiocarbon 40, 1085–1092.

Bertagnini, A., Landi, P., Rosi, M., Vigliargio, A., 1998. The Pomici di Base plinian eruption of Somma-Vesuvius. Journal of Volcanology and Geothermal Research 83, 219–239.

Boivin, P., Camus, G., De Goër, A., Gourgaud, A., Kieffer, G., Mergoil, J., Vincent, P., 1991. Volcanology of the Chaîne des Puys. Parc Naturel Régional des Volcans d'Auvergne, Imprimerie Moderne, Aurillac, 127pp.

Boygle, J., 1999. Variability of tephra in lake and catchment sediments, Svínavatn, Iceland. Global and Planetary Change 21, 129–149.

Brandt, U., Nowaczyk, N.R., Ramrath, A., Brauer, A., Mingram, J., Wulf, S., Negendank, J.F.W., 1999. Palaeomagnetism of Holocene and Late Pleistocene sediments from Lago di Mezzano and Lago Grande di Monticchio (Italy): initial results. Quaternary Science Reviews 18, 961–976.

Brauer, A., Mingram, J., Frank, U., Günter, C., Schettler, G., Wulf, S., Zolitschka, B., Negendank, J.F.W., 2000. Abrupt environmental oscillations during the Early Weichselian recorded at Lago Grande di Monticchio, southern Italy. Quaternary International 73/74, 79–90.

Brocchini, D., La Volpe, L., Laurenzi, M.A., Principe, C., 1994. Storia evolutiva del Monte Vulture. Plinius 12, 22–25.

Calanchi, N., Dinelli, E., Gasparotto, G., Lucchini, F., 1996a. Etnean tephra layer in Albano Lake and Adriatic Sea Cores: new findings of Y1-layer in the central Mediterranean area. Acta Vulcanologica 8, 7–13.

Calanchi, N., Dinelli, E., Lucchini, F., Mordenti, A., 1996b. Chemostratigraphy of late Quaternary sediments from Lake Albano and central Adriatic Sea cores (PALICLAS Project). In: Guilizzoni, P., Oldfield, F. (Eds.), Palaeoenvironmental Analysis of Italian Crater Lake and Adriatic Sediments. Memorie dell'Istituto italiano di Idrobiologia. 55, 247–263.

Calanchi, N., Cattaneo, A., Dinelli, E., Gasparotto, G., Lucchini, F., 1998. Tephra layers in Late Quaternary sediments of the central Adriatic Sea. Marine Geology 149, 191–209.

Cioni, R., Santacroce, R., Sbrana, A., 1999. Pyroclastic deposits as a guide for reconstructing the multi-stage evolution of the Somma-Vesuvius Caldera. Bulletin of Volcanology 60, 207–222.

Cioni, R., Levi, S., Sulpizio, R., 2000. Apulian Bronze Age pottery as a long-distance indicator of the Avellino Pumice eruption (Vesuvius, Italy). In: McGuire, W.G., Griffiths, D.R., Hancock, P.L., Stewart, I.S. (Eds.), The Archaeology of Geological Catastrophes, Vol. 171. Geological Society of London Special Publication, London, pp. 159–177.

Cioni, R., Sulpizio, R., Garruccio, N., 2003. Variability of the eruption dynamics during a Subplinian event: the Greenish Pumice Eruption of Somma-Vesuvius (Italy). Journal of Volcanology and Geothermal Research 124, 89–114.

Civetta, L., Cornette, Y., Crisci, G., Gillot, P.Y., Orsi, G., Requejo, C.S., 1984. Geology, geochronology and chemical evolution of the island of Pantelleria. Geological Magazine 121, 541–562.

Civetta, L., Orsi, G., Pappalardo, L., Fisher, R.V., Heiken, G., Ort, M., 1997. Geochemical zoning, mingling, eruptive dynamics and depositional processes; the Campanian Ignimbrite, Phlegrean Fields caldera, Italy. Journal of Volcanology and Geothermal Research 75, 183–219.

Coltelli, M., Del Carlo, P., Vezzoli, L., 2000. Stratigraphic constraints for explosive activity in the past 100 ka at Etna Volcano, Italy. International Journal of Earth Sciences 89, 665–677.

Cornette, Y., Crisci, G.M., Gillot, P.Y., Orsi, G., 1983. The recent volcanic history of Pantelleria: a new interpretation. Journal of Volcanology and Geothermal Research 17, 361–373.

D'Antonio, M., Civetta, L., Orsi, G., Pappalardo, L., Piochi, M., Carandente, A., de Vita, S., Di Vito, M.A., Isaia, R., 1999. The present state of the magmatic system of the Campi Flegrei caldera based on a reconstruction of its behavior in the past 12 ka. Journal of Volcanology and Geothermal Research 91, 247–268.

Deino, A.L., Curtis, G.H., Southon, J., Terrasi, F., Campajola, L., Orsi, G., 1994. ^{14}C and $^{40}Ar/^{39}Ar$ dating of the Campanian Ignimbrite, Phlegrean Fields, Italy. Abstract, ICOG-8. Berkeley, CA, pp. 77.

Delibrias, G., Di Paola, G.M., Rosi, M., Santacroce, R., 1979. La storia eruttiva del complesso vulcanico Somma Vesuvio ricostruita dalle successioni piroclastiche del Monte Somma. Reniconti Societa Italiana di Mineralogia e Petrologia 35, 411–438.

Delibrias, G., Guillier, M.-T., Labeyrie, J., 1986. Gif natural radiocarbon measurements X. Radiocarbon 28, 9–68.

De Rita, D., Zanetti, G., 1986. Caratteri vulcanologici e deposizionali delle piroclastiti di Stracciacappe (Sabatini Orientali, Roma). Memoirs Societa Geologica Italia 35, 667–677.

De Rita, D., Funiciello, R., Corda, L., Sposato, A., Rossi, U., 1993. Volcanic Units. In: Di Filippo, M. (Ed.), Sabatini Volcanic Complex. Consiglio Nazionale delle Ricerche Quaderni de 'La ricerca scientifica' 114(11), 33–79.

de Vita, S., Orsi, G., Civetta, L., Carandente, A., D' Antonio, M., Deino, A., di Cesare, T., Di Vito, M.A., Fisher, R.V., Isaia, R., Marotta, E., Necco, A., Ort, M., Pappalardo, L., Piochi, M., Southon, J., 1999. The Agnano-Monte Spina eruption (4100 years BP) in the restless Phlegrean Fields caldera (Italy). Journal of Volcanology and Geothermal Research 91, 269–301.

Di Vito, M.A., Sulpizio, R., Zanchetta, G., Calderoni, G., 1998. The geology of the south western slopes of Somma-Vesuvius, Italy, as inferred by borehole stratigraphies and cores. Acta Vulcanologica 10, 383–393.

Di Vito, M., Isaia, R., Orsi, G., Southon, J., di Vita, S., D' Antonio, M., Pappalardo, L., Piochi, M., 1999. Volcanism and deformation since 12,000 years at the Phlegrean Fields caldera (Italy). Journal of Volcanology and Geothermal Research 91, 221–246.

Druitt, T.H., Brenchley, P.J., Gökten, Y.E., Francaviglia, V., 1995. Late Quaternary rhyolitic eruptions from the Acigöl Complex, central Turkey. Journal of the Geological Society, London 152, 655–667.

Federico, M., Peccerillo, A., Barbieri, M., Wu, T.W., 1994. Mineralogical and geochemical study of granular xenoliths from the Alban Hills volcano, Central Italy: bearing on evolutionary processes in potassic magma chambers. Contributions to Mineralogy and Petrology 115, 384–401.

Fisher, R.V., Schmincke, H.-U., 1984. Pyroclastic rocks. Springer, Berlin, Heidelberg, 472pp.

Fornaseri, M., 1985. Geochronology of volcanic rocks from Latium (Italy). Rendiconti della Societa Italiana di Mineralogia e Petrologia 40, 73–106.

Fornaseri, M., Scherillo, A., Ventriglia, U., 1963. La regione vulcanica dei Colli Albani. Consiglio Nazionale delle Ricerche, Roma, 550pp.

Gillot, P.-Y., Keller, J., 1993. Radiochronological dating of Stromboli. Acta Vulcanologica 3, 69–77.

Giordano, G., De Rita, D., Cas, R., Rodani, S., 2002. Valley pond and ignimbrite veneer deposits in the small-volume phreatomagmatic 'Peperino Albano' basic ignimbrite, Lago Albano maar, Colli Albani volcano, Italy: influence of topography. Journal of Volcanology and Geothermal Research 118, 131–144.

Hajdas, I., Bonani, G., Zolitschka, B., Brauer, A., Negendank, J.F.W., 1998. ^{14}C ages of terrestrial macrofossils from Lago Grande di Monticchio (Italy). Radiocarbon 40, 803–807.

Hornig-Kjarsgaard, I., Keller, J., Koberski, U., Stadlbauer, E., Francalanci, L., Lenhart, R., 1993. Geology, stratigraphy and volcanological evolution of the island of Stromboli, Aeolian arc, Italy. Acta Vulcanologica 3, 21–68.

Hunt, J.B., Hill, P.G., 1993. Tephra geochemistry: a discussion of some persistent analytical problems. The Holocene 3, 271–278.

Hunt, J.B., Hill, P.G., 1996. An inter-laboratory comparison of the electron probe microanalysis of glass geochemistry. Quaternary International 34–36, 229–241.

Jahns, S., van den Bogaard, C., 1998. New palynological and tephrostratigraphical investigations of two salt lagoons on the island of Mljet, south Dalmatia, Croatia. Vegetation History and Archaeobotany 7, 219–234.

Keller, J., 1982. Mediterranean island arcs. In: Thorpe, R.S. (Ed.), Andesites. Wiley, Chichester, pp. 307–325.

Keller, J., Ryan, W.B.F., Ninkovich, D., Altherr, R., 1978. Explosive volcanic activity in the Mediterranean over the past 200,000 yr as recorded in deep-sea sediments. Geological Society of America Bulletin 89, 591–604.

Keller, J., Kraml, M., Morche, W., Negri, A., Scheld, A., A tephrochronological reference profile for the Ionian Sea: framework for the Upper Quaternary paleoceanographic record, in preparation.

Kraml, M., 1997. Laser-$^{40}Ar/^{39}Ar$-Datierungen an distalen marinen Tephren des jung-quartären mediterranen Vulkanismus (Ionisches Meer, METEOR-Fahrt 25/4). Ph.D. Thesis, Albert-Ludwigs-Universität Freiburg i.Br., 216pp.

Kraml, M., Keller, J., Henjes-Kunst, F., 1998. Tephrochronologische Zeitmarken für jung-quartäre Sedimente des Mittelmeeres. Abstract, Geo-Berlin '98. Berlin, Germany, pp. P96.

Landi, P., Bertagnini, A., Rosi, M., 1999. Chemical zoning and crystallization mechanisms in the magma chamber of the Pomici di Base plinian eruption of Somma-Vesuvius (Italy). Contributions to Mineralogy and Petrology 135, 179–197.

Le Bas, M.J., Le Maitre, R.W., Streckeisen, A., Zanettin, B., 1986. A chemical classification of volcanic rocks based on the Total Alkali-Silica diagram. Journal of Petrology 27, 745–750.

Lirer, L., Rolandi, G., Rubin, M., 1991. ^{14}C age of the "Museum Breccia" (Phlegrean Fields) and its relevance for the origin of the Campanian Ignimbrite. Journal of Volcanology and Geothermal Research 48, 223–227.

Lourens, L.J., Antonarakou, A., Hilgen, F.J., Van Hoof, A.A.M., Vergnaud-Grazzini, C., Zachariasse, W.J., 1996. Evaluation of the Plio-Pleistocene astronomical time scale. Paleoceanography 11, 391–413.

Mahood, G.A., Hildreth, W., 1986. Geology of the peralkaline volcano at Pantelleria, Strait of Sicily. Bulletin of Volcanology 48, 143–172.

McCoy, F.W., 1981. Areal distribution, redeposition and mixing of tephra within deep-sea sediments of the Eastern Mediterranean sea. In: Self, S., Sparks, R.S.J. (Eds.), Tephra studies. Reidel, Dordrecht, pp. 245–254.

Melluso, L., Morra, V., Perrotta, A., Scarpati, C., Adabbo, M., 1995. The eruption of the Breccia Museo (Phlegrean Fields, Italy): fractional crystallization processes in a shallow, zoned magma chamber and implications for the eruptive dynamics. Journal of Volcanology and Geothermal Research 68, 325–339.

Morche, W., 1988. Tephrochronologie der Äolischen Inseln. Ph.D. Thesis, Mineralogisch-Petrologisches Institut, Universität Freiburg/Br., 238pp.

Narcisi, B., 1993. Segnalazione di un livello piroclastico di provenienza etnea nell'area del Fucino (Italia Centrale). Il Quaternario 6, 87–92.

Narcisi, B., 1996. Tephrochronology of a late quaternary lacustrine record from the Monticchio Maar (Vulture Volcano, southern Italy). Quaternary Science Reviews 15, 155–165.

Narcisi, B., Vezzoli, L., 1999. Quaternary stratigraphy of distal tephra layers in the Mediterranean - an overview. Global and Planetary Change 21, 31–50.

Newton, A.J., Dugmore, A.J., 1993. Tephrochronology of Core C from Lago Grande di Monticchio. In: Negendank, J.F.W., Zolitschka, B. (Eds.), Paleolimnology of European Maar Lakes. Lecture Notes in Earth Sciences 49. Springer, Berlin, Heidelberg, pp. 333–348.

Nielsen, C.H., Sigurdsson, H., 1981. Quantitative methods for electron microprobe analysis of sodium in natural and synthetic glasses. American Mineralogist 66, 547–552.

Orsi, G., de Vita, S., Di Vito, M., 1996. The restless, resurgent Phlegrean Fields nested caldera (Italy): constraints on its evolution and configuration. Journal of Volcanology and Geothermal Research 74, 179–214.

Pappalardo, L., Civetta, L., D' Antonio, M., Deino, A., Di Vito, M., Orsi, G., Carandente, A., de Vita, S., Isaia, R., Piochi, M., 1999. Chemical and Sr-isotopical evolution of the Phlegrean magmatic system before the Campanian Ignimbrite and the Neapolitan Yellow Tuff eruptions. Journal of Volcanology and Geothermal Research 91, 141–166.

Paterne, M., Guichard, F., Labeyrie, J., Gillot, P.Y., Duplessy, J.C., 1986. Tyrrhenian Sea tephrochronology of the oxygen isotope record for the past 60,000 years. Marine Geology 72, 259–285.

Paterne, M., Guichard, F., Labeyrie, J., 1988. Explosive activity of the South Italian volcanoes during the past 80,000 years as determined by marine tephrochronology. Journal of Volcanology and Geothermal Research 34, 153–172.

Paterne, M., Labeyrie, J., Guichard, F., Mazaud, A., Maitre, F., 1990. Fluctuations of the Campanian explosive volcanic activity (South Italy) during the past 190,000 years, as determined by marine tephrochronology. Earth and Planetary Science Letters 98, 166–174.

Poli, S., Chiesa, S., Gillot, P.-Y., Gregnanin, A., Guichard, F., 1987. Chemistry versus time in the volcanic complex of Ischia (Gulf of Naples, Italy): evidence of successive magmatic cycles. Contributions to Mineralogy and Petrology 95, 322–335.

Ramrath, A., Nowaczyk, N.R., Negendank, J.F.W., 1999. Sedimentological evidence for environmental changes since 34,000 years BP from Lago di Mezzano, central Italy. Journal of Paleolimnology 21, 423–435.

Renne, P.R., Swisher, C.C., Deino, A.L., Karner, D.B., Owens, T.L., DePaolo, D.J., 1998. Intercalibration of standards, absolute ages and uncertainties in $^{40}Ar/^{39}Ar$ dating. Chemical Geology 145, 117–152.

Robinson, C., Shimmield, G.B., Creer, K.M., 1993. Geochemistry of Lago Grande di Monticchio, S. Italy. In: Negendank, J.F.W., Zolitschka, B. (Eds.), Paleolimnology of European Maar Lakes. Lecture Notes in Earth Sciences 49. Springer, Berlin, pp. 317–332.

Rolandi, G., 1988. Le ignimbriti della Piana Campana. Abstract, Atti 74° Congress Societa Geologica Italia, pp. 350–352.

Rolandi, G., Barrella, A.M., Borrelli, A., 1993a. The 1631 eruption of Vesuvius. Journal of Volcanology and Geothermal Research 58, 183–201.

Rolandi, G., Maraffi, S., Petrosino, P., Lirer, L., 1993b. The Ottaviano eruption of Somma-Vesuvio (8000 y B.P.): a magmatic alternating fall and flow-forming eruption. Journal of Volcanology and Geothermal Research 58, 43–65.

Rolandi, G., Petrosino, P., McGeehin, J., 1998. The interplinian activity at Somma-Vesuvius in the last 3500 years. Journal of Volcanology and Geothermal Research 82, 19–52.

Rosi, M., Sbrana, A., 1987. Phlegrean Fields. Consiglio Nazionale delle Ricerche, Roma, 176pp.

Rosi, M., Sbrana, A., Vezzoli, L., 1988. Stratigrafia delle Isole di Procida e Vivara. Bollettino del Gruppo Nazionale per la Vulcanologia 4, 500–525.

Rosi, M., Principe, C., Vecci, R., 1993. The 1631 Vesuvius eruption. A reconstruction based on historical and stratigraphical data. Journal of Volcanology and Geothermal Research 58, 151–182.

Rosi, M., Vezzoli, L., Castelmenzano, A., Grieco, G., 1999. Plinian pumice fall deposit of the Campanian Ignimbrite eruption (Phlegraean Fields, Italy). Journal of Volcanology and Geothermal Research 91, 179–198.

Santacroce, R., 1987. Somma-Vesuvius. Consiglio Nazionale delle Ricerche, Roma, 252pp.

Scandone, R., Bellucci, F., Lirer, L., Rolandi, G., 1991. The structure of the Campanian Plain and the activity of the Neapolitan volcanoes (Italy). Journal of Volcanology and Geothermal Research 48, 1–31.

Scarpati, C., Cole, P., Perrotta, A., 1993. The Neapolitan Yellow Tuff—a large volume multiphase eruption from Phlegrean Fields, Southern Italy. Bulletin of Volcanology 55, 343–356.

Schmidt, R., van den Bogaard, C., Merkt, J., Müller, J., 2002. A new Lateglacial chronostratigraphic tephra marker for the south-eastern Alps: the Neapolitan Yellow Tuff (NYT) in Längsee (Austria) in the context of a regional biostratigraphy and palaeoclimate. Quaternary International 88, 45–56.

Schmincke, H.-U., Park, C., Harms, E., 1999. Evolution and environmental impacts of the eruption of Laacher See Volcano (Germany) 12,900 a BP. Quaternary International 61, 61–72.

Siani, G., Paterne, M., Michel, E., Sulpizio, R., Sbrana, A., Arnold, M., Haddad, G., 2001. Mediterranean Sea surface radiocarbon reservoir age changes since the last glacial maximum. Science 294, 1917–1920.

Signorelli, S., Vaggelli, G., Francalanci, L., Rosi, M., 1999a. Origin of magmas feeding the Plinian phase of the Campanian Ignimbrite eruption, Phlegrean Fields (Italy): constraints based on

matrix-glass and glass-inclusion compositions. Journal of Volcanology and Geothermal Research 91, 199–220.

Signorelli, S., Vaggelli, G., Romano, C., 1999b. Pre-eruptive volatile (H_2O, F, Cl and S) contents of phonolitic magmas feeding the 3550-year old Avellino eruption from Vesuvius, southern Italy. Journal of Volcanology and Geothermal Research 93, 237–256.

Stoppa, F., Principe, C., 1998. Eruption style and petrology of a new carbonatitic suite from the Mt. Vulture (Southern Italy): the Monticchio Lakes formation. Journal of Volcanology and Geothermal Research 80, 137–153.

Stuiver, M., Reimer, P.J., Bard, E., Burr, G., Hughen, K., Kromer, B., McCormick, J., Spurk, M., 1998. The INTCAL 98 calibration curve. Radiocarbon 40, 1041–1083.

Sun, S.-s., McDonough, W.F., 1989. Chemical and isotopic systematics of oceanic basalts: implications for mantle compositions and processes. In: Saunders, A.D., Norry, M.J. (Eds.), Magmatism in the Ocean Basins. Geological Society of London, Special Publication, 42, pp. 313–345.

Thunell, R., Williams, D., Tappa, E., Rio, D., Raffi, I., 1979. The age, origin and volcanological significance of the Y-5 ash layer in the Mediterranean. Quaternary Research 12, 241–253.

Ton-That, T., Singer, B., Paterne, M., 2001. $^{40}Ar/^{39}Ar$ dating of latest Pleistocene (41 ka) marine tephra in the Mediterranean Sea: implications for global climate records. Earth and Planetary Science Letters 184, 645–658.

Trigila, R., 1995. The volcano of the Alban Hills. Tipografia della Scuola Grafica Salesiana, Roma, 283pp.

van den Bogaard, P., 1995. $^{40}Ar/^{39}Ar$ ages of sanidine phenocrysts from Laacher See Tephra (12,900 yr BP): chronostratigraphic and petrological significance. Earth and Planetary Science Letters 133, 163–174.

Vezzoli, L., 1988. Island if Ischia. Consiglio Nazionale delle Ricerche, Roma, 132pp.

Vezzoli, L., 1991. Tephra layers in Bannock Basin (Eastern Mediterranean). Marine Geology 100, 21–34.

Vinci, A., 1985. Distribution and chemical composition of tephra layers from Eastern Mediterranean abyssal sediments. Marine Geology 64, 143–155.

Vogel, J.S., Cornell, W., Nelson, D.E., Southon, J.R., 1990. Vesuvius/Avellino, one possible source of seventeenth century BC climatic disturbances. Nature 344, 534–537.

Washington, H.S., 1906. The Roman Comagmatic Region. Carnegie Institute, Washington, Publication 36, 1–220.

Watts, W.A., 1985. A long pollen record from Laghi di Monticchio, southern Italy: a preliminary account. Journal of the Geological Society of London 142, 491–499.

Watts, W.A., Allen, J.R.M., Huntley, B., 1996a. Vegetation history and palaeoclimate of the last glacial period at Lago Grande di Monticchio, southern Italy. Quaternary Science Reviews 15, 133–153.

Watts, W.A., Allen, J.R.M., Huntley, B., Fritz, S.C., 1996b. Vegetation history and climate of the last 15,000 years at Laghi di Monticchio, southern Italy. Quaternary Science Reviews 15, 113–132.

Wulf, S., 2000. Das tephrochronologische Referenzprofil des Lago Grande di Monticchio - Eine detaillierte Stratigraphie des süditalienischen explosiven Vulkanismus der letzten 100.000 Jahre. Ph.D. Thesis, University of Potsdam, Germany, Scientific Technical Report STR01/03, 124pp.

Zanchetta, G., Di Vito, M., Fallick, A.E., Sulpizio, R., 2000. Stable isotopes of pedogenic carbonates from the Somma-Vesuvius area, southern Italy, over the past 18 kyr: palaeoclimatic implications. Journal of Quaternary Science 15, 813–824.

Zolitschka, B., Negendank, J.F.W., 1996. Sedimentology, dating and palaeoclimatic interpretation of a 76.3 ka record from Lago Grande di Monticchio, southern Italy. Quaternary Science Reviews 15, 101–112.

5.2 Manuscript #2

"Towards a detailed distal tephrostratigraphy in the Central Mediterranean: the last 20,000 yrs record of Lago Grande di Monticchio" *(S. Wulf, M. Kraml & J. Keller, 2008: Journal of Volcanology and Geothermal Research)*

Scientific Technical Report STR14/01, Deutsches GeoForschungsZentrum GFZ. http://doi.org/10.2312/GFZ.b103-14010

Journal of Volcanology and Geothermal Research 177 (2008) 118–132

Contents lists available at ScienceDirect

Journal of Volcanology and Geothermal Research

journal homepage: www.elsevier.com/locate/jvolgeores

Towards a detailed distal tephrostratigraphy in the Central Mediterranean: The last 20,000 yrs record of Lago Grande di Monticchio

Sabine Wulf [a,*], Michael Kraml [b], Jörg Keller [c]

[a] GeoForschungsZentrum Potsdam, Section 3.3 Climate dynamics and sediments, Telegrafenberg, 14473 Potsdam, Germany
[b] Bundesanstalt für Geowissenschaften und Rohstoffe, Stilleweg 2, 30655 Hannover, Germany
[c] Institut für Mineralogie, Petrologie und Geochemie, Albert-Ludwigs.Universität Freiburg, Albertstrasse 23b, 79104 Freiburg i.Br., Germany

ARTICLE INFO

Article history:
Received 15 January 2007
Accepted 19 October 2007
Available online 12 November 2007

Keywords:
Central Mediterranean
Italian volcanism
tephrostratigraphy
Lago Grande di Monticchio
Late Pleistocene
Holocene

ABSTRACT

A detailed compilation of distal tephrostratigraphy comprising the last 20,000 yrs is given for the Central Mediterranean region. A total of 47 distinct ash layers identified in the maar lake sediments of Lago Grande di Monticchio (Basilicata, Southern Italy) are compared with proximal and distal terrestrial-marine tephra deposits in the circum-central Mediterranean region. The results of these studies provide valuable information for reconstructing the Late Pleistocene and the Holocene dispersal of pyroclastic deposits from south Italian explosive volcanoes, in particular Somma-Vesuvius, the Campi Flegrei caldera, Ischia Island and Mount Etna. Prominent tephras are discussed with respect to their reliability as dating and correlation tools in sedimentary records. Ashes from Plinian eruptions of Somma-Vesuvius (i.e. Avellino, Mercato, Greenish, Pomici di Base), for instance, are well-defined by their distribution patterns and their unique composition. The widespread Y-1 tephra from Mount Etna, on the other hand, derived most likely from two distinct Plinian events with changing wind conditions, and therefore becomes a less reliable stratigraphic marker. Statistical–numerical calculations are presented in order to discriminate between Holocene tephras from the Campi Flegrei caldera (i.e. Astroni 1–3, Agnano Monte Spina, Averno 1, Lagno Amendolare), since these ashes are characterized by an almost indistinguishable chemical fingerprint. As a highlight, numerous Campanian eruptions of proposed low-intensity have been identified in the distal site of Monticchio suggesting a revision of existing tephra dispersal maps and re-calculation of eruptive conditions. In summary, the tephra record of Monticchio is one of the key successions for linking both, terrestrial records from Central-southern Italy and marine sequences from the Tyrrhenian, Adriatic and Ionian Seas.

1. Introduction

Tephras deriving from high-magnitude explosive volcanic eruptions form important marker beds for dating and correlating sedimentary or ice core sequences from different environments. In Europe, numerous Pleistocene and Holocene distal tephras were described from Icelandic volcanoes (i.e. Thorarinsson, 1981), the Eifel volcanic field in south-western Germany (i.e. Van den Bogaard and Schmincke, 1985), and the Massif Central in France (i.e. Juvigné et al., 1992). The most appropriate region for tephrostratigraphic studies, in turn, is the Central-Eastern Mediterranean, which is divided in three main volcanic areas: i) Italian; ii) Aegean; and iii) Anatolian. The Italian volcanic area comprises the high-K-alkaline Tuscanian province, the K-alkaline Roman province (including Campanian volcanoes), the calc-alkaline to shoshonitic Aeolian Islands arc and the Na-alkaline Sicilian magmatism (e.g. Mount Etna, Ustica, Pantelleria and Linosa volcanoes) (Figs. 1 and 2). The Aegean volcanic area comprises the calc-alkaline Aegean Arc (e.g. Santorini, Kos, Nisyros, Mylos volcanoes), whereas the Anatolian volcanic area is linked to the Cappadocian volcanoes in central Turkey (e.g. Acigöl, Hasan Dag). These volcanic areas are characterized by high-frequent and large-magnitude explosive eruptions that generated a huge number of widespread tephras of quite different composition during the Late Quaternary.

First distal tephras in the Central-Eastern Mediterranean were detected and described in deep-sea sediments during the Swedish Deep-Sea Expedition of 1947–1948 (Mellis, 1954; Norin, 1958). Subsequent deep-sea drilling projects led to the development of a marine tephrostratigraphic framework for the last 300,000 yrs (e.g. Ryan, 1972; Cita et al., 1977; Keller et al., 1978; McCoy, 1980) (Fig. 3). More than 30 individual widespread tephras in numerous sediment cores from the Ionian, Aegean and Levantine Seas were assigned to large eruptions of Italian, Aegean Arc and Central Anatolian volcanoes and dated trough oxygen isotope and sapropel chronology of marine sediments (e.g. Keller et al., 1978; McCoy, 1980; Federman and Carey,

* Corresponding author. Present address: Institute for Geophysics, Jackson School of Geosciences, The University of Texas at Austin, J.J. Pickle Research Campus, Bldg. 196, 10100 Burnet Rd., Austin, TX 78758-4445, USA. Tel.: +1 512 471 0324; fax: +1 512 471 0348.
E-mail address: swulf@ig.utexas.edu (S. Wulf).

0377-0273/$ – see front matter © 2007 Elsevier B.V. All rights reserved.
doi:10.1016/j.jvolgeores.2007.10.009

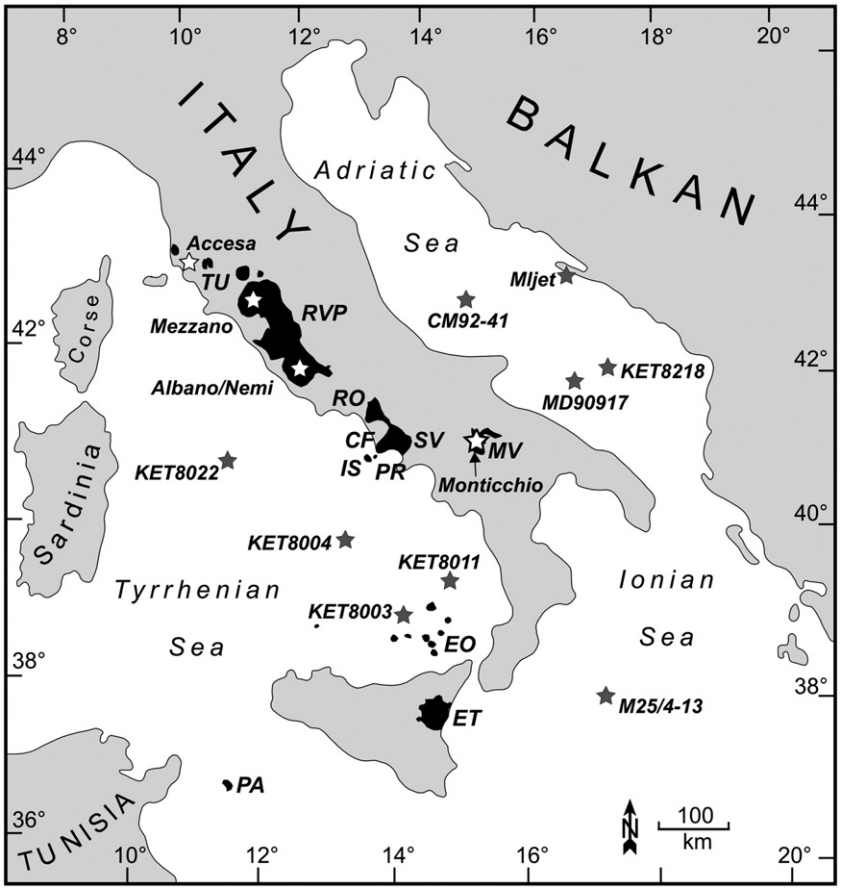

Fig. 1. Location of Lago Grande di Monticchio and main terrestrial and marine tephra sites in the Central Mediterranean mentioned in the text. Quaternary Italian volcanic sources are marked as black fields: *TU* Tuscany; *RVP* Roman Volcanic Province; *RO* Roccamonfina; *CF* Campi Flegrei, *SV* Somma-Vesuvius; *IS* Ischia; *PR* Procida-Vivara; *EO* Aeolian Islands; *ET* Mount Etna; *PA* Pantelleria.

1980; Cita et al., 1981; Vinci, 1985; Narcisi and Vezzoli, 1999). Due to the prevailing westerly winds, these ashes were exclusively distributed within the central and eastern part of the Mediterranean; so far, no tephra was found in the western part of the Mediterranean Sea.

For the last 20,000 yrs, tephrostratigraphic studies of Mediterranean deep-sea sediments revealed the detection of seven major eruptive events (Fig. 3, Table 1): the widespread rhyo-dacitic Y-2 (22,000 yr BP) and Z-2 (3600 yr BP) tephras from Santorini, the benmoreitic Y-1 tephra (17,000 yr BP) from Mount Etna, the poorly known Z-5, Z-4 and Z-3 tephras (10,000–8000 yr BP) of most likely Anatolian origin, and the tephriphonolitic Z-1 tephra (2000 yr BP) from Somma-Vesuvius (Keller et al., 1978; McCoy 1980). Findings of Santorini and Anatolian tephras are restricted to the Eastern part of the Mediterranean (Aegean, Levantine and Black Seas, and Greek and Turkish mainland), while the Italian Y-1 and Z-1 ashes form prominent marker layers in terrestrial and marine sediments in the Central Mediterranean (Fig. 2).

The Central Mediterranean itself was strongly influenced by intensive explosive volcanism in Central and Southern Italy during the Late Quaternary. Marine cores recovered from the Tyrrhenian, Adriatic and Ionian Seas (e.g. Keller et al., 1978; Paterne et al., 1986, 1988, 1990; Beccaluva et al., 1990; McCoy and Cornell, 1990; Vezzoli, 1991; Calanchi et al., 1994, 1998; Kallel et al., 2000; Siani et al., 2001, 2004; Oldfield et al., 2003; Insinga et al., 2006; Lowe et al., 2007), archaeological excavations and paleoclimate research programmes on lacustrine sequences and paleosols on the Italian mainland (e.g. Sullivan, 1988; Newton and Dugmore, 1993; Calanchi et al., 1996b; Narcisi, 1993, 1996, 1999a,b; Frezzotti and Narcisi, 1996; Karner et al., 1999; Ramrath et al., 1999; Sulpizio et al., 2003; Wulf et al., 2004, 2007; Munno and Petrosino, 2007; Magny et al., 2006) exhibited more than 350 individual ash layers for the last 150,000 yrs. The majority of marine and terrestrial distal tephras originated from Plinian to sub-Plinian explosive eruptions of the Campi Flegrei, Ischia Island, Somma-Vesuvius, Mount Etna and Aeolian Islands volcanoes. The correlation of these tephras with proximal and medial–distal volcanic counterparts was established on the basis of detailed work on the stratigraphy of proximal pyroclastic deposits, mainly carried out in the frame of volcanic hazard assessment and mitigation research projects (e.g. Rosi and Sbrana, 1987; Santacroce, 1987; Vezzoli, 1988; Pappalardo et al., 1999; Di Vito et al., 1999; Cioni et al., 2003; Sulpizio et al., 2003). For the last 20,000 yrs a huge number of tephras were recognised, particularly from Campanian volcanoes. As an example, Ischia Island alone exhibited more than 20 eruptions during the last 5000 yrs (Piochi et al., 1999), while ca. 70 explosive events from the Campi Flegrei caldera were identified for the last 12,000 yrs (Di Vito et al., 1999). Due to the increasing intensive search for cryptotephras, some of these ashes were also recognised in very distal sites like Austria, Croatia and the Macedonian/Albanian border (Jahns and van den Bogaard, 1998; Schmidt et al., 2002; Wagner et al., 2008-this issue). One of the most appropriate distal sites for tephrostratigraphic investigations is the Lago Grande di Monticchio in Southern Italy (Fig. 1). This small maar lake turned out to be an ideal archive for studying distal tephrostratigraphy in the Central Mediterranean due to: i) its vicinity to south Italian volcanoes (in particular the Campanian ones);, ii) the high and continuous sedimentation rate of lacustrine deposits; iii) the clear stratigraphic order; and, iv) the dating of tephras by a temporal high-resolution varve chronology. So far, a total of 344 distinct distal ashes were detected in the 135,000 yr sediment sequence (Fig. 3), and the most prominent ones ascribed to specific eruptive events (Newton and Dugmore, 1993; Narcisi, 1996; Wulf et al., 2004).

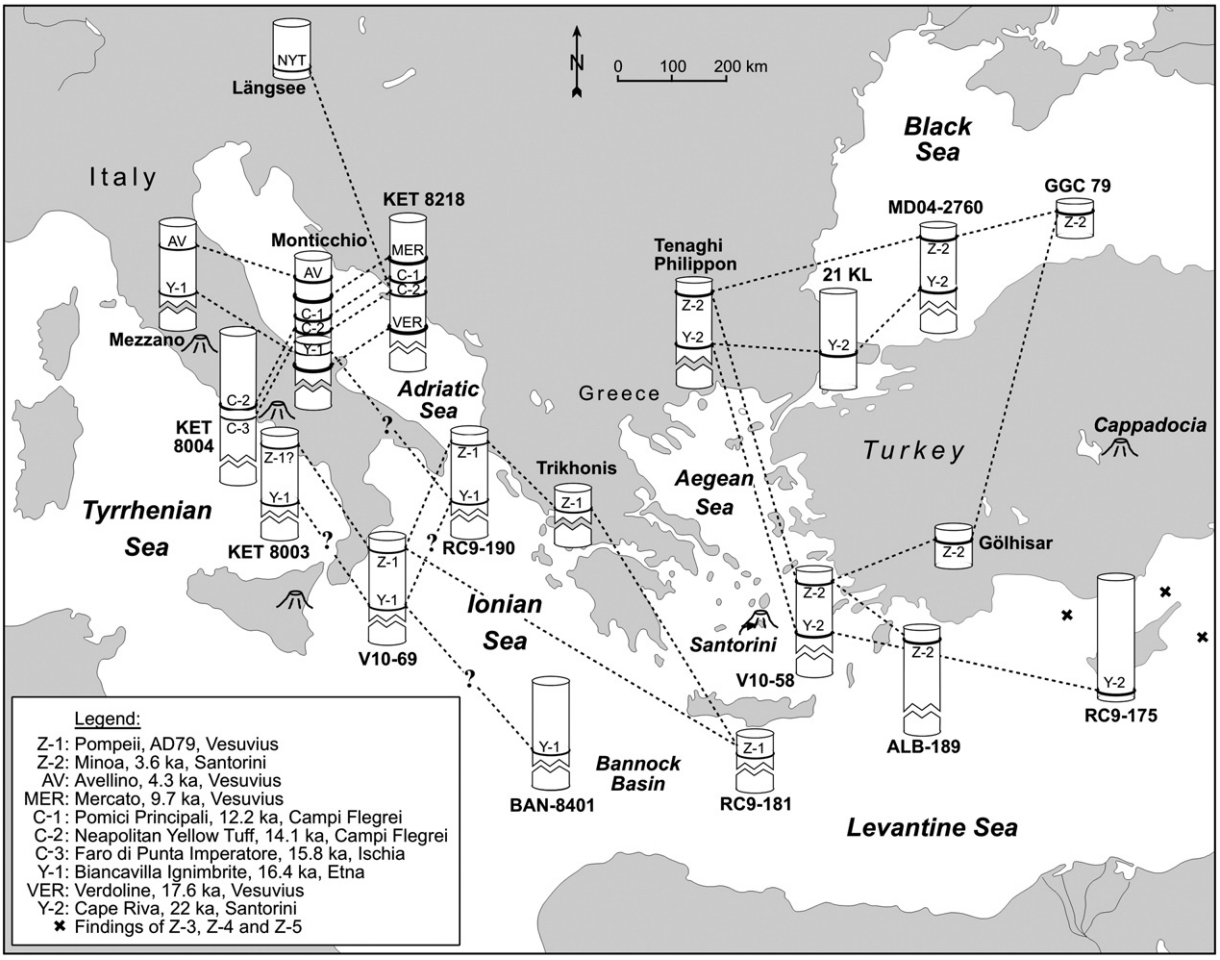

Fig. 2. Tephrostratigraphic constraints in the Eastern Mediterranean for the last ca. 20,000 yrs based on prominent ash layers of selected terrestrial and marine sediment records. Data from: Monticchio: Wulf et al. (2004), this study; Mezzano: Ramrath et al. (1999); Längsee: Schmidt et al. (2002); KET8003, KET8004, KET8218: Paterne et al. (1988); RC9-190, V10-69, RC9-181, V10-58, ALB-189, RC9-175: Keller et al. (1978); BAN-8401: Vezzoli (1991); Trikhonis: Creer et al. (1981); Tenaghi Philippon: Seymour et al. (2004); Gölhisar: Eastwood et al. (1999); 21KL: Wulf et al. (2002); MD04-2760: Kwiecien et al. (in press); GGC79: Guichard et al. (1993).

The main objective of this paper is to give a detailed overview of the distal tephrostratigraphy of both high- and low-intensity explosive eruptions of south Italian volcanoes for the last 20,000 yrs, based on new data from the Monticchio record, and their comparison with other terrestrial and marine archives in the Central Mediterranean.

2. Site, materials and methods

Lago Grande di Monticchio (40°56′N, 15°35′E, 656 m a.s.l., 36 m max. water depth) is the larger of two maar lakes in the Monte Vulture volcanic massif that formed 132,000±12,000 yrs ago (Brocchini et al., 1994). The lake is situated approximately 120 km east of Naples in a nearby favourable downwind position to Quaternary Campanian (100–200 km), Roman (200–350 km) and Sicilian–Aeolian volcanoes (300–600 km) (Fig. 1). Three coring surveys exhibited ca. 100 m of almost continuously laminated (ca. 90%) lacustrine sediments that span the last 135,000 calendar years (Zolitschka and Negendank, 1993; Brauer et al., 2000, 2007a). For the time interval of the last 20,000 calendar years, a total of 47 distal primary fallout ash layers were identified within the Monticchio sediments (Fig. 3). These tephras are well preserved due to the absence of bioturbation and retarded glass alteration processes, and well distinguishable from reworked ash layers. The latter are either mixed with washed-in plant material or occur as thin, fine-grained layers with more or less identical glass composition at the top of thick tephra deposits. Single tephras including cryptotephras (labelled as TM in numerical order from the youngest to the oldest deposits) were described on the basis of a continuous series of large-scale thin sections of sediments. This method provides information not only about the juvenile, mineral and lithic assemblage, but also about the original structure of tephra layers and grain size distribution of components. The chemical composition was determined on single glass shards on polished thin sections using microprobe techniques. Measurements were carried out at the WDS (wavelength dispersive spectrometry) CAMECA SX100 probe instrument at the GeoForschungsZentrum Potsdam (Germany). Conditions during the analyses were 15 kV for the accelerating voltage, 20 nA for the beam current and 10 to 20 μm for the beam diameter. Peak counting times for major-elements were 20 s except of Sodium analysed first at 10 s. For instrumental calibration inter-laboratory natural mineral and glass reference materials were used (Brauer et al., 2007b). The correlation of tephras is mainly based on the comparison of published WDS and SEM-EDS (scanning electron microscope-energy-dispersive spectrometry) major-element glass data and includes the numerical approach of the calculation of similarity coefficients (Borchardt et al., 1972). In cases where single grain chemical data were lacking, the Monticchio glass data were compared to XRF (X-ray fluorescence) and ICP-AES (inductively coupled plasma atomic emission spectrometry) whole rock analytical data in order to give a first idea of the origin of ashes.

Ages of distal tephras in the Monticchio record were obtained by the high-resolution varve and sedimentation rate chronology

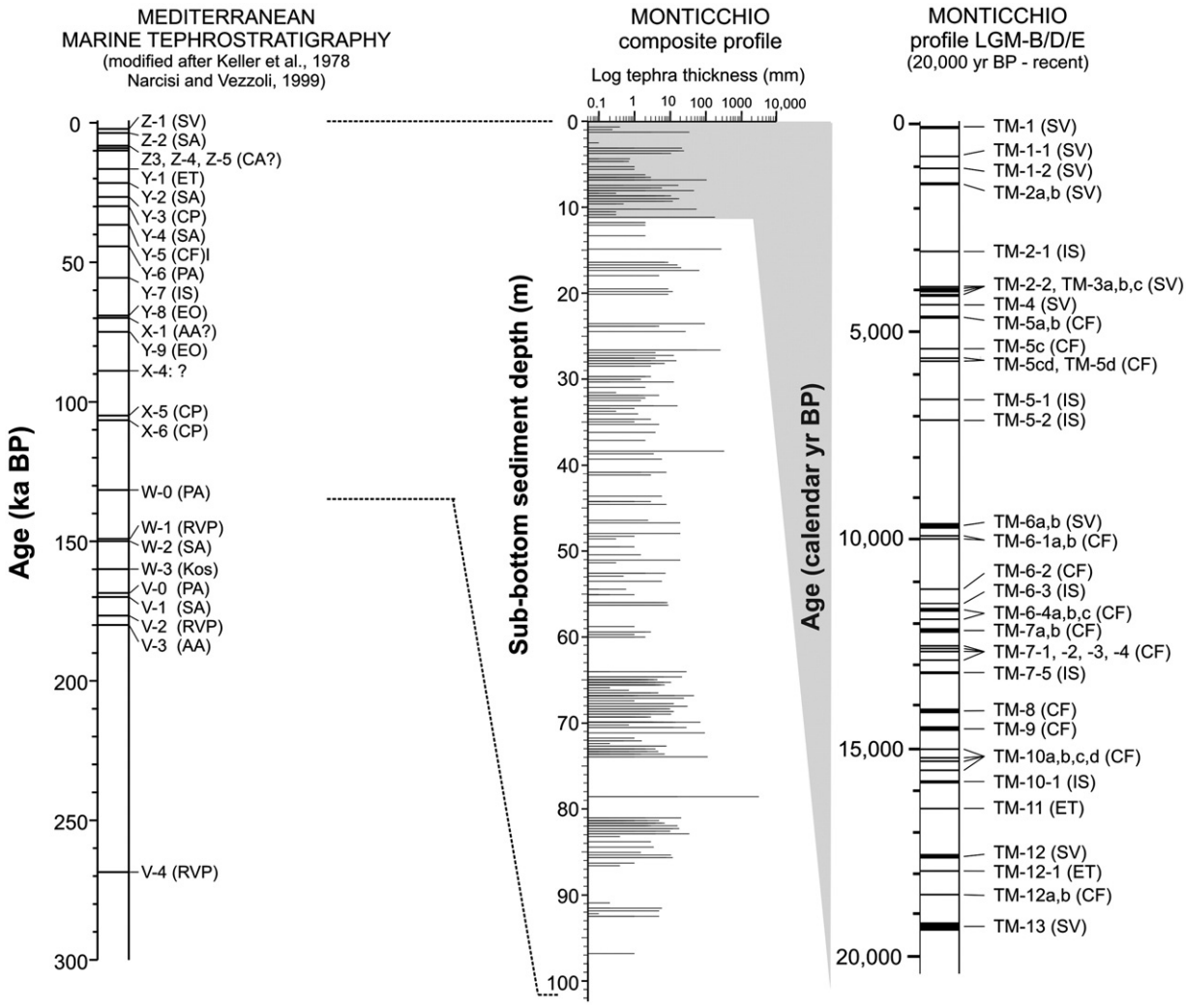

Fig. 3. Mediterranean marine tephrostratigraphy compared with the terrestrial tephra record of Lago Grande di Monticchio. Tephra sources in brackets: *SV* Somma-Vesuvius; *SA* Santorini; *CA* Cappadocia; *ET* Etna; *CP* Campanian Province; *CF* Campi Flegrei; *PA* Pantelleria; *IS* Ischia; *EO* Aeolian Islands; *AA* Aegean Arc; *RVP* Roman Volcanic Province.

(Zolitschka and Negendank, 1993) and are given as rounded calendar yr BP with an estimated error of ±5%. This chronology is based on the counting of annual layers and an interpolation of sedimentation rates in sections of poor lamination. Here the top sediments were used as the starting point for varve counting and assumed to represent AD 1950. For comparison, radiocarbon ages of tephra deposits obtained from literature were calibrated using INTCAL04 (Reimer et al., 2004) and MARINE04 programs (Hughen et al., 2004) and presented with a one sigma error as 'cal ^{14}C yr BP'.

3. Results

3.1. Description and origin of tephras

Distal tephra layers in the upper 20,000 yr sediment record of Monticchio range in thickness between 0.1 mm and 182 mm (Table 2). Different components (juvenile fragments, lithics and crystals) in each tephra layer are in general well sorted and show maximum grain sizes between 20 μm and 1.5 mm. Ashes show a wide range in major-element glass composition (Fig. 4, Table 3), but all of them indicate an origin from south Italian volcanoes. Most ashes are K-alkaline in composition and can be related to volcanic activity of the Campanian volcanoes. Only two tephras show a Na-alkaline benmoreitic composition, which is common for the Sicilian Province (i.e. Mount Etna, Ustica, Linosa, and Pantelleria volcanoes). Tephras deriving from Somma-Vesuvius show a wide compositional range from nearly saturated rocks (trachytes–phonolites) to highly under-saturated, high-K-alkaline rocks (leucititic phonolites–tephrites). Tephras from the Campi Flegrei caldera are in general high-K-trachy-phonolitic to trachyandesitic in composition, while Ischia ashes show a rather uniform and indistinguishable alkali-trachytic composition. To date, twenty four out of the forty-seven tephra layers were petrographically and chemically described by Wulf et al. (2004). A detailed description of the remaining twenty-three ash layers (ordered from the oldest to the youngest tephra layer) is given in the following:

TM-12-2a and *TM-12-2b* form a double-set of grey cryptotephras that date at 18,500±920 and 18,540±930 calendar yr BP. Components have a maximum grain size of 200 and 100 μm, respectively, and mainly comprise loose crystals of sanidine, plagioclase, biotite, clinopyroxene (augite), and volcanic rock fragments. Juvenile clasts are colourless to light brown and show a heterogeneous K-trachytic composition (Fig. 5a, Table 3).

TM-12-1 is a fine grained (<120 μm), dark brown, crystal-rich ash layer of 1.4 mm thickness. The main mineral phases are plagioclase, sanidine, clinopyroxene, orthopyroxene, apatite and amphibole. Brown glass shards are rare and reflect both a benmoreitic and rhyolitic composition (Fig. 4, Table 3). TM-12-1 dates at 17,980± 900 calendar yr BP.

TM-10-1 is a 12 mm thick vitric tephra layer, which dates at 15,820±790 calendar yr BP. Maximum grain sizes of components are

Table 1
Comparison of average major-element glass chemistry of widespread marine and terrestrial tephra markers in the Eastern Mediterranean

Tephra location	Z-1 # Ionian Sea M25/4-13	Z-2 [(1)] Black Sea MD04-2760	Avellino # Lago di Mezzano	Y-1 # Ionian Sea M25/4-13 phase A	Y-1 # Ionian Sea M25/4-13 phase B	Y-1 # Lago di Mezzano	Y-2 [(1)] Black Sea MD04-2760
SiO_2	55.54 (0.82)	71.87 (0.71)	55.58 (0.97)	61.46 (0.79)	63.65 (0.00)	60.32 (0.91)	71.30 (0.59)
TiO_2	0.41 (0.13)	0.30 (0.03)	0.18 (0.03)	1.23 (0.11)	0.78 (0.00)	1.38 (0.16)	0.48 (0.03)
Al_2O_3	21.52 (0.53)	13.42 (0.18)	23.29 (0.39)	17.11 (0.97)	17.52 (0.00)	17.46 (0.74)	14.24 (0.17)
FeO	3.78 (0.79)	2.06 (0.07)	1.95 (0.24)	4.24 (0.37)	2.08 (0.00)	5.09 (0.48)	3.15 (0.12)
MnO	0.15 (0.04)	0.07 (0.03)	0.14 (0.02)	0.15 (0.03)	0.05 (0.00)	0.17 (0.04)	0.12 (0.03)
MgO	0.50 (0.11)	0.30 (0.02)	0.22 (0.14)	1.50 (0.23)	0.51 (0.00)	1.82 (0.36)	0.43 (0.04)
CaO	4.68 (0.60)	1.46 (0.06)	2.18 (0.38)	3.90 (0.66)	1.74 (0.00)	4.45 (0.84)	1.80 (0.03)
Na_2O	5.91 (0.42)	4.93 (0.10)	8.35 (0.22)	6.10 (0.26)	7.06 (0.00)	5.89 (0.33)	4.34 (0.24)
K_2O	6.57 (1.08)	3.17 (0.08)	6.69 (0.38)	3.26 (0.66)	4.48 (0.00)	2.84 (0.61)	2.82 (0.07)
P_2O_5	0.11 (0.05)	0.04 (0.03)	0.03 (0.03)	0.47 (0.15)	0.22 (0.00)	0.56 (0.13)	0.09 (0.02)
Cl	0.86 (0.28)	0.29 (0.02)	0.64 (0.04)	0.30 (0.04)	0.10 (0.00)	0.30 (0.10)	0.26 (0.02)
F	0.00 (0.00)	0.00 (0.00)	0.35 (0.11)	0.00 (0.00)	0.00 (0.00)	0.00 (0.00)	0.00 (0.00)
Total	100.03 $n=8$	97.86 $n=42$	99.30 $n=9$	99.64 $n=14$	98.17 ($n=1$)	100.23 $n=9$	98.97 $n=13$

Two sigma standard deviations are given in brackets; n = number of shards analysed. Data from: # EMP (WDS) mean glass data (this study); [(1)] EMP (WDS) mean glass data (Kwiecien et al., in press).

200 μm. The mineral assemblage comprises sanidine, plagioclase, clinopyroxene (aegerine–augite) and amphibole. Lithics are rare and include volcanic rock fragments. Glass shards have a homogenous trachytic composition with Na_2O values ≥ K_2O (Fig. 5b, Table 3).

TM-10a and *TM-10c* are 4 mm and 1 mm thick white to pinkish vitric ashes that date at 15,030±750 and 15,300±770 calendar yr BP, respectively. Their mineral assemblage comprises sanidine, plagioclase, clinopyroxene and biotite crystals of 500 and 250 μm maximum grain size. Juvenile clasts are colourless and show a heterogeneous trachytic composition (Fig. 5a, Table 3).

TM-7-5 is a 1 mm thick white vitric ash that dates at 13,170±660 calendar yr BP. The mineral assemblage contains sanidine, plagioclase, clinopyroxene (aegerine–augite) and amphibole. Glass shards reveal a homogenous trachytic composition with Na_2O values ≥ K_2O (Fig. 5b, Table 3).

TM-7-4, *TM-7-3*, *TM-7-2* and *TM-7-1* are a succession of white cryptotephras, which are dated by varve counting between 12,910±650 and 12,590±630 calendar yr BP (Table 2). Tephras TM-7-4, TM-7-3 and TM-7-2 have a similar high-K-phonolitic glass composition (Fig. 5b, Table 3) and show maximum grain sizes of components between 50 μm and 100 μm. The main mineral phases are sanidine, plagioclase and biotite; volcanic rock fragments are present only in tephra TM-7-3. The younger TM-7-1 tephra differs in slightly higher silica contents, and, in addition, it contains augite phenocrysts. Maximum grain sizes for TM-7-1 tephra components are 40 μm.

TM-6-4 is made up of a succession of three distinct brown tephra layers dated at 11,980±600 (TM-6-4c, 3 mm thick), 11,890±590 (TM-6-4b, 1 mm thick) and 11,670±580 (TM-6-4a, 17 mm thick) calendar yr BP. Maximum grain sizes of components are 300 μm, 100 μm and 250 μm, respectively. Ash layers reveal a bimodal glass composition ranging from tephriphonolitic–phonolitic to trachyandesitic, whereas the TM-6-4a tephra show the most evolved composition (Fig. 5b, Table 3). The loose crystals and lithic fragments are similar for all three layers and include sanidine, plagioclase, clinopyroxene (augite), biotite and volcanic rock fragments.

TM-6-3 is a 1.3 mm thick, light-brownish tephra layer that comprises three distinct sub-layers of uniform trachytic composition (Fig. 5b; Table 3). The mineral assemblage includes loose crystals of sanidine, plagioclase, clinopyroxene (aegerine–augite) and amphibole with maximum grain sizes of 200 μm. Volcanic rock fragments are rare. TM-6-3 is dated at 11,520±580 calendar yr BP.

TM-6-2 forms a white, fine-grained (≤150 μm) double-layered cryptotephra of homogenous trachy-phonolitic composition (Fig. 5b, Table 3). The mineral assemblage is made up of sanidine, plagioclase, and clinopyroxene (augite) crystals. Volcanic rock fragments are also present. TM-6-2 is dated at 11,210±560 calendar yr BP.

TM-6-1 is a double-set of 3 mm and 1 mm thick ochre-brownish ash layers dated at 9960±500 (TM-6-1b) and 9890±490 calendar yr BP (TM-6-1a). The mineral assemblage contains sanidine, plagioclase, and clinopyroxene (augite) crystals of 200 μm maximum grain size. Volcanic rock fragments are also present. The glass chemistry of the TM-6-1a tephra reveals a trachytic to trachydacitic composition (Fig. 5b, Table 3).

TM-5-2 and *TM-5-1* are two distinct grey-brownish tephra layers of 1 and 2.5 mm thickness dated at 7150±360 and 6590±330 calendar yr BP, respectively. TM-5-1, in particular is divided into three distinct sub-layers that differ in maximum grain size between 100 μm and 200 μm. Both tephras are trachytic in glass composition with silica content of 63–64 wt.% and K_2O/Na_2O ratio around 1 (Fig. 5a, Table 3). Volcanic lithics and loose crystals are rare and comprise sanidine, plagioclase, clinopyroxene (aegerine–augite) and biotite.

TM-2-2 forms a coarse grained (≤300 μm), 1 mm thick grey ash layer, which is dated at 3940±200 calendar yr BP. The mineral assemblage comprises leucite, nepheline, sanidine, plagioclase, clinopyroxene (diopside) and biotite. Brown juvenile clasts are rich in leucite microcrystals and reveal a tephriphonolitic composition (Fig. 5c, Table 3).

TM-2-1 is a fine grained (≤120 μm) light-brownish cryptotephra with loose crystals of sanidine, plagioclase and amphibole and minor content of micro-pumices of trachytic composition (Fig. 5a, Table 3). TM-2-1 is dated at 3040±150 calendar yr BP.

TM-1-2 and *TM-1-1* are black cryptotephras that date at 1070±50 and 820±40 calendar yr BP, respectively. Maximum grain sizes are different and reveal values of 1000 μm for tephra TM-1-2 and 100 μm for tephra TM-1-1. Leucite, clinopyroxene, amphibole, plagioclase and sanidine form the main mineral phases for both ashes; volcanic rock fragments also occur. Juvenile clasts comprise dark brown scoria fragments that show a phonotephritic to trachyandesitic composition (Fig. 5c, Table 3).

4. Tephra correlation and dispersal

4.1. Last Glacial–Holocene transition (Termination I)

Between 20,000 and 10,000 calendar yr BP, twenty-five distal tephra layers are recorded in the Monticchio sequence (Fig. 3, Table 2). The oldest tephras, the thick trachytic to tephriphonolitic deposits of TM-13 (19,280±960 calendar yr BP) and TM-12 (17,560±880 calendar yr BP), were assigned by Narcisi (1996) and Wulf et al. (2004) to the caldera-forming Pomici di Base (21,790±290 cal ^{14}C yr BP) and the sub-Plinian Greenish (19,130±100 cal ^{14}C yr BP) eruptions of Somma-Vesuvius, respectively (Andronico et al., 1995; Bertagnini et al., 1998; Cioni et al., 2003). Both tephras were recently identified in the southern Adriatic Sea core MD90-917 (Siani et al., 2004) indicating a widespread eastward dispersal (Figs. 1 and 6). In the lacustrine record of Monticchio, the two Somma-Vesuvius tephras are separated by two thin ashes, TM-12-2a (18,500±920 calendar yr BP) and TM-12-2b (18,540±930 calendar yr BP), which may relate to an early stage of the Tufi Biancastri eruptions of the Campi Flegrei volcanic field at 17,900±

Table 2
Tephrostratigraphic details, origin, marine equivalents and referred ages of Late Pleistocene and Holocene tephras of the Lago Grande di Monticchio record

Tephra Monticchio	Depth (m)	Varve age (cal. yr BP) #	Thickness (mm)	Source	Eruption	Marine equivalent	Referred age in years BP (non-calibrated)
TM-1*	0.06	90±5	9	SV	1631	–	1631 AD (1)
TM-1-1	0.50	820±40	0.4	SV	?	–	–
TM-1-2	0.76	1070±50	0.25	SV	IIIme ?	–	−1140±60 (^{14}C terr.) (2)
TM-2a*	1.12	1420±70	3	SV	512 AD, PM1	–	512 AD (2)
TM-2b*	1.17	1440±70	35	SV	472 AD Pollena	–	472 AD (2)
TM-2-1	2.53	3040±150	0.1	IS	Cannavale/Chiarito ?	10–03 ?	2790±150 (^{14}C terr.) (3)
TM-2-2	3.11	3940±200	1	SV	AP5	–	–
TM-3a*	3.16	3990±200	22	SV	AP4	–	–
TM-3b*	3.20	4020±200	24	SV	AP3	–	2710±60 (^{14}C terr.) (2)
TM-3c* (2 sub-layers)	3.34	4150±210	31	SV	AP2	–	–
TM-4*	3.53	4310±220	6	SV	Avellino	–	3590±25 (^{14}C terr.) (4)
TM-5a*	3.74	4620±230	11	CF	Astroni 1–3	140–17	3820±50 (^{14}C terr.) (5)
TM-5b*	3.78	4660±230	3	CF	Astroni 1–3	160–17	3780±70 (^{14}C mar.) (6)
TM-5c*	4.27	5390±270	0.75	CF	Agnano Monte Spina	–	4130±50 (^{14}C terr.) (5)
TM-5cd	4.45	5640±280	0.7	CF	Averno 1 ?	167–17	4530±50 (^{14}C terr.) (5)
TM-5d*	4.48	5680±280	0.5	CF	Averno 1 ?	175–17	4600±70 (^{14}C mar.) (6)
TM-5-1(3 sub-layers)	5.09	6590±330	2.5	IS	Puzzillo 1–3 ?	10–04 ?	<8500 (^{14}C terr.)(7)
TM-5-2	5.44	7150±360	1	IS	Maisto ?	C0 ?	10,000>X>5,500 (8)
TM-6a*	6.45	9620±480	1	SV	Mercato top	V1	8010±35 (^{14}C terr.) (4)
TM-6b*	6.59	9680±480	106	SV	Mercato base		
TM-6-1a	6.67	9890±490	1	CF	Fondi di Baia	–	8560±70 (^{14}C terr.) (5)
TM-6-1b	6.69	9960±500	3	CF	Fondi di Baia		
TM-6-2(2 sub-layers)	7.26	11,210±560	0.2	CF	Casale	C(i)-1 ?	9580±100 (^{14}C terr.) (5)
TM-6-3(3 sub-layers)	7.38	11,520±580	1.3	IS ?	?	70–04 ?	–
TM-6-4a	7.46	11,670±580	17	CF	Soccavo 5 ?	275–17 ?	–
TM-6-4b	7.60	11,890±590	1	CF	Soccavo 4 ?	–	–
TM-6-4c	7.65	11,980±600	3	CF	Soccavo 4 ?	–	–
TM-7a*	7.75	12,170±610	6	CF	Agnano Pomici	C1, 310–17	10,320±50 (^{14}C terr.) (5)
TM-7b*	7.81	12,180±610	47	CF	Principali (APP)		10,430±90 (^{14}C mar.) (6)
TM-7-1	8.05	12,590±630	0.3	CF	Gaiola ?	–	–
TM-7-2	8.08	12,640±630	0.3	CF	La Pigna (LP)	–	−11,060±60 (^{14}C terr.) (5)
TM-7-3	8.13	12,770±640	0.1	CF	LP-NYT units 1–6 ?	–	–
TM-7-4	8.18	12,910±650	0.3	?	?	–	–
TM-7-5	8.36	13,170±660	1	IS ?	?	142–04 ?	–
TM-8* (3 sub-layers)	8.60	14,120±710	22	CF	Neapolitan Yellow Tuff (NYT)	C2, 395–17	14,900±400 (Ar/Ar) (9) 12,260±110 (^{14}C mar.) (6)
TM-9*	8.77	14,560±730	18	CF	Tufi Biancastri (GM1)	405–17	14,600±600 (Ar/Ar) (10) 12,600±110 (^{14}C mar.) (6)
TM-10a	8.97	15,030±750	4	CF	Lagno Amendolare (LA)	435–17	13,070±90 (^{14}C terr.) (11)
TM-10b*	9.04	15,220±760	7	CF	Lagno Amendolare (LA)		13,480±90 (^{14}C mar.) (6)
TM-10c	9.10	15,300±770	1	CF	Lagno Amendolare (LA)		
TM-10d*	9.18	15,550±780	4	CF	Lagno Amendolare (LA)		
TM-10-1	9.27	15,820±790	12	IS	St. Angelo Tuff ?	C3 ?	17,800±3200 (K/Ar) (12)
TM-11*	9.53	16,440±820	0.5	ET	Biancavilla	Y-1, Et1	14,180±200 (^{14}C terr.) (13) 15,520±70 (^{14}C terr.) (14) 14,650±90 (^{14}C mar.) (6)
TM-12*	10.02	17,560±880	55	SV	Verdoline	530–17	16,130±110 (^{14}C terr.) (4) 15,920±130 (^{14}C mar.) (6)
TM-12-1	10.19	17,980±900	1.4	ET	Ante-Biancavilla ?	–	–
TM-12-2a	10.43	18,500±920	0.3	CF	Tufi Biancastri ?	–	17,900±500 (Ar/Ar) (10)
TM-12-2b	10.44	18,540±930	0.2	CF	Tufi Biancastri ?		
TM-13*	11.07	19,280±960	182	SV	Pomici di Base	595–17	18,300±180 (^{14}C terr.) (4)

Sources: *SV* Somma-Vesuvius, *IS* Ischia, *CF* Campi Flegrei, *ET* Etna. *Data published in Wulf et al. (2004). References of tephra ages (non-calibrated): #varve ages derived from the Monticchio sediment chronology; (1)Rolandi et al. (1993a); (2)Rolandi et al. (1998); (3)Orsi et al. (1996); (4)Andronico et al. (1995); (5)Di Vito et al. (1999); (6)Siani et al. (2004); (7)Buchner et al. (1996); (8)de Vita et al. (2006); (9)Deino et al. (2004); (10)Pappalardo et al. (1999); (11)Andronico (1997); (12)Poli et al. (1987); (13)Delibrias et al. (1986); (14) Coltelli et al. (2000).

500 ^{39}Ar/^{40}Ar yr (Pappalardo et al., 1999). These tephras, however, were generated by low-intensity events, as hitherto suggested by their absence in any other distal terrestrial and marine record.

The Greenish tephra in the Monticchio record is preceded and followed by two thin benmoreitic tephras from Mount Etna. The older tephra layer TM-12-1 (17,980±900 calendar yr BP) is most likely generated by a sub-Plinian to Plinian eruption occurred prior to the Biancavilla–Montalto Ignimbrite eruption (16,950±360 cal ^{14}C yr BP; Delibrias et al., 1986). This tephra, however, has not been described in any other terrestrial or marine site, so far. The younger TM-11 tephra (16,440±820 calendar yr BP) was correlated by Wulf et al. (2004) with the marine Y-1 tephra, which is in turn directly related to the Biancavilla–Montalto Ignimbrite eruption of Mount Etna (Romano, 1982). The Y-1 tephra is widely dispersed in the Central Mediterranean Sea (e.g. Keller et al., 1978; Paterne et al., 1988; Vezzoli, 1991; Calanchi et al., 1996a; Siani et al., 2004) and on the central-southern Italian mainland (Narcisi, 1993; 1999b; Ramrath et al., 1999) (Fig. 2). The different dispersal axis directions of the Y-1 tephra to the east, southeast and north are still under discussion. Similarity coefficient calculations of the major-element composition (Table 4) suggest a close relationship between the younger TM-11 tephra in Monticchio and the Y-1 tephra identified in Lago di Mezzano, the central Adriatic Sea and the Bannock Basin (Fig. 2). The distal Etnean tephra in the southern Adriatic Sea, in turn, seems to relate to the Y-1 and Et1 tephras in the Ionian and Tyrrhenian Seas, respectively, as not only indicated by the glass composition but also by similar radiocarbon

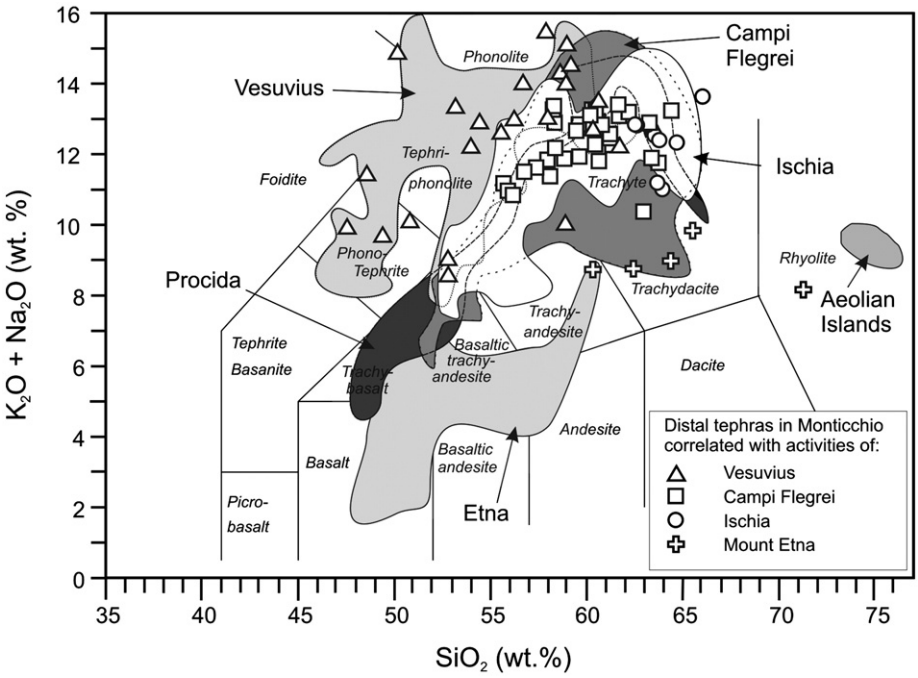

Fig. 4. Total alkali silica (TAS) plot of distal tephras (<20,000 yr BP) occurring in the Monticchio record. Fields indicate compositional variability of proximal tephra deposits for the last 20,000 yrs. Data sources for Somma-Vesuvius, Ischia and Campi Flegrei given in Fig. 5; Procida: De Astis et al. (2004); Etna: Coltelli et al. (2000); Aeolian Islands: Gioncada et al. (2005).

dates at 17,020±240 cal ^{14}C yr BP (southern Adriatic Sea; Siani et al., 2004) and 16,550±230 cal ^{14}C yr BP (Ionian Sea; Kraml, 1997). The hypothesis of at least two distinct Etnean eruptions during this time period is furthermore supported by the stratigraphic position of the Etnean layer Et1 in the Tyrrhenian Sea core KET8003, where it is more or less synchronously deposited with the Campanian C3 tephra. In the more distal site of KET8011, in turn, Et1 overlies C3, which corresponds to a reversed stratigraphic order of Y-1 and C3 tephra layers in the Monticchio succession. This might either imply: i) mixing and/or re-sedimentation processes occurred in the Tyrrhenian Sea cores, which resulted in an unclear stratigraphic order due to low sedimentation rates; ii) difficulties in tephra correlation among the different sites; and/or iii) an origin of the Etnean tephras Et1 (Tyrrhenian Sea) and TM-11 (Monticchio) from two distinct events. Despite the use of different analytical methods, all Y-1 findings correlate well with the proximal deposits of Unit D of the caldera-forming eruptions of the Ellittico volcano, Mount Etna (Coltelli et al., 2000). These large explosive events are related to the Biancavilla Ignimbrite eruption and dated at 18,770±60 and 18,250±110 cal ^{14}C yr BP (Coltelli et al., 2000). Based on dispersal maps of proximal tephra deposits (Coltelli et al., 2000), Y-1 in the Ionian Sea and the Bannock Basin would correspond to Unit D1b and D2b, respectively, whereas the northerly distributed Y-1/Et1 tephras on the Italian mainland and in Adriatic and Tyrrhenian Sea sediments might relate to atmospheric transport of finer clasts during these eruptions. Still unclear, however, remains the correlation of the 1500 yrs older Etnean tephra layer TM-12-1 in the Monticchio record due to the lack of comparable chemical data from proximal and distal sites. This requires, in general, a careful use of the Y-1 tephra(s) as reliable correlation marker in the Central Mediterranean.

The Y-1 tephra in the Monticchio record is overlain by the Ischia tephra layer TM-10-1 (15,820±790 calendar yr BP), which most likely relates to the explosive eruption of the St. Angelo Tuff from the Campotese volcano in the south-western part of the Island (17,800±3200 K/Ar yr; Poli et al., 1987). The marine tephra C3 in deep-sea cores KET8004, KET8003 and KET8011 of the Tyrrhenian Sea is similar in age and trachytic composition (Paterne et al., 1988) (Fig. 6), and is here considered to represent the same explosive event. The St. Angelo Tuff is succeeded by four single tephra layers, TM-10d, TM-10c, TM-10b and TM-10a, all of them characterized by a K-trachytic composition (Table 3). These tephras are dated between 15,550±780 and 15,030±750 calendar yr BP and were correlated by Wulf et al. (2004, this study) with the Lagno di Amendolare eruption of the Campi Flegrei caldera (15,430±190 cal ^{14}C yr BP; Andronico 1997). In the marine environment, a single Lagno Amendolare tephra layer was identified in core MD90-917 from the southern Adriatic Sea, and dated at 15,440±190 cal ^{14}C yr BP (LAM tephra layer; Siani et al., 2004). According to the results of similarity coefficient calculation (Table 5), this tephra can be correlated with tephra TM-10a in the Monticchio record. In addition, a still uncorrelated trachytic tephra recognised in two cores from the Central Adriatic Sea (Calanchi et al., 1998) shows a similar composition to tephra layers TM-10d and TM-10a (Table 5). This might indicate that the Lagno Amendolare tephras represent a quite complex eruptive succession, with alternating dispersal directions to the East and Northeast. Therefore, a careful use of these ashes as reliable stratigraphic marker is also required.

In the Monticchio record as well as in the MD90-917 core, the Lagno Amendolare tephras are followed by eleven tephra layers from the Campi Flegrei caldera. Tephra TM-9 (14,560±730 calendar yr BP; Wulf et al., 2004) and the marine ash sample 405-17 (14,040±150 cal ^{14}C yr BP; Siani et al., 2004) are both correlated with the late stage trachytic Tufi Biancastri/GM1 eruption (14,600±600 ^{39}Ar/^{40}Ar yr; Pappalardo et al., 1999). The limited recognition of this tephra in the Central Mediterranean area, suggests a restricted dispersal of this ash to the East. The Tufi Biancastri/GM1 tephra is overlain by the trachytic Neapolitan Yellow Tuff (NYT; 14,900±400 ^{39}Ar/^{40}Ar yr; Deino et al., 2004), which is correlated with tephra TM-8 in the Monticchio record (14,120±710 calendar yr BP; Wulf et al., 2004). The NYT pyroclastics have a widespread dispersal (Fig. 2). They form the prominent C2 tephra layer in the Tyrrhenian Sea cores KET8004 and KET8022 (Paterne et al., 1988), and were recognised in numerous terrestrial sites (Munno and Petrosino, 2007) up to 650 km northeast of their eruption centre (i.e. Frezzotti and Narcisi, 1996; Schmidt et al., 2002) (Fig. 2). The NYT tephra is overlain by a succession of four thin ash layers, TM-7-4, TM-7-3, TM-7-2 and TM-7-1 (12,910±650 to 12,590±

Table 3
Mean major-element glass composition (not normalized) of tephra layers of the Monticchio record

Tephra (glass fraction)	TM-1-1	TM-1-2	TM-2-1	TM-2-2	TM-5cd	TM-5-1	TM-5-2 (1)	(2)	TM-6-1a	TM-6-2
Varve age (cal. yr BP)	820	1070	3040	3940	5640	6590	7150		9890	11,210
Source	SV	SV	IS	SV	CF	IS	IS		CF	CF
SiO_2	49.55 (0.10)	46.87 (0.19)	60.99 (0.80)	53.03 (0.90)	59.87 (0.34)	64.08 (0.58)	62.90 (0.23)	64.53 (0.12)	62.24 (0.25)	59.01 (0.57)
TiO_2	0.83 (0.14)	1.14 (0.03)	0.65 (0.07)	0.60 (0.05)	0.47 (0.05)	0.71 (0.06)	0.67 (0.03)	0.45 (0.02)	0.44 (0.02)	0.45 (0.03)
Al_2O_3	19.82 (2.10)	17.56 (0.19)	18.60 (0.38)	19.56 (0.17)	18.32 (0.07)	19.13 (0.32)	18.52 (0.13)	18.40 (0.25)	18.81 (0.23)	18.21 (0.25)
FeO	8.61 (1.21)	9.26 (0.13)	2.89 (0.30)	5.35 (0.45)	3.47 (0.14)	2.83 (0.23)	2.72 (0.10)	1.41 (0.01)	3.22 (0.08)	3.98 (0.26)
MnO	0.24 (0.05)	0.20 (0.03)	0.16 (0.04)	0.16 (0.02)	0.16 (0.03)	0.21 (0.06)	0.18 (0.03)	0.03 (0.03)	0.16 (0.02)	0.14 (0.02)
MgO	1.90 (0.58)	3.59 (0.06)	0.47 (0.09)	1.09 (0.27)	0.67 (0.07)	0.46 (0.07)	0.43 (0.04)	0.22 (0.06)	0.56 (0.02)	0.88 (0.12)
CaO	8.47 (0.45)	8.78 (0.09)	1.33 (0.15)	5.79 (0.59)	2.49 (0.14)	1.36 (0.11)	1.32 (0.07)	0.84 (0.15)	2.46 (0.07)	2.90 (0.22)
Na_2O	5.11 (0.28)	3.80 (0.08)	6.27 (0.31)	5.04 (0.88)	4.77 (0.11)	5.18 (0.51)	6.19 (0.31)	7.41 (0.67)	3.76 (0.18)	3.68 (0.35)
K_2O	4.56 (0.92)	5.93 (0.11)	6.33 (0.16)	6.91 (1.14)	8.39 (0.45)	5.87 (0.37)	6.48 (0.23)	5.25 (0.97)	6.38 (0.26)	8.34 (0.36)
P_2O_5	0.50 (0.04)	1.02 (0.09)	0.06 (0.05)	0.18 (0.06)	0.13 (0.06)	0.08 (0.03)	0.08 (0.03)	0.04 (0.03)	0.09 (0.03)	0.18 (0.03)
Cl	0.90 (0.12)	0.51 (0.02)	0.50 (0.09)	0.66 (0.27)	0.70 (0.04)	0.54 (0.13)	0.46 (0.10)	0.03 (0.01)	0.79 (0.03)	0.60 (0.04)
F	0.00 (0.00)	0.00 (0.00)	0.00 (0.00)	0.00 (0.00)	0.00 (0.00)	0.01 (0.04)	0.00 (0.00)	0.00 (0.00)	0.00 (0.00)	0.05 (0.06)
Total	100.29 $n=3$	98.54 $n=10$	98.14 $n=8$	98.20 $n=6$	99.27 $n=7$	100.47 $n=17$	99.86 $n=11$	98.56 $n=2$	98.72 $n=11$	98.25 $n=18$

Tephra (glass fraction)	TM-6-3	TM-6-4a (1)	(2)	TM-6-4b (1)	(2)	TM-6-4c (1)	(2)	TM-7-1	TM-7-2	TM-7-3
Varve age (cal. yr BP)	11,520	11,670		11,890		11,980		12,590	12,640	12,770
Source	IS ?	CF		CF		CF		CF	CF	CF
SiO_2	63.73 (0.45)	56.36 (0.94)	59.50 (0.68)	54.54 (0.83)	59.28 (0.08)	53.66 (0.58)	56.35 (0.43)	57.47 (0.70)	55.57 (0.31)	54.70 (0.16)
TiO_2	0.55 (0.04)	0.68 (0.09)	0.40 (0.01)	0.71 (0.01)	0.41 (0.02)	0.59 (0.04)	0.54 (0.02)	0.47 (0.03)	0.49 (0.03)	0.51 (0.02)
Al_2O_3	18.72 (0.24)	18.14 (0.15)	18.23 (0.07)	17.86 (0.24)	18.02 (0.08)	17.82 (0.03)	17.99 (0.06)	18.42 (0.25)	18.08 (0.06)	17.77 (0.16)
FeO	2.47 (0.22)	5.51 (0.58)	3.68 (0.08)	5.79 (0.11)	2.94 (0.07)	5.35 (0.01)	4.47 (0.12)	3.74 (0.25)	3.86 (0.15)	3.74 (0.06)
MnO	0.22 (0.03)	0.15 (0.04)	0.12 (0.02)	0.15 (0.01)	0.12 (0.03)	0.12 (0.04)	0.15 (0.03)	0.13 (0.01)	0.11 (0.02)	0.13 (0.01)
MgO	0.28 (0.04)	1.58 (0.31)	0.77 (0.02)	1.86 (0.10)	0.48 (0.03)	1.92 (0.09)	1.17 (0.06)	0.79 (0.07)	0.78 (0.04)	0.74 (0.01)
CaO	1.15 (0.09)	3.78 (0.52)	2.37 (0.06)	4.82 (0.11)	2.18 (0.00)	5.13 (0.01)	3.44 (0.05)	3.12 (0.18)	3.24 (0.11)	3.10 (0.05)
Na_2O	6.44 (0.27)	3.40 (0.19)	3.17 (0.23)	3.38 (0.16)	4.48 (0.06)	3.20 (0.05)	3.75 (0.08)	3.20 (0.21)	3.68 (0.11)	3.55 (0.09)
K_2O	6.09 (0.14)	7.57 (0.36)	8.78 (0.04)	7.15 (0.11)	8.17 (0.10)	7.33 (0.16)	8.00 (0.12)	8.30 (0.69)	8.97 (0.06)	8.99 (0.28)
P_2O_5	0.04 (0.03)	0.39 (0.11)	0.19 (0.01)	0.43 (0.04)	0.10 (0.08)	0.37 (0.07)	0.22 (0.05)	0.17 (0.06)	0.15 (0.02)	0.14 (0.07)
Cl	0.65 (0.08)	0.56 (0.04)	0.38 (0.01)	0.54 (0.03)	0.64 (0.04)	0.49 (0.02)	0.58 (0.05)	0.62 (0.04)	0.61 (0.03)	0.61 (0.04)
F	0.00 (0.00)	0.00 (0.00)	0.00 (0.00)	0.00 (0.00)	0.00 (0.00)	0.00 (0.00)	0.00 (0.00)	0.12 (0.08)	0.00 (0.00)	0.00 (0.00)
Total	100.35 $n=26$	97.97 $n=10$	97.47 $n=2$	97.09 $n=4$	96.68 $n=3$	95.85 $n=2$	96.52 $n=6$	96.37 $n=5$	95.38 $n=4$	93.81 $n=2$

Tephra (glass fraction)	TM-7-5	TM-10a (1)	(2)	TM-10c	TM-10-1	TM-12-1 (1)	(2)	(3)	TM-12-2a	TM-12-2b
Varve age (cal. yr BP)	13,170	15,030		15,300	15,820	17,980			18,500	18,540
Source	IS ?	CF		CF	IS	ET			CF	CF
SiO_2	63.02 (0.27)	57.72 (0.70)	59.98 (0.77)	59.30 (0.61)	61.69 (1.24)	60.17 (0.75)	62.62	68.12	59.12 (0.50	59.35
TiO_2	0.56 (0.03)	0.47 (0.03)	0.43 (0.02)	0.41 (0.04)	0.50 (0.04)	1.05 (0.06)	1.65	0.11	0.38 (0.03)	0.35
Al_2O_3	18.60 (0.12)	17.63 (0.41)	17.48 (0.31)	17.58 (0.25)	18.73 (0.48)	19.47 (0.16)	14.63	17.42	18.01 (0.22)	16.60
FeO	2.59 (0.05)	3.60 (0.30)	2.64 (0.26)	2.55 (0.08)	2.81 (0.17)	1.64 (0.04)	5.00	0.38	3.37 (0.05)	2.61
MnO	0.23 (0.03)	0.12 (0.03)	0.13 (0.02)	0.12 (0.03)	0.33 (0.05)	0.03 (0.01)	0.18	0.01	0.10 (0.02)	0.12
MgO	0.31 (0.01)	0.88 (0.09)	0.45 (0.07)	0.37 (0.02)	0.28 (0.03)	0.17 (0.03)	1.02	0.05	0.80 (0.05)	0.50
CaO	1.11 (0.04)	3.13 (0.31)	2.14 (0.14)	1.98 (0.05)	0.99 (0.03)	4.74 (0.15)	2.71	1.60	2.54 (0.07)	2.13
Na_2O	6.83 (0.22)	3.70 (0.29)	4.20 (0.22)	4.63 (0.16)	6.83 (0.49)	5.86 (0.08)	4.50	4.81	2.95 (0.04)	3.63
K_2O	5.96 (0.07)	8.43 (0.56)	8.15 (0.47)	7.91 (0.13)	5.59 (0.20)	2.57 (0.24)	4.22	2.99	9.24 (0.10)	7.31
P_2O_5	0.04 (0.03)	0.17 (0.05)	0.07 (0.04)	0.06 (0.05)	0.03 (0.02)	0.51 (0.47)	0.46	0.04	0.20 (0.04)	0.10
Cl	0.66 (0.02)	0.43 (0.03)	0.52 (0.05)	0.53 (0.03)	0.76 (0.07)	0.19 (0.11)	0.34	0.04	0.31 (0.04)	0.51
F	0.00 (0.00)	0.00 (0.00)	0.00 (0.00)	0.00 (0.00)	0.01 (0.02)	0.00 (0.00)	0.00	0.00	0.00 (0.00)	0.00
Total	99.92 $n=9$	96.29 $n=13$	96.19 $n=5$	95.45 $n=3$	98.54 $n=6$	96.35 $n=2$	97.25 $n=1$	95.56 $n=1$	96.95 $n=3$	93.09 $n=1$

Totals are given after correcting Cl and F values as oxides. *N*=number of glass shards analysed; *SV* Somma-Vesuvius, *IS* Ischia, *CF* Campi Flegrei; *ET* Etna.

630 calendar yr BP), which derive from rather low-intensity eruptions. Due to its age and composition, tephra TM-7-2 can be correlated to the La Pigna explosive event (12,980±60 cal ^{14}C yr BP; Di Vito et al., 1999) (Fig. 5b). The older tephras TM-7-3 and TM-7-4 may represent two out of six ash layers deposited between the Neapolitan Yellow Tuff (14,900±400 ^{39}Ar/^{40}Ar yr; Deino et al., 2004) and La Pigna pyroclastics in proximal vent areas (Di Vito et al., 1999). The stratigraphic position of the youngest tephra TM-7-1, in turn, suggests a rough correlation with the poorly known Gaiola tephra event (Di Vito et al., 1999). Dating of this eruption is constrained in proximal sites by dates of the preceding Soccavo 1 event (12,140±90 cal ^{14}C yr BP) and the following Agnano Pomici Principali eruption (Di Vito et al., 1999). The TM7-4 to TM-7-1 succession is followed by the Agnano Pomici Principali eruption (APP; 12,140±100 cal ^{14}C yr BP; Di Vito et al., 1999), as indicated by the tephrostratigraphic position of two distinct phonolitic to trachyandesitic tephra layers in the lake sediments (TM-7b and TM-7a; 12,180±610 and 12,170±610 calendar yr BP; Wulf et al., 2004). The marine deposits of APP are known as C1 tephra in deep-sea sediments of the Central and southern Adriatic Sea (Paterne et al., 1988; Siani et al., 2004; Lowe et al., 2007), supporting a rather widespread tephra dispersal to the East (Figs. 1 and 4). The younger triple layer of the TM-6-4 tephra unit (11,980±600 to 11,670±580 calendar yr BP) is correlated with the Soccavo 4 and Soccavo 5 events of the Campi Flegrei Caldera dated between 12,140±100 cal ^{14}C yr BP (APP) and 11,010±60 cal ^{14}C BP (Pisani 3 tephra) (Di Vito et al., 1999). In particular, the Soccavo 5 tephra (TM6-4a) resembles the stratigraphic position and composition of the marine ash layer 275-17 recognised in the southern Adriatic Sea core MD90-917 (Figs. 6 and 7), which has tentatively been correlated with the Early Holocene activity of the Palinuro Seamount (Siani et al., 2004). Here, we suggest a

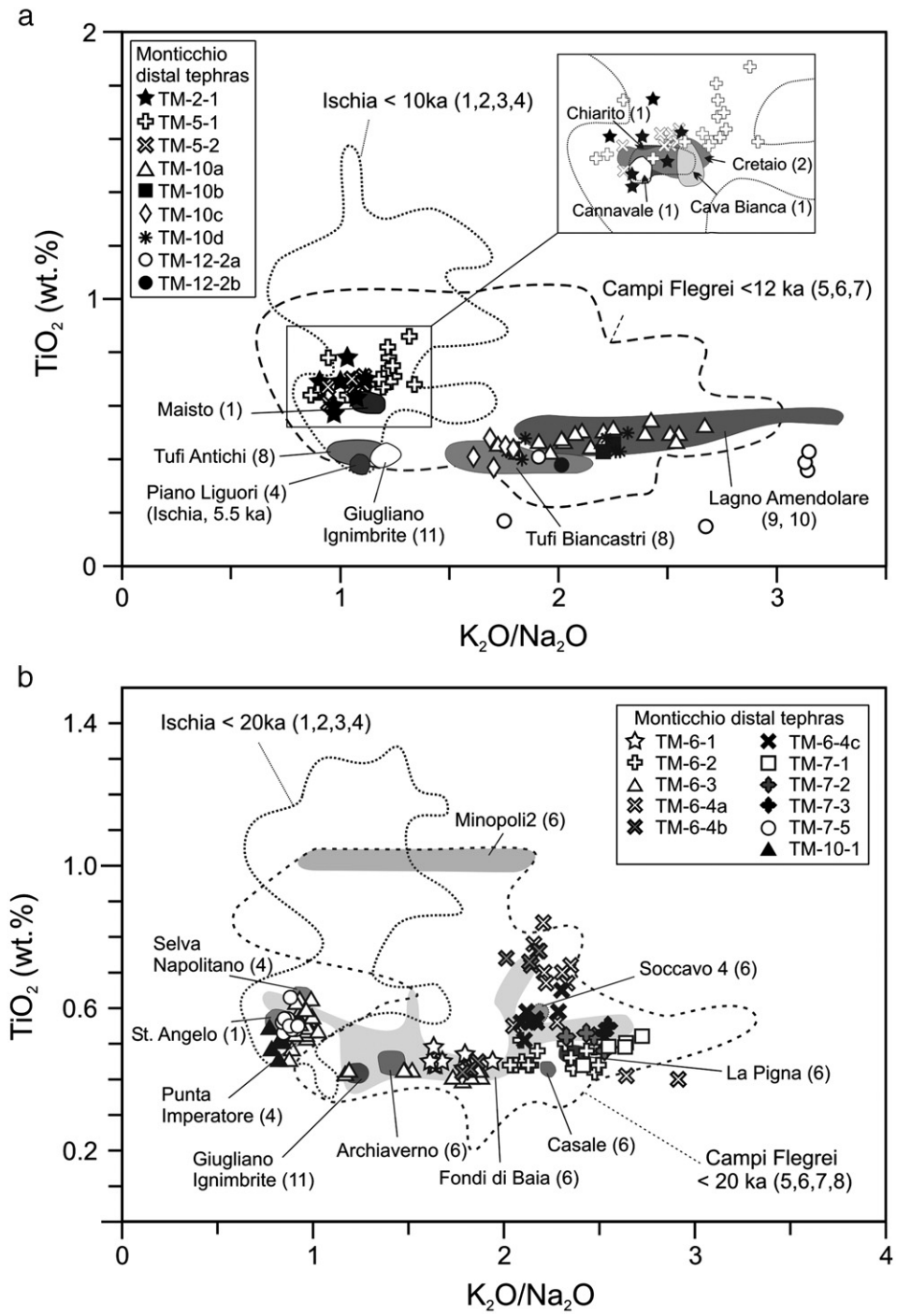

Fig. 5. a–d — Harker diagrams for discriminating and correlating distal tephras (<20,000 yr BP) in the Monticchio record to specific volcanic eruptions. Symbols represent normalized (re-calculated to 100 wt.%) glass chemical data (EPMA) of Monticchio tephras. Fields refer to published major-element XRF, ICP-AES, SEM and EPMA data of potential proximal correlative fallout units; data from: [1]Civetta et al. (1991); [2]Orsi et al. (1992); [3]Piochi et al. (1999); [4]Poli et al. (1987); [5]Rosi and Sbrana (1987); [6]D'Antonio et al. (1999); [7]de Vita et al. (1999); [8]Pappalardo et al. (1999); [9]Santacroce (1987); [10]Andronico (1997); [11]Fowler et al. (2007); [12]Rolandi et al. (1998); [13]Andronico and Cioni (2002); [14]Rolandi et al. (2004); [15]Turney et al. (in press).

correlation of this marine tephra rather to the Soccavo 5 event, which, in turn, implies a widespread easterly dispersal in the Central Mediterranean. The Soccavo succession in the Monticchio record is overlain by the triple-layered tephra TM-6-3 (11,520±580 calendar yr BP). This ash most likely relates to an unknown explosive eruption on Ischia Island that occurred more or less synchronously with the eruption of the Selva di Napolitano–Mt. Trippodi–Cannavale Lavas (10,400±900 K/Ar yr; Poli et al., 1987). TM-6-3 is chemically similar and in a comparable stratigraphic position (above the Agnano Pomici Principali tephra) with a marine tephra detected at 70 cm depth in the Tyrrhenian deep-sea core KET8004 (Paterne et al., 1988), and is here considered to represent the same eruptive event. The transition between Termination I and the Holocene in the Monticchio record is marked by the trachy-phonolitic TM-6-2 tephra (11,210±560 calendar yr BP) that most likely originates from an eruption of the Campi Flegrei caldera. At least nine volcanic centres were active during this time period; most of them, however, produced tephra of trachyandesitic to tephriphonolitic composition (Di Vito et al., 1999; D'Antonio et al.,

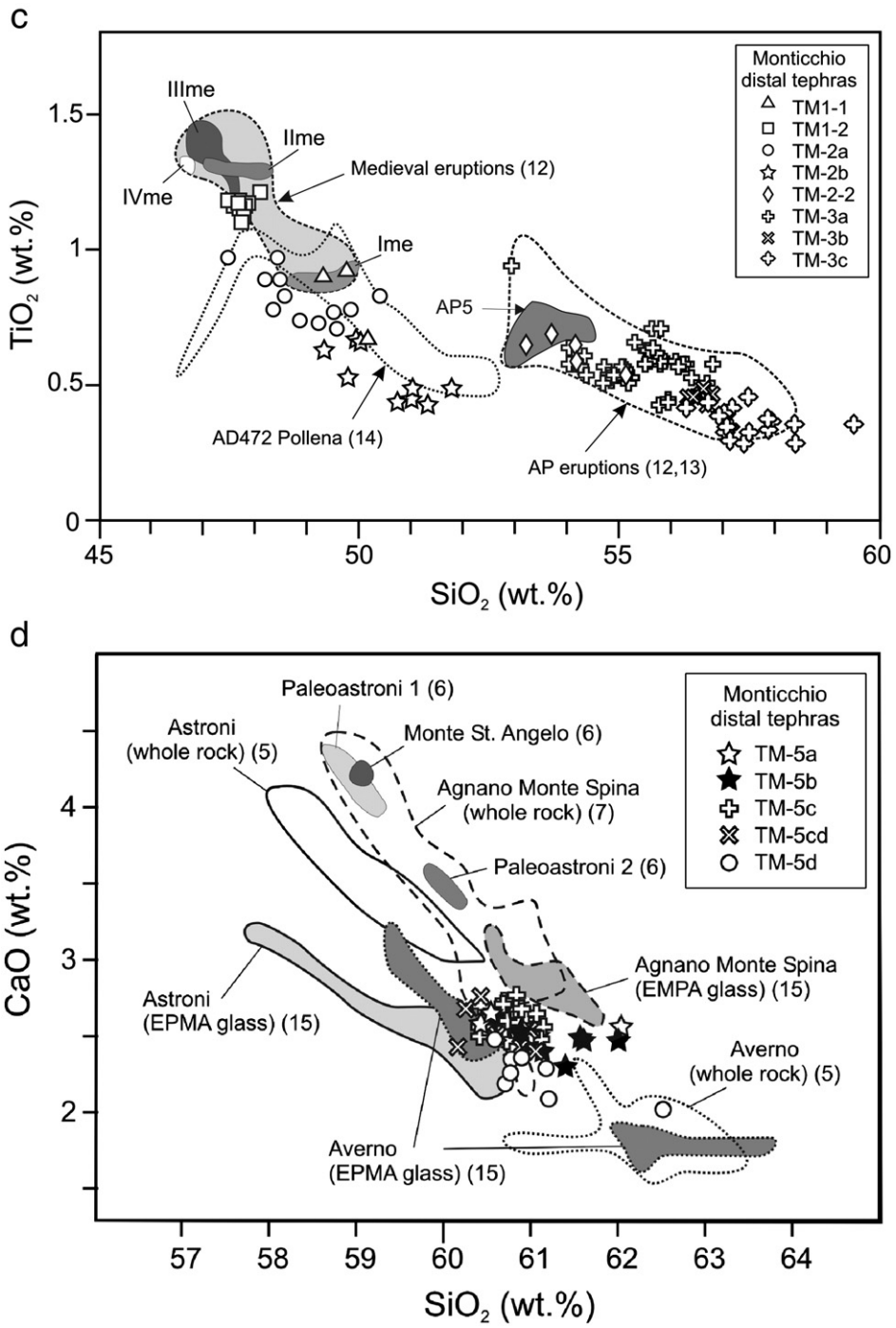

Fig. 5 (*continued*).

1999). The only potential correlative of TM-6-2 is given by the trachy-phonolitic Casale tephra (Fig. 5b), which erupted from an undefined centre more or less synchronously with the Pisani 3 tephra at 10,930± 170 cal ^{14}C yr BP (Di Vito et al., 1999). The age and composition of tephra TM-6-2 matches that of the marine tephra C(i)-1 from Tyrrhenian and southern Adriatic Sea cores (Paterne et al., 1988) (Fig. 6), indicating a widespread dispersal of the Casale tephra to the East.

4.2. Early Holocene (10,000–8000 cal yr BP)

The early Holocene succession of the Monticchio cores records major events occurring from the Campanian and Aeolian provinces (Table 2). The oldest of them is characterized by a double-set of thin tephra layers (TM-6-1b and TM-6-1a) dated by the varve chronology at 9960±500 and 9890±490 calendar yr BP, respectively. It can be correlated with the trachytic–trachydacitic Fondi di Baia eruption from the Campi Flegrei caldera (Fig. 5). To date, the Fondi di Baia tephra has not been described in any distal site in the Central Mediterranean. At 8890±30 cal ^{14}C yr BP the Plinian Mercato–Ottaviano eruption occurred from Somma-Vesuvius (Santacroce, 1987; Rolandi et al., 1993b; Andronico et al., 1995). This event dispersed its tephra far to the east and northeast. The related deposits in the Monticchio record are sub-divided in two tephra units (Wulf et al., 2004). The basal trachytic layer TM-6b (9680±480 calendar yr BP) probably represents the major Plinian event and occurs also as a single ash layer (V1) in Adriatic Sea core KET8218 and in cores from the

Table 4
Similarity coefficient calculation diagram (after Borchardt et al., 1972) for different samples of the Y-1/Et-1 tephra in the Central Mediterranean

	TM-11 phase A	TM-11 phase B	TM-12-1 phase A	Y-1 Mezzano	Y-1 Ionian Sea phase A	Y-1 Ionian Sea phase B	Y-1 Bannock Basin	Et1 Tyrrhenian Sea	Y-1 Southern Adriatic Sea	Y-1 Central Adriatic Sea	D1b Proximal	D2a Proximal
TM-11 phase A (1)												
TM-11 phase B (1)	0.722											
TM-12-1 phase A #	0.676	0.670										
Y-1 Mezzano #	0.931	0.710	0.727									
Y-1 Ionian Sea phase A #	0.902	0.790	0.730	0.886								
Y-1 Ionian Sea phase B #	0.625	0.845	0.689	0.617	0.678							
Y-1 Bannock Basin (2)	0.929	0.715	0.724	0.968	0.892	0.622						
Et1 (3) Tyrrhenian Sea	0.904	0.778	0.714	0.891	0.956	0.677	0.893					
Y-1 Southern Adriatic Sea (4)	0.884	0.749	0.622	0.835	0.854	0.668	0.826	0.873				
Y-1 Central Adriatic Sea (5)	0.937	0.757	0.668	0.914	0.889	0.656	0.909	0.916	0.898			
D1b Proximal (6)	0.929	0.745	0.704	0.896	0.907	0.657	0.903	0.929	0.854	0.907		
D2a Proximal (6)	0.867	0.626	0.675	0.880	0.790	0.558	0.877	0.798	0.791	0.829	0.831	
D2b Proximal (6)	0.934	0.689	0.706	0.931	0.867	0.611	0.933	0.883	0.831	0.888	0.921	0.901

Glass data from: # EMP-WDS, this study; [(1)]EMP-WDS, Wulf et al. (2004); [(2)]SEM-EDS, Vezzoli (1991); [(3)]SEM-EDS, Paterne et al. (1988); [(4)]SEM-EDS, Siani et al. (2004); [(5)]SEM-EDS, Calanchi et al. (1996a, 1998); [(6)]XRF, Coltelli et al. (2000).

Island of Mljet (Croatia; Fig. 1) east and northeast of Monticchio (Paterne et al., 1988; Jahns and van den Bogaard, 1998). The upper tephriphonolitic TM-6a tephra (9620±480 calendar yr BP) is correlated with the Pomici e Proietti unit of the Mercato eruption (Wulf et al., 2004), and was recently identified in Central Adriatic Sea cores (Lowe et al., 2007).

4.3. Middle Holocene (8000–4000 cal yr BP)

The Middle Holocene succession of the Monticchio sequence records nine explosive events from Campanian volcanoes (Table 2). The TM-5-2 and TM-5-1 tephras (dated at 7150±360 and 6590±330 calendar yr BP) most likely relate to the Maisto and Puzzillo 1–3 eruptions of Ischia Island. The Maisto phreatomagmatic event preceded the Phase 1 of Holocene activity of Ischia Island and comprises two major ash fallout beds exposed in the eastern part of the Ischia Island (de Vita et al., 2006). Its age is constrained by the underlying Selva del Napolitano–Mt. Trippodi–Cannavale Lavas (10,400±900 K/Ar yr BP; Poli et al., 1987) and the overlying Piano Liguori unit (5520±230 cal ^{14}C yr BP; Orsi et al., 1996). The Puzzillo eruptions formed three thick fallout deposits (de Vita and Piochi, pers. comment) and are dated at<8500 ^{14}C yr BP (Buchner et al., 1996). Due to the similar composition and stratigraphic position above the Casale tephra, TM-5-2 and TM-5-1 might correspond to the marine ash layers C0 (7000 interpolated yr BP) and 10-04 (5700 interpolated yr BP), recognised in the Tyrrhenian Sea core KET8004 (Paterne et al., 1988) (Figs. 6 and 7).

The TM-5-2 and TM-5-1 tephras are followed by five ash layers from the Campi Flegrei caldera with similar phono-trachytic glass composition (Fig. 5d). According to the date of deposition between 5680±280 and 5390±270 calendar yr BP for TM-5d, TM-5cd, and TM-5c, and 4660±230 calendar yr BP for TM-5b and TM-5a, these tephra layers were correlated with the Agnano Monte Spina (AMS; 4620±40 cal ^{14}C yr BP; Di Vito et al., 1999) and Astroni eruptions (AST; 4220±

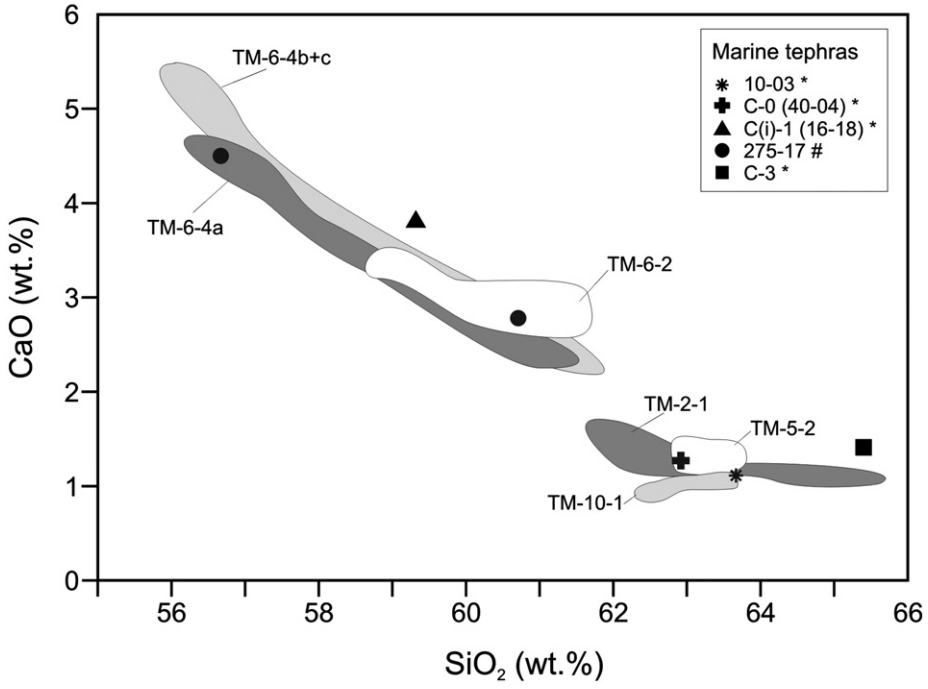

Fig. 6. SiO_2 vs. CaO diagram of Monticchio tephra layers (EPMA glass data) correlated with Central Mediterranean marine ash layers; EDS glass data from: * Paterne et al. (1988); # Siani et al. (2004).

Table 5
Comparison of chemical data of marine tephra layers from central and southern Adriatic Sea cores (SEM-EDS data from (a) Calanchi et al., 1998; (b) Siani et al., 2004) and Monticchio tephra layers on the basis of similarity coefficient calculation (after Borchardt et al., 1972)

Lagno Amendolare (15.5–15.0 ka BP)							
Lago Grande di Monticchio	Ref.	TM-10a(1)	TM-10a(2)	TM-10b	TM-10c	TM-10d(1)	TM-10d(2)
LAM, 434 cm	(a)	0.929	0.834	0.801	0.796	0.900	0.877
PAL94-66, 266 cm	(b)	0.889	0.848	0.829	0.816	0.872	0.887
CM92-41, 270 cm	(b)	0.887	0.849	0.829	0.817	0.870	0.888
Astroni 1–3 (AST), Agnano Monte Spina (AMS) and Averno (AV) (5.7–4.6 ka BP)							
Lago Grande di Monticchio	Ref.	TM-5a+b(AST)	TM-5c(AMS)	TM-5cd(AV?)	TM-5d (1)(AV?)	TM-5d (2)(AV?)	
MD90917 AMS, 175 cm	(a)	0.921	0.899	0.924	0.904	0.858	
MD90917 AMS, 167 cm	(a)	0.921	0.933	0.948	0.899	0.887	
MD90917 AST, 160 cm	(a)	0.929	0.889	0.920	0.911	0.839	
MD90917 AST, 140 cm	(a)	0.926	0.891	0.913	0.899	0.842	
CM92-43, 150 cm	(b)	0.934	0.959	0.937	0.892	0.915	
PAL94-66, 64 cm	(b)	0.893	0.913	0.897	0.851	0.874	
IN68-21, 100 cm	(b)	0.934	0.941	0.938	0.892	0.899	
PAL94-8, 128–124 cm	(b)	0.914	0.950	0.917	0.873	0.915	
RF93-77, 83 cm	(b)	0.937	0.948	0.941	0.895	0.907	
PAL94-77, 140 cm	(b)	0.940	0.951	0.944	0.898	0.910	
IN68-22, 133 cm	(b)	0.938	0.953	0.947	0.900	0.910	
CM92-41, 70 cm	(b)	0.935	0.950	0.938	0.892	0.896	
Avellino and AP eruptions (4.3–4.0 ka BP)							
Lago Grande di Monticchio	Ref.	TM-2-2(AP5)	TM-3a(AP4)	TM-3b(AP3)	TM-3c(AP2)	TM-4(Avellino)	
RF93-30, 530 cm	(b)	0.794	0.850	0.930	0.863	0.568	

70 cal ^{14}C yr BP; Di Vito et al., 1999; Isaia et al., 2004), respectively (Wulf et al., 2004). Recently published EPMA glass chemical data of Holocene Campi Flegrei pyroclastics (Turney et al., in press) suggest a new correlation of the tephras TM-5d and TM-5cd to the Averno 1 eruption (5150±30 cal ^{14}C yr BP; Di Vito et al., 1999) (Fig. 5d). The comparison of the Monticchio tephras with marine ash layers from the southern and central Adriatic Seas provides further constraints for source and proximal counterparts correlation. The results of similarity coefficient calculation (Table 5) suggest a correlation of tephra TM-5cd with two tephras at 175 and 167 cm depth in southern Adriatic sea core MD90-917, previously correlated with the Agnano Monte Spina eruption (Siani et al., 2004). According to the new chemical data, a correlation of these marine tephras with the Averno 1 eruption should be considered. The tephra layers TM-5b/TM-5a can be assigned to the marine tephras at 160 and 140 cm depth of core MD90-917, and corresponds to the Astroni 1–3 eruption as already proposed by Siani

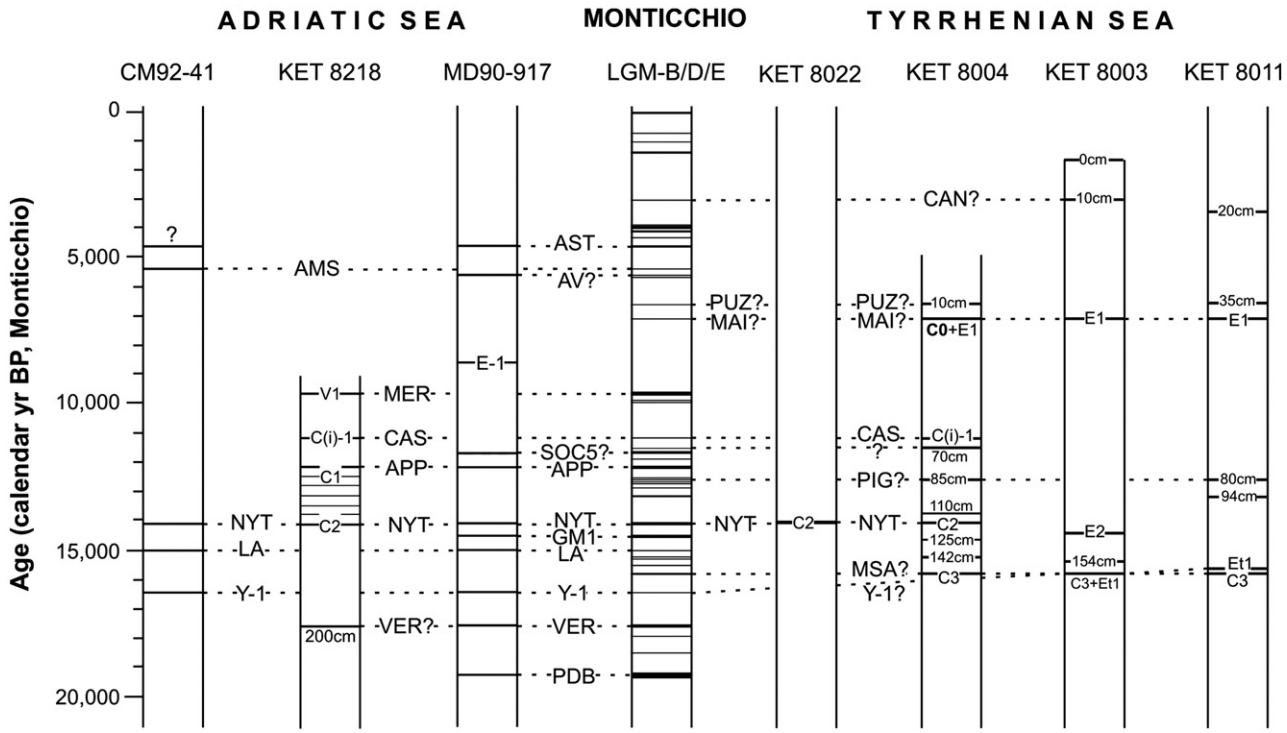

Fig. 7. Comparison of the 20,000 yr tephrostratigraphic record of Monticchio (LGM-B/D/E) with representative Tyrrhenian Sea (Paterne et al., 1988), central (CM-92-41; Calanchi et al., 1998) and southern Adriatic Sea cores (MD90-917, Siani et al., 2004; KET8218, Paterne et al., 1988). *AMS* Agnano Monte Spina, *APP* Agnano Pomici Principali, *AST* Astroni 1–3, *AV* Averno 1, *CAN* Cannavale, *CAS* Casale, *GM1* Tufi Biancastri, *LA* Lagno Amendolare, *MAI* Maisto, *MER* Mercato, *MSA* Monte St. Angelo, *NYT* Neapolitan Yellow Tuff, *PDB* Pomici di Base, *PIG* La Pigna, *PUZ* Puzzillo 1–3, *SOC5* Soccavo 5, *VER* Greenish, *Y-1* Biancavilla–Montalto.

et al. (2004). A distinct tephra found in numerous cores from the central Adriatic Sea and identified as AMS tephra (Calanchi et al., 1998; Lowe et al., 2007), in turn, chemically corresponds to the Monticchio tephra TM-5c (Table 5), and is different to the proposed AMS tephras in south Adriatic Sea core MD90-917. These results indicate an ENE dispersal for the Averno 1 and Astroni 1–3 tephras, and a rather north-easterly distribution of the Agnano Monte Spina tephra. However, the use of either one of these ashes as dating and correlation tools requires a careful inspection and consistent analytical standard methods (i.e. EPMA).

The Agnano Monte Spina and Astroni tephras in the Monticchio record are followed by a succession of Plinian and sub-Plinian distal deposits from Somma-Vesuvius. The Na-phonolitic Avellino tephra (TM-4), dated at 4310±220 calendar yr BP (Wulf et al., 2004), forms the most widespread Middle Holocene ash horizon in terrestrial archives of central and southern Italy. In the Monticchio record, it comprises a basal white micro-pumice deposits and a top thin grey ash layer. The Avellino tephra was found in the lacustrine sediments of Lago di Albano, Lago di Nemi (Calanchi et al., 1996b), Lago di Mezzano (Ramrath et al., 1999) and Lago dell' Accesa (Magny et al., 2006) north of Somma-Vesuvius (Fig. 1), and in the Basento basin in southern Italy (Sulpizio et al., 2008-this issue). Marine studies exhibit also an occurrence of the Avellino tephra in the Tyrrhenian (Kallel et al., 1997) and central Adriatic Seas (Lowe et al., 2007).

Four phonolitic to tephriphonolitic tephra layers from Somma-Vesuvius, TM-3c, TM-3b, TM-3a and TM-2-2, were deposited between 4150±210 and 3940±200 calendar yr BP in the Monticchio lake sediments (Wulf et al., 2004; this study). These leucite-bearing ashes have been correlated with the interplinian Avellino–Pompeii activities of Somma-Vesuvius (AP2, AP3, AP4 and AP5 eruptions; Rolandi et al., 1998; Andronico and Cioni, 2002) (Fig. 5c). In proximal sites, ages of 3160±230 cal ^{14}C yr BP and 2810±50 cal ^{14}C yr BP were reported for the AP2 and AP3 eruptions (Andronico and Cioni, 2002). Distal ashes from the AP2 and AP4 eruptions were recently found in Central and Southern Adriatic Sea cores (Lowe et al., 2007). An unidentified phonolitic tephra layer described in Adriatic Sea core RF93-30 (Calanchi et al., 1998) most likely correlates with the AP3 event (Table 5). Based on their thickness in the Monticchio record (from 14 mm to 24 mm; Wulf et al., 2004), the AP2-4 tephras are expected to be widely dispersed to the East-Northeast.

4.3. Late Holocene (4000 cal yr BP–present)

The Late Holocene succession of the Monticchio sequence starts recording an explosive activity from Ischia Island. Numerous volcanic centres were active during this period (de Vita et al., 2006), but only a few eruptions generated widespread ash deposits. Those include the Cannavale (2920±160 cal ^{14}C yr BP; Orsi et al., 1996), Chiarito (ca. VIII century B.C.; Gialanella, 1994), Cava Bianca (ca. 400 BC; Civetta et al., 1999) and Cretaio (1790±80 cal ^{14}C yr BP; Orsi et al., 1992) events. The cryptotephra TM-2-1 (3040±150 calendar yr BP) in the Monticchio succession records this activity, although it is not possible to chemically distinguish between the Cannavale and Chiarito eruptions, due to their similar age and composition (Fig. 5a). The Cretaio event, however, can be excluded as a correlative for TM-2-1 due to the lack of amphibole phenocrysts (Piochi, pers. comment). A discrete Ischia tephra recognised at 10 cm sediment depth in Tyrrhenian Sea core KET8003 shows a similar age (2550 interpolated yr BP; Paterne at al., 1988) and represents a potential marine counterpart for tephra TM-2-1 (Figs. 6 and 7).

Somma-Vesuvius generated several high-intensity explosive eruptions during historical times at AD 79, AD 472 Pollena, AD 512, and AD 1631 (Santacroce, 1987). Deposits of the latter three eruptions have been recognised as tephra layers in the Monticchio record (TM-2b, TM-2a and TM-1; Wulf et al., 2004). Despite the reported easterly dispersal direction none of these ashes has been found in the Adriatic Sea, yet. Tephra fallout of the AD 79 (Pompeii) eruption is mainly distributed to the south and southeast (Barberi et al., 1983), and, apart from the Monticchio site, reported in numerous terrestrial and marine successions in the southern Central Mediterranean (tephra Z-1; Keller et al., 1978).

In the Monticchio record, two cryptotephras TM-1-2 (1070±50 calendar yr BP) and TM-1-1 (820±40 calendar yr BP) are intercalated between the AD 512 and AD 1631 sub-Plinian event. These scoria layers can be correlated with medieval low-intensity eruptions of Somma-Vesuvius. In particular, TM-1-2 correlates with tephra unit IIIme (1030±60 cal ^{14}C yr BP; Rolandi et al., 1998), while the source event for tephra TM-1-1 has to remain undefined.

5. Conclusions

According to the results of tephra studies of the uppermost 11 m sediment section of the Lago Grande di Monticchio succession, at least forty-seven tephra layers record different intensity explosive eruptions from the Italian volcanoes during Termination I and the Holocene. The majority of these tephras were generated by Campanian volcanoes, particularly Somma-Vesuvius, the Campi Flegrei caldera and Ischia Island. Most of them show a more or less easterly dispersal. Rather widespread ashes of Campanian origin were produced by the Avellino, Mercato (Somma-Vesuvius) and the Neapolitan Yellow Tuff (Campi Flegrei) eruptions. These tephras were dispersed to the North and East-Northeast (Fig. 2) and can be easily distinguished from other Late Pleistocene and Holocene Campanian tephras due to their unique glass chemistry. The Y-1/Biancavilla–Montalto–Ignimbrite eruptions of Mount Etna formed one of the most widespread but complex tephra deposits in the Central Mediterranean. Findings of the Y-1 ash as well as other tephras from the Campi Flegrei activity (Astroni 1–3, Agnano Monte Spina and Lagno Amendolare) require a detailed discrimination by using either trace-element or mineral phase composition before using them as reliable dating and correlation tools.

The tephra record of Monticchio is one of the key successions for linking both, terrestrial records from Central-southern Italy and marine sequences from the Tyrrhenian, Adriatic and Ionian Seas by using numerous widespread tephra markers (Figs. 2 and 7). At least twelve tephras form reliable correlation marker in central and south Adriatic Sea cores of the last 20,000 yrs (Fig. 7). Tyrrhenian deep-sea sediments and new sequences recovered near the Sorrento peninsula (Insinga et al., 2006) exhibit more than nine distinct tephra layers that provide potential for tephra linking. In the Ionian Sea, only two tephras have been detected for the considered time span, so far (Fig. 2).

One major problem with respect to tephrochronological studies in the Central Mediterranean is still the quality, diversity and comparability of tephra chemical data. In order to guarantee reliable tephra correlations a statistical approach is required, and this implies data collection from single grains of both distal and proximal tephra layers using consistent high-quality analytical techniques (i.e. EPMA or laser ablation ICP-MS).

Acknowledgments

We gratefully acknowledge the support by M. Köhler and G. Arnold for preparation of polished thin sections and O. Appelt for assistance during EPMA measurements at the GeoForschungsZentrum Potsdam. We thank Roberto Sulpizio, Gianni Zanchetta, Monica Piochi and Lucia Civetta for fruitful discussion, as well as David Lowe and an anonymous reviewer who greatly helped to improve this manuscript. This project was funded by the German Research Council (DFG) and related to the 'International Continental Drilling Program/Kontinentales Tiefbohrprogramm der Bundesrepublik Deutschland' (ICDP/KTB) project no. NE 154/33-1,-2 and -3 and the GeoForschungsZentrum Potsdam.

References

Andronico, D., 1997. La Stratigrafia dei prodotti dell'eruzione di Lagno Amendolare (Phlegrean Fields, Napoli). Atti della SocietaÁ toscana di scienze naturali residente in Pisa. Memorie. Serie A 104, 165–178.

Andronico, D., Cioni, R., 2002. Contrasting styles of Mount Vesuvius activity in the period between the Avellino and Pompeii Plinian eruptions, and some implications for assessment of future hazards. Bulletin of Volcanology 64, 372–391.

Andronico, D., Calderoni, G., Cioni, R., Sbrana, A., Sulpizio, R., Santacroce, R., 1995. Geological map of Somma-Vesuvius Volcano. Periodico di Mineralogia 64, 77–78.

Barberi, F., Rosi, M., Santacroce, R., Sheridan, M.F., 1983. Volcanic hazard zonation: Mt. Vesuvius. In: Tazieff, H., Sabroux, J.-C. (Eds.), Forecasting volcanic events. Developments in Volcanology, vol. 1. Elsevier, Amsterdam-Oxford-New York-Tokyo, pp. 149–161.

Beccaluva, L., Bonatti, E., Dupuy, C., Ferrara, G., Innocenti, F., Lucchini, F., Macera, P., Petrini, R., Rossi, P.L., Serri, G., Seyler, M., Siena, F., 1990. Geochemistry and mineralogy of volcanic rocks from ODP sites 650, 651, 655 and 654 in the Tyrrhenian Sea. Proceedings of the Ocean Drilling Program 107, 49–74.

Bertagnini, A., Landi, P., Rosi, M., Vigliargio, A., 1998. The Pomici di Base plinian eruption of Somma-Vesuvius. Journal of Volcanology and Geothermal Research 83, 219–239.

Borchardt, G.A., Aruscavage, P.J., Millard Jr., H.T., 1972. Correlation of the Bishop ash, a Pleistocene marker bed, using instrumental neutron activation analysis. Journal of Sedimentary Petrology 42, 301–306.

Brauer, A., Mingram, J., Frank, U., Günter, C., Schettler, G., Wulf, S., Zolitschka, B., Negendank, J.F.W., 2000. Abrupt environmental oscillations during the Early Weichselian recorded at Lago Grande di Monticchio, southern Italy. Quaternary International 73/74, 79–90.

Brauer, A., Allen, J.R.M., Mingram, J., Dulski, P., Wulf, S., Huntley, B., 2007a. Evidence for last interglacial chronology and environmental change from Southern Europe. PNAS 104, 450–455.

Brauer, A., Wulf, S., Mangili, C., Appelt, O., Moscariello, A., 2007b. Tephrochronological dating of varved interglacial lake deposits from Piànico-Sèllere (Southern Alps, Italy) to around 400 ka: a reply to D. Pinti, V. Rouchon, X. Quidelleur, P.-Y. Gillot, S. Chiesa, C. Ravazzi. Journal of Quaternary Science 22 (4), 415–418.

Brocchini, D., La Volpe, L., Laurenzi, M.A., Principe, C., 1994. Storia evolutiva del Monte Vulture. Plinius 12, 22–25.

Buchner, G., Italiano, A., Vita-Finzi, C., 1996. Recent uplift of Ischia, southern Italy. In: Mc Guire, W.J., Jones, A.P., Neuberg, J. (Eds.), Volcano Instability on the Earth and other planets. Geol. Soc., vol. 110, pp. 249–252 (Special Paper).

Calanchi, N., Gasparotto, G., Romagnoli, C., 1994. Glass chemistry in volcaniclastic sediments of ODP Leg 107, Site 650, sedimentary sequence: provenance and chronological implications. Journal of Volcanology and Geothermal Research 60, 59–85.

Calanchi, N., Dinelli, E., Gasparotto, G., Lucchini, F., 1996a. Etnean tephra layer in Albano Lake and Adriatic Sea Cores: new findings of Y1-layer in the Central Mediterranean area. Acta Vulcanologica 8, 7–13.

Calanchi, N., Dinelli, E., Lucchini, F., Mordenti, A., 1996b. Chemostratigraphy of late Quaternary sediments from Lake Albano and central Adriatic Sea cores (PALICLAS Project). In: Guilizzoni, P., Oldfield, F. (Eds.), Palaeoenvironmental Analysis of Italian Crater Lake and Adriatic Sediments. Memorie dell'Istituto italiano di Idrobiologia, vol. 55, pp. 247–263.

Calanchi, N., Cattaneo, A., Dinelli, E., Gasparotto, G., Lucchini, F., 1998. Tephra layers in Late Quaternary sediments of the central Adriatic Sea. Marine Geology 149, 191–209.

Cioni, R., Sulpizio, R., Garruccio, N., 2003. Variability of the eruption dynamics during a Subplinian event: the Greenish Pumice eruption of Somma-Vesuvius (Italy). Journal of Volcanology and Geothermal Research 124, 89–114.

Cita, M.B., Vergnaud-Grazzini, C., Robeck, C., Chamley, H., Ciaranfi, N., D'Onofrio, S., 1977. Paleoclimatic record of a long deep sea core from the eastern Mediterranean. Quaternary Research 8, 205–235.

Cita, M.B., McCoy, F.W., Coughlin, S., 1981. Tephrochronology of the Mediterranean Deep-Sea Record. New data from the Western Mediterranean Ridge and from the Tyrrhenian Basin. Rendiconti della Società Italiana di Mineralogia e Petrologia 4, 255–258.

Civetta, L., Gallo, G., Orsi, G., 1991. Sr- and Nd-isotope and trace element constraints on the chemical evolution of the magmatic system of Ischia (Italy) in the last 55 ka. Journal of Volcanology and Geothermal Research 46, 213–230.

Civetta, L., De Vivo, A., Orsi, G., Polara, G., 1999. Il vulcanismo a Ischia in età greco romana secondo le evidenze geologiche e le testimonianze storico-letterarie. In: Vichiana, Loffredo (Ed.), Napoli, pp. 15–32.

Coltelli, M., Del Carlo, P., Vezzoli, L., 2000. Stratigraphic constraints for explosive activity in the past 100 ka at Etna Volcano, Italy. International Journal of Earth Sciences 89, 665–677.

Creer, K.M., Readman, P.W., Papamarinopoulos, S., 1981. Geomagnetic secular variations in Greece through the last 6000 years obtained from lake sediment studies. Geophysical Journal of the Royal Astronomical Society 66, 193–219.

D'Antonio, M., Civetta, L., Orsi, G., Pappalardo, L., Piochi, M., Carandente, A., de Vita, S., Di Vito, M.A., Isaia, R., 1999. The present state of the magmatic system of the Campi Flegrei caldera based on a reconstruction of its behavior in the past 12 ka. Journal of Volcanology and Geothermal Research 91, 247–268.

De Astis, G., Pappalardo, L., Piochi, M., 2004. Procida volcanic history: new insights into the evolution of the Phlegraean Volcanic District (Campania region, Italy). Bulletin of Volcanology 66, 622–641.

de Vita, S., Orsi, G., Civetta, L., Carandente, A., D' Antonio, M., Deino, A., di Cesare, T., Di Vito, M.A., Fisher, R.V., Isaia, R., Marotta, E., Necco, A., Ort, M., Pappalardo, L., Piochi, M., Southon, J., 1999. The Agnano–Monte Spina eruption (4100 years BP) in the restless Phlegrean Fields caldera (Italy). Journal of Volcanology and Geothermal Research 91, 269–301.

de Vita, S., Sansivero, F., Orsi, G., Marotta, E., 2006. Cyclical slope instability and volcanism related to volcano-tectonism in resurgent calderas: the Ischia island (Italy) case study. Engineering Geology 86, 148–165.

Deino, A.L., Orsi, G., de Vita, S., Piochi, M., 2004. The age of the Neapolitan Yellow Tuff caldera-forming eruption (Campi Flegrei caldera — Italy) assed by $^{40}Ar/^{39}Ar$ dating method. Journal of Volcanology and Geothermal Research 133, 157–170.

Delibrias, G., Guillier, M.-T., Labeyrie, J., 1986. Gif natural radiocarbon measurements X. Radiocarbon 28, 9–68.

Di Vito, M., Isaia, R., Orsi, G., Southon, J., di Vita, S., D' Antonio, M., Pappalardo, L., Piochi, M., 1999. Volcanism and deformation since 12,000 years at the Phlegrean Fields caldera (Italy). Journal of Volcanology and Geothermal Research 91, 221–246.

Eastwood, W.J., Pearce, N.J.G., Westgate, J.A., Perkins, W.T., Lamb, H.F., Roberts, N., 1999. Geochemistry of Santorini tephra in lake sediments from Southwest Turkey. Global and Planetary Change 21, 17–29.

Federman, A.N., Carey, S.N., 1980. Electron microprobe correlation of tephra layers from Eastern Mediterranean abyssal sediments and the island of Santorini. Quaternary Research 13, 160–171.

Fowler, S.J., Spera, F.J., Bohrson, W.A., Belkin, H.E., De Vivo, B., 2007. Phase equilibria constraints on the chemical and physical evolution of the Campanian Ignimbrite. Journal of Petrology 48, 459–493.

Frezzotti, M., Narcisi, B., 1996. Late Quaternary tephra-derived palaeosols in central Italy's carbonate Apennine Range: stratigraphical and paleoclimatological implications. Quaternary International 34–36, 147–153.

Gialanella, C., 1994. Pithecusa: gli insediamenti di Punta Chiarito. Relazione preliminare. Annali di Archeologia e Storia Antica — APOIKIA. I.U.O. 1, 169–204.

Gioncada, A., Mazzuoli, R., Milton, A.J., 2005. Magma mixing at Lipari (Aeolian Islands, Italy): insights from textural and compositional features of phenocrysts. Journal of Volcanology and Geothermal Research 145, 97–118.

Guichard, F., Carey, S., Arthur, M.A., Sigurdsson, H., Arnold, M., 1993. Tephra from the Minoan eruption of Santorini in sediments of the Black Sea. Nature 363, 610–612.

Hughen, K.A., Baillie, M.G.L., Bard, E., Bayliss, A., Beck, J.W., Bertrand, C., Blackwell, P.G., Buck, C.E., Burr, G., Cutler, K.B., Damon, P.E., Edwards, R.L., Fairbanks, R.G., Friedrich, M., Guilderson, T.P., Kromer, B., McCormac, F.G., Manning, S., Bronk Ramsey, C., Reimer, P.J., Reimer, R.W., Remmele, S., Southon, J.R., Stuiver, M., Talamo, S., Taylor, F.W., van der Plicht, J., Weyhenmeyer, C.E., 2004. Marine04 marine radiocarbon age calibration, 0–26 kyr BP. Radiocarbon 46, 1059–1086.

Insinga, D., Fedele, L., Morra, V., Sacchi, M., 2006. Tephrostratigraphy of Naples and Salerno Bays (eastern Tyrrhenian Sea): implications for the Lake Pleistocene–Holocene evolution of volcanic activity in the Campania region. Workshop Abstract, Tefrostratigrafia del Quaternario recente italiano, Roma 21.–23. June 2006, pp. 48.

Isaia, R., D'Antonio, M., Dell'Erba, F., Di Vito, M., Orsi, G., 2004. The Astroni volcano: the only example of closely spaced eruptions in the same vent area during the recent history of the Campi Flegrei caldera (Italy). Journal of Volcanology and Geothermal Research 133, 171–192.

Jahns, S., van den Bogaard, C., 1998. New palynological and tephrostratigraphical investigations of two salt lagoons on the island of Mljet, south Dalmatia, Croatia. Vegetation History and Archaeobotany 7, 219–234.

Juvigné, E.H., Kroonenberg, S.B., Veldkamp, A., El Arabi, A., Vernet, G., 1992. Widespread Alleröd and Boreal trachyandesitic to trachytic tephra layers as stratigraphic markers in the Massif Central, France. Quaternaire 3, 137–146.

Kallel, N., Paterne, M., Labeyrie, L., Duplessy, J.C., Arnold, M., 1997. Temperature and salinity records of the Tyrrhenian Sea during the last 18,000 years. Palaeogeography, Palaeoclimatology, Palaeoecology 135, 97–108.

Kallel, N., Duplessy, J.C., Labeyrie, L., Fontugne, M., Paterne, M., Montacer, M., 2000. Mediterranean pluvial periods and sapropel formation over the last 200.000 years. Palaeogeography, Palaeoclimatology, Palaeoecology 157, 45–58.

Karner, D.B., Juvigné, E., Brancaccio, L., Cinque, A., Russo Ermolli, E., Santangelo, N., Bernasconi, S., Lirer, L., 1999. A potential early middle Pleistocene tephrostratotype for the Mediterranean Basin: the Valle di Diano, Campania, Italy. Global and Planetary Change 21, 1–15.

Keller, J., Ryan, W.B.F., Ninkovich, D., Altherr, R., 1978. Explosive volcanic activity in the Mediterranean over the past 200,000 yrs as recorded in deep-sea sediments. Geological Society of America Bulletin 89, 591–604.

Kraml, M., 1997. Laser-$^{40}Ar/^{39}Ar$-Datierungen an distalen marinen Tephren des jung-quartären mediterranen Vulkanismus (Ionisches Meer, METEOR-Fahrt 25/4). Ph.D. Thesis, Albert-Ludwigs-Universität Freiburg i.Br., 216 pp.

Kwiecien, O., Arz, H., Lamy, F., Wulf, S., Roehl, C., Haug, G.H., in press. Estimated reservoir ages of the Glacial Black Sea. Radiocarbon 50 (1).

Lowe, J.J., Blockley, S., Trincardi, F., Asioli, A., Cattaneo, A., Matthews, I.P., Pollard, M., Wulf, S., 2007. Age modeling of late Quaternary marine sequences in the Adriatic: towards improved precision and accuracy using volcanic event stratigraphy. Continental Shelf Research 27, 560–582.

Magny, M., De Beaulieu, J-L., Drescher-Schneider, R., Vannière, B., Walter-Simonnet, A-V., Millet, L., Bossuet, G., Peyron, O., 2006. Climatic oscillations in central Italy during the Last Glacial–Holocene transition: the record from Lake Accesa. Journal of Quaternary Science 21, 311–320.

McCoy, F.W., 1980. The upper Thera (Minoan) ash in deep-sea sediments: distribution and comparison with other ash layers. In: Dumas, C. (Ed.), Thera and the Aegean world. Papers and Proceedings of the 2nd International Scientific Congress, Santorini, Greece, August 1978. The Thera Foundation, pp. 57–78.

McCoy, F., Cornell, W., 1990. Volcaniclastic sediments in the Tyrrhenian basin. In: Kastens, K.A., Mascle, J., et al. (Eds.), Proceedings of ODP Scientific Results. Ocean Drilling Program, vol. 107, pp. 291–305. College Station, TX.

Mellis, O., 1954. Volcanic ash-horizons in deep-sea sediments from the eastern Mediterranean. Deep-Sea Research 2, 89–92.
Munno, R., Petrosino, P., 2007. The late Quaternary tephrostratigraphical record of the San Gregorio Magno basin (southern Italy). Journal Quaternary Science 22 (3), 247–266.
Narcisi, 1999a. Neapolitan Yellow Tuff tephra in the lacustrine sediments of the Valle di Castiglione crater (Alban Hills). Acta Vulcanologica 11, 265–269.
Narcisi, 1999b. Nuovi ritrovamenti del tefra tardiglaciale Etneo in Italia centrale. Il Quaternario 12, 69–78.
Narcisi, B., 1993. Segnalazione di un livello piroclastico di provenienza etnea nell'area del Fucino (Italia Centrale). Il Quaternario 6, 87–92.
Narcisi, B., 1996. Tephrochronology of a late quaternary lacustrine record from the Monticchio Maar (Vulture Volcano, southern Italy). Quaternary Science Reviews 15, 155–165.
Narcisi, B., Vezzoli, L., 1999. Quaternary stratigraphy of distal tephra layers in the Mediterranean— an overview. Global and Planetary Change 21, 31–50.
Newton, A.J., Dugmore, A.J., 1993. Tephrochronology of Core C from Lago Grande di Monticchio. In: Negendank, J.F.W., Zolitschka, B. (Eds.), Paleolimnology of European Maar Lakes. Lecture Notes in Earth Sciences, vol. 49. Springer-Verlag, Berlin, Heidelberg, pp. 333–348.
Norin, E., 1958. The sediments of the central Tyrrhenian Sea. In: Pettersson, H. (Ed.), Reports of the Swedish Deep-Sea Expedition, 1947–1948. Elanders Boktryckeri Aktiebolag, Göteborg. 136.
Oldfield, F., Asioli, A., Accorsi, C.A., Mercuri, A.M., Juggins, S., Langone, L., Rolph, T., Trincardi, F., Wolff, G., Gibbs, Z., Vigliotti, L., Frignani, M., van der Post, K., Branch, N., 2003. A high resolution late Holocene palaeo environmental record from the central Adriatic Sea. Quaternary Science Reviews 22, 319–342.
Orsi, G., Gallo, G., Heiken, G., Wohletz, K., Yu, E., Bonani, G., 1992. A comprehensive study of the pumice formation and dispersal: the Cretaio Tephra of Ischia (Italy). Journal of Volcanology and Geothermal Research 53, 329–354.
Orsi, G., Piochi, M., Campajola, L., D'Onofrio, A., Gialanella, L., Terrasi, F., 1996. ^{14}C geochronological constraints for the volcanic history of the island of Ischia (Italy) over the last 5000 years. Journal of Volcanology and Geothermal Research 71, 249–257.
Pappalardo, L., Civetta, L., D' Antonio, M., Deino, A., Di Vito, M., Orsi, G., Carandente, A., de Vita, S., Isaia, R., Piochi, M., 1999. Chemical and Sr-isotopical evolution of the Phlegrean magmatic system before the Campanian Ignimbrite and the Neapolitan Yellow Tuff eruptions. Journal of Volcanology and Geothermal Research 91, 141–166.
Paterne, M., Guichard, F., Labeyrie, J., 1988. Explosive activity of the South Italian volcanoes during the past 80,000 years as determined by marine tephrochronology. Journal of Volcanology and Geothermal Research 34, 153–172.
Paterne, M., Guichard, F., Labeyrie, J., Gillot, P.Y., Duplessy, J.C., 1986. Tyrrhenian Sea tephrochronology of the oxygen isotope record for the past 60,000 years. Marine Geology 72, 259–285.
Paterne, M., Labeyrie, J., Guichard, F., Mazaud, A., Maitre, F., 1990. Fluctuations of the Campanian explosive volcanic activity (South Italy) during the past 190,000 years, as determined by marine tephrochronology. Earth and Planetary Science Letters 98, 166–174.
Piochi, M., Civetta, L., Orsi, G., 1999. Mingling in the magmatic system of Ischia (Italy) in the past 5 ka. Mineralogy and Petrology 66, 227–258.
Poli, S., Chiesa, S., Gillot, P.-Y., Gregnanin, A., Guichard, F., 1987. Chemistry versus time in the volcanic complex of Ischia (Gulf of Naples, Italy): evidence of successive magmatic cycles. Contributions to Mineralogy and Petrology 95, 322–335.
Ramrath, A., Zolitschka, B., Wulf, S., Negendank, J.F.W., 1999. Late Pleistocene climatic variations as recorded in two Italian maar lakes (Lago di Mezzano, Lago Grande di Monticchio). Quaternary Science Reviews 18, 977–992.
Reimer, P.J., Baillie, M.G.L., Bard, E., Bayliss, A., Beck, J.W., Bertrand, C., Blackwell, P.G., Buck, C.E., Burr, G., Cutler, K.B., Damon, P.E., Edwards, R.L., Fairbanks, R.G., Friedrich, M., Guilderson, T.P., Hughen, K.A., Kromer, B., McCormac, F.G., Manning, S., Bronk Ramsey, C., Reimer, R.W., Remmele, S., Southon, J.R., Stuiver, M., Talamo, S., Taylor, F.W., van der Plicht, J., Weyhenmeyer, C.E., 2004. Intcal04 terrestrial radiocarbon age calibration, 0–26 cal kyr BP. Radiocarbon 46, 1029–1058.
Rolandi, G., Barrella, A.M., Borrelli, A., 1993a. The 1631 eruption of Vesuvius. Journal of Volcanology and Geothermal Research 58, 183–201.
Rolandi, G., Maraffi, S., Petrosino, P., Lirer, L., 1993b. The Ottaviano eruption of Somma–Vesuvio (8000 y B.P.): a magmatic alternating fall and flow-forming eruption. Journal of Volcanology and Geothermal Research 58, 43–65.
Rolandi, G., Petrosino, P., McGeehin, J., 1998. The interplinian activity at Somma-Vesuvius in the last 3500 years. Journal of Volcanology and Geothermal Research 82, 19–52.
Rolandi, G., Munno, R., Postiglione, I., 2004. The A.D. 472 eruption of the Somma volcano. Journal of Volcanology and Geothermal Research 129, 291–319.
Romano, R., 1982. Succession of the volcanic activity in the Etnean area. Memorie della Societa Geologica Italiana 23, 27–48.
Rosi, M., Sbrana, A., 1987. Phlegrean Fields. Consiglio Nazionale delle Ricerche (CNR), Roma 14 (9).
Ryan, W.B.F., 1972. Stratigraphy of Late Quaternary sediments in the Eastern Mediterranean. In: Stanley, D.J. (Ed.), The Mediterranean Sea. Dowden, Hutchinson & Ross, Stroudsburg, pp. 149–169.
Santacroce, R., 1987. Somma-Vesuvius. CNR, Roma. 252 pp.
Schmidt, R., van den Bogaard, C., Merkt, J., Müller, J., 2002. A new Late Glacial chronostratigraphic tephra marker for the south-eastern Alps: the Neapolitan Yellow Tuff (NYT) in Längsee (Austria) in the context of a regional biostratigraphy and palaeoclimate. Quaternary International 88, 45–56.
Seymour, K.St., Christanis, K., Bouzinos, A., Papazisimou, S., Papatheodorou, G., Moran, E., Dénès, G., 2004. Tephrostratigraphy and tephrochronology in the Philippi peat basin, Macedonia, Northern Hellas (Greece). Quaternary International 121, 53–65.
Siani, G., Paterne, M., Michel, E., Sulpizio, R., Sbrana, A., Arnold, M., Haddad, G., 2001. Mediterranean sea surface radiocarbon reservoir age changes since the Last Glacial Maximum. Science 294, 1917–1920 [+5 p. Suppl.].
Siani, G., Sulpizio, R., Paterne, M., Sbrana, A., 2004. Tephrostratigraphy study for the last 18,000 ^{14}C years in a deep-sea sediment sequence for the South Adriatic. Quaternary Science Reviews 23, 2485–2500.
Sullivan, D.G., 1988. The discovery of Santorini Minoan tephra in western Turkey. Nature 333, 552–554.
Sulpizio, R., Zanchetta, G., Paterne, M., Siani, G., 2003. A review of tephrostratigraphy in central and southern Italy during the last 65 ka. Il Quat. It. J. Quat. Sc. 16, 91–108.
Sulpizio, R., Bonasia, R., Dellino, P., Di Vito, M.A., La Volpe, L., Mele, D., Zanchetta, G., Sadori, L., 2008. Discriminating the long distance dispersal of fine ash from sustained columns or near ground ash clouds: the example of the Pomici di Avellino eruption (Somma-Vesuvius, Italy). Journal of Volcanology and Geothermal Research 177, 263–276 (this issue).
Thorarinsson, S., 1981. Greetings from Iceland. Ash-fall and volcanic aerosols in Scandinavia. Geografiska Annaler 63A, 109–118.
Turney, C.S.M., Blockley, S.P.E., Lowe, J.J., Wulf, S., Branch, N.P., Mastrolorenzo, G., Swindle, G., Nathan, R., Pollard, A.M., in press. Chemical characterization of Quaternary tephras from the Campanian Province, Italy. Quaternary International. doi:10.1016/j.quaint.2007.02.007.
Van den Bogaard, P., Schmincke, H.-U., 1985. Laacher See Tephra: a widespread isochronous late Quaternary tephra layer in central and northern Europe. Geological Society of America Bulletin 96, 1554–1571.
Vezzoli, L., 1988. Island of Ischia. Consiglio Nazionale delle Ricerche (CNR), Roma 114 (10).
Vezzoli, L., 1991. Tephra layers in Bannock Basin (Eastern Mediterranean). Marine Geology 100, 21–34.
Vinci, A., 1985. Distribution and chemical composition of tephra layers from Eastern Mediterranean abyssal sediments. Marine Geology 64, 143–155.
Wagner, B., Sulpizio, R., Zanchetta, G., Wulf, S., Wessel, M., Daut, G., 2008. The last 40 ka tephrostratigraphic record of Lake Ohrid, Albania: a very distal archive for ash dispersal from Italian volcanoes. Journal of Volcanology and Geothermal Research 177, 71–80 (this issue).
Wulf, S., Kraml, M., Kuhn, T., Schwarz, M., Inthorn, M., Keller, J., Kuscu, I., Halbach, P., 2002. Marine tephra from the Cape Riva eruption (22 ka) of Santorini in the Sea of Marmara. Marine Geology 183, 131–141.
Wulf, S., Kraml, M., Keller, J., Negendank, J.F.W., 2004. Tephrochronology of the 100 ka lacustrine sediment record of Lago Grande di Monticchio (southern Italy). Quaternary International 122, 7–30.
Wulf, S., Brauer, A., Mingram, J., Zolitschka, B., Negendank, J.F.W., 2007. Distal tephras in the sediments of Monticchio maar lakes. In: Principe, C. (Ed.), Geologia del Monte Vulture. Bollettino della Societa Geologica Italiana, pp. 105–122.
Zolitschka, B., Negendank, J.F.W., 1993. Lago Grande di Monticchio (southern Italy): a high resolution sedimentary record of the last 70,000 years. In: Negendank, J.F.W., Zolitschka, B. (Eds.), Paleolimnology of European Maar lakes. Lecture Notes in Earth Sciences, vol. 49. Springer-Verlag, Berlin, Heidelberg, pp. 277–288.

5.3 Manuscript #3

"The 100-133 ka record of Italian explosive volcanism and revised tephrochronology of Lago Grande di Monticchio" *(S. Wulf, J. Keller, M. Paterne, J. Mingram, S. Lauterbach, S. Opitz, G. Sottili, B. Giaccio, P.G. Albert, C. Satow, E.L. Tomlinson, M. Viccar &, A. Brauer (2012): Quaternary Science Reviews)*

Scientific Technical Report STR14/01, Deutsches GeoForschungsZentrum GFZ. http://doi.org/10.2312/GFZ.b103-14010

Quaternary Science Reviews 58 (2012) 104–123

Contents lists available at SciVerse ScienceDirect

Quaternary Science Reviews

journal homepage: www.elsevier.com/locate/quascirev

The 100–133 ka record of Italian explosive volcanism and revised tephrochronology of Lago Grande di Monticchio

Sabine Wulf [a,*], Jörg Keller [b], Martine Paterne [c], Jens Mingram [a], Stefan Lauterbach [a], Stephan Opitz [d], Gianluca Sottili [e], Biagio Giaccio [e], Paul G. Albert [f], Chris Satow [g], Emma L. Tomlinson [f,h], Marco Viccaro [i], Achim Brauer [a]

[a] GFZ German Research Centre for Geosciences, Section 5.2 – Climate Dynamics and Landscape Evolution, Telegrafenberg, 14473 Potsdam, Germany
[b] Institute of Geosciences, Mineralogy – Geochemistry, Albert-Ludwigs-University Freiburg, Albertstrasse 23b, 79104 Freiburg, Germany
[c] Laboratoire des Sciences du Climat et de l'Environnement (IPSL-CEA-CNRS-UVSQ), Domaine du CNRS Bât. 12, Avenue de la Terrasse, 91198 Gif-sur-Yvette, France
[d] Alfred Wegener Institute, Telegrafenberg A43, 14473 Potsdam, Germany
[e] Istituto di Geologia Ambientale e Geoingegneria, CNR, Via Salaria km 29,300, 00015 Rome, Italy
[f] Department of Earth Sciences, Royal Holloway University of London, Egham TW20 0EX, United Kingdom
[g] Department of Geography, Royal Holloway University of London, Egham TW20 0EX, United Kingdom
[h] Department of Geology, Trinity College Dublin, College Green, Dublin 2, Ireland
[i] Dipartimento di Scienze Biologiche Geologiche e Ambientali, Università di Catania, Corso Italia 57, 95129 Catania, Italy

ARTICLE INFO

Article history:
Received 16 June 2012
Received in revised form
27 September 2012
Accepted 5 October 2012
Available online

Keywords:
Tephrochronology
Italian volcanism
Lago Grande di Monticchio
Central Mediterranean

ABSTRACT

Laminated sediments of the maar lake Lago Grande di Monticchio in southern Italy exhibit a unique sequence of numerous primary tephra events that provide both insights into the Late Quaternary eruptive history of Italian volcanoes and an archive of essential marker horizons for dating and linking palaeoclimate records throughout the Central and Eastern Mediterranean. The acquisition of new sediment cores from this lake now extends the existing 100 ka-tephra record back to 133 ka BP, the end of the penultimate Glacial. The additional ca 30 m of sediments host a total number of 52 single tephra layers forming 21 tephra clusters that have been characterised on the basis of detailed geochemical and petrographical examinations. Tephras can be assigned to hitherto poorly known Plinian to sub-Plinian eruptive events of the nearby Campanian (Ischia Island, Phlegrean Fields), Roman (Sabatini volcanic district) and Aeolian-Sicilian volcanoes (Etna, Stromboli, Salina) and are dated according to the varve and sedimentation rate chronology of Monticchio sediments. The most prominent tephra layers within the interval of investigation – TM-25 and TM-27 – can be firmly correlated with Ionian Sea tephras X-5 (ca 105 ka BP) and X-6 (ca 108–110 ka BP). In addition, a further 26 tephra layers are correlated with radiometrically and radioisotopically dated volcanic events providing the basis for a robust revised tephrochronology of the entire Monticchio sediment sequence for the last 133 ka.

1. Introduction

During the past decades, tephra studies in the Central Mediterranean facilitated the dating and linking of numerous distal terrestrial and marine palaeoenvironmental records leading to a continuous development of detailed tephrostratigraphies of Italian explosive volcanism for at least the last 100 ka BP (e.g., Keller et al., 1978; Paterne et al., 1986; Siani et al., 2004; Wulf et al., 2004, 2008; Lowe et al., 2007; Calanchi and Dinelli, 2008; Paterne et al., 2008; Sulpizio et al., 2010).

Tephrostratigraphies, in general, require a complete record of major eruptive events, reliable dating, a clear stratigraphic order and an unambiguous identification of tephras, which in combination are difficult to derive from a single archive. Proximal volcanic areas (up to 5–15 km from vent), for example, are ideal for dating tephra deposits, but may lack complete stratigraphies due to burial and erosional processes. Distal environments may record only large-magnitude eruptions and miss small-scale events, but have the potential to document the stratigraphic interfingering and super-positioning of tephras from multiple volcanic sources. However, the dating of tephras in distal sedimentary archives can be problematic due to the lack of datable material. In this respect, annually laminated crater lake sediments are exceptionally valuable archives since they provide both eruptive evidence from

* Corresponding author. Tel.: +49 (0) 331 2881381; fax: +49 (0) 331 2881302.
E-mail address: swulf@gfz-potsdam.de (S. Wulf).

0277-3791/$ – see front matter © 2012 Elsevier Ltd. All rights reserved.
http://dx.doi.org/10.1016/j.quascirev.2012.10.020

adjacent volcanic centres and robust chronologies (e.g., Brauer et al., 1999; Wulf et al., 2004). In the central Mediterranean, such an archive is provided by the maar lake Lago Grande di Monticchio in southern Italy. A total of 293 visible tephra fallout layers from volcanic sources in central and southern Italy, which are located between 100 and 540 km away, were previously identified in the Monticchio sediments providing a detailed tephrostratigraphy of the explosive volcanism in Italy for the last 100 ka BP (Newton and Dugmore, 1993; Narcisi, 1996; Wulf et al., 2004, 2006, 2008). Detailed studies created a large data set of chronostratigraphical and geochemical information of individual tephras that are widely used as references for the correlation and dating of other distal and proximal tephra deposits (e.g., Lowe et al., 2007; Bourne et al., 2010; Smith et al., 2011; Giaccio et al., 2012).

The extended sediment record from Lago Grande di Monticchio (Brauer et al., 2007) exhibits another 52 tephra layers providing a record of Italian volcanism for the period 100–133 ka BP. Petrography and geochemistry of the tephras are described and interpreted in this paper. The ages of tephra deposition are provided by a combination of new varve counting for the extended 30 m section and a partial revision of the varve and sedimentation chronology of the <100 ka profile (Brauer et al., 2007). These data contribute to the establishment of a reliable tephrostratigraphical record in the Central Mediterranean.

2. The study site

Lago Grande di Monticchio (40°56′N, 15°35′E, 656 m a.s.l.) is located about 120 km east of Naples in the Monte Vulture volcanic complex in the region of Basilicata, southern Italy (Fig. 1a). It is the larger of two adjacent maar lakes that were formed during the final phreatomagmatic eruptions of Monte Vulture at 132 ± 12 ka BP (Lago Grande di Monticchio; Brocchini et al., 1994; Stoppa and Principe, 1998) and 141 ± 11 ka BP (Lago Piccolo di Monticchio; Villa and Buettner, 2009), respectively. Lago Grande di Monticchio has a total surface area of 0.4 km^2, a maximum water depth of 36 m, and has no major in- or outflows (Fig. 1b).

Lying 100–350 km away, the site is in a favourable downwind position to the active volcanoes of the alkaline Roman Co-magmatic Province (RCP). The RCP is subdivided into the Campanian and Roman volcanic area. The Campanian area includes the volcanic fields of Monte Vulture, Roccamonfina, Somma-Vesuvius, the Phlegrean Fields and the Islands of Ischia, Procida-Vivara and Ponza. Most of these centres are still active, while activities of Procida-Vivara and Roccamonfina ceased at ca 14 ka BP (Scandone et al., 1991) and 130 ka BP (Radicati di Brozolo et al., 1988), respectively. Volcanism in the Roman area is older than in the Campanian area. The youngest tephra producing eruptions are known from the Alban Hills (560–33 ka BP; Giaccio et al., 2009; Marra et al., 2011), the Sabatini Volcanic District (800–86 ka BP; Sottili et al., 2010) and the Vico volcanic centre (≥420 to 95 ka BP; Sollevanti, 1983; Laurenzi and Villa, 1987). Activities of both the Campanian and Roman volcanoes produced huge amounts of tephra fallout, mainly K-alkaline trachytic–phonolitic in composition. Lago Grande di Monticchio is furthermore located 280–540 km northeast of the active volcanic centres of the Aeolian Islands (280 km), Mount Etna (360 km) and the Island of Pantelleria in the Strait of Sicily (540 km). Erupted material of these volcanoes ranges in composition from calcalkaline (Aeolian Islands) to Na-alkaline and pantelleritic (Etna, Pantelleria). Some of these

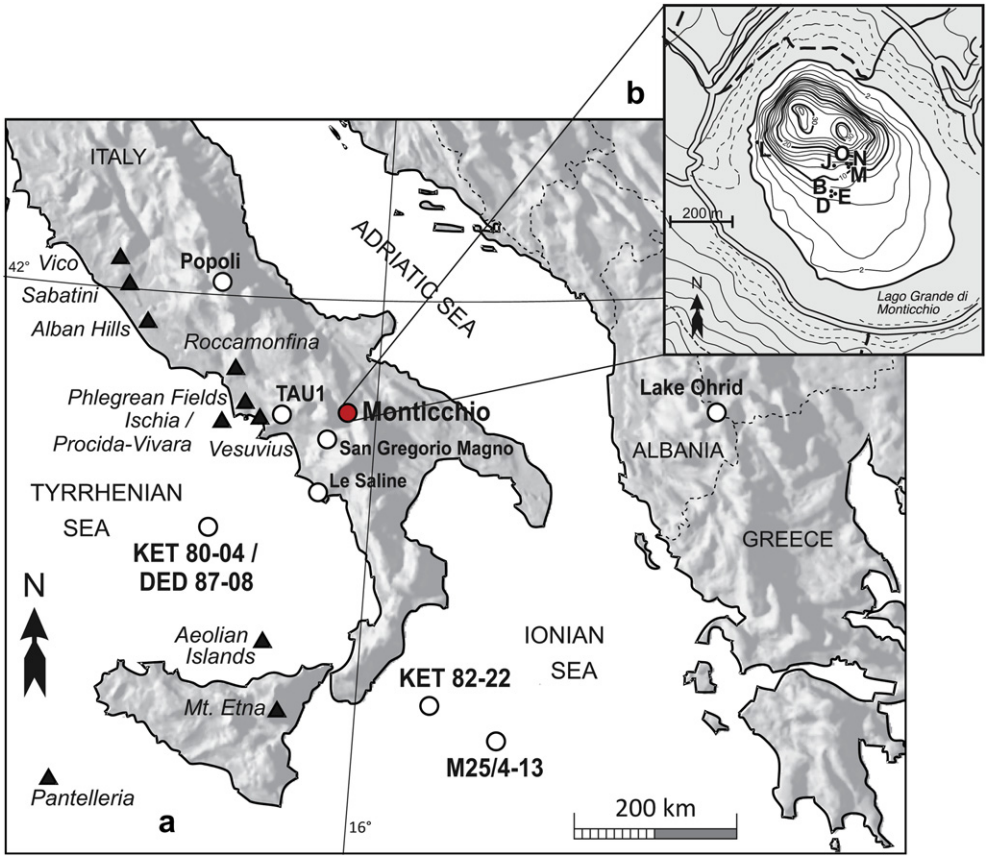

Fig. 1. a) Site map of Italy showing major volcanic centres, the location of Lago Grande di Monticchio and distal correlation sites mentioned in the text. b) Bathymetric map of Lago Grande di Monticchio with coring sites.

eruptions were highly explosive, and the erupted tephra material was widely dispersed in the Central Mediterranean (e.g., Keller et al., 1978; Paterne et al., 1986, 2008; Vezzoli, 1991).

3. Material and chronology

Lago Grande di Monticchio has been the focus of intense studies for palaeoclimatic reconstruction since the early 1980s (e.g., Watts, 1985; Watts et al., 1996; Zolitschka and Negendank, 1996; Allen et al., 1999; Brauer et al., 2000, 2007). Three subsequent coring campaigns (1990, 1994 and 2000) were carried out within the lake basin recovering eight overlapping sediment cores (Fig. 1b) that provide a continuous composite profile of 103.1 m total length (Brauer et al., 2007) (Fig. 2). Counting of varved sections and calculating sedimentation rates in sections of poor varve preservation dated the base of the Monticchio composite profile at 132,900 calendar years BP (Zolitschka and Negendank, 1996; Brandt et al., 1999; Brauer et al., 2007). The chronology of the upper <100 ka sediments was corroborated by independent time constraints such as radiocarbon dating (Zolitschka and Negendank, 1996; Hajdas et al., 1998) and tephrochronology (Narcisi, 1996; Wulf et al., 2004). A total of 293 single tephra layers are recorded

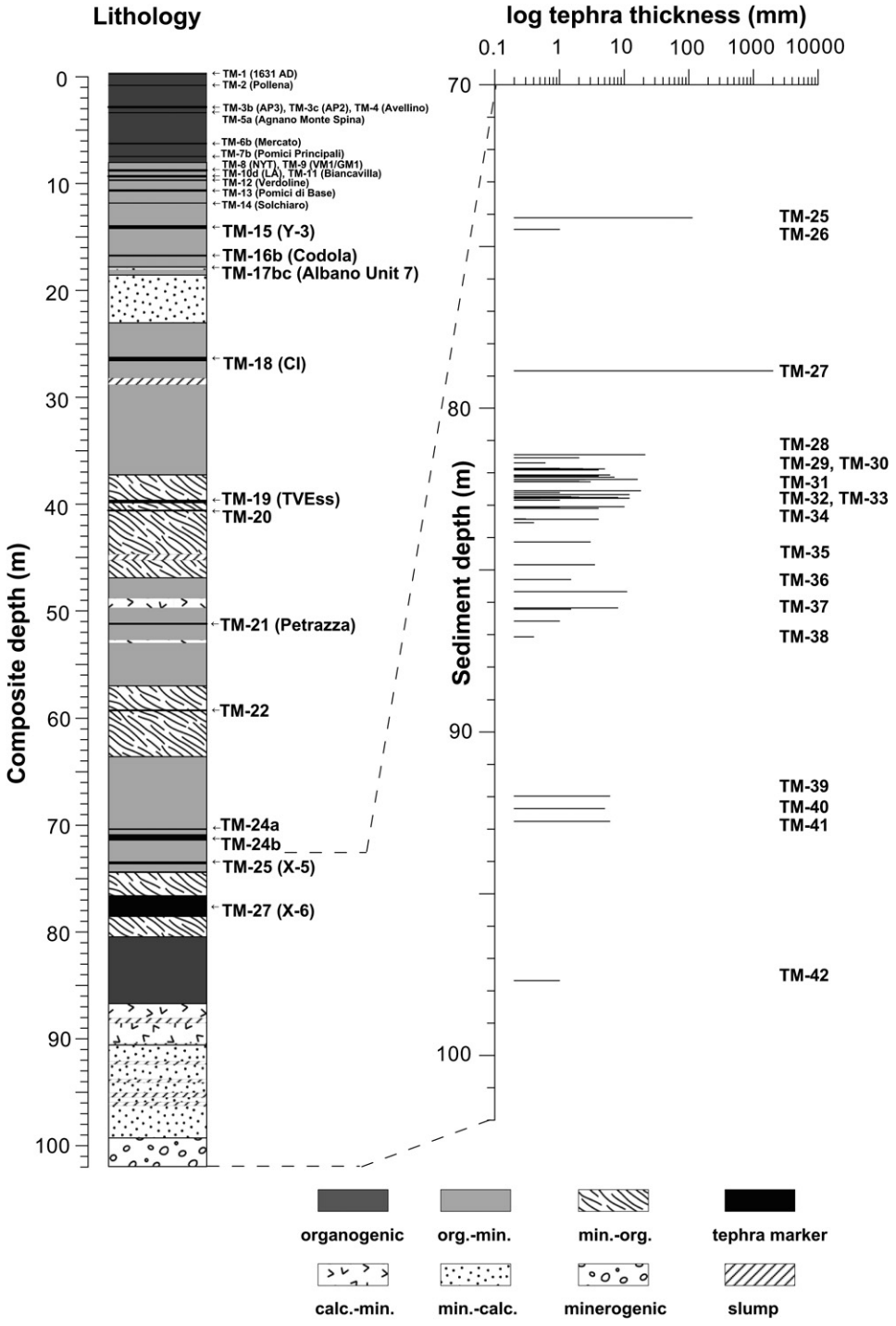

Fig. 2. Lithology and tephrostratigraphy of the composite profile LGM-B/D/E/J/M/O with focus on the 100–133 ka BP tephras.

in the <100 ka sequence, of which 68 are correlated with volcanic events and published by Narcisi (1996) and Wulf et al. (2004, 2008).

The 100–133 ka sediment section contains another 52 visible, distal tephra layers that range in thickness between 0.2 mm and >2 m (Fig. 2). Host sediments of these ash layers are organo-clastic muds that are annually laminated for the entire section except for the lowermost part (>131 ka BP), which is characterised by the intercalation of thick turbidites (Brauer et al., 2007). Detailed studies of the 52 tephra layers were performed including petrographical, geochemical and grain size analyses.

4. Tephrochronological methods

Tephra layers are labelled in accordance to Wulf et al. (2004, 2006) as tephra marker "TM" with the respective ascendant numbers starting from the youngest of the >100 ka tephras (TM-25) to the oldest deposit (TM-42). Clusters of tephra layers of similar composition (here labelled "units") are distinguished by adding an additional number (e.g., TM-29-1), and layers within these clusters (here labelled "sub-layers") are furthermore labelled in alphabetic order from the youngest to the oldest layer (e.g., TM-29-1a, TM-29-1b, etc.). In consequence, a total of 52 tephra layers form 21 tephra clusters (Table 1).

Tephra layers were described in respect to their mineral/lithic assemblage, maximum grain sizes and thickness using large-scale thin sections of in situ sediment blocks (Brauer et al., 2000). The major-element composition of volcanic glass was analysed on polished thin sections of loose tephra material that was extracted and cleaned with a 10% hydrogen peroxide solution. Electron probe microanalyses (EPMA) were carried out at the GFZ German Research Centre for Geosciences in Potsdam using a Cameca SX-100 electron microprobe (WDS). Measurements were obtained at 15 kV (accelerating voltage) and 20 nA (beam current) with beam sizes of 15 μm or 20 μm. Peak counting times were 20 s for each element, except for Na (10 s). Between 5 and 22 glass shards were analysed per tephra layer. Instrumental calibration used inter-laboratory natural mineral and glass reference materials such as the Lipari obsidian (Hunt and Hill, 1996). Analytical precision is based on the secondary standard and is listed for each element in Supplementary Table A.

Tephras TM-24a, TM-24b (Wulf et al., 2004) and TM-27 were additionally analysed using a JEOL 8600 wavelength-dispersive electron microprobe in the Research Laboratory for Archaeology and the History of Art, University of Oxford, U.K. An analytical setup was chosen at 15 kV acceleration voltage, 6 nA current and 10 μm beam diameter. Element analysis times were 30 s for each element, except for P and Cl (60 s), and Na (10 s). Glass reference materials Atho-G and StHs6/80-G were used (Jochum et al., 2005) (Supplementary Table B). EPMA analyses showing totals lower than 95 wt% were excluded from all data sets. Petrological classification of tephras was based on normalized data of the glass major-element composition using the Total–Alkali–Silica diagram after Le Bas et al. (1986). Tephra compositional data are summarized in Tables 1 and 2 and provided in full in the Supplementary Tables A and B.

EPMA glass data of Monticchio tephras were compared with SEM–EDS glass data of marine tephras from Tyrrhenian and Ionian Sea sediment cores (Paterne, 1985; Paterne et al., 2008; this study). Here, major elements of individual glass shards of tephras were measured on a JEOL/EDS instrument (core DED 87-08; see details in Paterne et al., 2008) and on a CAMEBAX/SEM equipment (cores KET 80-04 and KET 82-22; see details in Paterne, 1985; Paterne et al., 1986, 1988, 2008) at CNRS-CEA, Gif-sur-Yvette, France. The EDS glass compositions of tephras from core DED 8708 were cross-checked at the Jussieu Camparis microprobe facility using the Vedde Ash standard (Bard et al., 1994). The measurement of major element compositions of tephras from the older KET cores used the Beloc meteoric glass standard (Jéhanno et al., 1992), and a number of glass shards analysed were cross-checked at the Orsay microprobe facility. No significant offset was observed between the EDS and EPMA data.

Grain-specific trace element glass data of selected tephras (TM-24a, TM-24b, TM-25, POP3) were obtained at the Department of Earth Sciences, Royal Holloway University London using a Agilent 7500ce coupled to a Resonetics 193 nm ArF excimer laser-ablation system (RESOlution M-50 prototype) with a two-volume ablation cell (Müller et al., 2009). The laser spot size was 25 μm, the repetition rate was 5 Hz and the count time was 40 s (200 pulses) on the sample and 40 s on the gas blank (background). Concentrations were calibrated using NIST612 with ^{29}Si as the internal standard. Data reduction was performed manually using Microsoft Excel allowing removal of portions of the signal compromised by the occurrence of microcrysts. Full details of the analytical and data reduction methods are given in Tomlinson et al. (2010). Accuracy was verified using secondary glass standards from the Max Planck Institute, Leipzig, Germany (MPI-DING suite; Jochum et al., 2006) and is typically better than ±5%. Trace element data is fully provided in Supplementary Table C.

5. Results

In the following section, detailed compositional and chronostratigraphical descriptions of each tephra occurring in the 100–133 ka BP section are given, starting from the youngest to the oldest deposit (see also Tables 1 and 2). Calendar ages with 5% uncertainty for tephras are provided according to the Monticchio varve and sedimentation rate chronology after Brauer et al. (2007).

TM-25 is an 11.3 cm thick and coarse-grained (max. 1.5 mm) white pumice fallout at 74.11 m composite depth. It is dated by the Monticchio varve and sedimentation rate chronology at 105,480 ± 5270 calendar years BP. Coarse phenocrysts of sanidine, zoned plagioclase, biotite, amphibole, green clinopyroxene, and olivine xenocrystals are common in this tephra (Fig. 3a). Apatite often occurs as micro-crystal inclusions in juvenile clasts. Minor amounts of volcanic lithics and altered tuffs are also visible. Pumice fragments are highly vesicular (Fig. 3a) and show a K-trachytic composition with alkali ratios (K_2O/Na_2O) of ~2 (Fig. 4a). Trace element concentrations in the glasses show some significant variation (i.e., 251–289 ppm Zr; 615–711 ppm Sr; 776–1470 ppm Ba; 17–23 ppm Th). The tephra layer is mixed with fine organic sedimentary material towards the top of the deposit.

TM-26 is a 1 mm thick, fine-grained, grey-brownish ash layer (Fig. 3b) at 74.47 m composite depth that is dated at 106,300 ± 5320 calendar years BP. It is dominated by loose crystals of plagioclase, orthopyroxene, greenish clinopyroxene, rare sanidine, olivine, amphibole, Fe–Ti-oxides, and abundant tachylites. Glass shards are light and brown in colour, show low to moderate vesicularity and are often rich in apatite microcrysts. The glass chemical data reflect a heterogeneous Na-pronounced trachydacitic composition showing high SiO_2 concentrations of ca 65 wt% (normalized data) (Fig. 4b).

TM-27 positioned at 78.85 m composite depth and dated at 108,330 ± 5420 calendar years BP is one of the most prominent tephra deposits in the Monticchio sequence. Its base encompasses a 1.6 cm thick coarse-grained (max. 1.3 mm) pumice fallout that is overlain by ca 2 m of finer grained, vitric ash. Due to its fine grain size the vitric ash is interpreted as a co-ignimbrite that is mixed with lacustrine sedimentary material towards the top of the deposit. The basal fallout is composed of highly vesicular, colourless to light brownish pumice fragments, abundant phenocrysts of

Table 1
Core depths, composite depths, varve ages, thicknesses, maximum grain sizes and sources of Monticchio tephra layers deposited between 100 and 133 ka BP. CP = Campanian Province, E = Etna, PF = Phlegrean Fields, STR = Stromboli Island, IS = Ischia Island, SAL = Salina Island, SAB = Sabatini Volcanic District.

Tephra layer		Core depth (base of tephra)	Composite depth (m)	Varve age (cal. a BP) ± 5% error	Thickness (mm)	Maximum grain size (μm)	Source
TM-25		M49u, 97.5 cm	74.108	105,480 ± 5270	113.0	1500	CP
TM-26		O49u, 40.4 cm	74.471	106,300 ± 5320	1.0	80	E
TM-27		O53u, 45.6 cm	78.847	108,330 ± 5420	2000.0	1300	CP
TM-28	a	M59u, 48.8 cm	81.437	110,410 ± 5520	21.0	160	CP
	b	M59u, 52.5 cm	81.531	110,830 ± 5540	2.0	400	CP
TM-29-1	a	M59u, 68.5 cm	81.691	111,480 ± 5570	0.6	280	PF ?
	b	O58u, 16.4 cm	81.862	112,180 ± 5610	1.0	100	PF ?
	c	O58u, 16.7 cm	81.87	112,210 ± 5610	1.0	180	PF ?
	d	O58u, 16.8 cm	81.8709	112,230 ± 5610	0.2	100	PF ?
	e	O58u, 17.0 cm	81.871	112,230 ± 5610	0.5	190	PF ?
	f	O58u, 17.3 cm	81.8714	112,250 ± 5610	2.3	300	PF ?
	g	O58u, 17.9 cm	81.88	112,310 ± 5620	0.3	100	PF ?
	h	O58u, 18.6 cm	81.881	112,330 ± 5620	5.0	400	PF ?
	i	O58u, 21.7 cm	81.912	112,460 ± 5620	4.0	260	PF ?
TM-29-2	a	M62u, 60.5 cm	82.065	112,520 ± 5630	6.0	220	PF ?
	b	M62u, 60.9 cm	82.075	112,540 ± 5630	2.5	160	PF ?
	c	M62u, 61.1 cm	82.077	112,560 ± 5630	0.5	110	PF ?
	d	M62u, 61.5 cm	82.081	112,580 ± 5630	2.5	200	PF ?
	e	M62u, 63.0 cm	82.096	112,620 ± 5630	4.0	140	PF ?
	f	M62u, 67.3 cm	82.131	112,790 ± 5640	7.0	180	PF ?
	g	M62u, 73.4 cm	82.20	112,990 ± 5650	16.0	400	PF ?
	h	M62u, 73.9 cm	82.203	113,020 ± 5650	2.5	140	PF ?
TM-30-1	a	M62u, 79.5 cm	82.261	113,370 ± 5670	2.0	100	PF ?
	b	M62u, 80.9 cm	82.276	113,490 ± 5670	3.0	280	PF ?
	c	M64u, 20.7 cm	82.552	113,660 ± 5680	18.0	300	PF ?
	d	M64u, 20.8 cm	82.5524	113,670 ± 5680	0.5	100	PF ?
	e	M64u, 26.9 cm	82.61	113,880 ± 5690	1.0	90	PF ?
	f	M64u, 33.9 cm	82.672	114,000 ± 5700	12.0	700	PF ?
TM-30-2	a	M64u, 39.3 cm	82.738	114,440 ± 5720	1.5	300	PF ?
	b	M64u, 40.5 cm	82.751	114,530 ± 5730	2.0	300	PF ?
	c	M64u, 42.0 cm	82.762	114,600 ± 5730	8.0	100	PF ?
	d	M64u, 43.9 cm	82.785	114,720 ± 5740	12.0	800	PF ?
TM-31		M64u, 44.5 cm	82.791	114,770 ± 5740	0.5	180	PF ?
TM-32		M64u, 50.2 cm	82.846	115,250 ± 5760	1.0	120	STR ?
TM-33-1	a	M64u, 71.2 cm	83.047	115,720 ± 5790	10.0	320	IS
	b	M64u, 71.5 cm	83.061	115,750 ± 5790	1.0	100	IS
	c	M64u, 75.5 cm	83.101	116,110 ± 5810	4.0	240	IS
TM-33-2	a	M65u, 28.0 cm	83.427	118,190 ± 5910	0.3	110	IS
	b	M65u, 28.7 cm	83.434	118,210 ± 5910	4.0	250	IS
TM-34		M65u, 39.8 cm	83.542	118,810 ± 5940	0.4	100	SAL ?
TM-35	a	O62u, 63.0 cm	84.137	120,670 ± 6030	3.0	650	CP
	b	O63u, 59.5 cm	84.841	121,940 ± 6100	3.5	230	CP
TM-36		M70u, 22.9 cm	85.296	123,030 ± 6150	1.5	300	SAB
TM-37	a	M70u, 61.5 cm	85.676	124,080 ± 6200	11.0	200	IS
	b	M71o, 76.3 cm	86.176	124,330 ± 6220	8.0	500	IS
	c	M71o, 80.3 cm	86.216	124,360 ± 6220	1.5	150	IS
	d	M71u, 13.0 cm	86.588	124,860 ± 6240	1.0	90	IS
TM-38		M72o, 64.0 cm	87.074	125,550 ± 6280	0.4	150	CP
TM-39		O70u, 52.7 cm	91.982	130,530 ± 6530	6.0	170	CP
TM-40		O70u, 88.0 cm	92.366	130,860 ± 6540	5.0	170	IS
TM-41		M77u, 34.0 cm	92.766	131,020 ± 6550	6.0	300	CP
TM-42		O74u, 70.3 cm	97.686	132,110 ± 6610	1.0	300	IS

sanidine, biotite, plagioclase, clinopyroxene and amphibole as well as fragments of older volcanic rocks and limestones. Juvenile clasts are phonolitic to trachytic in composition and show a heterogeneous character with respect to CaO concentrations (1.6–2.1 wt%) and K_2O/Na_2O ratios (0.9–1.4) (Fig. 4a).

TM-28 consists of two distinct vitric ash layers of similar composition at 81.44 m (110,410 ± 5520 calendar years BP) and 81.53 m composite depth (110,830 ± 5540 calendar years BP). The upper tephra TM-28a is a 2.1 cm thick and relatively fine-grained layer. Its phenocryst content comprises sanidine, alkali feldspar (anorthoclase?), biotite and orange–brown amphibole. Juvenile clasts with microcrysts dominate the top part of this deposit. The lower tephra TM-28b is only 2 mm thick and reveals coarser grain sizes (max. 400 μm). The mineral assemblage is made up of sanidine, plagioclase, biotite, green Ti–augite and brown amphibole phenocrysts. Mafic and intermediate lava rock fragments are common as well. Highly vesicular, brownish juvenile clasts characterise both tephra layers. Their trachytic to phonolitic

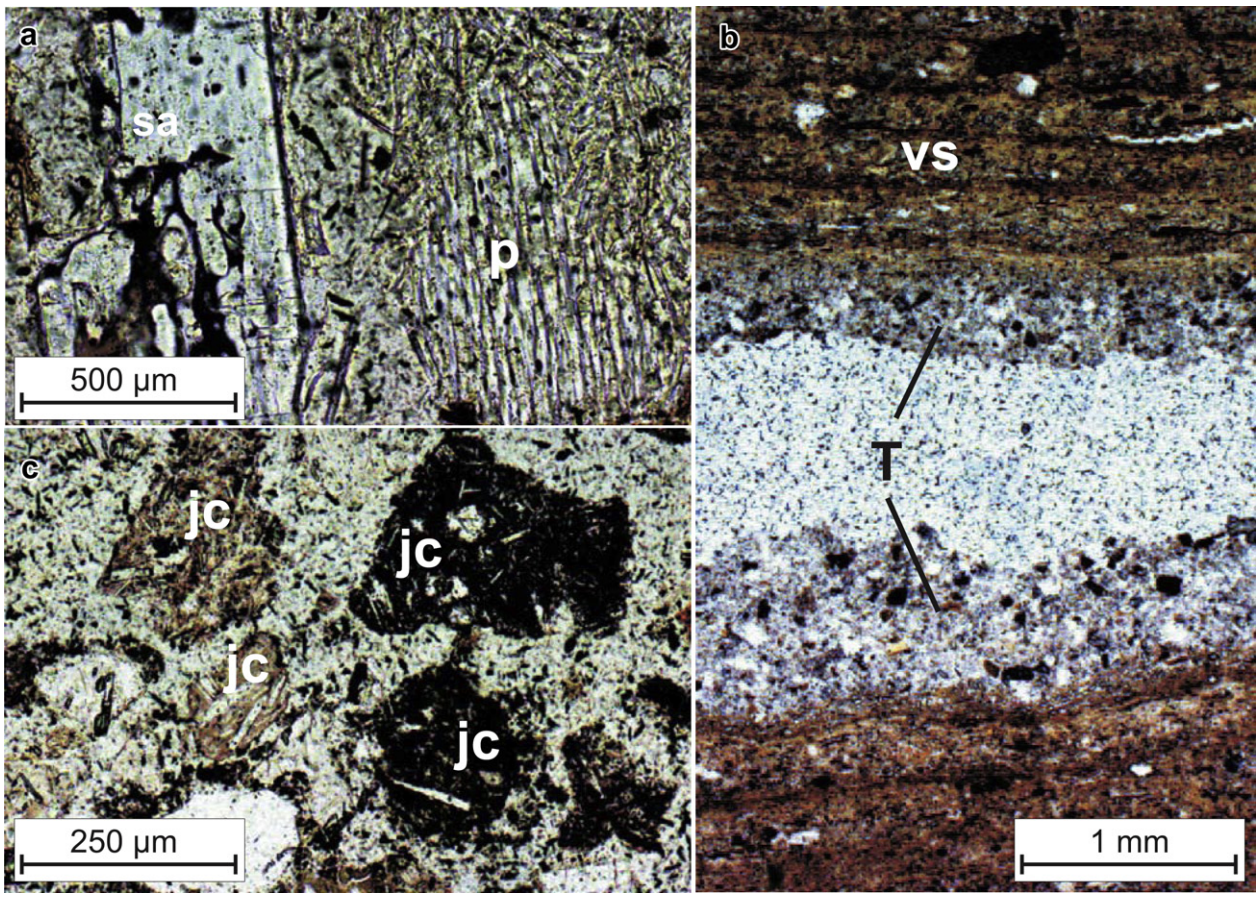

Fig. 3. Images under optical microscope of prominent tephras in the 100–133 ka BP sediment section of Lago Grande di Monticchio. a) TM-25: Large sanidine phenocryst (sa) and micropumice (p); b) TM-26: Crystal-rich tephra layer (t) embedded in varved Monticchio sediments (vs); c) TM-30-1c: Brown and black juvenile clasts (jc) rich in microcrysts.

composition resembles that of tephra TM-27 and only differs in slightly lower K_2O concentrations (Fig. 4a, Table 2).

TM-29 and TM-30 comprise a total of four tephra units (TM-29-1, TM-29-2, TM-30-1 and TM-30-2) of similar composition, each made up of multiple distinct tephra fallout layers. Each unit displays variations in the chemical composition from silicic to more mafic rock composition (Fig. 4c, Table 2) reflecting the emptying of normally and compositionally stratified volcanic systems.

The uppermost tephra unit *TM-29-1* at 81.69 m–81.91 m composite depth is dated between 111,480 ± 5570 and 112,460 ± 5620 calendar years BP. It is made up of nine 0.2–5 mm thick, grey-brownish ash layers labelled as TM-29-1a to TM-29-1i. All tephra layers contain light-brownish, non- to low-vesicular, blocky glass shards. The glass composition is heterogeneous latitic, basaltic–andesitic, tephriphonolitic to phonotephritic for the five basal layers (TM-29-1e to TM-29-1i) and homogenous phonotephritic for the four top layers (TM-29-1a to TM-29-1d). SiO_2 values decrease from the basal to the top layer from 54.6 to 49.7 wt% (Fig. 4c). Alkali totals are low (7.9–10.8 wt%), while the K_2O/Na_2O ratios show high values of 1.7–2.7. Abundant phenocrysts of alkali feldspar (anorthoclase?), pale greenish clinopyroxene, biotite as well as leucite and apatite microcrystals are present in all layers. Lithic fragments comprise lava rocks and greenish tuffs. A remarkable decrease of lithic and phenocryst concentration is visible from the basal (TM-29-1i) to the top deposits (TM-29-1a).

The underlying tephra unit *TM-29-2* is made up of eight distinct grey-brownish tephra layers, TM-29-2a to TM-29-2h, occurring between 82.06 m and 82.20 m composite depth and dated between 112,520 ± 5630 and 113,020 ± 5650 calendar years BP. The mineral and lithic assemblage is equivalent to that of tephra succession TM-29-1. Glasses are also brownish in colour, blocky and display low vesicularity, but show a slightly more differentiated trachytic to basaltic trachyandesitic composition (Fig. 4c). SiO_2 values range from 60.4 to 51.6 wt% from the basal to the top layer. Within all layers, tephra components are set in a grey-brownish fine ash matrix.

The underlying tephra unit *TM-30-1* contains six grey to black-brownish tephra layers (TM-30-1a to TM-30-1f) between 82.26 m and 82.67 m composite depth that are dated between 113,370 ± 5670 and 114,000 ± 5700 calendar years BP. The basal layer of 12 mm thickness is the lightest and most coarse-grained (<700 µm) tephra deposit within TM-30-1. It comprises both high-vesicular, light pumice fragments and green-brownish, non- to low-vesicular, blocky glass shards with abundant apatite microcrystals (Fig. 3c). The two types of juvenile clasts reflect a bimodal chemical composition. Brown glass shards are concentrated in the younger five tephra layers TM-30-1a to TM-30-1e and have a latitic composition. Mean SiO_2 concentrations are between 56.4 and 57.9 wt% (Fig. 4c). Light pumice fragments, in turn, are abundant in the basal layer TM-30-1f, and show a homogenous trachytic composition with SiO_2 values of about 60 wt%. In addition, tephra particles of the uppermost tephras TM-30-1a and TM-30-1b are embedded in a dark-brownish, ashy matrix. The mineral assemblage of all layers within the TM-30-1 unit consists of coarse crystals of zoned plagioclase, sanidine, biotite, greenish clinopyroxene and rare olivine xenocrysts; leucite and apatite microcrystals in the juvenile phase occur as well. Lithics are abundant and

comprise lava rock fragments, altered greenish tuffs and feldspar cumulates.

Tephra unit *TM-30-2* is deposited between 82.74 and 82.78 m composite depth and dates between 114,440 ± 5720 and 114,720 ± 5740 calendar years BP. TM-30-2 comprises four distinct tephra layers of which the basal tephra TM-30-2d is the most prominent and coarse-grained layer. It consists of two types of juvenile clasts characterised by a distinct chemical composition: a) light, high-vesicular pumice fragments – rich in Fe–Ti–Oxide microcrysts – showing a trachytic composition and b) rare brownish, low to moderate-vesicular glass shards of trachyandesitic composition that are more abundant in the overlying tephras TM-30-2a to TM-30-2c (Fig. 4c). Phenocrysts of all tephras of succession TM-30-2 encompass zoned plagioclase, sanidine, greenish clinopyroxene, biotite and apatite. Lithics are abundant and comprise altered tuffs (altered pumices and lava rock fragments with leucite inclusions) and mafic to intermediate volcanic rocks.

TM-31 is a 0.5 mm thin fine-grained, white vitric ash layer at 82.79 m composite depth, which is directly underlying the basal tephra of TM-30-2. It is dated by varve counting at 114,770 ± 5740 calendar years BP. TM-31 comprises both colourless, high-vesicular pumice fragments of heterogeneous dacitic–trachydacitic composition (63–68 wt% SiO_2; K_2O/Na_2O ratios of 2.3–3.6; alkali totals 6.0–8.7 wt%) and moderate-vesicular glasses of phonotephritic to basaltic trachyandesitic composition (ca 52 wt% SiO_2) (Fig. 4c). Only a few loose crystals of plagioclase, sanidine, biotite and clinopyroxene as well as lava rock fragments occur.

TM-32 is a 1 mm thin, fine-grained and light-brown ash layer at 82.85 m composite depth. It is dated at 115,250 ± 5760 calendar years BP. Phenocrysts present include K-feldspar, zoned plagioclase, light-greenish clinopyroxene, orthopyroxene and olivine. In addition, rare lithic clasts of quenched feldspar crystals and tachylites occur. The juvenile phase is made up of greyish-brownish, non- to low-vesicular volcanic glass that exhibits a rather heterogeneous calc-alkaline, trachyandesitic composition. Glass shards of TM-32 show SiO_2 concentrations of ca 60 wt%, high FeO_{total} values of about 6.5 wt%, and concentrations of CaO, Na_2O and K_2O of about 4–5 wt%, respectively (Fig. 4d, Table 2).

TM-33 comprises two tephra units, TM-33-1 and TM-33-2, hosting a set of several tephra layers of similar composition. Tephra unit TM-33-1 is made up of three light-brownish, vitric ash layers up to 11 mm in thickness, deposited at 83.05–83.10 m composite depth and dated between 115,720 ± 5790 and 116,110 ± 5810 calendar years BP. Tephra unit TM-33-2, in turn, comprises two thin tephra layers at ca 83.43 m composite depth, which are dated at 118,190 and 118,210 calendar years BP, respectively. Tephras of units TM-33-1 and TM-33-2 all consist of abundant light-brownish, medium- to high-vesicular pumice fragments and few large sanidine, plagioclase, biotite and rare clinopyroxene (aegerine–augite) phenocrysts. Scarce lithics comprise clasts of volcanic and sedimentary rock fragments (sandstones, siltstones). Glass shards of each tephra unit show a bimodal trachytic composition (Fig. 4e). The major element chemistry within each unit differs in the concentration of SiO_2 (60.8–63.1 wt%) and CaO (1.0–2.1 wt%). The K_2O/Na_2O ratios show values of 0.8 and 1.4 for the lower and the upper tephra layers, respectively.

TM-34 is a 0.4 mm thick tephra layer at 83.54 m composite depth that is dated at 118,810 ± 5940 calendar years BP. This fine-grained ash consists of blocky, non- to low-vesicular brown, apatite-bearing glass shards. Phenocrysts are comprised of the minerals plagioclase and pale-greenish clinopyroxene with adherent glass. Additionally, a few lava lithics are also present. Glass is heterogeneous Na-calcalkaline, trachyandesitic to basaltic trachyandesitic in composition, showing significant variations in SiO_2 (54.4–57.8 wt%) as well as high FeO_{total} (8.4–11.3 wt%), MgO (2.4–3.8 wt%) and CaO (6.2–8.2 wt%) concentrations (Fig. 4f, Table 2).

TM-35 comprises two tephra layers of similar colour and mineral composition, TM-35a (120,670 ± 6030 calendar years BP) and TM-35b (121,940 ± 6100 calendar years BP) at 84.14 m and 84.84 m composite depth, respectively. Both tephras consist of light, high-vesicular pumice fragments and large phenocrysts of sanidine, plagioclase, biotite and rare green clinopyroxene. Lithics comprise clasts of lava rocks and altered tuffs. Geochemical data are only available for the more coarse-grained tephra TM-35a. This tephra reveals a homogeneous trachytic composition with CaO concentrations of about 2 wt% and K_2O/Na_2O ratios of ~1.5 (Fig. 4a).

TM-36 is a fine-grained, brown-blackish ash layer at 85.30 m composite depth, which is dated at 123,030 ± 6150 calendar years BP. It contains light, high-vesicular pumice fragments, abundant large phenocrysts of sanidine, leucite, nepheline, biotite, apatite and green clinopyroxene, as well as rare altered tuffs and limestone fragments. Tephra components are set in a black (base) and brown (top) fine-grained matrix. Glass shards show a phonolitic composition with high Al_2O_3 values of 20.3–20.8 wt% and CaO concentrations of 4.1–5.3 wt% (Table 2, Fig. 4g).

TM-37 is a succession of four single tephra layers deposited between 85.68 m and 86.59 m composite depth. Layer thicknesses range between 1 and 11 mm. The oldest tephra TM-37d (124,860 ± 6240 calendar years BP) is a white, fine-grained, almost pure vitric ash with high-vesicular glass components. It is overlain by a pumice bed, TM-37c (124,360 ± 6220 calendar years BP), that is rich in lithic fragments (lava lithics and altered green tuffs with feldspar xenocrystals) and phenocrysts of sanidine, plagioclase, biotite, green clinopyroxene and amphibole. Here, high-vesicular white pumice clasts and rare brown glass shards are common. The slightly younger tephra TM-37b (124,330 ± 6220 calendar years BP) is similar in composition but thicker and coarser-grained than TM-37c and TM-37d. The thickest tephra layer is the youngest deposit TM-37a (124,070 ± 6200 calendar years BP). It is twice reversely graded and mainly composed of high-vesicular white pumice fragments. Abundant phenocrysts and lithics comparable with those in layers TM-37b and TM-37c occur at the base of the deposit. All tephra layers of unit TM-37 are homogeneous and trachytic in composition showing low CaO concentrations (1.0–1.3 wt%) and K_2O/Na_2O ratios between 0.8 and 1.0 (Fig. 4e, Table 2).

TM-38 (formerly labelled as TM-38a in Wulf et al., 2006) is a fine-grained, vitric ash at 87.07 m composite depth. It is composed of light-coloured glass shards of homogeneous high-K-phonolitic composition (Fig. 4a). A few loose crystals of sanidine and biotite also occur. Tephra TM-38 is dated by the Monticchio chronology at 125,550 ± 6280 calendar years BP.

TM-39 is a brownish tephra layer of 4 mm thickness at 91.98 m composite depth. It comprises brown and light, low to moderately vesicular glass shards of similar homogeneous phonolitic composition that exhibit higher FeO_{total} (4.5 wt%) and CaO (3.3 wt%) concentrations and lower K_2O/Na_2O ratios (1.3–1.7) than tephra TM-38 (Fig. 4a). The phenocryst assemblage encompasses the minerals plagioclase, sanidine, green clinopyroxene, and amphibole. Leucite and apatite microcrystals occur as well as lithics of lava rocks. TM-39 is dated at 130,530 ± 6530 calendar years BP.

TM-40 at 92.37 m composite depth is a white vitric ash of 5 mm thickness dated at 130,860 ± 6540 calendar years BP. It bears phenocrysts of sanidine, biotite and greenish clinopyroxene. Lithics are rare and comprise lava rock fragments. The main juvenile phase is characterised by light high-vesicular and few brownish glass shards of inhomogeneous trachytic composition.

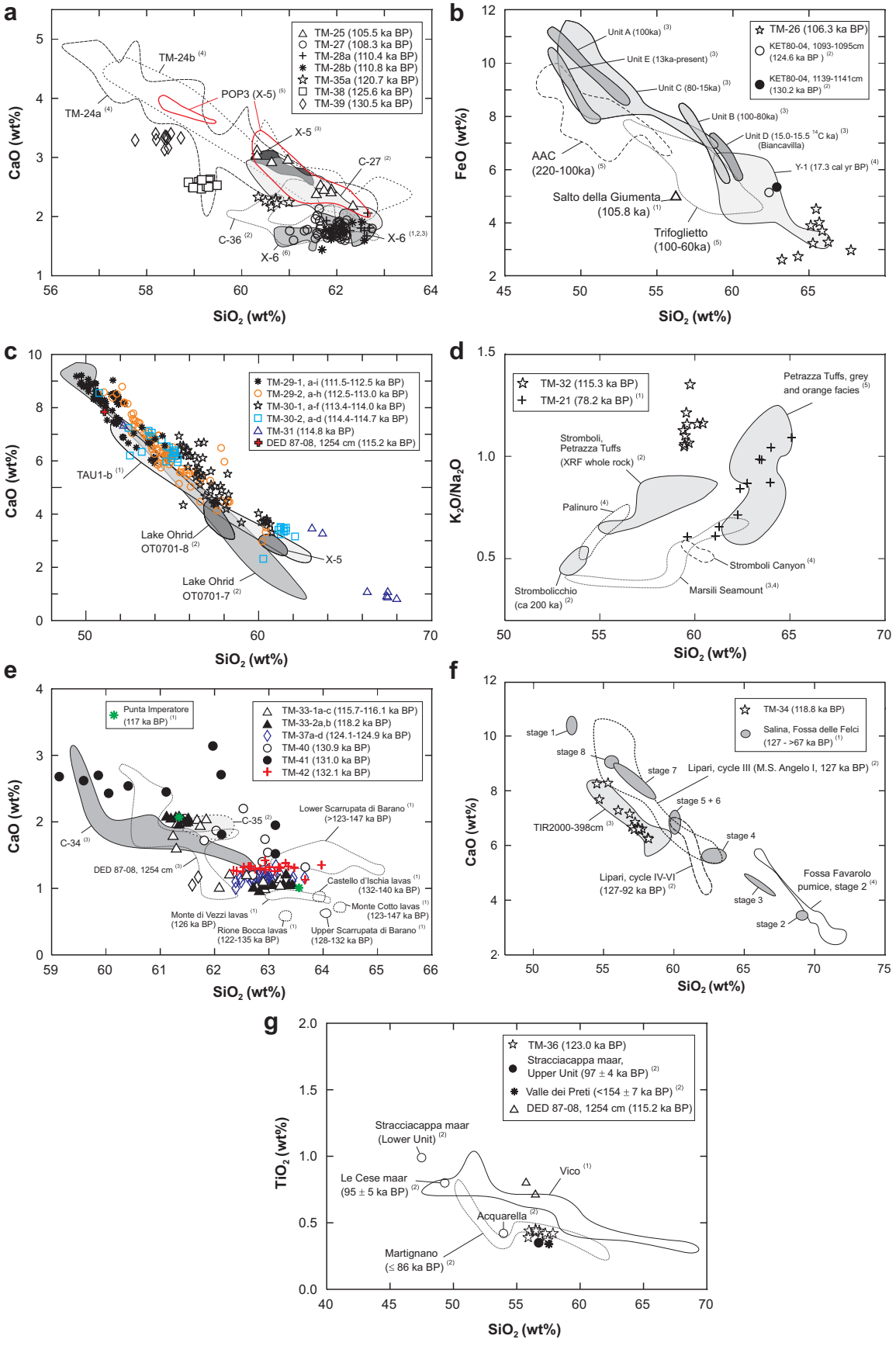

Fig. 4. a: Harker diagram SiO_2 vs. CaO for chemical discrimination of Monticchio tephras from the Campanian province (undefined): (1) mean SEM–EDS glass data (Munno and Petrosino, 2007; Marciano et al., 2008); (2) SEM–EDS glass data (Paterne et al., 2008); (3) EPMA glass data (Scheld, 1995); (4) EPMA glass data (Wulf et al., 2004; this study); (5)

K_2O/Na_2O ratios are ~1 and CaO concentrations are variable between 1.2 and 2.2 wt% (Fig. 4e).

TM-41 (formerly labelled as TM-38b in Wulf et al., 2006) is a double layered, light brownish tephra of 6 mm thickness. It occurs at 92.77 m composite depth and is dated at 131,020 ± 6550 calendar years BP. Glass shards are light to brownish in colour and display low-vesicularity. The glass composition is heterogeneous trachytic to phonolitic, reflecting variable concentration of CaO (1.5–3.1 wt%), FeO_{total} (1.2–3.5 wt%), K_2O/Na_2O ratios (1.4–2.4) and high Al_2O_3 values (19.3–21.0 wt%) (Fig. 4e, Table 2). The mineral assemblage encompasses phenocrysts of sanidine, plagioclase, biotite, clinopyroxene and apatite microcrystals. Rare volcanic rock fragments also occur.

TM-42 is a 1 mm thick, light ash at 97.69 m composite depth. It is the oldest tephra layer in the Monticchio record dated at 132,110 ± 6610 calendar years BP. The mineral assemblage is composed of sanidine, plagioclase, biotite and minor green clinopyroxene crystals. Lithics are rare and comprise clasts of lava rocks of intermediate composition. The juvenile phase is made up of light high-vesicular pumice fragments of homogenous trachytic character (Table 2, Fig. 4e).

6. Discussions

6.1. Tephra origin and distal correlation

In the following, the potential sources of tephras deposited in the Monticchio record between ca 100 ka and 133 ka as well as correlations with proximal and distal equivalents are discussed.

6.1.1. TM-25 (X-5)

The youngest tephra in the 100–133 ka Monticchio sediment section, TM-25 (ca 105.5 ± 5.3 ka BP), is a thick and coarse grained deposit that densely clusters within the K-trachytic chemical fields of the marine X-5 tephra (Fig. 4a). The widely distributed tephra layer X-5 and the associated X-6 have been defined as first-order marker beds in the marine record of the Ionian Sea by Keller et al. (1978), and later confirmed by new sediment cores of the *Meteor* cruise M25-4 (Scheld, 1995; Keller et al., 1996; Kraml, 1997; Keller and Kraml, 2004). For X-5, a $^{40}Ar/^{39}Ar$ date of 105 ± 2 ka has been obtained by Kraml (1997) in accordance with its position directly below sapropel S-4 (mid-sapropel age 102 ka BP) and with the marine oxygen isotope curve (e.g., Allen et al., 1999). In the Tyrrhenian Sea cores DED 87-08/KET 80-04 an equivalent tephra marker, C-27 (103.5 ka), is correlated with the X-5 tephra (Paterne, 1985; Paterne et al., 2008) (Table 3). X-5 was also identified in terrestrial archives of the Central Mediterranean. In volcaniclastic deposits on Salina – (Aeolian Islands), X-5 forms an up to 25 cm thick pink tephra layer (Morche, 1988; Lucchi et al., 2008). Keller (2006) first pointed out the occurrence of the two superimposed tephra layers, X-5 (1 m thick) and X-6 (0.5 m thick), in Cilento post-Tyrrhenian coastal deposits (Le Saline, southern Italy, ca 140 km SSW′ from Lago Grande di Monticchio, Fig. 1), which were recently geochemically confirmed by Marciano et al. (2008) (samples SM1, SM2, SA = X-6), Giaccio et al. (2012) (samples CIL1 = X-5 and CIL2 = X-6) and Albert (2012) (Palinuro Tephra/LeS1 = X-5 and LeS2 = X-6). In the San Gregorio Magno basin, located ca 40 km SW′ of Monticchio (Fig. 1), the X-5 tephra was correlated with sample S11 forming a 30 cm thick marker horizon in the lake sediments (Munno and Petrosino, 2007). A recent finding in the lacustrine succession of the Sulmona Basin (Popoli, Central Italy, ca 240 km NW′ of Monticchio) revealed a new $^{40}Ar/^{39}Ar$ age of 106.2 ± 1.3 ka BP for the 1.5 cm thin POP3/X-5 layer (Giaccio et al., 2012) confirming the initial dating by Kraml (1997). The X-5 tephra was furthermore identified in further distal settings such as Lake Ohrid (Balkans), where it shows a thickness of 3 cm (Sulpizio et al., 2010).

The composition of X-5 in general points to a Campanian origin (Keller et al., 1978; Morche, 1988; Scheld, 1995; Keller and Kraml, 2004; Di Vito et al., 2008; Giaccio et al., 2012), but the proximal source of X-5 has not yet been defined.

Marine tephras X-5 and C-27 were originally assigned to the two distinct Monticchio tephras TM-24a (ca 101.8 ka BP) and TM-24b (ca 102.8 ka BP) in the Monticchio record based on initial major and trace element data (Wulf et al., 2004). Additional major element glass data obtained on TM-24a and TM-24b (this study) prove a wider range in glass composition and therefore differ from the rather homogenous X-5 glass compositions (Fig. 4a). Given the major element geochemical overlap of the trachytic components of the TM-24a, TM-24b and TM-25 tephras, trace element glass data are used in an attempt to distinguish these tephras. Using Th as a fractionation index, Ba and Sr concentrations in the TM-25 glasses are clearly distinguishable from the TM-24a/TM-24b glasses and appear to reside upon separate evolutionary trends (Fig. 5). Ba is most diagnostic, extending to lower concentrations in the TM-25 glasses compared to those of the TM-24a/TM-24b glasses (Fig. 5b). Trace element data confirm the correlation of TM-25 to the terrestrial and marine X-5 tephra (Fig. 5). Furthermore, the stratigraphical position and the varve age of Monticchio tephra TM-25 is in much closer agreement with the position of X-5 in marine cores and the $^{40}Ar/^{39}Ar$ ages obtained directly on the X-5 tephra by Kraml (1997) and Giaccio et al. (2012).

6.1.2. TM-26 (Salto della Giumenta Unit, Etna)

The Na-alkaline glass composition and mineral assemblage of tephra TM-26 (ca 106.3 ± 5.3 ka BP) strongly resemble the composition of pyroclastics of Mount Etna, i.e., from the Biancavilla/Y-1 tephra (17.3 ka BP) (Fig. 4b). We therefore propose a correlation of TM-26 with an older Plinian eruption of this volcano. Explosive behaviour of Mount Etna during the considered time period of >100 ka BP developed during activities of the Valle del Bove centres and the Timpe Phase (Coltelli et al., 2000; Branca et al., 2008; Nicotra et al., 2011), and include the units of the Ancient Alkaline Centres (220–100 ka BP) and Trifoglietto (100–60 ka BP) previously defined by Romano (1982). Based on the comparison with bulk rock geochemical data (Fig. 4b) we assume a correlation of TM-26 with the proximal pyroclastics of the "Salto della Giumenta Unit" that has been assigned to activities of the "Tarderia" volcano (Nicotra et al., 2011). This correlation is further supported by a $^{40}Ar/^{39}Ar$ age of

EPMA glass data (Giaccio et al., 2012); [6] SEM–EDS glass data (Sulpizio et al., 2010). b: Harker diagram SiO_2 vs. FeO_{total} for chemical discrimination of Monticchio tephras from Mount Etna: [1] XRF whole rock data of pyroclasts (Nicotra et al., 2011); [2] SEM–EDS glass data (this study); [3] XRF whole rock data of pyroclasts (Coltelli et al., 2000); [4] EPMA glass data (Wulf et al., 2004, 2008); [5] XRF whole rock data of lava (M. Viccaro, this study). c: Harker diagram SiO_2 vs. CaO for chemical discrimination of Monticchio tephras TM-29, TM-30 and TM-31 from the Campanian volcanic province (Phlegrean Fields?): [1] SEM–EDS glass data (Di Vito et al., 2008); [2] SEM–EDS glass data (Sulpizio et al., 2010). d:Harker diagram SiO_2 vs. alkali ratio for chemical discrimination of Monticchio tephras from Stromboli Island: [1] EPMA glass data (Wulf et al., 2004); [2] XRF whole rock data (Hornig-Kjarsgaard et al., 1993); [3] XRF whole rock data (Trua et al., 2002); [4] XRF whole rock data (Beccaluva et al., 1985); [5] EPMA glass data (this study, see Supplementary Table B). e: Harker diagram SiO_2 vs. CaO for chemical discrimination of Monticchio tephras from Ischia Island: [1] XRF whole rock data of pumice (Poli et al., 1987); [2] SEM–EDS glass data (Paterne et al., 2008); [3] SEM–EDS glass data (Paterne, 1985; this study). f: Harker diagram SiO_2 vs. CaO for chemical discrimination of Monticchio tephras from Salina Island: [1] XRF whole rock (Gertisser and Keller, 2000); [2] XRF whole rock (Esperança et al., 1992); [3] EPMA glass data (Albert et al., 2012; this study, see Supplementary Table B); [4] EPMA glass data, this study (see Supplementary Table B). g: Harker diagram SiO_2 vs. TiO_2 for chemical discrimination of Monticchio tephras from the Sabatini Volcanic District: [1] XRF whole rock data (Perini et al., 1997, 2004); [2] EPMA glass data (Sottili et al., 2012).

Table 2
Mean values of non-normalized EPMA glass data and 2σ standard deviation (italics) of tephra layers occurring in the Monticchio sequence between 100 and 133 ka BP. Totals are corrected for chlorine concentrations. Full analytical data of individual glass measurements are provided in Supplementary Table A.

Sample	TM-30-1d		TM-30-1e		TM-30-1f		TM-30-2b		TM-30-2c		TM-30-2d	
SiO_2	59.10	*1.37*	64.23	*1.57*	60.11	*0.76*	60.22	*0.65*	60.75	*0.74*	49.39	*0.53*
TiO_2	0.39	*0.05*	0.54	*0.09*	0.45	*0.03*	0.46	*0.03*	0.48	*0.02*	1.14	*0.04*
Al_2O_3	17.95	*0.39*	16.82	*1.25*	18.17	*0.26*	18.41	*0.18*	18.45	*0.19*	17.81	*0.21*
FeO	3.32	*0.34*	3.38	*0.59*	2.79	*0.15*	2.94	*0.21*	3.09	*0.08*	8.57	*0.31*
MnO	0.13	*0.02*	0.13	*0.03*	0.23	*0.06*	0.25	*0.05*	0.29	*0.03*	0.15	*0.03*
MgO	0.62	*0.13*	0.94	*0.37*	0.40	*0.08*	0.28	*0.03*	0.31	*0.02*	3.52	*0.15*
CaO	2.54	*0.30*	3.14	*0.75*	1.80	*0.10*	1.74	*0.12*	1.71	*0.11*	8.71	*0.25*
Na_2O	3.85	*0.23*	4.78	*0.34*	6.19	*0.70*	5.97	*0.52*	6.11	*0.41*	2.69	*0.16*
K_2O	8.31	*0.18*	3.79	*0.48*	7.10	*0.48*	6.30	*0.17*	6.61	*0.14*	5.58	*0.30*
P_2O_5	0.16	*0.05*	0.21	*0.04*	0.06	*0.04*	0.04	*0.02*	0.04	*0.02*	0.94	*0.06*
Cl	0.39	*0.03*	0.25	*0.04*	0.70	*0.14*	0.83	*0.14*	0.89	*0.04*	0.25	*0.02*
Total	96.67		98.14		97.86		97.25		98.63		98.70	
Analyses	$n = 10$		$n = 9$		$n = 22$		$n = 10$		$n = 16$		$n = 13$	
	TM-29-1b		TM-29-1c		TM-29-1d		TM-29-1e		TM-29-1f		TM-29-1g	
SiO_2	49.25	*1.14*	50.21	*0.32*	50.38	*0.58*	51.67	*1.65*	50.80	*0.32*	51.69	*0.60*
TiO_2	1.10	*0.03*	1.12	*0.04*	1.10	*0.03*	1.11	*0.02*	1.10	*0.04*	1.09	*0.07*
Al_2O_3	17.67	*0.45*	18.00	*0.11*	18.17	*0.06*	17.89	*0.37*	17.96	*0.20*	17.96	*0.12*
FeO	7.90	*0.17*	8.04	*0.12*	7.85	*0.13*	7.88	*0.15*	7.91	*0.18*	7.75	*0.23*
MnO	0.14	*0.02*	0.15	*0.01*	0.15	*0.03*	0.16	*0.03*	0.13	*0.02*	0.15	*0.03*
MgO	3.29	*0.15*	3.47	*0.15*	3.49	*0.29*	3.10	*0.40*	3.33	*0.22*	2.90	*0.36*
CaO	8.13	*0.21*	8.41	*0.32*	8.44	*0.60*	7.61	*0.98*	7.83	*0.37*	7.17	*0.63*
Na_2O	2.93	*0.04*	2.91	*0.06*	2.96	*0.12*	2.95	*0.11*	2.88	*0.06*	3.00	*0.16*
K_2O	5.78	*0.14*	5.80	*0.14*	5.75	*0.36*	5.79	*0.08*	5.87	*0.28*	6.36	*0.28*
P_2O_5	0.77	*0.10*	0.70	*0.05*	0.73	*0.05*	0.68	*0.03*	0.69	*0.04*	0.72	*0.04*
Cl	0.35	*0.03*	0.34	*0.01*	0.34	*0.02*	0.33	*0.02*	0.35	*0.02*	0.40	*0.03*
Total	97.24		99.07		99.29		99.09		98.76		99.09	
Analyses	$n = 5$		$n = 7$		$n = 5$		$n = 5$		$n = 8$		$n = 5$	
	TM-29-1h		TM-29-1i		TM-29-2a		TM-29-2b		TM-29-2c		TM-29-2d	
SiO_2	52.17	*1.27*	51.54	*1.03*	52.15	*1.24*	52.55	*0.79*	53.91	*0.52*	54.19	*0.34*
TiO_2	1.02	*0.05*	1.10	*0.06*	1.06	*0.05*	1.09	*0.04*	1.13	*0.03*	1.09	*0.03*
Al_2O_3	18.08	*0.32*	17.91	*0.23*	17.46	*0.33*	17.76	*0.35*	17.36	*0.17*	17.39	*0.17*
FeO	7.49	*0.36*	7.43	*0.22*	7.59	*0.26*	7.69	*0.27*	7.72	*0.06*	7.69	*0.22*
MnO	0.15	*0.03*	0.12	*0.02*	0.15	*0.03*	0.14	*0.02*	0.14	*0.03*	0.15	*0.04*
MgO	2.65	*0.57*	3.38	*0.36*	2.87	*0.39*	2.96	*0.38*	2.51	*0.16*	2.37	*0.11*
CaO	6.98	*0.86*	7.89	*0.72*	7.11	*0.94*	7.38	*0.63*	6.38	*0.32*	6.10	*0.21*
Na_2O	3.16	*0.35*	2.76	*0.12*	2.93	*0.21*	2.94	*0.21*	3.13	*0.09*	3.14	*0.04*
K_2O	6.01	*0.54*	5.56	*0.34*	5.54	*0.24*	5.56	*0.22*	5.85	*0.26*	5.90	*0.17*
P_2O_5	0.67	*0.07*	0.66	*0.05*	0.65	*0.09*	0.69	*0.06*	0.67	*0.04*	0.64	*0.04*
Cl	0.37	*0.05*	0.33	*0.03*	0.32	*0.02*	0.32	*0.02*	0.33	*0.01*	0.33	*0.02*
Total	98.67		98.60		97.76		99.02		99.05		98.91	
Analyses	$n = 15$		$n = 16$		$n = 9$		$n = 14$		$n = 5$		$n = 14$	
	TM-29-2e		TM-29-2f		TM-29-2g		TM-30-1a		TM-30-1b		TM-30-1c	
SiO_2	53.15	*1.19*	54.57	*0.91*	56.91	*2.04*	53.22	*0.72*	56.43	*0.70*	55.52	*0.70*
TiO_2	1.04	*0.09*	1.13	*0.11*	0.82	*0.18*	0.75	*0.08*	0.60	*0.09*	0.80	*0.13*
Al_2O_3	17.46	*0.45*	17.85	*0.21*	18.31	*1.06*	16.73	*0.77*	18.64	*1.30*	17.59	*0.46*
FeO	7.65	*0.35*	6.78	*0.32*	5.50	*1.26*	6.20	*0.42*	5.29	*0.58*	6.66	*0.83*
MnO	0.15	*0.03*	0.14	*0.03*	0.14	*0.03*	0.14	*0.03*	0.14	*0.04*	0.14	*0.04*
MgO	2.45	*0.24*	2.59	*0.32*	1.79	*0.83*	1.97	*0.21*	1.61	*0.29*	2.04	*0.49*
CaO	6.30	*0.64*	6.14	*0.53*	4.91	*1.25*	5.69	*0.57*	5.14	*0.88*	5.49	*0.86*
Na_2O	3.15	*0.20*	3.31	*0.17*	3.69	*0.25*	2.96	*0.18*	3.49	*0.16*	3.16	*0.17*
K_2O	5.89	*0.43*	6.07	*0.24*	6.35	*0.92*	5.77	*0.24*	6.26	*0.66*	6.35	*0.75*
P_2O_5	0.65	*0.06*	0.64	*0.07*	0.38	*0.14*	0.51	*0.07*	0.37	*0.05*	0.47	*0.12*
Cl	0.33	*0.03*	0.33	*0.03*	0.37	*0.10*	0.32	*0.03*	0.28	*0.04*	0.40	*0.10*
Total	98.14		99.46		99.09		94.18		98.19		98.52	
Analyses	$n = 15$		$n = 19$		$n = 18$		$n = 6$		$n = 10$		$n = 12$	
	TM-30-1d		TM-30-1e		TM-30-1f		TM-30-2b		TM-30-2c		TM-30-2d	
SiO_2	54.64	*0.91*	55.76	*0.78*	57.95	*1.89*	52.39	*0.90*	54.24	*0.73*	59.85	*0.80*
TiO_2	0.65	*0.02*	0.66	*0.07*	0.64	*0.22*	1.05	*0.12*	0.81	*0.05*	0.50	*0.03*
Al_2O_3	17.70	*0.68*	17.62	*0.61*	17.54	*0.33*	17.71	*0.64*	18.02	*0.25*	17.91	*0.44*
FeO	5.93	*0.19*	5.55	*1.15*	5.00	*1.38*	7.17	*0.69*	6.68	*0.35*	3.76	*0.29*
MnO	0.16	*0.03*	0.14	*0.04*	0.12	*0.03*	0.15	*0.03*	0.15	*0.02*	0.16	*0.03*
MgO	1.56	*0.08*	1.32	*0.35*	1.30	*0.71*	2.85	*0.44*	2.65	*0.25*	0.88	*0.15*
CaO	5.01	*0.51*	4.46	*0.78*	4.21	*1.20*	6.60	*0.74*	6.29	*0.34*	3.20	*0.34*
Na_2O	3.41	*0.30*	3.49	*0.25*	3.48	*0.33*	3.12	*0.49*	3.04	*0.11*	4.14	*0.30*

(*continued on next page*)

Table 2 (*continued*)

Sample	TM-30-1d		TM-30-1e		TM-30-1f		TM-30-2b		TM-30-2c		TM-30-2d	
K_2O	6.55	*0.37*	6.61	*0.29*	6.91	*0.82*	5.73	*0.48*	6.13	*0.17*	6.62	*0.38*
P_2O_5	0.42	*0.04*	0.45	*0.06*	0.31	*0.20*	0.52	*0.08*	0.58	*0.07*	0.17	*0.03*
Cl	0.43	*0.05*	0.42	*0.15*	0.43	*0.08*	0.32	*0.05*	0.34	*0.02*	0.47	*0.03*
Total	96.37		96.37		97.80		97.60		98.90		97.57	
Analyses	$n = 5$		$n = 6$		$n = 13$		$n = 10$		$n = 11$		$n = 10$	
	TM-31		TM-32		TM-33-1a		TM-33-1c		TM-33-2a		TM-33-2b	
SiO_2	61.10	*5.48*	59.73	*0.59*	59.83	*0.64*	61.64	*0.59*	61.14	*1.21*	58.57	*0.50*
TiO_2	0.73	*0.18*	0.77	*0.04*	0.46	*0.02*	0.67	*0.03*	0.62	*0.01*	0.43	*0.02*
Al_2O_3	18.43	*0.46*	16.95	*0.33*	18.66	*0.17*	18.45	*0.23*	18.01	*0.38*	18.31	*0.17*
FeO	4.18	*1.77*	6.47	*0.40*	3.03	*0.06*	2.98	*0.26*	2.77	*0.08*	2.95	*0.13*
MnO	0.24	*0.09*	0.16	*0.03*	0.25	*0.03*	0.29	*0.05*	0.28	*0.03*	0.19	*0.03*
MgO	1.12	*1.11*	1.94	*0.19*	0.41	*0.01*	0.35	*0.05*	0.31	*0.04*	0.38	*0.04*
CaO	2.86	*2.58*	4.38	*0.29*	1.86	*0.13*	1.05	*0.07*	1.00	*0.06*	1.92	*0.04*
Na_2O	2.03	*0.48*	4.17	*0.13*	5.49	*0.42*	6.96	*0.31*	6.99	*0.42*	5.27	*0.12*
K_2O	5.58	*0.64*	4.76	*0.24*	7.27	*0.07*	5.75	*0.14*	5.74	*0.18*	7.40	*0.10*
P_2O_5	0.22	*0.25*	0.45	*0.05*	0.06	*0.02*	0.05	*0.03*	0.06	*0.03*	0.07	*0.02*
Cl	0.59	*0.16*	0.37	*0.04*	0.77	*0.03*	0.69	*0.04*	0.70	*0.02*	0.65	*0.03*
Total	96.99		100.07		97.93		98.71		97.46		95.99	
Analyses	$n = 9$		$n = 10$		$n = 9$		$n = 10$		$n = 9$		$n = 7$	
	TM-34		TM-35a		TM-36		TM-37a		TM-37b		TM-37c	
SiO_2	56.13	*1.53*	58.99	*0.58*	54.00	*0.83*	60.68	*0.60*	60.87	*0.83*	60.84	*0.67*
TiO_2	1.26	*0.10*	0.41	*0.02*	0.40	*0.02*	0.61	*0.03*	0.63	*0.03*	0.61	*0.03*
Al_2O_3	15.69	*0.74*	18.66	*0.21*	19.56	*0.26*	17.91	*0.18*	17.89	*0.41*	18.10	*0.32*
FeO	9.46	*0.83*	2.86	*0.09*	3.53	*0.41*	2.61	*0.11*	2.56	*0.03*	2.62	*0.14*
MnO	0.21	*0.03*	0.17	*0.04*	0.17	*0.01*	0.23	*0.04*	0.22	*0.03*	0.25	*0.06*
MgO	2.88	*0.37*	0.40	*0.02*	0.27	*0.04*	0.31	*0.01*	0.33	*0.01*	0.35	*0.05*
CaO	6.85	*0.61*	2.18	*0.05*	4.55	*0.33*	1.07	*0.03*	1.10	*0.02*	1.11	*0.07*
Na_2O	3.81	*0.26*	5.14	*0.16*	5.29	*0.36*	6.63	*0.35*	6.44	*0.42*	7.12	*0.58*
K_2O	2.41	*0.19*	7.94	*0.17*	7.33	*0.76*	5.90	*0.10*	5.87	*0.15*	5.99	*0.14*
P_2O_5	0.48	*0.06*	0.05	*0.02*	0.04	*0.02*	0.04	*0.02*	0.07	*0.02*	0.07	*0.02*
Cl	0.21	*0.03*	0.58	*0.03*	0.13	*0.01*	0.62	*0.03*	0.56	*0.04*	0.47	*0.07*
Total	99.35		97.26		95.24		96.46		96.41		97.44	
Analyses	$n = 15$		$n = 7$		$n = 10$		$n = 8$		$n = 7$		$n = 7$	
	TM-37d		TM-38		TM-39		TM-40		TM-41		TM-42	
SiO_2	61.10	*0.45*	57.58	*0.60*	56.67	*0.51*	60.37	*0.84*	59.07	*1.26*	61.89	*0.53*
TiO_2	0.63	*0.02*	0.48	*0.02*	0.58	*0.02*	0.61	*0.05*	0.48	*0.06*	0.66	*0.04*
Al_2O_3	18.17	*0.16*	19.03	*0.12*	18.35	*0.23*	18.09	*0.16*	19.17	*0.56*	18.65	*0.19*
FeO	2.55	*0.11*	3.34	*0.08*	4.39	*0.25*	2.78	*0.22*	2.60	*0.75*	2.53	*0.09*
MnO	0.19	*0.03*	0.17	*0.03*	0.19	*0.02*	0.19	*0.04*	0.12	*0.04*	0.20	*0.03*
MgO	0.36	*0.02*	0.68	*0.02*	0.93	*0.07*	0.49	*0.13*	0.58	*0.18*	0.40	*0.02*
CaO	1.16	*0.06*	2.48	*0.05*	3.21	*0.09*	1.61	*0.31*	2.33	*0.45*	1.28	*0.06*
Na_2O	6.47	*0.28*	4.49	*0.26*	4.79	*0.25*	5.67	*0.31*	4.34	*0.70*	5.84	*0.56*
K_2O	6.16	*0.15*	8.42	*0.12*	7.45	*0.32*	6.27	*0.25*	7.51	*0.38*	6.36	*0.18*
P_2O_5	0.07	*0.04*	0.10	*0.04*	0.20	*0.03*	0.13	*0.04*	0.11	*0.02*	0.05	*0.03*
Cl	0.51	*0.04*	0.51	*0.03*	0.47	*0.03*	0.40	*0.07*	0.39	*0.13*	0.51	*0.02*
Total	97.25		97.28		97.13		96.50		96.61		98.25	
Analyses	$n = 13$		$n = 13$		$n = 11$		$n = 9$		$n = 11$		$n = 19$	

105.8 ± 4.5 ka BP obtained from the groundmass of related lava flows of the Tarderia activities (Branca et al., 2008), which is in good agreement with the varve age of TM-26.

Apart from XRF whole rock data of proximal pyroclastics, tephra TM-26 can only be compared with SEM–EDS data of glass of Etnean origin found in 1093–1095 cm and 1139–1141 cm sediment depth in Tyrrhenian Sea core KET 80-04 (Fig. 4b, Table 3). Those distal shards dated at 124.6 ka and 130.2 ka BP, respectively, are significantly older than TM-26, but are similar in composition and therefore confirm the considered correlation with older Etnean deposits.

6.1.3. TM-27 (X-6), TM-28a and TM-28b (Campanian)

The glass composition and mineral assemblage of the thickest Monticchio tephra TM-27 (ca 108.3 ± 5.4 ka BP) match the widespread marine X-6 tephra (Fig. 4a). The X-6 tephra forms a prominent marker horizon in the deep-sea sediments of the Ionian Sea (Keller et al., 1978; Morche, 1988) and in terrestrial sequences of central and southern Italy (Marciano et al., 2008; Giaccio et al., 2012) and the Balkans (Sulpizio et al., 2010). The age of X-6 is, so far, only constrained by interpolation of the sapropel chronology of the Ionian Sea between sapropels S4 and S5 at ca 108–110 ka BP (Keller et al., 1978; Kraml, 1997; Keller and Kraml, 2004), which is in good agreement with the varve age of Monticchio tephra TM-27. Furthermore, the comparison of single grain glass data shows that TM-27/X-6 can be attributed to the marine C-31 tephra (107 ka BP) that forms a thick and coarse grained marker layer in sediment cores KET 80-04, DED 87-08 and KET 82-22 in the Central Tyrrhenian and Ionian Seas (Paterne et al., 2008) (Table 3). Composition and thickness in the Monticchio record strongly support the assumption that

Table 3
List of major element data of distal and proximal tephras used for correlation with Monticchio tephras (see text). Data from: * this study; (1) Paterne et al. (2008), (2) Sulpizio et al. (2010), (3) Di Vito et al. (2008), (4) Sottili et al. (2012), (5) Poli et al. (1987), (6) Fuchs (1873).

Distal tephra correlatives

Sample	C-27, KET 80-04, 930–945 cm	C-27, KET 80-04, 930–945 cm	C-31, KET 80-04, 975–985 cm	TAU1-b?, DED 87-08, 1254 cm	Sabatini rew?, DED 87-08, 1254 cm	C-34 reworked?, DED 87-08, 1254 cm	C-34, DED 87-08, 1260 cm	C-35, KET 82-22, 485 cm	C-36, KET 80-04, 1083 cm	C-36, KET 80-04, 1083 cm	Etnean, KET 80-04, 1095 cm	Etnean, KET 80-04, 1141 cm
SiO_2	60.46	61.87	61.80	51.10	56.11 *(0.37)*	61.20 *(0.60)*	60.92 *(0.78)*	61.97	61.42	61.22	62.38	62.55
TiO_2	0.47	0.40	0.45	1.70	0.76 *(0.05)*	0.46 *(0.12)*	0.42 *(0.10)*	0.44	0.30	0.44	0.85	0.83
Al_2O_3	18.31	18.21	18.11	17.38	19.73 *(0.08)*	18.37 *(0.19)*	18.43 *(0.25)*	18.57	19.27	18.43	17.95	17.24
FeO	3.51	3.08	3.16	8.59	4.25 *(0.20)*	3.11 *(0.28)*	3.11 *(0.15)*	3.17	2.95	3.10	5.11	5.28
MnO	0.16	0.22	0.28	0.22	0.18 *(0.05)*	0.24 *(0.12)*	0.23 *(0.10)*	0.00	0.00	0.21	–	–
MgO	0.75	0.39	0.31	3.15	1.16 *(0.10)*	0.38 *(0.21)*	0.33 *(0.12)*	0.31	0.34	0.33	1.40	1.25
CaO	2.59	1.79	1.76	7.85	3.95 *(0.09)*	1.83 *(0.47)*	1.80 *(0.19)*	1.92	2.71	1.82	4.64	4.19
Na_2O	3.69	5.82	5.64	3.30	5.38 *(0.35)*	5.61 *(1.29)*	5.91 *(0.38)*	6.58	4.47	5.63	4.38	4.92
K_2O	9.23	7.10	7.34	5.38	7.67 *(0.27)*	7.81 *(1.09)*	7.63 *(0.49)*	7.05	8.55	7.63	3.30	3.22
P_2O_5	0.01	0.00	0.02	0.77	0.15 *(0.15)*	0.00 *(0.00)*	0.01 *(0.04)*	0.00	0.00	0.00	–	–
Total	99.18	98.88	98.87	99.92	99.32	99.01	98.80	100.01	100.01	98.81	100.01	99.48
Age	*103.6 ka*	*103.6 ka*	*107 ka*	*115.2 ka*	*115.2 ka*	*115.2 ka*	*116.1 ka*	*121.5 ka*	*123.2 ka*	*125.4 ka*	*124.6 ka*	*130.2 ka*
Ref.	(1)	(1)	(1)	*N = 1	*N = 2	*N = 18	*N = 19	(1)	(1)	(1)	*N = 1	*N = 1

Distal and proximal tephra correlatives

Sample	C-38, DED 87-08, 1370 cm	C-39, DED 87-08, 1370 cm	C-39, DED 87-08, 1370 cm	Lake Ohrid, OT0701-7a	Lake Ohrid, OT0701-7b	TAU1-b sc	TAU1-b ch	VDP1, Valle dei Preti, Sabatini	Punta, Imperatore, Ischia		Monte Vezzi, lavas, Ischia	Upper, Scarrupata, Ischia	Lower, Scarrupata, Ischia
SiO_2	61.22	62.61	61.95	50.86	58.30	51.99	62.13	54.28	63.56	61.05	62.85	61.74	62.63
TiO_2	0.45	0.64	0.38	1.15	0.63	1.25	0.60	0.32	0.77	0.00	0.67	0.66	0.44
Al_2O_3	18.44	18.12	18.26	18.55	19.75	19.33	18.56	19.76	19.09	18.35	18.76	17.91	18.84
Fe_2O_3	–	–	–	–	–	–	–	–	1.99	4.21	2.17	2.78	0.89
FeO	3.08	2.75	3.05	8.33	3.62	7.10	2.98	2.78	1.37	2.12	0.81	0.25	1.63
MnO	0.21	0.22	0.12	0.22	0.15	0.23	0.17	0.25	0.24	0.04	0.18	0.21	0.09
MgO	0.22	0.15	0.49	3.19	0.82	2.76	0.68	0.15	0.81	0.90	0.42	0.29	0.51
CaO	1.65	1.01	2.06	8.47	3.41	7.10	2.48	3.05	1.00	2.05	0.86	0.65	1.37
Na_2O	5.90	6.85	4.18	3.27	4.54	4.00	4.59	6.41	5.54	5.94	6.57	6.37	4.27
K_2O	7.65	6.56	8.75	5.40	8.36	6.22	7.81	7.32	5.85	5.28	5.96	6.07	6.95
P_2O_5	0.00	0.00	0.00	0.28	0.01	–	–	0.01	0.00	0.00	0.03	0.01	0.04
Total	98.82	98.91	99.24	99.99	99.99	99.98	100.00	94.36	101.37	100.26	99.27	96.92	97.67
Age	*137 ka*	*137 ka*	*137 ka*					*<154 ka*	*118.5 ka*	*118.5 ka*	*126 ka*	*130 ka*	*≥133 ka*
Ref.	(1)	(1)	(1)	(2)	(2)	(3)	(3)	(4)	(5)	(6)	(5)	(5)	(5)

Scientific Technical Report STR14/01, Deutsches GeoForschungsZentrum GFZ. http://doi.org/10.2312/GFZ.b103-14010

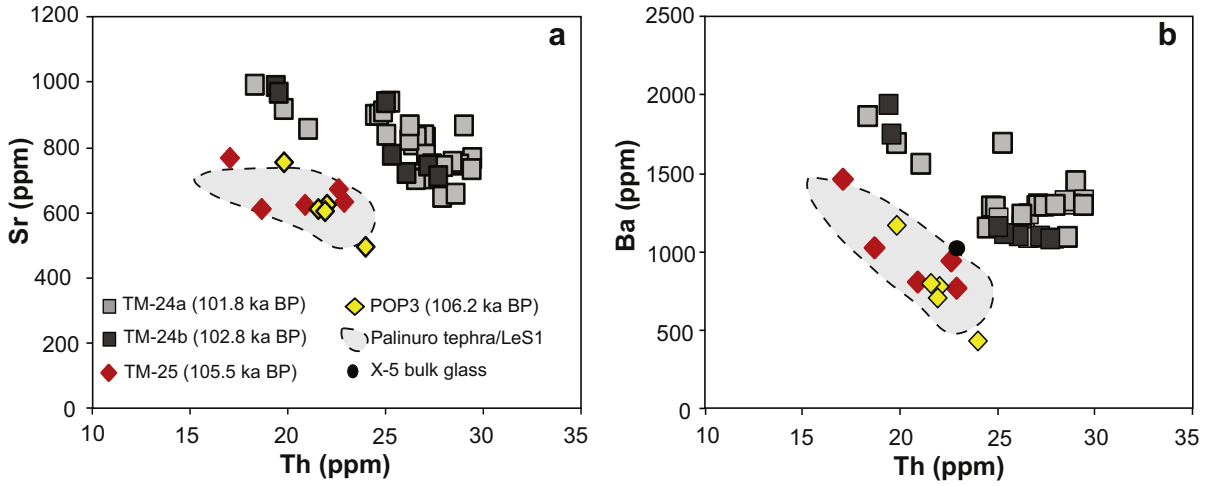

Fig. 5. Trace element plots of Monticchio tephras TM-24a, TM-24b and TM-25 vs. the X-5 tephra identified in terrestrial (POP3; Giaccio et al., 2012; Palinuro Tephra/LeS1; Albert, 2012) and marine settings (X-5 bulk glass; Wulf et al., 2004). Note the distinct composition of Monticchio tephras TM-24a and TM-24b in comparison to tephra TM-25, which closely matches the X-5 composition.

the X-6 tephra originates from the nearby Campanian volcanoes (Keller et al., 1978; Keller and Kraml, 2004; Marciano et al., 2008; Giaccio et al., 2012). However, the exact Campanian source volcano of X-6 remains unknown.

The TM-27/X-6 tephra in the Monticchio sequence is preceded by two thin and fine-grained layers, TM-28a and TM-28b, which are chemically almost identical to TM-27. These tephras are approximately 2000 and 2500 calendar years older and probably derive from the same unknown Campanian volcanic source as X-6.

6.1.4. TM-29, TM-30 and TM-31 (TAU-1b)

Based on the highly variable chemical composition (50–62 wt% SiO_2), lithology and time of deposition between ca 111.5 ± 5.6 and 114.8 ± 5.7 ka BP, tephra successions TM-29 and TM-30 and tephra layer TM-31 can be correlated with the TAU1-b pumice fallout deposit occurring in medial-distal outcrops in the Campanian Plain that was tentatively attributed to an unknown Phlegrean Field eruption (Di Vito et al., 2008). The TAU1-b pyroclastic unit consists of a well-sorted lapilli deposit made up of both light- and dark-coloured pumices that show a widely variable composition from latitic to trachytic, similar to those of TM-29, TM-30 and TM-31 (Fig. 4c). The TAU1-b deposit is indirectly dated between the MIS 5e high stand (125 ka BP) and the Campanian Ignimbrite (ca 39 ka BP) and was miscorrelated with the considerably younger TM-24b tephra (102.8 ka BP, previously X-5 tephra; Wulf et al., 2004) in the Monticchio record (Di Vito et al., 2008). The TAU-1b/TM-24b/X-5 correlation was mainly based on trace element data (Di Vito et al., 2008), though major element composition and lithological features of TAU1-b do not match the more evolved and homogeneous glass chemistry of the light vitric ash TM-24b.

A similar miscorrelation is proposed for the distal OT0701-7 tephra in Lake Ohrid core Co1201 (Balkans; Fig. 1a). Sulpizio et al. (2010) interpreted this tephra as a correlative of tephra OT0702-8 in a different Ohrid core (Co1202), that is underlain by the marine X-6 tephra and that matches the homogeneous trachytic composition of the marine X-5 tephra rather than that of the TAU1-b pumices. However, the heterogeneous latitic to phonolitic composition of tephra OT0701-7 is in strong agreement with the composition of Monticchio tephras TM-29 and TM-30, which we here relate to the TAU1-b eruption (Fig. 4c).

Although TAU1-b has not been detected in the marine environment, a single glass component occurring in a mixed tephra layer in 1254 cm sediment depth in Tyrrhenian Sea core DED 87-08 resembles the composition of Monticchio tephra layer TM-29-1g (Table 3, Fig. 4c). The age of this marine tephra at 115.2 ka BP is well within the time frame of the eruption of tephras TM-29/TM-30/TM-31; however, a detailed correlation requires more analytical data.

6.1.5. TM-32 (Stromboli)

The trachyandesitic glass composition of tephra TM-32 (ca 115.3 ± 5.8 ka BP) resembles the glass data of the 75.3 ka BP Petrazza Pyroclastic Series of Stromboli (Aeolian Islands; Gillot and Keller, 1993; Hornig-Kjarsgaard et al., 1993) and the distal tephra equivalent TM-21/Y-9 (Wulf et al., 2004), though it is characterised by higher FeO_{total} and K_2O and lower SiO_2 concentrations (Fig. 4d). However, Stromboli pyroclastic activity in the considered time period has not yet been identified (Gillot and Keller, 1993; Hornig-Kjarsgaard et al., 1993), thus leaving a precise correlation of TM-32 unresolved.

6.1.6. TM-33 (Punta Imperatore Formation, Ischia)

The chemical composition of most tephras of unit TM-33 (ca 115.7 ± 5.8–118.2 ± 5.9 ka BP) strongly resembles that of Ischia pyroclastics (Fig. 4e). During the considered time period 100–133 ka, three phonolitic pyroclastic fall deposits – the Punta Imperatore, the Upper and Lower Scarrupata di Barano Formations – are recognized in proximal sites from Ischia Island (Vezzoli, 1988; Brown et al., 2008). These explosive phases are accompanied by lava dome and flow activities of the Monte di Vezzi/Castello d'Ischia, Rione Bocca and Monte Cotto/La Guardiola volcanic centres (Vezzoli, 1988). A wide and overlapping range of ages is given for most of the Ischia volcanic units mainly due to the use of different dating material such as whole rock material, groundmass and sanidine crystals (Gillot et al., 1982; Vezzoli, 1988; Poli et al., 1989). However, the only consistent age constraint is provided for the Punta Imperatore Formation (116 ± 2.6 ka BP to 123 ± 2.7 ka BP; K/Ar dates of groundmass and sanidine; Gillot et al., 1982). This timing in combination with geochemical evidence (Fig. 4e) provides a reliable proximal correlative from Ischia for tephra succession TM-33.

In distal marine archives, several tephra layers are recognised during the considered time period showing a glass composition typical for Ischia products. Here, tephra C-35 (ca 121.5 ka BP) in the Ionian Sea core KET 82-22 (485 cm; Paterne et al., 2008) as well as tephra C-34 (ca 116.1 ka BP) and an overlying mixed layer (ca

115.2 ka BP) in 1260 cm and 1254 cm sediment depth in Tyrrhenian Sea core DED 87-08 (this study) provide the nearest compositional correlative of the Monticchio tephra unit TM-33 (Table 3, Fig. 4e).

6.1.7. TM-34 (Salina)

Comparison with published major element data of pyroclastics and lava products strongly suggests that the calcalkaline tephra TM-34 (ca 118.8 ± 5.9 ka BP) derives from the Aeolian Islands (Fig. 4f). Explosive volcanism during the considered time interval is recognized on the Islands of Salina and Lipari. On Lipari, on the one hand, the Monte San Angelo center was explosively active between 127 ± 8 ka BP and 92 ± 10 ka BP (Esperança et al., 1992), and erupted pyroclastics of the related cycles III and IV of Lipari are chemically (bulk samples) similar to TM-34 (Fig. 4f). On the other hand, the Fossa delle Felci stratovolcanic center on Salina produced several sub-Plinian to strombolian fallout deposits within two distinct eruptive sequences of older basaltic (127 ± 5 ka BP, K/Ar; Gillot, 1987; Gertisser and Keller, 2000) and younger andesitic to dacitic volcanics (Keller, 1980; Gertisser and Keller, 2000). The latter comprise pyroclastics of the stages 5–8 showing a bulk composition that best resembles the glass composition of tephra TM-34. Volcanism of the Fossa delle Felci is supposed to have lasted no longer than a few ten thousand years (Gertisser and Keller, 2000) and therefore the age of its younger products (<127 ka BP) is well in the time frame of the deposition of TM-34 in Monticchio. However, the best chemical match of glass data is given by a secondary glass component of a coarse-grained turbidite found in Marsili Basin core TIR2000-398 cm from the Tyrrhenian Sea (Fig. 4f) (Albert et al., 2012). These components are tentatively interpreted to represent older, so far undated activity of Salina that was incorporated during a younger collapse of the island. In summary, a reliable correlation of tephra TM-34 with a dated proximal counterpart is not possible at this moment, but the source can most likely be narrowed down to Salina Island.

6.1.8. TM-35a (Campanian)

The trachytic tephra TM-35a (ca 120.7 ± 6 ka BP) can be most likely associated with compositionally similar pyroclastic units recognised in the Neapolitan area, dated between 125 ka and 39 ka BP (e.g., Pappalardo et al., 1999; Di Vito et al., 2008). Based on field evidence, these units were tentatively attributed to early unknown explosive activities localised in the Phlegrean Fields area (Di Vito et al., 2008).

Furthermore, the glass composition of TM-35a approximates that of the distal marine tephra layer C-36 (ca 123.2 ka BP) occurring in Tyrrhenian Sea core KET 80-04 (Paterne et al., 2008) and supporting a Campanian provenance (Fig. 4a, Table 3).

6.1.9. TM-36 (Valle dei Preti unit, Sabatini Volcanic District)

The phonolitic composition of tephra TM-36 (ca 123 ± 6.2 ka BP) suggests an origin from the Sabatini Volcanic District (SVD; Roman area) (Fig. 4g). The last activities of the SVD produced a cluster of predominantly hydromagmatic and subordinate magmatic eruptions of similar phonolitic composition (Sottili et al., 2010, 2012). A good geochemical match for TM-36 is given, for instance, by the Upper Stracciacappa unit (Fig. 4g), though this unit is significantly younger (97 ± 4 ka BP; Sottili et al., 2012) than the varve age obtained for tephra TM-36. The Baccano Lower Unit (131 ± 2 ka BP; Sottili et al., 2012), described as a leucite/analcime bearing white pumice fall deposit, was produced by an eruption more temporally comparable with TM-36, however, this proximal unit has not yet been geochemically characterised. The closest chemical and chronological matches are given by the pyroclastics of the Valle dei Preti unit (VdP; Sottili et al., 2012) (Fig. 4g). The VdP unit was formerly dated at >296 ± 3 ka BP (Sottili et al., 2012). However, new stratigraphical data indicate a much younger formation age that is closer to the considered time frame of the deposition of tephra TM-36 (i.e., younger than the Cornacchia Lava dated at 154 ± 7 ka BP; Nappi and Mattioli, 2003). A detailed correlation requires more analytical data of proximal pyroclasts, which is currently in progress.

Equivalents of the tephra TM-36 are not yet identified distally. Marine core DED 87-08 (Tyrrhenian Sea), at a sediment depth of 1254 cm, presents a mix of volcanic glass showing different compositions. Within this mixed marine tephra deposit a phonolitic component is identified that is comparable with TM-36 glasses (Table 3, Fig. 4g). However, this marine tephra layer is dated at 115.2 ka BP and therefore considerably younger than TM-36.

6.1.10. TM-37 (Ischia)

The trachytic composition of tephra layers within unit TM-37 (ca 124.1 ± 6.2–124.9 ± 6.2 ka BP) is typical of Ischia products (Fig. 4e). However, during this time interval volcanic activity on Ischia is thought to be restricted to the formation of lava domes and minor lava flows from the Castello d'Ischia and Monte di Vezzi volcanic centres (126 ± 4 ka BP; K/Ar on whole rock; Gillot et al., 1982). It is speculative whether these activities were accompanied by the eruption of larger amounts of tephra material, and thus a specific correlation of tephra unit TM-37 with proximal pyroclastic deposits of Ischia remains open.

6.1.11. TM-38 and TM-39 (Campanian area)

The high-K phonolitic glass composition of tephras TM-38 (ca 125.6 ± 6.3 ka BP) and TM-39 (ca 130.5 ± 6.5 ka BP) is similar to pyroclastics of Campanian provenance (Di Vito et al., 2008), but a detailed correlation with proximal and distal tephra deposits is not possible at this time.

6.1.12. TM-40 (Ischia)

The heterogeneous trachytic composition of tephra TM-40 (ca 130.9 ± 6.5 ka BP) suggests an origin from Ischia Island. In particular, the Upper Scarrupata di Barano Formation (USB), dated at 128.7 ± 3.1 ka BP and 132.7 ka ± 3.2 ka BP (K/Ar whole rock data of lava; Vezzoli, 1988), is consistent with the considered time period. However, the USB is poorly characterised with limited geochemical data available for this deposit, indeed only a single whole rock pumice analysis is available in the literature (Poli et al., 1987). This composition does not reflect the heterogeneous composition of the TM-40 tephra (Fig. 4e) and therefore leaves a reliable correlation with the USB open until further geochemical investigations of the proximal USB pyroclastics are conducted.

6.1.13. TM-41 (Campanian area)

Tephra TM-41 (ca 131 ± 6.6 ka BP) reveals a Campanian provenance based on its heterogeneous K-trachytic glass composition. However, a precise correlation with a proximal or distal tephra equivalent is not possible at this time.

6.1.14. TM-42 (Ischia)

In respect to the oldest tephra in the Monticchio record, TM-42 (ca 132.1 ± 6.6 ka BP), geochemical similarities are identified with the Lower Scarrupata di Barano Formation (LSB) of Ischia (Fig. 4e) based on bulk rock data of pumices. However, the dating of the LSB appears problematic. The only time constraints derive from K/Ar dates of the overlying Monte Cotto and La Guardiola lavas that propose minimum ages of the LSB between 123 ± 3.4 ka BP (Sanidine) and 147 ± 3 ka BP (groundmass) (Vezzoli, 1988). The consequence of a wide proximal age range and the lack of comparable EPMA glass data is that the correlation of tephra TM-42 with the proximal LSB deposits on Ischia Island remains ambiguous.

6.2. Revising tephrochronology

The revision of the varve and sedimentation rate chronology of the Monticchio sediments (Brauer et al., 2007) lead to changes of the timing of tephras deposited prior to the TM-13/Pomici di Base eruption (19,280 calendar years BP; Wulf et al., 2004). As a result, tephra ages became systematically older, i.e. the TM-15/Y-3 tephra now dates at 27,260 ± 1360 calendar years BP instead of 23,930 calendar years BP (Wulf et al., 2004), whereas the timing of the TM-18/Campanian Ignimbrite tephra layer is corrected to a varve age of 36,770 ± 1840 calendar years BP compared to 39.3 ka Ar/Ar. A complete list of revised ages of main tephra markers defined in Wulf et al. (2004) is provided in Table 4. Those dates in addition to three new tephra varve dates resulting from the extended Monticchio 100–133 ka BP section are used to re-built a tephrochronological framework, which is then compared with updated radiometric and radioisotopic ages of correlated counterparts obtained from other proximal and distal records elsewhere (weighted mean ages with 2σ error range; Fig. 6, Table 4). The juxtaposition of both chronologies generally shows a good agreement, though in some sections large and variable uncertainties are noticeable:

- *Section 1* (0–1.15 m composite depth): sediments of the topmost 50 cm are homogenous and the laminations are not well preserved. The varve age of 90 ± 5 calendar years of tephra TM-1/AD 1631 in 6 cm depth is estimated to be too young, either indicating missing sediments or an underestimation of varves in the top section. In turn, sediments in the lower section are laminated (organic varves). Here, the calendar ages of tephras TM-2a/AD 512 and TM-2b/AD 472 Pollena agree well with a 5% uncertainty with the historically documented ages of tephra events. However, this relatively good fit indicates an overestimation of varves between the TM-1 and TM-2a tephras.
- *Section 2* (1.15–10.15 m composite depth): approximately 90% of the Monticchio sediments in this section between 1500 and 18,000 calendar years BP are annually laminated (organic varves). The varve age of the TM-4/Avellino tephra of 4310 ± 220 calendar years BP in the upper part is within the 2σ error range of radiocarbon ages obtained in proximal and distal deposits (Table 3), but shows an older age with a difference of 7% compared to the weighted mean radiometric age of correlated equivalents. Varve ages of the directly overlying tephras TM-3b/AP3 (4020 ± 200 calendar years BP) and TM-3c/AP2 (4150 ± 210 calendar years BP), in turn, are significant older than the respective ^{14}C ages of proximal correlatives (41% and 18% uncertainty). However, based on the good preservation of varves in the section between ca 3500 and 4500 calendar years BP large varve counting errors and/or a hiatus can be excluded which instead suggests an overestimation of varves in the younger sediment section (1500–3500 calendar years BP). Monticchio varve ages of the TM-4/Avellino underlying tephras TM-5a/Agnano Mt. Spina, TM-7/Pomici Principali, TM-8/Neapolitan Yellow Tuff, TM-9/GM1 and TM-10d/Lagno

Table 4
Revised tephrochronology of Lago Grande di Monticchio for the last 133 ka. V = Vesuvius; PF = Phlegrean Fields; E = Etna; PV = Procida-Vivara; A = Alban Hills; IS = Ischia; STR = Stromboli; PA = Pantelleria; CP = Campanian Volcanic Province; RP = Roman Province. Conventional and AMS radiocarbon dating were calibrated using CALIB 6.0.1 with the IntCal09 or Marine09 calibration curves (Stuiver and Reimer, 1993; Reimer et al., 2009). Dates of correlatives were chosen on the basis of dating precision and reliability of tephra correlation (dates of distal tephras). References for dates of correlatives are: (1) Rolandi et al. (1993), (2) Rolandi et al. (1998), (3) Vogel et al. (1990), (4) Santacroce et al. (2008), (5) Andronico et al. (1995), (6) Zanchetta et al. (2011), (7) Passariello et al. (2009), (8) Sevink et al. (2011), (9) Marzocchella et al. (1994), (10) de Vita et al. (1999), (11) Siani et al. (2004), (12) Di Vito et al. (1999), (13) Deino et al. (2004), (14) Pappalardo et al. (1999), (15) Andronico (1997), (16) Delibrias et al. (1986), (17) Kraml (1997), (18) Siani et al. (2001), (19) Bertagnini et al. (1998), (20) Alessio et al. (1976), (21) Sulpizio et al. (2003), (22) Buccheri et al. (2002a), (23) Buccheri et al. (2002b), (24) Paterne et al. (1999) in Giaccio et al. (2008), (25) Giaccio et al. (2009), (26) Freda et al. (2006), (27) De Vivo et al. (2001), (28) Gillot et al. (1982), (29) Gillot and Keller (1993), (30) Civetta et al. (1984), (31) Giaccio et al. (2012), (32) Keller and Kraml (2004).

Monticchio tephra	Tephra event (Source)	Monticchio varve age ± 5% uncertainty (calendar a BP)	Weighted mean age of tephra correlative (cal a BP)	2σ error range of ages of correlatives (cal a BP)	Tephra dating method (and total number of dates) of correlatives	Reference (dating of correlative)
TM-1	AD 1631 (V)	90 ± 5	369	369	Historical record	1
TM-2a	AD 512 (V)	1420 ± 70	1488	1488	Historical record	2
TM-2b	Pollena AD472 (V)	1440 ± 70	1528	1528	Historical record	2
TM-3b	AP3 (V)	4020 ± 200	2850	2740–2950	^{14}C (1)	2
TM-3c	AP2 (V)	4150 ± 210	3520	3420–3770	^{14}C (3)	2, 3, 4
TM-4	Pomici di Avellino (V)	4310 ± 220	4000	3530–4830	^{14}C (20)	2, 3, 4, 5, 6, 7, 8, 9
TM-5a	Agnano Mt. Spina (PF)	4620 ± 230	4740	4580–4880	^{14}C (1)	10
TM-6b	Pomici di Mercato (V)	9680 ± 480	8910	8710–9070	^{14}C (2)	4, 5
TM-7b	Pomici Principali (PF)	12,180 ± 610	12,030	11,290–12,440	^{14}C (2)	11, 12
TM-8	NYT (PF)	14,120 ± 710	13,860	13,480–15,700	^{40}Ar/^{39}Ar (1), ^{14}C (1)	11, 13
TM-9	VM1/GM1 (PF)	14,560 ± 730	14,400	13,400–15,800	^{40}Ar/^{39}Ar (1), ^{14}C (2)	11, 14
TM-10d	Lagno Amendolare (PF)	15,550 ± 780	15,830	15,230–16,500	^{14}C (1)	15
TM-11	Biancavilla/Y-1 (E)	16,440 ± 820	17,400	16,860–17,960	^{14}C (3)	11, 16, 17
TM-12	Pomici Verdoline (V)	17,560 ± 880	19,070	18,570–20,380	^{14}C (5)	4, 5, 11, 18
TM-13	Pomici di Base (V)	19,280 ± 960	22,040	21,340–23,980	^{14}C (5)	4, 5, 11, 19
TM-14	Solchiaro (PV)	21,260 ± 1060	23,350	22,570–24,130	^{14}C (1)	20
TM-15	Y-3 (PF?)	[a]27,260 ± 1360	30,650	30,230–31,180	^{14}C (3)	21, 22, 23
TM-16b	Codola (V/PF?)	31,120 ± 1560	34,270	32,530–36,010	^{14}C (1)	24
TM-17bc	Albano Unit 7 (A)	31,830 ± 1590	35,880	29,000–40,000	^{40}Ar/^{39}Ar (3)	25, 26
TM-18	CI/Y-5 (PF)	[a]36,770 ± 1840	39,290	38,900–39,700	^{40}Ar/^{39}Ar (2)	21, 27
TM-19	TVEss (IS)	[a]60,060 ± 3000	54,910	46,300–61,700	^{40}Ar/^{39}Ar (1), K/Ar (5)	17, 28
TM-20	UMSA (IS)	61,370 ± 3070	56,000	48,000–64,000	^{40}Ar/^{39}Ar (1)	17
TM-21	Petrazza/Y-9 (STR)	78,340 ± 3920	75,300	69,300–81,300	K/Ar (1)	29
TM-22	Ignimbrite Z/P-10 (PA)	89,130 ± 4460	82,910[b]	72,000–95,000	K/Ar (2)	30
TM-23-11	POP1/C-22 (CP or RP)	95,180 ± 4760	92,400	87,800–97,000	^{40}Ar/^{39}Ar (1)	31
TM-25	X-5/C-27 (CP)	105,480 ± 5270	106,090	101,000–109,000	^{40}Ar/^{39}Ar (2)	17, 31
TM-27	X-6/C-31 (CP)	108,330 ± 5420	109,000	105,000–113,000	Sapropel (1)	17, 32
TM-33-2b	Punta Imperatore (IS)	118,210 ± 5910	118,510	110,800–128,400	K/Ar (4)	28

[a] Additional ^{40}Ar/^{39}Ar dates were obtained on these samples (Watts et al., 1996; Wulf et al., 2004).
[b] Oxygen isotope dating of marine tephra equivalent P-10 reveals an age of ca 84 ka (Paterne et al., 1990).

Amendolare (4620 ± 230–15,550 ± 780 calendar years BP) are in good agreement with ^{14}C and $^{39}Ar/^{40}Ar$ ages of correlatives with a mean uncertainty of less than 2%. The TM-6b/Mercato tephra (9680 ± 480 calendar years BP) is the only outlier, showing an older varve age in respect to the radiometric dating (9% uncertainty). In the lowermost section (9.5–10.15 m), the ages of the TM-11/Biancavilla tephra (16,440 ± 820 calendar years BP) and the TM-12/Verdoline tephra (17,560 ± 880 calendar years BP) appear to be too young, and a systematic increase of deviation up to 8% (ca 1500 years) between varve and radiometric ages of tephras is notable. This difference is most likely based on an underestimation of varves in this section of poor varve preservation.

- *Section 3* (10.15–18.00 m composite depth): below the TM-12/Verdoline tephra, the annual lamination of the organic-clastic sediments is poorly preserved and therefore likely lead to an underestimation of varves. Age uncertainties increase to an average of 11% which corresponds to ca 2800 years for the TM-13/Pomici di Base tephra (19,280 ± 960 calendar years BP) and up to ca 4000 years for the TM-17bc/Albano unit 7 tephra (31,830 ± 1590 calendar years BP). Marker tephras TM-14/Solchiaro, TM-15/Y-3 and TM-16b/Codola are re-dated to 21,260 ± 1060, 27,260 ± 1360 and 31,120 ± 1560 calendar years BP, respectively.
- *Section 4* (18.00–27.00 m composite depth): the annual lamination of the minerogenic–calcareous sediments is exceptionally well preserved in the new cores LGM-M and LGM-O between tephras TM-17bc/Albano unit 7 and TM-18/Campanian Ignimbrite, and therefore has been re-counted (Funk, 2004). As a result, the new varve age of 36,770 ± 1840 calendar years BP for the TM-18/Campanian Ignimbrite tephra is now well within the 2σ error range of two $^{40}Ar/^{39}Ar$ dates of proximal and distal correlatives and shows an uncertainty of ca 6% in respect to the weighted mean age (Table 4).
- *Section 5* (27.00–60.00 m composite depth): the section between 37,000 and 90,000 calendar years BP (MIS 3 to 5b) exhibits organic-minerogenic sediments that are poorly laminated with an exception between 50 and 58 m sediment depth (76,000–88,000 calendar years BP, MIS 5a). Major tephra markers occur in the lower part between 40 and 60 m and

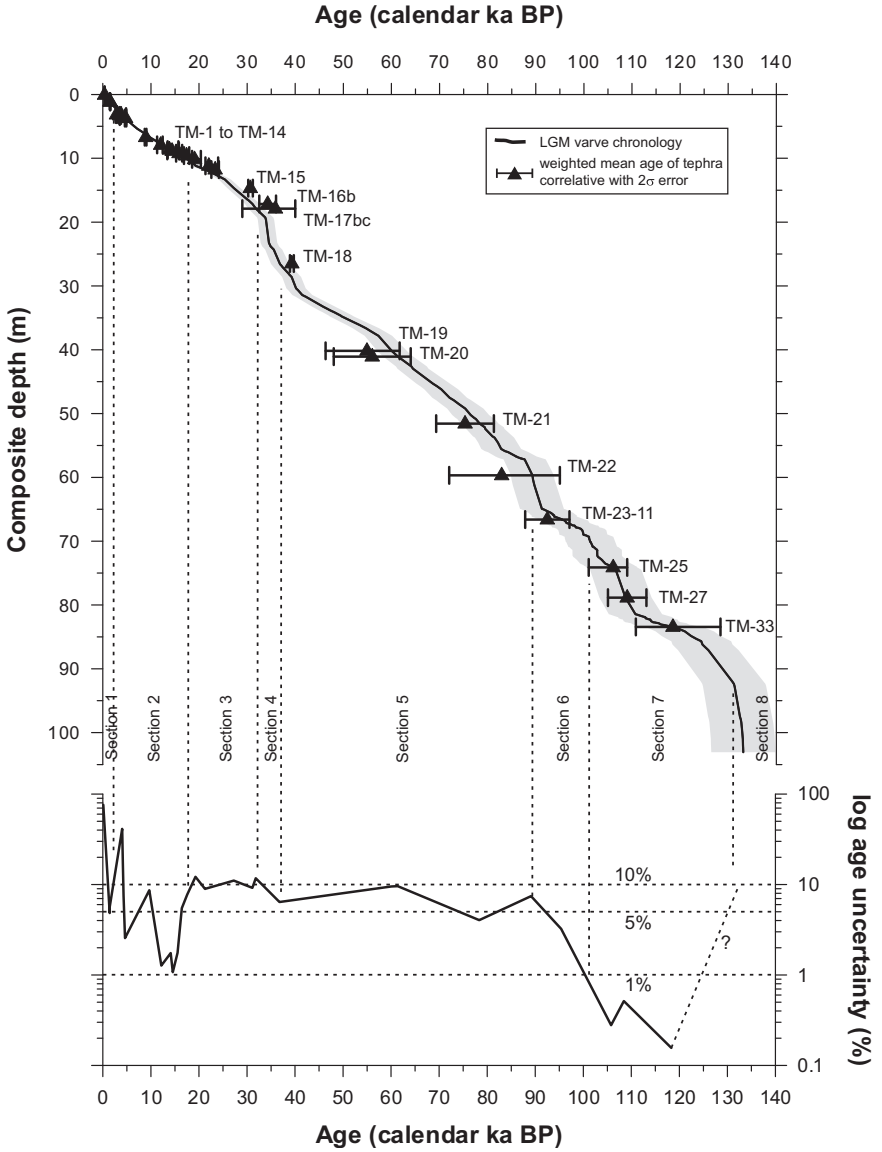

Fig. 6. Synthesis of revised tephrochronology and varve-supported sedimentation rate chronology including 5% age uncertainty (grey area) of the 133 ka Monticchio sequence (upper diagram) and 2σ age uncertainties calculated by the discrepancy between mean radiometric/radioisotopic and Monticchio varve ages of tephras (lower diagram).

include TM-19/Tufo Verde Epomeo *sensu stricto* (TVE*ss*), TM-20/Unitá di Monte San Angelo (UMSA), TM-21/Petrazza and TM-22/Ignimbrite Z. The two Ischia tephra layers TM/19/TVE*ss* and TM-20/UMSA are re-dated in the Monticchio sediments from previously 56,250 and 57,570 calendar years BP to 60,060 ± 3000 and 61,370 ± 3070 calendar years BP, respectively. However, the new varve ages appear too old, though they are still within the 2σ error range of $^{39}Ar/^{40}Ar$ and K/Ar ages obtained on proximal and distal correlatives. This assumption is supported by the varve age of the preceding TM-21/Petrazza tephra (78,340 ± 3920 calendar years BP), which is ca 3000 years older than the K/Ar age of 75.3 ka BP (Gillot and Keller, 1993) of its proximal correlative. The varve age of tephra TM-22 (Ignimbrite Z of Pantelleria, marine tephra layer P-10) is corrected from previously 85,320 calendar years (Wulf et al., 2004) to 89,130 ± 4460 calendar years BP, and is now 5100–6200 years older than the mean age of two K/Ar dates of proximal pyroclastics and the marine oxygen isotope age of 84 ka of the P-10 equivalent in the Tyrrhenian Sea (Paterne et al., 1990). In total, the mean age uncertainty is approximately 8% indicating an overestimation of varve ages in this section.

- *Section 6* (60.00–70.20 m composite depth): the section between 90,000 and 101,000 calendar years BP (MIS 5b/5c) constitutes minerogenic–organic sediments that are more or less well laminated in the upper 70% of the succession. In the lower part, varve preservation is poor. Though a total of 81 tephra fallout layers occur in this section, only one tephra could be assigned to a dated correlative. The trachytic tephra TM-23-11 was recently matched with the terrestrial POP1 tephra occurring in the Popoli section, Sulmona Basin (Latium) and dated by $^{40}Ar/^{39}Ar$ at 92.4 ± 4.6 ka BP (Giaccio et al., 2012). Here, the Monticchio varve age of 95,180 ± 4760 calendar years BP is well within the 2σ error range, but ca 3000 years older than the mean radioisotopic age of its correlative, indicating an overestimation of varves with an age uncertainty of ca 3% in this section.
- *Section 7* (70.20–92.50 m composite depth): the newly studied section between 101,000 and 131,000 calendar years BP is well laminated, showing a variety of varve types of organic–minerogenic (MIS 5c), organic (MIS 5e) and calcareous–minerogenic (MIS 6) composition. Prominent tephra marker layers such as TM-25/X-5 and TM-27/X-6 occur in the upper part of this section providing valuable dating points at 105,480 ± 5270 and 108,330 ± 5420 calendar years BP. These are in very good agreement (0.3 and 0.5% uncertainty) with the dates obtained from the marine and terrestrial equivalents (Table 4). This implies an underestimation of varve ages in the poorly laminated section 6. In the lower part of section 7, the tentative correlation of the TM-33 succession (118,210 ± 5910 calendar years BP) with the Punta Imperatore Formation confirms the Monticchio chronology with an even lower uncertainty of ca 0.2%.
- *Section 8* (92.50–103.10 m composite depth): the basal part of the Monticchio record is characterised by the deposition of a large number of turbidites formed during the early phase of lake development. So far, no robust time control is given for the sediments older than 131,000 calendar years BP, though an underestimation of varves of at least 10% is possible (Brauer et al., 2007).

7. Conclusions

The Monticchio tephra record exhibits 345 visible tephra fallout layers that are distributed throughout the last 133 ka and dated by the revised varve and sedimentation rate chronology of Monticchio sediments (Brauer et al., 2007). This chronology is in reasonable concordance with 28 radiometric and radioisotopic dates of prominent tephra correlatives with a mean age uncertainty of 5% (Table 4). The detailed study of 52 tephras layers occurring between 100 and 133 ka BP allows defining sources in the southern and central Italian volcanic area and an assignment to 21 distinct eruptive units. To date, most of these ashes were not described in distal environments elsewhere, thus reliable assignments to single eruptive events were only possible on a limited basis. These exceptions are correlations with the prominent marine tephras X-5 (ca 105 ka BP) and X-6 (ca 108–110 ka BP) which are varve dated with an uncertainty of less than 1% (Brauer et al., 2007). Other less well constrained correlations are based either on age constraints or tentative geochemical matches. This brings up three main issues that need to be resolved by the tephra community in the future:

1. The description of tephra deposits, particularly in proximal sites, often lacks in EPMA glass data. These data are essential for reliably correlating distal findings and should thus be provided for all ash layers in any type of archive.
2. Detailed chronological constraints of tephras are well derived for major eruptive events like, for example, the Avellino (4 ka BP), Neapolitan Yellow Tuff (14 ka BP) and Campanian Ignimbrite (39 ka) eruptions, and are lacking for lower-magnitude events. To overcome this issue and to achieve a more comprehensive data set of Mediterranean explosive volcanism, efforts should be made to also date tephras from small-scale eruptions in sedimentary archives.
3. The similarity of major element glass composition of tephras from the same source volcanoes (i.e., Phlegrean Fields, Ischia) often prevents a reliable correlation with a specific event. This problem can be overcome by additional trace element analyses (e.g., Smith et al., 2011; Tomlinson et al., 2012) and $^{87}Sr/^{86}Sr$ isotopic measurements (e.g., Di Renzo et al., 2007; Giaccio et al., 2007; Roulleau et al., 2009).

These data build upon the existing Monticchio tephra data set and will contribute to an improved Late Quaternary tephrostratigraphy in the Mediterranean.

Acknowledgements

We thank D. Berger, M. Köhler, M. Prena, R. Scheuss, and D. Axel for the retrieval of sediment cores during the coring campaign in 2000. Special thanks are due to G. Arnold, M. Köhler and D. Berger for thin section preparation, O. Appelt and V. Smith for technical support, quantification and calibration during EPMA measurements, and A. Hendrich and M. Dziggel for graphical support. We also warmly thank the reviewers Christine Lane and Roberto Sulpizio for their detailed and constructive feedback. The coring campaign and tephra studies were funded by the GFZ German Research Centre for Geosciences, Potsdam, Germany. This study is a contribution to the Helmholtz-Association climate initiative REKLIM (Topic 8 'Rapid Climate Change from Proxy data'). ELT and PGA were funded by NERC RESET Consortium (NE/E015905/1).

Appendix A. Supplementary material

Supplementary material associated with this article can be found, in the online version, at http://dx.doi.org/10.1016/j.quascirev.2012.10.020.

References

Albert, P.G., 2012. Volcanic glass geochemistry of Italian proximal deposits linked to distal archives in the central Mediterranean region. Unpublished thesis, Royal Holloway University of London, 352 pp.

Albert, P.G., Tomlinson, E.L., Smith, V.C., Di Roberto, A., Todman, A., Rosi, M., Marani, M., Müller, W., Menzies, M.A., 2012. Marine-continental tephra correlations: volcanic glass geochemistry from the Marsili basin and the Aeolian Islands, Southern Tyrrhenian Sea, Italy. Journal of Volcanology and Geothermal Research 229–230, 74–94.

Alessio, M., Bella, F., Improta, S., Belluomini, G., Calderoni, G., Cortesi, C., Turi, B., 1976. University of Rome Carbon-14 dates XIV. Radiocarbon 18, 321–349.

Allen, J.R.M., Brandt, U., Brauer, A., Hubberten, H.-W., Huntley, B., Keller, J., Kraml, M., Mackensen, A., Mingram, J., Negendank, J.F.W., Nowaczyk, N.R., Oberhänsli, H., Watts, W.A., Wulf, S., Zolitschka, B., 1999. Rapid environmental changes in southern Europe during the last glacial period. Nature 400, 740–743.

Andronico, D., 1997. La Stratigrafia dei prodotti dell'eruzione di Lagno Amendolare (Campi Flegrei, Napoli). Atti Società Toscana di Scienze naturali Memorie, Serie A 104, 165–178.

Andronico, D., Calderoni, G., Cioni, R., Sbrana, A., Sulpizio, R., Santacroce, R., 1995. Geological map of Somma-Vesuvius Volcano. Periodico di Mineralogia 64, 77–78.

Bard, E., Arnold, M., Mangerud, J., Paterne, M., Labeyrie, L., Dupart, J., Melieres, M., Sonstegaard, E., Duplessy, J., 1994. The North-Atlantic atmosphere–sea surface ^{14}C gradient during the Younger Dryas climatic event. Earth and Planetary Science Letters 126, 275–287.

Beccaluva, L., Gabbianelli, G., Lucchini, F., Rossi, P.L., Savelli, C., 1985. Petrology and K/Ar ages of volcanics dredged from the Eolian seamounts: implications for geodynamic evolution of the southern Tyrrhenian basin. Earth and Planetary Science Letters 74, 187–208.

Bertagnini, A., Landi, P., Rosi, M., Vigliargio, A., 1998. The Pomici di Base plinian eruption of Somma-Vesuvius. Journal of Volcanology and Geothermal Research 83, 219–239.

Bourne, A.J., Lowe, J.J., Trincardi, F., Asioli, A., Blockley, S., Wulf, S., Matthews, I.P., Piva, A., Vigliotti, L., 2010. Distal tephra record for the last ca 105,000 years from core PRAD 1–2 in the central Adriatic Sea: implications fro marine tephrostratigraphy. Quaternary Science Reviews 29, 3079–3094.

Branca, S., Coltelli, M., De Beni, E., Wijbrans, J., 2008. Geological evolution of Mount Etna volcano (Italy) from earliest products until the first central volcanism (between 500 and 100 ka ago) inferred from geochronological and stratigraphic data. International Journal of Earth Science 97, 135–152.

Brandt, U., Nowaczyk, N.R., Ramrath, A., Brauer, A., Mingram, J., Wulf, S., Negendank, J.F.W., 1999. Palaeomagnetism of Holocene and Late Pleistocene sediments from Lago di Mezzano and Lago Grande di Monticchio (Italy): initial results. Quaternary Science Reviews 18, 961–976.

Brauer, A., Allen, J.R.M., Mingram, J., Dulski, P., Wulf, S., Huntley, B., 2007. Evidence for last interglacial chronology and environmental change from Southern Europe. Proceedings of the National Academy of Sciences 104, 450–455.

Brauer, A., Endres, C., Negendank, J.F.W., 1999. Lateglacial calendar year chronology based on annually laminated sediments from Lake Meefelder Maar, Germany. Quaternary International 61, 17–25.

Brauer, A., Mingram, J., Frank, U., Günter, C., Schettler, G., Wulf, S., Zolitschka, B., Negendank, J.F.W., 2000. Abrupt environmental oscillations during the Early Weichselian recorded at Lago Grande di Monticchio, southern Italy. Quaternary International 73/74, 79–90.

Brocchini, D., La Volpe, L., Laurenzi, M.A., Principe, C., 1994. Storia evolutiva del Monte Vulture. Plinius 12, 22–25.

Brown, R.J., Orsi, G., de Vita, S., 2008. New insights into Late Pleistocene explosive volcanic activity and caldera formation on Ischia (southern Italy). Bulletin of Volcanology 70, 583–603.

Buccheri, G., Bertoldo, G., Coppa, M.G., Munno, R., Pennetta, M., Siani, G., Valente, A., Secchione, C., 2002a. Studio multidisciplinare della successione sedimentaria tardo-quaternaria proveniente dalla scarpata continentale del Golfo di Policastro (Tirreno meridionale). Bollettino della Societa Geologica Italiana 121, 187–210.

Buccheri, G., Capretto, G., Di Donato, V., Esposito, P., Ferruzza, G., Pescatore, T., Russo Ermolli, E., Senatore, M.R., Sprovieri, M., Bertoldo, G., Carella, D., Madonia, G., 2002b. A high resolution record of the last deglaciation in the southern Tyrrhenian Sea: environmental and climatic evolution. Marine Geology 186, 447–470.

Calanchi, N., Dinelli, E., 2008. Tephrostratigraphy of the last 170 ka in sedimentary successions from the Adriatic Sea. Journal of Volcanology and Geothermal Research 177, 81–95.

Civetta, L., Cornette, Y., Crisci, G., Gillot, P.Y., Orsi, G., Requejo, C.S., 1984. Geology, geochronology and chemical evolution of the island of Pantelleria. Geological Magazine 121, 541–668.

Coltelli, M., Del Carlo, P., Vezzoli, L., 2000. Stratigraphic constraints for explosive activity in the past 100 ka at Etna Volcano, Italy. International Journal of Earth Sciences 89, 665–677.

Deino, A.L., Orsi, G., de Vita, S., Piochi, M., 2004. The age of the Neapolitan Yellow Tuff caldera-forming eruption (Campi Flegrei caldera – Italy) assessed by $^{40}Ar/^{39}Ar$ dating method. Journal of Volcanology and Geothermal Research 133, 157–170.

Delibrias, G., Guillier, M.-T., Labeyrie, J., 1986. Gif natural radiocarbon measurements X. Radiocarbon 28, 9–68.

de Vita, S., Orsi, G., Civetta, L., Carandente, A., D'Antonio, M., Deino, A., di Cesare, T., Di Vito, M.A., Fisher, R.V., Isaia, R., Marotta, E., Necco, A., Ort, M., Pappalardo, L., Piochi, M., Southon, J., 1999. The Agnano-Monte Spina eruption (4100 years BP) in the restless Campi Flegrei caldera (Italy). Journal of Volcanology and Geothermal Research 91, 269–301.

De Vivo, B., Rolandi, G., Gans, P.B., Calvert, A., Bohrson, W.A., Spera, F.J., Belkin, H.E., 2001. New constraints on the pyroclastic eruptive history of the Campanian volcanic plain (Italy). Mineralogy and Petrology 73, 47–65.

Di Renzo, V., Di Vito, M.A., Arienzo, I., Carandente, A., Civetta, L., D'Antonio, M., Giordano, F., Orsi, G., Tonarini, S., 2007. Magmatic history of Somma-Vesuvius on the basis of new geochemical and isotopic data from a deep borehole (Camaldoli della Torre). Journal of Petrology 48, 753–784.

Di Vito, M., Isaia, R., Orsi, G., Southon, J., di Vita, S., D'Antonio, M., Pappalardo, L., Piochi, M., 1999. Volcanism and deformation since 12,000 years at the Campi Flegrei caldera (Italy). Journal of Volcanology and Geothermal Research 91, 221–246.

Di Vito, M.A., Sulpizio, R., Zanchetta, G., D'Orazio, M., 2008. The late Pleistocene pyroclastic deposits of the Campanian Plain: new insights into the explosive activity of Neapolitan volcanoes. Journal of Volcanology and Geothermal Research 177, 19–48.

Esperança, S., Crisci, G.M., de Rosa, R., Mazzuoli, R., 1992. The role of the crust in the magmatic evolution of the island of Lipari (Aeolian Islands, Italy). Contributions to Mineralogy and Petrology 112, 450–462.

Freda, C., Gaeta, M., Karner, D.B., Marra, F., Renne, P.R., Taddeucci, J., Scarlato, P., Christensen, J.N., Dallai, L., 2006. Eruptive history and petrologic evolution of the Albano multiple maar (Alban Hills, Central Italy). Bulletin of Volcanology 68, 567–591.

Fuchs, C.W.C., 1873. Monografia geologica dell'isola d'Ischia, con carta geologica 1: 25.000. Mem. per serv. alla descrizione carta geologica d'Italia 2/1, 1.

Funk, S., 2004. Mikrofazielle Untersuchungen an Seesedimenten des Zeitfensters 37–25 ka vor heute aus dem Lago Grande di Monticchio, Italien, und deren paläoklimatische Bedeutung, Institute for Geosciences. University of Potsdam, Potsdam, p. 94.

Gertisser, R., Keller, J., 2000. From basalt to dacite: origin and evolution of the calc-alkaline series of Salina, Aeolian Arc, Italy. Contributions to Mineralogy and Petrology 139, 607–626.

Giaccio, B., Sposato, A., Gaeta, M., Marra, F., Palladino, D.M., Taddeucci, J., Barbieri, M., Messina, P., Rolfo, M.F., 2007. Mid-distal occurrences of the Albano Maar pyroclastic deposits and their relevance for reassessing the eruptive scenarios of the most recent activity at the Colli Albani Volcanic District, Central Italy. Quaternary International 171–172, 160–178.

Giaccio, B., Isaia, R., Fedele, F.G., Di Canzio, E., Hoffecker, J., Ronchitelli, A., Sinitsyn, A.A., Anikovich, M., Lisitsyn, S.N., Popov, V.V., 2008. The Campanian Ignimbrite and Codola tephra layers: two temporal/stratigraphic markers for the Early Upper Palaeolithic in southern Italy and eastern Europe. Journal of Volcanology and Geothermal Research 177, 208–226.

Giaccio, B., Marra, F., Hajdas, I., Karner, D.B., Renne, P.R., Sposato, A., 2009. $^{40}Ar/^{39}Ar$ and ^{14}C geochronology of the Albano maar deposits: implications for defining the age and eruptive style of the most recent explosive activity at Colli Albani Volcanic District, Central Italy. Journal of Volcanology and Geothermal Research 185, 203–213.

Giaccio, B., Nomade, S., Wulf, S., Isaia, R., Sottili, G., Cavuoto, G., Galli, P., Messina, P., Sposato, A., Sulpizio, R., Zanchetta, G., 2012. The late MIS 5 Mediterranean tephra markers: a reappraisal from peninsular Italy terrestrial records. Quaternary Science Reviews 56, 31–45.

Gillot, P.-Y., Keller, J., 1993. Radiochronological dating of Stromboli. Acta Vulcanologica 3, 69–77.

Gillot, P.Y., 1987. Histoire volcanique des iles éoliennes: arc insulaire ou complexe orogénique annulaire? IGAL, Paris, pp. 35–42.

Gillot, P.Y., Chiesa, S., Pasquare, G., Vezzoli, L., 1982. <33.000 yr K/Ar dating of the volcano-tectonic horst of the isle of Ischia, Gulf of Naples. Nature 299, 242–245.

Hajdas, I., Bonani, G., Zolitschka, B., Brauer, A., Negendank, J.F.W., 1998. ^{14}C ages of terrestrial macrofossils from Lago Grande di Monticchio (Italy). Radiocarbon 40, 803–807.

Hornig-Kjarsgaard, I., Keller, J., Koberski, U., Stadlbauer, E., Francalanci, L., Lenhart, R., 1993. Geology, stratigraphy and volcanological evolution of the island of Stromboli, Aeolian arc, Italy. Acta Vulcanologica 3, 21–68.

Hunt, J.B., Hill, P.G., 1996. An inter-laboratory comparison of the electron probe microanalysis of glass geochemistry. Quaternary International 34–36, 229–241.

Jéhanno, C., Boclet, D., Froget, L., Lambert, B., Robin, E.R., Rocchia, R., Turpin, L., 1992. The Cretaceous–Tertiary boundary at Beloc, Haiti: no evidence for an impact in the Caribbean Area. Earth and Planetary Science Letters 109, 229–241.

Jochum, K.P., Pfänder, J., Woodhead, J.D., Willbold, M., Stoll, B., Herwig, K., Amini, M., Abouchami, W., Hofmann, A.W., 2005. MPI-DING glasses: new geological reference materials for in situ Pb isotope analysis. Geochemistry, Geophysics, Geosystems 6. http://dx.doi.org/10.1029/2005GC000995.

Jochum, K.P., et al., 2006. MPI-DING reference glasses for in situ microanalysis: new reference values for element concentrations and isotope ratios. Geochemistry, Geophysics, Geosystems 7 (2).

Keller, J., 1980. The island of Salina. Rendiconti Società Italiana di Mineralogia e Petrologia 36, 489–524.

Keller, J., 2006. The Ionian Sea as tephrochronological archive for major paroxysms in Italian explosive volcanism of the Upper Quaternary. Workshop CNR-AIQUA Roma, 21–23 June 2006.

Keller, J., Kraml, M., 2004. Tephrochronological archives for known and unknown paroxysms in Italian explosive volcanism of the upper Quaternary. IAVCEI General Assembly, Nov. 2004, Pucón, Chile.
Keller, J., Ryan, W.B.F., Ninkovich, D., Altherr, R., 1978. Explosive volcanic activity in the Mediterranean over the past 200,000 yr as recorded in deep-sea sediments. Geological Society of America Bulletin 89, 591–604.
Keller, J., Kraml, M., Scheld, A., 1996. Late Quaternary tephrochronological correlation between deep-sea sediments and the land record in the Central Mediterranean. In: 30th International Geological Congress, Beijing, vol. 3, p. 204.
Kraml, M., 1997. Laser-^{40}Ar/^{39}Ar-Datierungen an distalen marinen Tephren des jung-quartären mediterranen Vulkanismus (Ionisches Meer, METEOR-Fahrt 25/4), Geowissenschaftliche Fakultät. Albert-Ludwigs-Universität Freiburg i.Br., Freiburg i. Br., p. 216.
Laurenzi, M.A., Villa, I.M., 1987. ^{40}Ar/^{39}Ar chronostratigraphy of Vico ignimbrites. Periodico di Mineralogia 56, 285–293.
Le Bas, M.J., Le Maitre, R.W., Streckeisen, A., Zanettin, B., 1986. A chemical classification of volcanic rocks based on the Total Alkali–Silica diagram. Journal of Petrology 27, 745–750.
Lowe, J.J., Blockley, S., Trincardi, F., Asioli, A., Cattaneo, A., Matthews, I.P., Pollard, M., Wulf, S., 2007. Age modelling of late Quaternary marine sequences in the Adriatic: towards improved precision and accuracy using volcanic event stratigraphy. Continental Shelf Research 27, 560–582.
Lucchi, F., Tranne, C.A., De Astis, G., Keller, J., Losito, R., Morche, W., 2008. Brown tuffs on the Aeolian Islands (southern Italy). Journal of Volcanology and Geothermal Research 177, 49–70.
Marciano, R., Munno, R., Petrosino, P., Santo, A.P., Villa, I., 2008. Late quaternary tephra layers along the Cilento coastline (southern Italy). Journal of Volcanology and Geothermal Research 177, 227–243.
Marra, F., Deocampo, D., Jackson, M.D., Ventura, G., 2011. The Alban Hills and Monti Sabatini volcanic products used in ancient Roman masonry (Italy): an integrated stratigraphic, archaeological, environmental and geochemical approach. Earth-Science Reviews 108, 115–136.
Marzocchella, A., Calderoni, G., Nisbet, R., 1994. Sarno e Frattaminore: evidenze dagli abitati. In: Livadie, A. (Ed.), L'eruzione vesuviana delle "Pomici di Avellino" e la facies di Palma Campania (Bronzo Antico). Edipuglia, Bari, pp. 157–202.
Morche, W., 1988. Tephrochronologie der Äolischen Inseln. Mineralogisch-Petrologisches Institut, Universität Freiburg/Br., p. 238.
Müller, W., Shelley, M., Miller, P., Broude, S., 2009. Initial performance metrics of a new custom-designed ArF excimer LA–ICPMS system coupled to a two-volume laser-ablation cell. Journal of Analytical Atomic Spectrometry 24, 209–214.
Munno, R., Petrosino, P., 2007. The late Quaternary tephrostratigraphical record of the San Gregorio Magno basin (southern Italy). Journal of Quaternary Science 22, 247–266.
Nappi, G., Mattioli, M., 2003. Evolution of the Sabatinian Volcanic District (central Italy) as inferred by stratigraphic successions of its northern sector and geochronological data. Periodico di Mineralogia 72, 79–102.
Narcisi, B., 1996. Tephrochronology of a late quaternary lacustrine record from the Monticchio Maar (Vulture Volcano, southern Italy). Quaternary Science Reviews 15, 155–165.
Newton, A.J., Dugmore, A.J., 1993. Tephrochronology of Core C from Lago Grande di Monticchio. In: Negendank, J.F.W., Zolitschka, B. (Eds.), Paleolimnology of European Maar Lakes. Springer-Verlag, Berlin, Heidelberg, pp. 333–348.
Nicotra, E., Ferlito, C., Viccaro, M., Cristofolini, R., 2011. Volcanic geology and petrology of the Val Calanna succession (Mt. Etna, Southern Italy): discovery of a new eruptive center. Periodico di Mineralogia 80, 287–307.
Pappalardo, L., Civetta, L., D'Antonio, M., Deino, A., Di Vito, M., Orsi, G., Carandente, A., de Vita, S., Isaia, R., Piochi, M., 1999. Chemical and Sr-isotopical evolution of the Phlegrean magmatic system before the Campanian Ignimbrite and the Neapolitan Yellow Tuff eruptions. Journal of Volcanology and Geothermal Research 91, 141–166.
Passariello, I., Livadie, C.A., Talamo, P., Lubritto, C., DÓnofrio, A., Terrasi, F., 2009. ^{14}C chronology of Avellino pumices eruption and timing of human reoccupation of the devastated region. Radiocarbon 51, 803–816.
Paterne, M., 1985. Reconstruction de l'activité explosive des volcans de l'Italie du Sud par tephrochronologie marine. Thèse Doctorat-Etat, Université Paris-Sud Orsay, 141 pp.
Paterne, M., Guichard, F., Labeyrie, J., Gillot, P.Y., Duplessy, J.C., 1986. Tyrrhenian Sea tephrochronology of the oxygen isotope record for the past 60,000 years. Marine Geology 72, 259–285.
Paterne, M., Guichard, F., Labeyrie, J., 1988. Explosive activity of the South Italian volcanoes during the past 80,000 yrs as determined by marine tephrochronology. Journal of Volcanology and Geothermal Research 34, 153–172.
Paterne, M., Labeyrie, J., Guichard, F., Mazaud, A., Maitre, F., 1990. Fluctuations of the Campanian explosive volcanic activity (South Italy) during the past 190,000 years, as determined by marine tephrochronology. Earth and Planetary Science Letters 98, 166–174.
Paterne, M., Kallel, N., Labeyrie, L., Vautravers, M., Duplessy, J.C., Rossignol-Strick, M., Cortijo, E., Arnold, M., Fontugne, M., 1999. Hydrological relationship between the North Atlantik Ocean and the Mediterranean Sea during the past 15–75 kyr. Paleoceanography 14, 626–638.
Paterne, M., Guichard, F., Duplessy, J.C., Siani, G., Sulpizio, R., Labeyrie, J., 2008. A 90,000–200,000 yrs marine tephra record of Italian volcanic activity in the Central Mediterranean Sea. Journal of Volcanology and Geothermal Research 177, 187–196.
Perini, G., Conticelli, S., Francalanci, L., 1997. Inferences on the volcanic history of the Vico volcano, Roman Magmatic Province, Central Italy: stratigraphic, petrographic and geochemical data. Mineralogica et Petrographica Acta 40, 67–93.
Perini, G., Francalanci, L., Davidson, J.P., Conticelli, S., 2004. Evolution and genesis of magmas from Vico Volcano, central Italy: multiple differentiation pathways and variable parental magmas. Journal of Petrology 45, 139–182.
Poli, S., Chiesa, S., Gillot, P.-Y., Gregnanin, A., Guichard, F., 1987. Chemistry versus time in the volcanic complex of Ischia (Gulf of Naples, Italy): evidence of successive magmatic cycles. Contributions to Mineralogy and Petrology 95, 322–335.
Poli, S., Chiesa, S., Gillot, P.-Y., Guichard, F., Vezzoli, L., 1989. Time dimension in the geochemical approach and hazard estimates of a volcanic area: the Isle of Ischia case (Italy). Journal of Volcanology and Geothermal Research 36, 327–335.
Radicati di Brozolo, F., Di Girolamo, P., Turi, B., Oddone, M., 1988. ^{40}Ar–^{39}Ar and K–Ar dating of K-rich rocks from the Roccamonfina Volcano, Roman Comagmatic Region, Italy. Geochimica et Cosmochimica Acta 52, 1435–1441.
Reimer, P.J., Baillie, M.G.L., Bard, E., Bayliss, A., Beck, J.W., Blackwell, P.G., Bronk Ramsey, C., Buck, C.E., Burr, G.S., Edwards, R.L., Friedrich, M., Grootes, P.M., Guilderson, T.P., Hajdas, I., Heaton, T.J., Hogg, A.G., Hughen, K.A., Kaiser, K.F., Kromer, B., McCormac, F.G., Manning, S.W., Reimer, R.W., Richards, D.A., Southon, J.R., Talamo, S., Turney, C.S.M., van der Plicht, J., Weyhenmeyer, C.E., 2009. IntCal09 and Marine09 radiocarbon age calibration curves, 0–50,000 years cal BP. Radiocarbon 51, 1111–1150.
Rolandi, G., Barrella, A.M., Borrelli, A., 1993. The 1631 eruption of Vesuvius. Journal of Volcanology and Geothermal Research 58, 183–201.
Rolandi, G., Petrosino, P., McGeehin, J., 1998. The interplinian activity at Somma-Vesuvius in the last 3500 years. Journal of Volcanology and Geothermal Research 82, 19–52.
Romano, R., 1982. Succession of the volcanic activity in the Etnean area. Memorie della Società Geologica Italiana 23, 27–48.
Roulleau, E., Pinti, D.L., Rouchon, V., Quidelleur, X., Gillot, P.-Y., 2009. Tephrochronostratigraphy of the lacustrine interglacial record of Pianico, Italian Southern Alps: identifying the volcanic sources using radiogenic isotopes and trace elements. Quaternary International 204, 31–43.
Santacroce, R., Cioni, R., Marianelli, P., Sbrana, A., Sulpizio, R., Zanchetta, G., Donahue, D.J., Joron, J.L., 2008. Age and whole rock–glass compositions of proximal pyroclastics from the major explosive eruptions of Somma-Vesuvius: a review as a tool for distal tephrostratigraphy. Journal of Volcanology and Geothermal Research 177, 1–18.
Scandone, R., Bellucci, F., Lirer, L., Rolandi, G., 1991. The structure of the Campanian Plain and the activity of the Neapolitan volcanoes (Italy). Journal of Volcanology and Geothermal Research 48, 1–31.
Scheld, A., 1995. Tephralagen in "METEOR-Kernen" des Ionischen Meeres. Universität Freiburg i.Br., p. 83.
Sevink, J., van Bergen, M.J., van der Pflicht, J., Feiken, H., Anastasia, C., Huizinga, A., 2011. Robust date for the Bronze Age Avellino eruption (Somma-Vesuvius): 3945 +/− 10 calBP (1995 +/− 10 cal BC). Quaternary Science Reviews 30, 1035–1046.
Siani, G., Paterne, M., Michel, E., Sulpizio, R., Sbrana, A., Arnold, M., Haddad, G., 2001. Mediterranean Sea surface radiocarbon reservoir age changes since the last glacial maximum. Science 294, 1917–1920.
Siani, G., Sulpizio, R., Paterne, M., Sbrana, A., 2004. Tephrostratigraphy study for the last 18,000 ^{14}C years in a deep-sea sediment sequence for the South Adriatic. Quaternary Science Reviews 23, 2485–2500.
Smith, V.C., Isaia, R., Pearce, N.J.G., 2011. Tephrostratigraphy and glass compositions of post-15 kyr Campi Flegrei eruptions: implications for eruption history and chronostratigraphic markers. Quaternary Science Reviews 30, 3638–3660.
Sollevanti, F., 1983. Geologic, volcanologic, and tectonic setting of the Vico-Cimino area, Italy. Journal of Volcanology and Geothermal Research 17, 203–217.
Sottili, G., Palladino, D.M., Marra, F., Jicha, B., Karner, D.B., Renne, P., 2010. Geochronology of the most recent activity in the Sabatini Volcanic District, Roman Province, central Italy. Journal of Volcanology and Geothermal Research 196, 20–30.
Sottili, G., Palladino, D.M., Gaeta, M., Masotta, M., 2012. Origins and energetics of maar volcanoes: examples from the ultrapotassic Sabatini Volcanic District (Roman Province, Central Italy). Bulletin of Volcanology 74, 163–186.
Stoppa, F., Principe, C., 1998. Eruption style and petrology of a new carbonatitic suite from the Mt. Vulture (Southern Italy): the Monticchio Lakes Formation. Journal of Volcanology and Geothermal Research 80, 137–153.
Stuiver, M., Reimer, P.J., 1993. Extended ^{14}C data base and revised calib 3.0 ^{14}C age calibration program. Radiocarbon 35, 215–230.
Sulpizio, R., Zanchetta, G., Paterne, M., Siani, G., 2003. A review of tephrostratigraphy in central and southern Italy during the last 65 ka. Il Quaternario 16, 91–108.
Sulpizio, R., Zanchetta, G., D'Orazio, M.D., Vogel, H., Wagner, B., 2010. Tephrostratigraphy and tephrochronology of lakes Ohrid and Prespa, Balkans. Biogeosciences Discussions 7, 3931–3967.
Tomlinson, E.L., Thordarson, T., Müller, W., Thirlwall, M., Menzies, M.A., 2010. Micro analysis of tephra by LA–ICP–MS – strategies, advantages and limitations assessed using the Thorsmork ignimbrite (Southern Iceland). Chemical Geology 279, 73–89.
Tomlinson, E.L., Arienzo, I., Civetta, L., Wulf, S., Smith, V.C., Hardiman, M., Lane, C.S., Carandente, A., Orsi, G., Rosi, M., Müller, W., Thirlwall, M.F., Menzies, M.A., 2012. Geochemistry of the Phlegrean Fields (Italy) proximal sources for major Mediterranean tephras. Geochimica et Cosmochimica Acta 93, 102–128.

Trua, T., Serri, G., Marani, M., Renzulli, A., Gamberi, F., 2002. Volcanological and petrological evolution of Marsili Seamount (southern Tyrrhenian Sea). Journal of Volcanology and Geothermal Research 114, 441–464.
Vezzoli, L., 1988. Island if Ischia. CNR, Roma.
Vezzoli, L., 1991. Tephra layers in Bannock Basin (Eastern Mediterranean). Marine Geology 100, 21–34.
Villa, I.M., Buettner, A., 2009. Chronostratigraphy of Monte Vulture volcano (southern Italy): secondary mineral microtextures and ^{39}Ar–^{40}Ar systematic. Bulletin of Volcanology 71, 1195–1208.
Vogel, J.S., Cornell, W., Nelson, D.E., Southon, J.R., 1990. Vesuvius/Avellino, one possible source of seventeenth century BC climatic disturbances. Nature 344, 534–537.
Watts, W.A., 1985. A long pollen record from Laghi di Monticchio, southern Italy: a preliminary account. Journal of the Geological Society, London 142, 491–499.
Watts, W.A., Allen, J.R.M., Huntley, B., 1996. Vegetation history and palaeoclimate of the last glacial period at Lago Grande di Monticchio, southern Italy. Quaternary Science Reviews 15, 133–152.
Wulf, S., Brauer, A., Kraml, M., Keller, J., Negendank, J.F.W., 2004. Tephrochronology of the 100 ka lacustrine sediment record of Lago Grande di Monticchio (southern Italy). Quaternary International 122, 7–30.
Wulf, S., Brauer, A., Mingram, J., Zolitschka, B., Negendank, J.F.W., 2006. Distal tephras in the sediments of Monticchio maar lakes. In: Principe, C. (Ed.), La geologia del monte Vulture. Consiglio Nazionale delle Ricerche, pp. 105–122.
Wulf, S., Kraml, M., Keller, J., 2008. Towards a detailed distal tephrostratigraphy in the Central Mediterranean: the last 20,000 yrs record of Lago Grande di Monticchio. Journal of Volcanology and Geothermal Research, 118–132.
Zanchetta, G., Sulpizio, R., Roberts, N., Cioni, R., Eastwood, W.J., Siani, G., Caron, B., Paterne, M., Santacroce, R., 2011. Tephrostratigraphy, chronology and climatic events of the Mediterranean basin during the Holocene: an overview. The Holocene 21, 33–52.
Zolitschka, B., Negendank, J.F.W., 1996. Sedimentology, dating and palaeoclimatic interpretation of a 76.3 ka record from Lago Grande di Monticchio, southern Italy. Quaternary Science Reviews 15, 101–112.

5.4 Manuscript #4

"Marine tephra from the Cape Riva eruption (22 ka) of Santorini in the Sea of Marmara" *(S. Wulf, M. Kraml, T. Kuhn, M. Schwarz, M. Inthorn, J. Keller, I. Kuscu & P. Halbach, 2002: Marine Geology)*

Scientific Technical Report STR14/01, Deutsches GeoForschungsZentrum GFZ. http://doi.org/10.2312/GFZ.b103-14010

ELSEVIER

Marine Geology 183 (2002) 131–141

MARINE GEOLOGY
INTERNATIONAL JOURNAL OF MARINE GEOLOGY, GEOCHEMISTRY AND GEOPHYSICS

www.elsevier.com/locate/margeo

Marine tephra from the Cape Riva eruption (22 ka) of Santorini in the Sea of Marmara

S. Wulf [a,*], M. Kraml [b], T. Kuhn [c], M. Schwarz [b], M. Inthorn [d], J. Keller [b], I. Kuscu [e], P. Halbach [d]

[a] *GeoForschungsZentrum Potsdam, PB 3.3 – Sedimentation and Basin Analysis, Telegrafenberg, D-14473 Potsdam, Germany*
[b] *Institute of Mineralogy, Petrology and Geochemistry, Albert-Ludwigs-University Freiburg, Albertstrasse 23b, D-79104 Freiburg i.Br., Germany*
[c] *Department of Economic Geology and Leibniz-Laboratory for Applied Marine Research, Freiberg University of Mining and Technology, Brennhausgasse 14, D-09596 Freiberg, Germany*
[d] *Institute of Geology, Free University of Berlin, Malteserstr. 74-100, D-12249 Berlin, Germany*
[e] *Marine Geology and Geophysics, MTA, 06520 Ankara, Turkey*

Received 11 July 2001; accepted 3 December 2001

Abstract

A discrete tephra layer has been discovered in three marine sediment cores from the Sea of Marmara, eastern Mediterranean. The rhyodacitic glass chemistry and the stratigraphical position suggest a Santorini provenance and, in particular, a correlation with the marine Y-2 tephra that is known from the southern Aegean Sea and eastern Levantine Basin. This tephra represents the distal facies of the Cape Riva eruption of Santorini, which has been dated by ^{14}C on land at 21 950 cal. yr BP. Hitherto, the Y-2 tephra has been detected only in marine sediment cores recovered south to southeast of its volcanic source. The new occurrence in the Sea of Marmara approximately 530 km NNE of the Santorini eruptive centre suggests a more north-easterly dispersal of fallout products of the Cape Riva eruption than previously supposed.

Keywords: Cape Riva eruption; Santorini volcano; marine tephrochronology; Sea of Marmara; Late Quaternary

1. Introduction

Tephra layers, produced by explosive volcanic eruptions, are widespread isochronous markers, which can be used for dating and correlating sediment sequences across environmental boundaries. Several explosive Quaternary volcanoes occur in the eastern Mediterranean and provide considerable potential for detailed tephrochronological correlations of palaeoceanographic events (e.g. Ninkovich and Heezen, 1967; Keller et al., 1978; Paterne et al., 1988; Vezzoli, 1991; Narcisi and Vezzoli, 1999). In particular, volcanoes of the Hellenic Arc and the Italian peninsula are characterised by numerous highly explosive eruptions. During the Quaternary, the main phase of volcanic activity of the Hellenic Arc was concentrated on the islands of Methana, Milos, Santorini, Kos, Yali and Nisyros (Druitt et al., 1999). The most prominent volcanic island of the Hel-

* Corresponding author. Fax: +49-331-288-1302.
E-mail address: wulf@gfz-potsdam.de (S. Wulf).

0025-3227/02/$ – see front matter
PII: S0025-3227(01)00302-4

lenic Arc is Santorini. The Santorini volcanic activity recorded on land started during the Middle Pleistocene and lasts until recent times (Druitt et al., 1999). At least 12 major explosive eruptions have occurred during the past ~300 kyr forming the so-called "Thera Pyroclastic Formation" (Druitt et al., 1989, 1999). Each of these major explosive events is characterised by an initial Plinian phase forming large pumice fall deposits. The calc-alkaline composition of the eruptive products ranges from andesite to rhyodacite. The youngest major explosive event was represented by the Minoan eruption (3570 ± 20 cal. yr BP; Betancourt and Michael, 1987). Its fallout products are widely dispersed and documented as the Z-2 tephra layer in many deep-sea cores of the Eastern Mediterranean and in lake sediments from southwest Turkey and the Nile Delta (Fig. 1; Ninkovich and Heezen, 1965; Keller and Ninkovich, 1972; Federman and Carey, 1980; Vinci, 1985; Stanley and Sheng, 1986; Sullivan, 1988; Guichard et al., 1993; Eastwood et al., 1999).

A similar tephra succession originating from a major Santorini explosive event of comparable magnitude, the so-called Cape Riva Tuff underlies the Minoan pyroclastic deposits (Druitt, 1985; Druitt et al., 1989). The Cape Riva eruption produced four distinct eruptive units composed of an initial pumice fall deposit (CR-A), a red-brown, partly welded ignimbrite formed by collapse of the Plinian column (CR-B), a co-ignimbritic lithic lag breccia (CR-C) representing the proximal facies of CR-B and an additional welded ignimbrite (CR-D). The pumice fall deposits exposed at Santorini are largely dacitic or rhyodacitic in composition and indicate an east–northeast trending dispersion axis (Druitt et al., 1989). Radiocarbon ages on charcoal from the lower part of the terrestrial pumice flow deposits of unit CR-B (Akrotiri, Santorini) revealed ages of approximately 22 cal. ka BP (Pichler and Friedrich, 1976).

One of the pyroclastic units of the Cape Riva eruption is considered to be the terrestrial equivalent of the widespread marine Y-2 tephra (Pichler and Friedrich, 1976; Federman and Carey, 1980; Vinci, 1985, 1987), which has been dated by an interpolated oxygen isotope stratigraphy at roughly 18 ka BP (Thunell et al., 1977; Keller et al., 1978). The occurrence of the rhyodacitic Y-2 tephra in deep-sea cores from the north-eastern part of the Mediterranean Sea (Aegean Sea and Levantine Basin) suggests at first an easterly dispersal direction for the Cape Riva ash plume (e.g. Keller et al., 1978; Federman and Carey, 1980; Vinci, 1985, 1987; Guichard et al., 1993; Hardiman, 1999; Schwarz, 2000; Fig. 1). This paper reports a new occurrence of the Y-2 tephra in marine sediment cores from the Sea of Marmara and its significance for the reconstruction of the Y-2 dispersal direction.

2. Palaeoceanography and sedimentology of the Sea of Marmara

The Sea of Marmara is an intra-continental marginal sea in the Mediterranean, which is connected to the brackish Black Sea by the Bosphorus Strait and to the normal marine Aegean Sea by the shallow strait of the Dardanelles. In order to reconstruct the palaeoceanographic conditions during the late Glacial–Holocene, three sediment piston cores (20 KLG, 21 KL, 40 KL) up to 10.61 m long have been recovered during the R/V *Meteor* cruise M44/1 in January/February 1999 from a central plateau rising several hundred meters above a deep basin of the central Sea of Marmara (Fig. 1, Table 1). These cores were lithologically described, and organic carbon content (C_{org}) was obtained on core 20 KLG (Fig. 2). In general, the sediments are composed of silty clay of different colours (Kuhn et al., 2000). The sediment surface is characterised by a mm-thick brownish-grey surface layer (core 20 KLG) proving slightly oxidising conditions in the current bottom water. The underlying sediments are olive-grey, olive-black and greenish-grey in colour (Fig. 2) due to changing redox conditions as indicated by pore water Eh profiles (Mn^{4+}-, Fe^{3+}-, sulphate-reducing zone; Pekdeger et al., 2000). Several black horizons occur within these sediments consisting of Fe monosulphides, organic components and clay minerals (Kuhn et al., 2000). The black horizons may be interpreted as freshwater deposits as they resemble banded clays

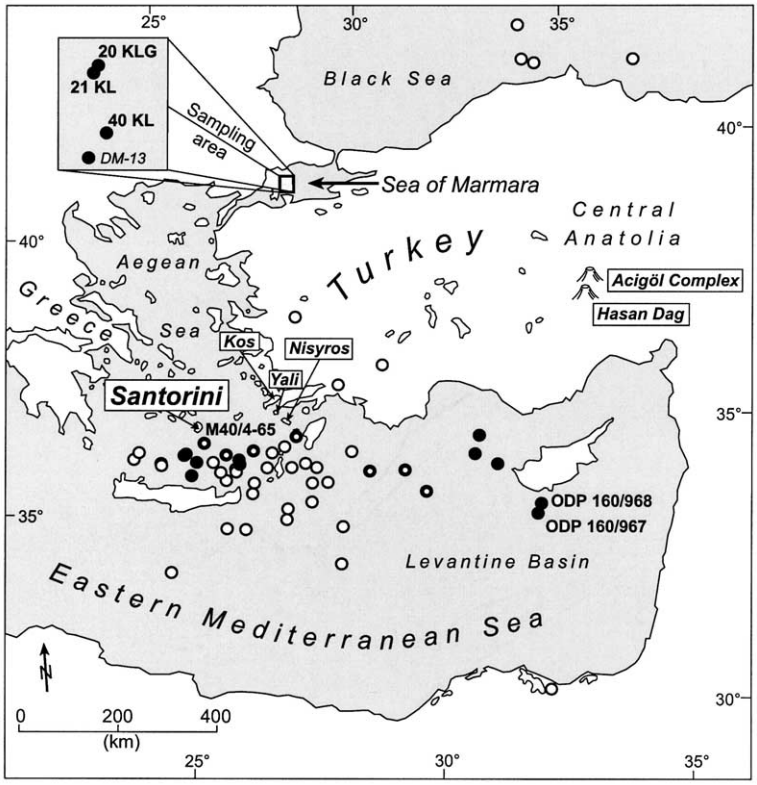

Fig. 1. Map of the Eastern Mediterranean illustrating the location of Quaternary volcanoes, coring sites used in this study, occurrence of the Z-2/Minoan ash (open circles) and the Y-2/Cape Riva tephra (filled circles) in lacustrine sediment sequences and deep-sea cores from the Aegean, Levantine and Black Seas. Bold black circles with grey dots mark the occurrence of both, the Z-2 and the Y-2 tephra. Locations of deep-sea drilling sites are taken from Keller et al. (1978), Federman and Carey (1980), Vinci (1985, 1987), Guichard et al. (1993), Hardiman (1999), Schwarz (2000) and Çagatay et al. (2000); coring positions of terrestrial sequences are from Eastwood et al. (1999) and Stanley and Sheng (1986).

from the Black Sea, which were formed under Pleistocene freshwater conditions (Calvert, 1990). The following general palaeoceanographic model of the Sea of Marmara has been considered (see also Aksu et al., 1999; Çagatay et al., 2000): The black horizons were deposited under glacial conditions during and after the last glacial maximum. The low global sea level and the sill of the Dardanelles (today 65 m water depth) caused the Sea of Marmara to be cut off from the Aegean Sea and filled by freshwater or brackish water. Global warming led to sea level rise starting about 12 ka BP and to seawater ingression into the Sea of Marmara between 10.6 and 6.4 ka BP. The Black Sea, also filled with seawater since 7.15 ka BP, drained its freshwater through the Sea of Mar-

Table 1
Location of drilling sites and length of studied piston cores of the Sea of Marmara

Core number	Longitude E	Latitude N	Water depth (m)	Core recovery (cm)
20 KLG	27°45.79′	40°50.51′	566	1061
21 KL	27°45.77′	40°50.50′	566	720
40 KL	27°46.31′	40°47.12′	702	900

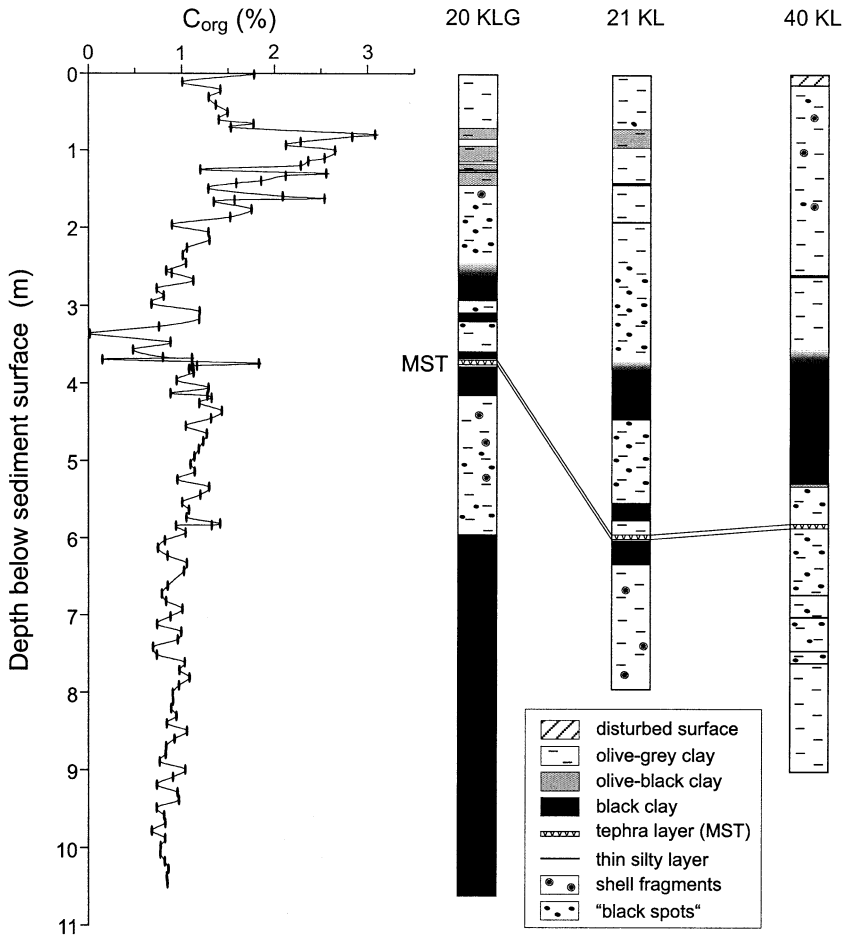

Fig. 2. Core logs of sediment cores 20 KLG, 21 KL and 40 KL from the Sea of Marmara showing the stratigraphic position of ash layer MST. Black spots are interpreted as bioturbations filled with organic material. Organic carbon content (C_{org}) was obtained on core 20 KLG using a LECO–CS analyser at the Free University of Berlin (Inthorn, 2000).

mara, leading to a stratified water column (Aksu et al., 1999). Both conditions caused the formation of sapropelic layers in the Sea of Marmara between 10.6 and 3.2 ka BP (Çagatay et al., 2000). The current hydrological conditions were established 3.2 kyr ago.

3. Macroscopic and microscopic features of tephra layer

A discrete tephra layer, here simplified called Marmara Sea Tephra (MST), is intercalated in all three sediment cores, occurring in-between or below the black horizons, which proves a deposition before the last seawater ingression (see above). The thickness of the tephra layer varies between 1 cm in core 40 KL and 7 cm in cores 20 KLG and 21 KL, respectively. The tephra layer intercalated in the sediment cores recovered from 566 m water depth (20 KLG, 21 KL) is mixed with calcareous ooze causing enhanced thicknesses. Generally, the tephra is red-brownish to ochre in colour and made up of silt to sand-sized particles (max. 230–270 μm). It mainly consists of volcanic glass composed of colourless to brownish

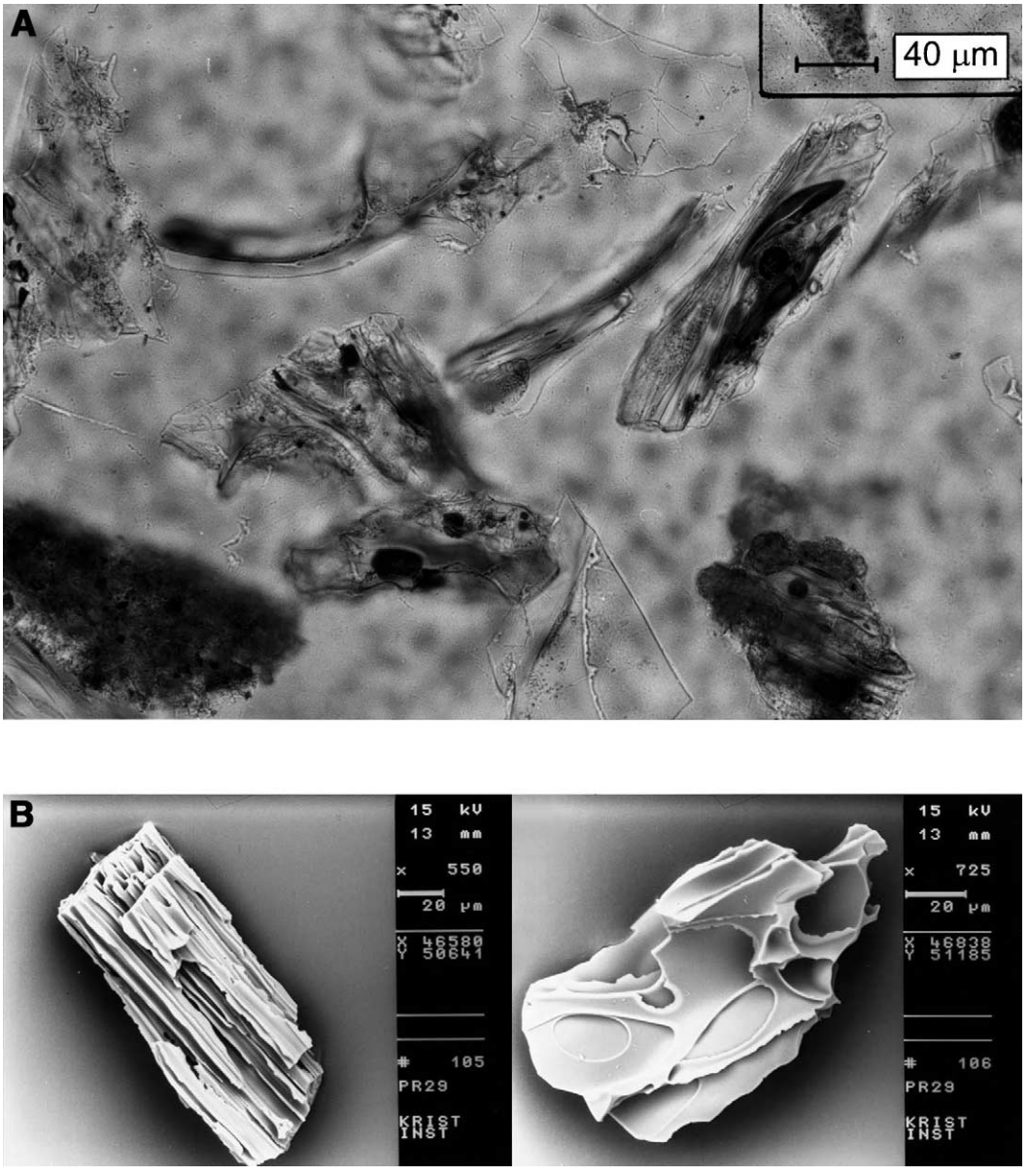

Fig. 3. (A) Microscopic photo of the MST showing volcanic glass shards and phenocrysts of the MST. (B) SEM images of pumice fragments from the Y-2 tephra occurring in core M40/4-65 of the Aegean Sea (Schwarz, 2000).

bubble wall shards with subordinate colourless pumice fragments displaying sub-parallel pipe vesicles (Fig. 3). Some of the glass shards are covered by orange to red coloured iron oxides. Minerals such as plagioclase, augite, hypersthene, apatite and magnetite are rare. Sand-sized volcanic rock fragments occur sporadically.

4. Tephrochronological methods

From each sediment core the petrographical and chemical composition of the MST was determined using polished thin sections. First, the tephra samples were carefully cleaned with 30% H_2O_2 in order to remove the organic matter and

surface coatings. The silt-sand fraction was dried and sieved with a series of fine mesh polyester sieves (200, 100 and 63 μm). The coarsest fraction was chosen for the preparation of thin sections. Major-element EMP analyses on single glass shards were carried out at the GFZ Potsdam, using a Cameca SX-100 electron probe (WDS) with an accelerating voltage of 15 kV and a beam current of 20 nA. Because of the known loss of sodium of volcanic glass during the EMP analysis (Nielsen and Sigurdsson, 1981; Hunt and Hill, 1993), a large beam size of 15 μm diameter was chosen. Peak counting times were 20 s for each element. Instrumental calibration used interlaboratory natural mineral and glass reference materials (Lipari obsidian; Hunt and Hill, 1996).

The chemical composition of the terrestrial Cape Riva pumice and Y-2 glass from the deep-sea cores M40/4-65 of the Aegean Sea (29.5 cm thick tephra layer) as well as ODP 160/967 C and ODP 160/968 C of the Levantine Basin (2 cm thick ash layers, respectively) was determined by a Cameca SX 100 electron microprobe (WDS) at IMPG Freiburg. The operating conditions for these measurements were similar to the GFZ instrument: 15 kV accelerating voltage, 10 nA beam current, defocused beam of 10 μm diameter and peak counting times of 20 s except of Na analysed 10 s. Comparable international mineral and obsidian standards were used for instrumental calibration (USNM 7285, KN18, KE12; Nielsen and Sigurdsson, 1981; Devine et al., 1995).

5. Geochemistry and origin of MST

The chemical composition of glass shards from the MST is rhyodacitic and defines a homogenous population (Table 2, Fig. 4). According to the results of sedimentological data, an age of >10.6 ka BP (see second paragraph) has to be assumed for the deposition of MST. Taking into account both, the geochemical and stratigraphical features, the following volcanic fields characterised by young Quaternary explosive silicic eruptions can be considered as possible sources for the MST: (a) the Aeolian Islands in the Southern Tyrrhenian Sea (Italy), (b) the larger stratovolca-

Table 2
Mean values and 1σ standard deviation of major element chemistry obtained by microprobe analyses on single glass shards from the distal MST and Y-2 tephra as well as on pumice from the proximal Cape Riva unit CR-A[a]

Unit	MST 20	σ	MST 21	σ	MST 40	σ	Y-2	σ	Y-2	σ	Y-2	σ	Cape Riva	σ	Cape Riva	σ
Sample	KLG		KL		KL		#65gl29[a]		#65gl26[a]		ODP968C		ODP967C		Sa 17[a]		Sa 4[a]	
SiO_2	72.79	0.60	72.57	0.73	72.68	0.85	71.72	0.21	71.39	0.79	71.48	0.75	71.37	1.06	71.05	0.41	71.78	0.20
TiO_2	0.46	0.03	0.46	0.02	0.46	0.02	0.46	0.03	0.50	0.08	0.50	0.03	0.48	0.04	0.48	0.05	0.46	0.04
Al_2O_3	14.43	0.15	14.47	0.21	14.48	0.23	14.84	0.11	14.83	0.10	14.75	0.19	14.70	0.27	14.77	0.13	14.81	0.11
FeO	3.06	0.06	3.16	0.10	3.22	0.15	3.33	0.12	3.44	0.37	3.05	0.11	3.04	0.08	3.46	0.21	3.31	0.09
MnO	0.11	0.04	0.12	0.03	0.12	0.02	0.12	0.04	0.13	0.05	0.13	0.03	0.13	0.03	0.13	0.04	0.13	0.04
MgO	0.43	0.02	0.42	0.02	0.43	0.02	0.43	0.02	0.46	0.08	0.42	0.02	0.43	0.02	0.47	0.05	0.42	0.02
CaO	1.76	0.04	1.78	0.04	1.79	0.04	1.75	0.07	1.79	0.18	1.80	0.06	1.85	0.06	1.81	0.12	1.76	0.07
Na_2O	3.99	0.15	4.04	0.12	3.81	0.35	4.27	0.13	4.35	0.17	4.95	0.16	5.03	0.28	4.62	0.15	4.19	0.17
K_2O	2.88	0.08	2.90	0.08	2.94	0.06	2.91	0.09	2.93	0.09	2.82	0.09	2.86	0.09	3.06	0.19	2.98	0.06
P_2O_5	0.07	0.02	0.06	0.02	0.07	0.03	0.15	0.08	0.16	0.09	0.10	0.03	0.10	0.03	0.15	0.07	0.14	0.07
Total	100.00		100.00		100.00		100.00		100.00		100.00		100.00		100.00		100.00	
	$n=13$		$n=12$		$n=16$		$n=23$		$n=23$		$n=18$		$n=17$		$n=23$		$n=24$	

[a] Data of the Y-2 tephra occurring in deep-sea core M40/4-65 from the Aegean Sea (Schwarz, 2000).
n = number of analysed glass shards.

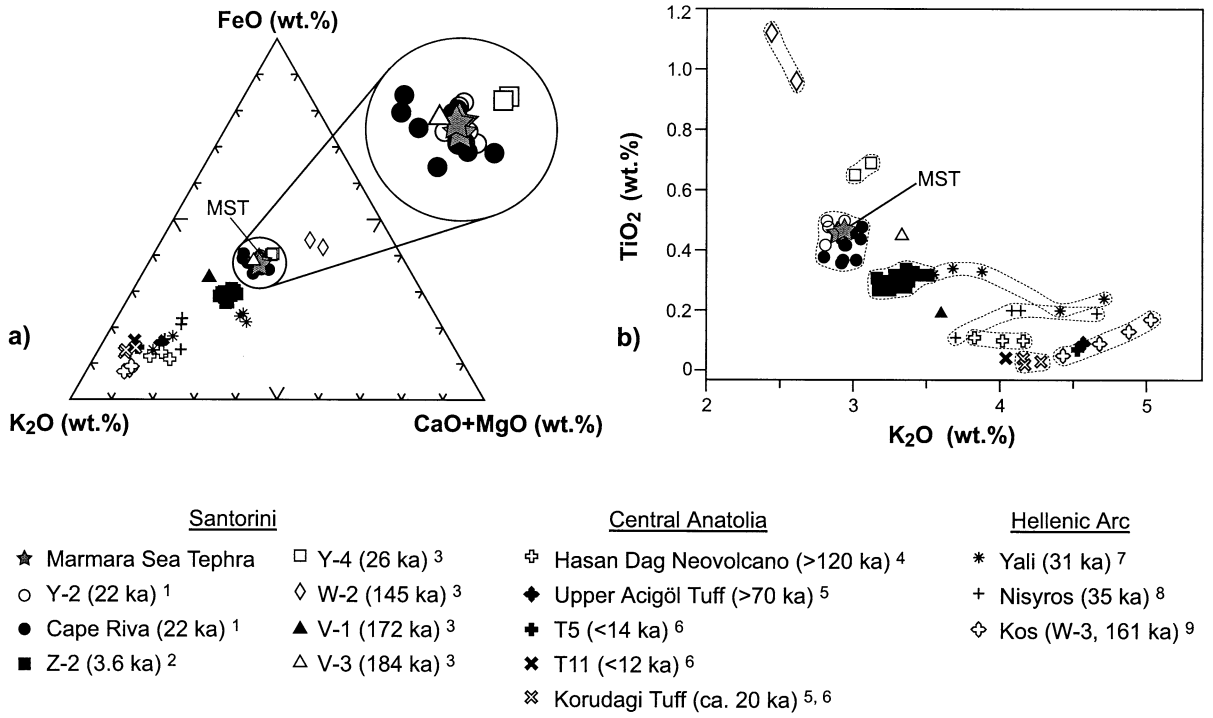

Fig. 4. Chemical discrimination of the MST and prominent Quaternary tephra layers from Santorini, Yali, Nisyros, Kos and Central Anatolia (see Table 3 for references). Element chemistry referred from literature is obtained on single glass shards or glass concentrates using mainly EMP and minor SEM–EDS, ICP–AES and XRF techniques. Note that the comparison of data resulted from single component analyses (EMP, SEM–EDS) with data derived from bulk sample analyses (ICP–AES, XRF) may show some discrepancies, particular in respect of the alkali contents (Keller, 1981). Data of tephra ages are from (1) Pichler and Friedrich (1976), (2) Betancourt and Michael (1987), (3) Schwarz (2000), (4) Deniel et al. (1998), (5) Druitt et al. (1995), (6) Kuzucuoğlu et al. (1998), (7) Federman and Carey (1980), (8) Hardiman (1999) and (9) Smith et al. (1996).

noes of Central Anatolia (Turkey) and (c) the volcanic islands of the Hellenic Arc (Aegean Sea, Greece). Pyroclastic products of rhyodacitic composition from the Aeolian Islands are known from Lipari, which were erupted during the last ~20 kyr (Crisci et al., 1983). However, these tephra deposits are only dispersed on a local scale as indicated by their absence in deep-sea cores from the Ionian (Keller et al., 1978; Kraml, 1997) and Adriatic Sea (Calanchi et al., 1998; Paterne et al., 1988) as well as in lacustrine sediment records from central and southern Italy (Calanchi et al., 1996; Narcisi, 1996; Narcisi and Anselmi, 1998; Ramrath et al., 1999; Wulf, 2000). Prominent stratovolcanoes like the Hasan Dağ and the Acigöl volcanic complex in Central Anatolia (Druitt et al., 1995; Deniel et al., 1998; Kuzucuoğlu et al., 1998) have produced silicic pyroclastic material of distinctly different chemical composition as shown in Fig. 4 and Table 3. In contrast to the Aeolian Islands and Central Anatolia, the Hellenic Arc provides a more likely source for the MST. Here, the major tephra deposits originating from the islands of Kos, Yali and Nisyros partly erupted within the time span of interest, but they do not match the geochemical composition of the MST (Fig. 4, Table 3). On the other hand, the Santorini volcano has produced several ash layers, namely from the oldest to the youngest V-3, V-1, W-2, Y-4, Y-2 and Z-2 tephra. As shown in Fig. 4a, microprobe data of glass shards from the marine V-3, Y-4 and Y-2 tephra define a narrow cluster. Using the discriminating Harker diagram (Fig. 4b) and calculated similarity coefficients after Borchardt et al. (1972) – 0.83 for the Y-4 tephra, 0.91 for the V-3 tephra and

Table 3
Similarity coefficients (after Borchardt et al., 1972) of the MST versus mean glass analyses of the most likely silicic tephra sources in the eastern Mediterranean

Volcanic event	SiO_2	TiO_2	Al_2O_3	FeO	MgO	CaO	Na_2O	K_2O	Mean
Santorini Y-2[a–c]	0.98	0.98	0.98	1.00	0.99	0.99	0.80	0.99	0.97
Santorini Cape Riva[a,d]	0.98	0.90	0.99	0.97	0.92	0.97	0.74	0.98	0.93
Santorini Minoan (Z-2)[b–i]	0.99	0.65	0.97	0.64	0.59	0.80	0.81	0.88	0.79
Santorini Y-4[c]	0.96	0.69	0.97	0.79	0.66	0.81	0.83	0.95	0.83
Santorini Middle Pumice (W-2)[b,c]	0.90	0.44	0.93	0.54	0.31	0.48	0.91	0.87	0.67
Santorini Lower Pumice 2 (V-1)[c]	0.98	0.41	0.97	0.78	0.40	0.59	0.88	0.81	0.73
Santorini V-3[c]	0.96	0.97	0.95	0.90	0.85	0.99	0.75	0.87	0.91
Yali-1[j]	0.95	0.43	0.87	0.37	0.28	0.53	0.99	0.66	0.64
Yali-2[b,c]	0.99	0.71	1.00	0.57	0.90	0.92	0.88	0.79	0.84
Yali-3[j]	0.94	0.53	0.84	0.28	0.41	0.38	0.92	0.62	0.61
Nisyros Lower Pumice[j]	0.96	0.43	0.91	0.47	0.28	0.52	0.90	0.71	0.65
Nisyros Upper Pumice[j]	0.95	0.44	0.89	0.43	0.05	0.60	0.95	0.70	0.63
Nisyros marine[c,j]	0.94	0.32	0.86	0.30	0.33	0.51	0.98	0.70	0.62
Kos Plateau Tuff (W-3)[b,c,j]	0.95	0.24	0.87	0.16	0.10	0.31	0.99	0.61	0.53
Hasan Dag rhyolitic Tuffs[k]	0.95	0.23	0.91	0.21	0.41	0.40	0.92	0.73	0.59
Upper Acigöl Tuff[l]	0.96	0.19	0.95	0.32	0.31	0.45	0.98	0.64	0.60
Korudagi Tuff[l,m]	0.94	0.07	0.92	0.23	0.07	0.20	0.88	0.69	0.50
Acigöl Göl T5[m]	0.95	0.15	0.96	0.27	0.12	0.28	0.85	0.64	0.53
Acigöl Göl T11[m]	0.92	0.09	0.93	0.27	–	0.22	0.59	0.72	0.47

[a] This work.
[b] Federman and Carey (1980).
[c] Vinci (1985).
[d] Druitt et al. (1999).
[e] Eastwood et al. (1999).
[f] Sullivan (1988, 1990).
[g] Watkins et al. (1978).
[h] Guichard et al. (1993).
[i] Keller (1980).
[j] Hardiman (1999).
[k] Deniel et al. (1998).
[l] Druitt et al. (1995).
[m] Kuzucuoğlu et al. (1998).

0.97 for Y-2 tephra (Table 3) – the MST is most likely identical to the marine Y-2 tephra.

6. Discussion and concluding remarks

Based on geochemical, mineralogical and stratigraphical data, the MST can be correlated with the marine Y-2 tephra from Quaternary deep-sea cores in the Eastern Mediterranean Sea. This correlation supports a tentative correlation of a 3 cm thick ash layer that occurs in sediment core DM13 (Çagatay et al., 2000) recovered from a location close to core 40 KL (Fig. 1). Because of the stratigraphical position and the rhyodacitic composition obtained by semi-quantitative SEM-EDX analyses on glass shards, this ash layer has been preliminarily attributed to the Y-2 tephra (Çagatay et al., 2000). However, detailed tephrochronological studies are required to confirm this correlation.

According to the high similarity coefficients (Table 3), the MST and the marine Y-2 tephra can be correlated with Unit CR-A/CR-B of the Cape Riva eruption (see also Schwarz, 2000). The related pyroclastic units have been dated using various methods. Uncalibrated radiocarbon ages of terrestrial charcoal ranging from 18 050 to 18 880 a BP (Pichler and Friedrich, 1976; Eriksen et al., 1990), give an average calibrated age of

21.95 ka BP (after Bard et al., 1998). Corresponding ages of 22.3 ka and 24.8 ka BP for the Y-2 tephra is interpolated from the independent sapropel chronology (after Lourens et al., 1996) of deep-sea cores ODP 160/967 and ODP 160/968, respectively. Considering the analytical uncertainty of the astronomically calibrated sapropel chronology (a few thousand years) and the radiometric ^{14}C chronology, these ages are in good agreement.

So far, the Y-2 tephra has been detected in marine sediment cores recovered at maximum distances of 615 km south to southeast of the Santorini eruptive centre (Vinci, 1987; Fig. 1). This study provides evidence of both the more widespread dispersal to the east–southeast (710 km) as indicated by the occurrence of the Y-2 tephra in deep-sea cores ODP 160/967 and ODP 160/968, and furthermore a widespread distribution to the northeast (530 km) as demonstrated by the identification of Y-2 tephra in sediments of the Sea of Marmara. This implies that the Cape Riva eruption was probably of higher magnitude and with a more north-easterly dispersal of its fallout products than previously supposed, similar to the recent evidence of the Holocene Minoan eruption (Guichard et al., 1993; Eastwood et al., 1999). In the cores of the Sea of Marmara the discrete Y-2 tephra provides an additional independent time marker for the marine sediments at ca. 22 ka cal. BP.

Acknowledgements

We are grateful to Captain Kull and the officers and crew of R/V *Meteor* who contributed to the success of the cruise M 44/1. We are also grateful to our Turkish partners O. Algan and N. Çagatay from MTA and Istanbul University for their logistic support and scientific discussions. In addition, we wish to thank M. Köhler and G. Arnold (GFZ) for the preparation of thin sections, and Warren Fastwood and an anonymous referee for their reviews. Financial support for this work was provided by the German Research Council (DFG project No. HA 563/31, NE 154/33, KE 136/37, KE 136/35).

References

Aksu, A.E., Hiscott, R.N., Yasar, D., 1999. Oscillating Quaternary water levels of the Marmara Sea and vigorous outflow into the Aegean Sea from the Marmara Sea–Black Sea drainage corridor. Mar. Geol. 153, 275–302.

Bard, E., Arnold, M., Hamelin, B., Tisnerat-Laborde, N., Cabioch, G., 1998. Radiocarbon calibration by means of mass spectrometric $^{230}Th/^{234}U$ and ^{14}C ages of corals: an updated data base including samples from Barbados, Muruoa and Tahiti. Radiocarbon 40, 1085–1092.

Betancourt, P.P., Michael, H.N., 1987. Dating the Aegean Late Bronze age with radiocarbon: addendum. Archaeometry 29, 212–213.

Borchardt, G.A., Aruscavage, P.J., Millard, H.T., Jr., 1972. Correlation of the Bishop ash, a Pleistocene marker bed, using instrumental neutron activation analysis. J. Sediment. Petrol. 42, 301–306.

Çagatay, M.N., Görür, N., Algan, O., Eastoe, C., Tchapalyga, A., Ongan, D., Kuhn, T., Kuscu, I., 2000. Late Glacial–Holocene palaeoceanography of the Sea of Marmara: timing of connections with the Mediterranean and the Black Sea. Mar. Geol. 167, 191–206.

Calanchi, N., Dinelli, E., Lucchini, F., Mordenti, A., 1996. Chemostratigraphy of late Quaternary sediments from Lake Albano and central Adriatic Sea cores (PALICLAS Project). In: Guilizzoni, P., Oldfield, F. (Eds.), Palaeoenvironmental Analysis of Italian Crater Lake and Adriatic Sediments. Mem. Istit. Ital. Idrobiol., pp. 247–263.

Calanchi, N., Cattaneo, A., Dinelli, E., Gasparotto, G., Lucchini, F., 1998. Tephra layers in Late Quaternary sediments of the central Adriatic Sea. Mar. Geol. 149, 191–209.

Calvert, S.E., 1990. Geochemistry and origin of Holocene sapropel in the Black Sea. In: Ittekot, V., Kempe, S., Michaelis, W., Spitzy, A. (Eds.), Facets of Modern Biogeochemistry. Springer, Berlin, pp. 326–352.

Crisci, G.M., Delibrias, G., De Rosa, R., Mazzuoli, R., Sheridan, M.F., 1983. Age and petrology of the Late-Pleistocene Brown Tuffs on Lipari, Italy. Bull. Volcanol. 46, 381–391.

Deniel, C., Aydar, E., Gourgau, A., 1998. The Hasan Dağı stratovolcano (Central Anatolia, Turkey): evolution from calc-alkaline to alkaline magmatism in a collision zone. J. Volcanol. Geotherm. Res. 87, 275–302.

Devine, J.D., Gardner, J.E., Brack, H.P., Layne, G.D., Rutherford, M.J., 1995. Comparison of microanalytical methods for estimation of H_2O-contents of silicic volcanic glasses. Am. Mineral. 80, 319–328.

Druitt, T.H., 1985. Vent evolution and lag breccia formation during the Cape Riva eruption of Santorini, Greece. J. Geol. 93, 439–454.

Druitt, T.H., Mellors, R.A., Pyle, D.M., Sparks, R.S.J., 1989. Explosive volcanism on Santorini, Greece. Geol. Mag. 126, 95–126.

Druitt, T.H., Brenchley, P.J., Gökten, Y.E., Francaviglia, V., 1995. Late Quaternary rhyolitic eruptions from the Acigöl Complex, central Turkey. J. Geol. Soc. London 152, 655–667.

Druitt, T.H., Edwards, L., Mellors, R.M., Pyle, D.M., Sparks, R.S.J., Lanphere, M., Davies, M., Barriero, B., 1999. Santorini Volcanol. Geol. Soc. Spec. Publ., Geological Society of London, 19, 165 pp.

Eastwood, W.J., Pearce, N.J.G., Westgate, J.A., Perkins, W.T., Lamb, H.F., Roberts, N., 1999. Geochemistry of Santorini tephra in lake sediments from Southwest Turkey. Global Planet. Change 21, 17–29.

Eriksen, U., Friedrich, W.L., Buchardt, B., Tauber, H., Thomson, M.S., 1990. The Stronghyle Caldera: geological, palaeontological and stable isotope evidence from radiocarbon dated stromatolites from Santorini. In: Hardy, D.A., Keller, J., Galanopoulos, V.P., Flemming, N.C., Druitt, T.H. (Eds.), Thera and the Aegean World III. Santorini, Greece, pp. 139–150.

Federman, A.N., Carey, S.N., 1980. Electron microprobe correlation of tephra layers from Eastern Mediterranean abyssal sediments and the island of Santorini. Quat. Res. 13, 160–171.

Guichard, F., Carey, S., Arthur, M.A., Sigurdsson, H., Arnold, M., 1993. Tephra from the Minoan eruption of Santorini in sediments of the Black Sea. Nature 363, 610–612.

Hardiman, J.C., 1999. Deep sea tephra from Nisyros Island, eastern Aegean Sea, Greece. In: Firth, C.R., McGuire, W.J. (Eds.), Volcanoes in the Quaternary. Geological Society of London, London, pp. 69–88.

Hunt, J.B., Hill, P.G., 1993. Tephra geochemistry: a discussion of some persistent analytical problems. Holocene 3, 271–278.

Hunt, J.B., Hill, P.G., 1996. An inter-laboratory comparison of the electron probe microanalysis of glass geochemistry. Quat. Int. 34/36, 229–241.

Inthorn, M., 2000. Bathymetrie und Tektonik des tiefen Marmarameeres/Türkei. Diploma Thesis, Free University of Berlin, 58 pp.

Keller, J., 1980. Prehistoric pumice tephra on Aegean islands. In: Doumas, C. (Ed.), Thera and the Aegean World II. The Thera Foundation, London, pp. 49–56.

Keller, J., 1981. Quaternary tephrochronology in the Mediterranean region. In: Self, S., Sparks, R.S.J. (Eds.), Tephra Studies. Reidel, Dordrecht, pp. 227–244.

Keller, J., Ninkovich, D., 1972. Tephra-Lagen in der Ägäis. Z. Dtsch. Geol. Ges. 123, 579–587.

Keller, J., Ryan, W.B.F., Ninkovich, D., Altherr, R., 1978. Explosive volcanic activity in the Mediterranean over the past 200 000 yr as recorded in deep-sea sediments. Geol. Soc. Am. Bull. 89, 591–604.

Kraml, M., 1997. Laser-$^{40}Ar/^{39}Ar$-Datierungen an distalen marinen Tephren des jung-quartären mediterranen Vulkanismus (Ionisches Meer, METEOR-Fahrt 25/4). Ph.D. Thesis, Albert-Ludwigs-University of Freiburg i.Br., Germany, 216 pp.

Kuhn, T., Richter, S., Algan, O., 2000. Core descriptions. In: Pätzold, J., Halbach, P.E., Hempel, G., Weikert, H. (Eds.), Östliches Mittelmeer–Nördliches Rotes Meer 1999, Cruise No. 44, 22 January–16 May. METEOR-Berichte, Universität Hamburg, pp. 37–39.

Kuzucuoğlu, C., Pastre, J.-F., Black, S., Ercan, T., Fontugne, M., Guillou, H., Hatté, C., Karabıyıkoglu, M., Orth, P., Türkecan, A., 1998. Identification and dating of tephra layers from Quaternary sedimentary sequences of Inner Anatolia, Turkey. J. Volcanol. Geotherm. Res. 85, 153–172.

Lourens, L.J., Antonarakou, A., Hilgen, F.J., Van Hoof, A.A.M., Vergnaud-Grazzini, C., Zachariasse, W.J., 1996. Evaluation of the Plio-Pleistocene astronomical timescale. Paleoceanography 11, 391–413.

Narcisi, B., 1996. Tephrochronology of a late quaternary lacustrine record from the Monticchio Maar (Vulture Volcano, southern Italy). Quat. Sci. Rev. 15, 155–165.

Narcisi, B., Anselmi, B., 1998. Sedimentological investigations on a late quaternary lacustrine core from the Lagaccione crater (Central Italy): palaeoclimatic and palaeoenvironmental inferences. Quat. Int. 47/48, 21–28.

Narcisi, B., Vezzoli, L., 1999. Quaternary stratigraphy of distal tephra layers in the Mediterranean – an overview. Global Planet. Change 21, 31–50.

Nielsen, C.H., Sigurdsson, H., 1981. Quantitative methods for electron microprobe analysis of sodium in natural and synthetic glasses. Am. Mineral. 66, 547–552.

Ninkovich, D., Heezen, B.C., 1965. Santorini tephra, Proceedings of the Seventeenth Symposium of the Colston Res. Society. Colston Research Papers 17. Butterworths Scientific Publications, London, pp. 413–452.

Ninkovich, D., Heezen, B.C., 1967. Physical and chemical properties of volcanic glass shards from Pozzuolana Ash, Thera Island, and from Upper and Lower Ash Layers in Eastern Mediterranean deep-sea sediments. Nature 213, 582–584.

Paterne, M., Guichard, F., Labeyrie, J., 1988. Explosive activity of the South Italian volcanoes during the past 80 000 years as determined by marine tephrochronology. J. Volcanol. Geotherm. Res. 34, 153–172.

Pekdeger, A., Knappe, A., Kuhn, T., 2000. Vertical distribution of Eh and pH. In: Pätzold, J., Halbach, P.E., Hempel, G., Weikert, H. (Eds.), Östliches Mittelmeer–Nördliches Rotes Meer 1999, Cruise No. 44, 22 January–16 May. METEOR-Berichte, Universität Hamburg, pp. 48–49.

Pichler, H., Friedrich, W., 1976. Radiocarbon dates of Santorini volcanics. Nature 262, 373–374.

Ramrath, A., Nowaczyk, N.R., Negendank, J.F.W., 1999. Sedimentological evidence for environmental changes since 34 000 years BP from Lago di Mezzano, central Italy. J. Paleolimnol. 21, 423–435.

Schwarz, M., 2000. Tephrakorrelation im östlichen Mittelmeer (Meteor M40/4 Kerne). Diploma Thesis, Albert-Ludwigs-University of Freiburg i.Br., 257 pp.

Smith, P.E., York, D., Chen, Y., Evensen, N.M., 1996. Single crystal ^{40}Ar–^{39}Ar dating of a Late Quaternary paroxysm on Kos, Greece: Concordance of terrestrial and marine age. Geophys. Res. Lett. 23, 3047–3050.

Stanley, D.J., Sheng, H., 1986. Volcanic shards from Santorini (Upper Minoan ash) in the Nile Delta, Egypt. Nature 320, 733–735.

Sullivan, D.G., 1988. The discovery of Santorini Minoan tephra in Western Turkey. Nature 333, 552–554.

Sullivan, D.G., 1990. Minoan tephra in lake sediments in western Turkey, dating eruption and assessing the atmospheric dispersal of ash. In: Hardy, D.A., Renfrew, A.C. (Eds.), Thera and the Aegean World III. The Thera Foundation, London, pp. 114–119.

Thunell, R.C., Williams, D., Federman, A., Sparks, R.S.J., 1977. Late Quaternary tephra chronology of Eastern Mediterranean sediments. Geol. Soc. Am. Abstr. Prog. 9, 1200.

Vezzoli, L., 1991. Tephra layers in Bannock Basin (Eastern Mediterranean). Mar. Geol. 100, 21–34.

Vinci, A., 1985. Distribution and chemical composition of tephra layers from Eastern Mediterranean abyssal sediments. Mar. Geol. 64, 143–155.

Vinci, A., 1987. The 'Cape Riva tephra layer' Y-2 (Santorini volcano) in deep-sea sediments from eastern Mediterranean Sea. Boll. Oceanol. Teor. Appl. 5, 117–123.

Watkins, N.D., Sparks, R.S.J., Sigurdsson, H., Huang, T.C., Federman, A., Carey, S., Ninkovich, D., 1978. Volume and extent of the Minoan tephra from Santorini volcano: new evidence from deep-sea cores. Nature 271, 122–126.

Wulf, S., 2000. Das tephrochronologische Referenzprofil des Lago Grande di Monticchio – Eine detaillierte Stratigraphie des süditalienischen explosiven Vulkanismus der letzten 100 000 Jahre. Ph.D. Thesis, University of Potsdam, Germany, Scientific Technical Report STR01/03, 124 pp.

ISSN 2190-7110